Measurement of some Parameters of a PN Junction Solar Cell and Analysis of its Time Dependent Response at Different Injection Levels

A Thesis
submitted in partial fulfilment of the
requirements of the degree of
DOCTOR OF PHILOSOPHY

by

MAHESH KUMAR MADAN

PHYSICS GROUP

Birla Institute of Technology and Science

Pilani (Rajasthan) India

January, 1981

DEDICATED

TO THOSE WHO ARE INVOLVED DIRECTLY OR INDIRECTLY IN THE EFFORTS TO MAKE SOLAR CELLS A VIABLE SOURCE OF ELECTRIC POWER

BIRLA INSTITUTE OF TECHNOLOGY & SCIENCE
PILANI (RAJASTHAN)

CERTIFICATE

Thia is to certify that the thesis entitled "MEASUREMENT OF SOME PARAMETERS OF A p-n JUNCTION SOLAR CELL AND ANALYSIS OF ITS TIME DEPENDENT RESPONSE AT DIFFERENT INJECTION LEVELS" and submitted by Mr. Mahesh Kumar Madan ID No. 76S85001 for award of Ph.D degree of the Institute, embodies original work done by him under my supervision.

Signature in full of the Supervisor: V K Tewary

Name in capital block letters: V. K. TEWARY

Designation: Professor of Physics and Dean of Research and Consultancy Division

Date: February 6, 1981.

ACKNOWLEDGEMENT

It gives me immense pleasure to place on record my deep sense of gratitude towards Dr. V.K. Tewary, Professor of Physics and Dean of Research and Consultancy Division, B.I.T.S., Pilani who not only initiated, guided and encouraged me throughout the course of this work but also took a very personal interest in it. I am indeed grateful to him.

I owe my sincere and heartfelt thanks to Dr. L.K. Maheshwari, Dr. P.R. Marweri, Dr. A. Subramanian and Shri T.N.R.K. Kurup for taking keen interest in my work. My thanks are also due to Mr. R.S. Mahwar and Mr. R.S. shekhawat for helping me in all possible ways.

I am thankful to the staff of Physics Group, Instrumentation Unit, Electrical and Electronics Engineering Group, Information Processing Unit, Library, Workshop and various laboratories of B.I.T.S., Pilani who helped me in various ways. I also thank Dean Faculty Division III and Director B.I.T.S., Pilani for providing the necessary facilities.

I wish to thank Dr. S.C. Jain, Director, Solid State Physics Laboratory, Ministry of Defence, Delhi,

for granting permission to do some experimental work there, I also wish to thank the staff of Solar Cell Division of S.S.P.L, for taking keen interest in my work.

There are many who made my stay at Pilani enjoyable during the course of this work. I would be able to name only a few of them s Mr. Ravinder Seru, Dr. V.S. Kulhar, Dr. G.S. Tyagi, Dr. S.c. Sharma, Dr. N.K. Swami, Mr. A, Shrimali, Mr. N. Jagadle, Mr. Sohan Lal, Dr. Animesh Jain, Dr. S.K. Jain, Dr. (Miss) A. Agarwala, Mr. S.K. Sharma, Miss M. Rajeshwari, Mrs. Anita Dubey, Mr. Murlidhar, Mr. Sanjay Gaur, Mr. Rajnesh Mahajan, Mr. V. Krishnan, Dr. Lalit Kumar.

I am grateful to the University Grants Commission, India for the award of a research fellowship.

My special thanks are to Mr. M.K. Joshi for sincere typing and Mr. N.K. Sharma for tracing and printing the diagrams.

I affectionately thank my sisters and parents who have been a constant source of inspiration throughout this seemingly unending task.

mk madan

(MAHESH KUMAR MADAN)

ABSTRACT

This thesis deals with the measurement and analysis of steady state characteristics and transient response of p-n junction solar cells in dark as well as illuminated mode at various injection or illumination levels. Since in dark mode p-n junction solar cell characteristics are similar to those of p-n junction diode# experimental studies on some p-n junction diodes also have been done.

In steady state# the saturation of junction voltage across a forward biased p-n junction at high injection levels is exploited for a determination of series resistance and diffusion potential of a p-n junction device, similarly# shunt resistance and reverse saturation current# in principle, may be determined from the reverse I-V characteristic of a p-n junction device taking into account the fact that in case of reverse bias# whole of the voltage appears across the p-n junction. It is shown that this method can be used to study the effect of illumination level and wavelength of light on these parameters of a solar cell.

Transient response has been studied by three methods. Two of them, i.e. open circuit voltage decay (dark) and reverse recovery, are based on injection of carriers and hence can be used for solar cells as well as diodes. The third one is based on generation of carriers by exposing solar cell to light pulses.

For the open circuit voltage decay (OCVD) in a p-n junction device, a theoretical analysis is presented which is based on an old but hitherto unused expression given by North and which accounts for the p-n coupling between the emitter and the base of the device. The p-n coupling makes a significant contribution in modern p-n diodes/solar cells because of gap shrinkage effects caused by heavy doping in the diffuse layer. The p-n coupling introduces a sharp, almost vertical, drop in voltage in the initial stages of the decay which is added to the voltage drop due to the series resistance of the diode/solar cell. The two contributions can be separated by measuring the current dependense of the total initial voltage drop. Thus the theory explains the observed injection current dependence of the series resistance which is determined from the OCVD data without separating the p-n coupling contribution. Experiments on OCVD in p-n junction devices have been conducted which illustrate

the basic features of the theory. The results of these experiments as well as those of Neugroschel et. al. can be fitted quite well with the theory. This analysis yields the value of the excess carrier lifetime and an estimate of the gap shrinkage. It has been reported that Neugroschel's results could not be fitted by the usual linear theory.

A theoretical analysis of reverse recovery transients is presented which also includes the effect of p-n coupling in the calculation of storage time by appropriately modifying the North’s formula, when p-n coupling is neglected the present formulation for storage time reduces to the usual Kingston’s formula. Results of experimental studies on reverse recovery, and their fitting with the theory is presented here. This analysis also yields the value of the excess carrier lifetime and an estimate of the gap shrinkage, and can be used to supplement OCVD results.

The experimental studies on photo voltage decay (PVD) indicate that slope of the decay is independent of intensity in a certain region (presumably where saturation effects and space charge effects are negligible) • Also the value of slope of the linear region of the PVD curve is nearly same as that of the OCVD

curve, unlike the results reported by Mahan et. al. The similarity of the aforementioned slopes is in accordance with our theoretical analysis based upon Jain's theory which gives that at large values of time the slope is independent of wavelength of light. Generally, our experimental results are in qualitative agreement with Jain's theory.

C O N T E N T S

Certificate

Acknowledgements

ABSTRACT

Contents

CHAPTER I I GENERAL INTRODUCTION 1

1. Introduction 2

2. Theory of p-n Junction C

2.1 Theory of p-n Junction Diode 3

2.2 Theory of p-n Junction Solar Cells. 10

3. Effect of p-n Coupling 13

4. Objective and Scope of the Present Investigation 17

5. Summary of the hork Reported in this Thesis. K

References 24

Table 27

Figure Captions 28

Figures. 2y

CHAPTER II» STEADY STATE MEASUREMENTSAND ANALYST 3i

1. Introduction 32

2. Theory 5 5

2.1 I-V Characteristic of an Ideal. Diode 33

2.2 Effect of R_y and on R_{sh} . I-V Characteristic 37

2.3 I-V Characteristic of a Solar Cell. 40

3. Experimental Study 40

4. Analysis of Results 43

5. Conclusions 44

References 46

Tables 4 S

Figure Captions SO

Figures 54

CHAPTER III* OPEN CIRCUIT VOLTAGE DECAY 13

1. Introduction SO

2. Theory of OCVD 87

3. Theoretical Analysis of OCVD and Measurement of Device Parameters 93

3.1 Theoretical Behaviour of OCVD 93

3.2 Method to Determine Solar Cell Parameters Using OCVD 106

3.3 Comparison with Earlier Experimental Data 108

4. Experimental Study and Analysis 40

4.1 Experimental Arrangements 110

4.2 Experimental Results of OCVD 114

4.3 Measurement of Initial Drop 1*5

4.4 Analysis of Experimental Results 11(3

5. Conclusions 124

References 126

Tables 129

Figure Captions 135

Figures 144

CHAPTER IV : REVERSE RECOVERY ISO

1. Introduction iSi

2. Theory and Analysis iS4

2.1 Theory of Constant Current Phase i$4

2.2 Qualitative Analysis I S3

3. Experimental Study <52

3.1 Experimental Arrangements 192

3.2 Results and Analysis |53

4. Conclusions HG

References i97

Tables |jg

Figure Captions 2 <37

Figures 210

CHAPTER V s PHOTO VOLTAGE DECAY 221

1. Introduction 2 22

2• Theory 2 23

3* Experimental Study 227

4. Conclusions 232

References 233

Tables 234

FiguresCaptions 23G

Figures 239

CHAPTER I

GENERAL INTRODUCTION

CHAPTER I

GENERAL INTRODUCTION

1. Introduction

After the successful demonstration of the principle of photovoltaic energy conversion using solar cells in 1954 by Bell Telephone Laboratories, there has been a tremendous improvement in the technology of fabrication and understanding of physics of the same. The main advantages of solar cells over other energy conversion devices are its light weight, high efficiency, high reliability, almost no maintenance requirements no pollution and zero fuel cost. These advantages have made it indespensable in space applications and many satellites are now being powered by solar cells. The main disadvantages with solar cells are the requirement of high investments initially and intermittent availability of power. This has limited their use in terrestrial applications, with the effects right now being put in to improve the efficiency and reduce the cost, it is expected that within a few years, solar cells may compete with the conventional sources of energy.

The first solar cells developed were made of silicon and till today, silicon is the most widely used material for fabricating solar cells. Though there are other materials which are theoretically expected to give higher efficiencies, but the technology and physics of silicon are perhaps the best understood, out of these materials, as regards their use in making solar cells is concerned. Fig. 1.1 gives a curve of theoretical maximum efficiency versus energy gap of the material (1). Table 1.1 gives a list of some selected materials and the types of solar cells being explored and their present status in terms of efficiency (2).

To determine the usefulness of a device in varying conditions and to determine design parameters to improve its efficiency, or to otherwise study the device/Whatever context it may be it is necessary to have reliable testing and characterization methods for the device and they have to be updated with the improvements in the device. Some of the most important parameters of a solar cell are series resistance, shunt resistance and minority carrier lifetime which directly affect its efficiecy. This thesis deals with the theoretical and experimental analysis of some methods of measurement of these and some other related parameters.

Though the theory of semiconductors is quite well understood, but there are maby questions about p-n junctions which are yet to be answered satisfactorily, from practical point of view as well as for the theoretical understanding. In this context, reliability of the method of determination of a parameter plays an important role.

Solar cell measurements are normally made in two modesi steady state and transient;and both of these modes can be studied in dark or under light. Many parameters can be determined in steady state as well as transients and some of them by more than one method in each mode (for example minority carrier lifetime).

Series resistance is one of the most important parameters of a solar cell , To reduce the overall cost, solar cells may be used at high intensities with concentrators which will make high currents flow through the cell. In these conditions series resistance of the cell may become one of the most inhibiting factors. Hence a study of this parameter is important. As we shall see later, there are various methods to determine the value of series resistance. Most of them extract the value of this parameter from steady state analysis, though it has been reported that its value can be measured using the method of open circuit voltage decay (OCVD) (3), (4). In (5) result

of a study of series resistance variation with respect to current when determined by OCVD, is reported. It shows a large variation of series resistance with current which is not substantiated by other methods and theoretically not understood. This, perhaps, requires a new look into the validity of the method of interpretation used in OCVD to determine series resistance. We shall discuss this problem in detail in chapter 3 and show that when the OCVD data Is interpreted as proposed in that chapter, we get an acceptable value of series resistance.

In the analysis of most of the transient methods, the contribution of diffuse layer is neglected. It has been assumed that the contribution of this part to the total current is negligible. However, recent studies (6) - (9) have shown that energy band gap narrowing due to heavy doping may take place in the diffuse region which may increase its contribution. It is in this context that p-n coupling (introduced in chapter 3) becomes important and may account for the observed descrepancy in the variation of series resistance with current as well as rest of the open circuit voltage decay. We investigate the effect of p-n coupling on OCVD in chapter 3 and on reverse recovery transients in chapter 4.

In the next section, a brief discussion of the p-n junction theory is given. In section 3 a discussion on the effect of p-n coupling on various measurements is discussed. In section 4 objective of the present investigations is given and in last section a summary of the work presented in this thesis is given.

2. Theory of P-n Junction

The analysis reported here is based on a model of a planar p-n junction based on the usual approximations (10). P is taken as heavily doed compared to n-region. The junction is at $x = 0$ and n-region extends from 0 to ∞.

The general equations describing the behaviour of carriers can, then be written (10) - (14) in the n-region as follows:

$$\frac{\partial p}{\partial t} = -\frac{p}{\tau_p} - \frac{\partial J_p}{\partial x} + g \tag{1.1}$$

$$\frac{\partial n}{\partial t} = -\frac{n}{\tau_n} - \frac{\partial J_n}{\partial x} + g \tag{1.2}$$

$$J_p = -D_p \frac{\partial p}{\partial x} \tag{1.3}$$

$$J_n = D_n \frac{\partial n}{\partial x} \tag{1.4}$$

$$J = J_p + J_n$$

In these equations J_n, J_p and J represent the electron and hole and total flux densities respectively; p and n are the excess carrier densities and p_{no} and n_{no} are thermal equilibrium densities of holes and electrons respectively; τ_p, τ_n, D_p, D_n, μ_p and μ_n are the lifetimes, diffusion coefficients, and mobilities of the holes and electrons; g is the generation rate of electron hole pairs. Please note that usually δp and δn are used to represent excess carrier concentration, but here brevity we shall use only p and n.

Similar equations can be written for p-region also.

In most cases, it is assumed that condition of charge neutrality at every point exists; drift current (due to electric field) is negligible and concentration of minority carriers is much less than that of majority carriers (low injection level).

Thus, for minority carriers on n-side the continuity equation can be written as

$$D_p \frac{\partial^2 p}{\partial x^2} - \frac{p}{\tau_p} + g = \frac{\partial p}{\partial t} \qquad (1.5)$$

It is assumed that carrier densities are never high enough to disobey the Boltzmann Statistics (for discussion on a general boundary condition, please see chapter 2). In such a case, carrier density injected

at the junction is given by

$$p(o) = P_{no}(\exp(qV/kT) - 1) \tag{1.6}$$

where p(o) is the excess hole density on n-side at the junction, V is the applied voltage, q is the electronic charge, k is Boltzmann constant and T is temperature on the absolute scale. Another boundary condition is

$$p(x,t) = 0 \text{ at } x = \infty \tag{1.7}$$

which represents ohmic contact at the back.

2.1 Theory of P-n Junction Diode

In a diode, in steady state

$$g = 0 \tag{1.8}$$

$$\text{and} \quad \frac{\partial p}{\partial t} = 0; \quad \frac{\partial n}{\partial t} = 0 \tag{1.9}$$

Hence eq.(1.5) will reduce to

$$D_p \frac{\partial^2 p}{\partial x^2} - \frac{p}{\tau_p} = 0 \tag{1.10}$$

with the boundary conditions already described

$$p(x) = p(o) \exp(-x/L_p) \tag{1.11}$$

$$\text{where } L_p^2 = D_p \tau_p \tag{1.12}$$

Similarly in p region, equation for electrons would be

$$n(x) = n(o)\ \exp(VL_n) \tag{1.13}$$

$$L_n^2 = D_n \tau_n \tag{1.14}$$

Total flux current will be given by

$$J = D_n \frac{dn(o)}{dx} - D_p \frac{dp(o)}{dx} \tag{1.15}$$

$$\text{or} \quad J = \frac{D_n}{L_n} n(o) - \frac{D_p}{L_p} p(o) \tag{1.16}$$

Using the relation (1.6), eq.(1.16) can be written as

$$J = J_o\ (\exp(qV/kT) - 1) \tag{1.17}$$

$$\text{where} \quad J_o = \frac{n_{po} D_n}{L_n} + \frac{p_{no} D_p}{L_p} \tag{1.18}$$

The current density I will be given by

$$I = qJ \tag{1.19}$$

$$\text{and} \quad I_o = qJ_o \tag{1.20}$$

where I_o is called the reverse saturation current,

Eq.(1.17) coupled with eq.(1.19) and (1.20) can be written as

$$I = I_o\ (\exp(qV/kT) - 1) \tag{1.21}$$

This equation describes the I-V relation for a diode.

In transient state

$$\frac{\partial p}{\partial t} \neq 0 \tag{1.22}$$

Hence for transient state eq.(1.5) can be written as

$$L_p \frac{\partial^2 p}{\partial x^2} - \frac{p}{\tau_p} = \frac{\partial p}{\partial t} \tag{1.23}$$

Similarly an equation for p region can also be written.

To solve eq.(1.23), along with the equation for p-region, to find an expression for V(t) all the boundary conditions mentioned for the steady case have to be satisfied along with the conditon that at t a 0, the carrier profile is given be eqs.(1.11) and (1.13). The solution of transient state for a diode is discussed in detail in chapter III.

2.2 <u>Theory of P-n Junction Solar Cells</u>

We consider a solar cell as shown in Fig. 1.2 whose junction is at x = 0 and diffuse layer thickness is *1 .

The excess carrier generation rate is then given

(10) by

$$g^*(x) = \alpha N_o e^{-\alpha(x+d)} \tag{1.24}$$

where N_o is the number of photons per unit area per unit time falling at the front surface of solar cell, α is the absorption coefficient. The incident light is taken as monochromatic.

The boundary condition at surface is

$$D_n \left(\frac{dn_p}{dx}\right)_{-d} = s\, n_p(-d) \tag{1.25}$$

where s is the surface recombination velocity. Apart from this, other boundary conditions are same as those given for diode.

The solutions of eq. (1.1) and (1.2) are then given (10) by

$$n_p(x) = A \cosh\frac{x}{L_n} + B \sinh\frac{x}{L_n} + \frac{\alpha N_o \tau_n}{1-\alpha^2 L_n^2} e^{-\alpha(x+d)} \tag{1.26}$$

$$p_n(x) = D e^{-x/L_p} + \frac{\alpha N_o \tau_p}{1-\alpha^2 L_p^2} e^{-\alpha(x+d)} \tag{1.27}$$

where

$$D = p_{no}(e^{qV/kT} - 1) - \frac{\alpha N_o \tau_p}{1-\alpha^2 L_p^2} e^{-\alpha d} \tag{1.28}$$

$$A - n_{po}(e^{qV/kT} - 1) - \frac{\alpha N_o L_n^2}{1-\alpha^2 L_n^2} e^{-\alpha d} \tag{1.29}$$

and

$$G = A \left[\frac{s \operatorname{Cosh} \frac{d}{L_n} + \frac{D_n}{L_n} \operatorname{Sinh} \frac{d}{L_n}}{\frac{D_n}{L_n} \operatorname{Cosh} \frac{d}{L_n} + s \operatorname{Sinh} \frac{d}{L_n}} \right] +$$

$$\frac{\alpha N_o L_n^2}{1-\alpha^2 L_n^2} \left[\frac{s_n + D\alpha}{\frac{D_n}{L_n} \operatorname{Cosh} \frac{d}{L_n} + s \sinh \frac{d}{L_n}} \right] \tag{1.30}$$

The junction current is given by

$$I = I_o(e^{qV/kT} - 1) - I_g \tag{1.31}$$

where

$$I_o = q \left[\frac{p_{no} D_p}{L_p} + \frac{n_{po} D_n}{L_n} \; \frac{s \operatorname{Cosh} \frac{d}{L_n} + \frac{D_n}{L_n} \operatorname{Sinh} \frac{d}{L_n}}{\frac{D_n}{L_n} \operatorname{Cosh} \frac{d}{L_n} + s \operatorname{Sinh} \frac{d}{L_n}} \right] \tag{1.32}$$

and

$$I_g = \frac{q \alpha N_o L_p^2 e^{-\alpha d}}{1-\alpha^2 L_p^2} \left(\frac{1}{L_p} - \alpha \right) + \frac{q \alpha N_o L_n^2}{1-\alpha^2 L_n^2}$$

$$x \left\{ \frac{1}{L_n} \left[\frac{\left(s \operatorname{Cosh} \frac{d}{L_n} + \frac{D_n}{L_n} \operatorname{Sinh} \frac{d}{L_n}\right) e^{-\alpha d} - s - \alpha L_n}{\frac{D_n}{L_n} \operatorname{Cosh} \frac{d}{L_n} + s \sinh \frac{d}{L_n}} \right] + \alpha e^{-\alpha d} \right\}$$

The transient case has been discussed in chapter 5.

3. Effect of p-n coupling

Eq.(1.6) shows that concentration of holes at $x \ll 0$ on n-side is related to the voltage atross the junction. A similar relation exists between concentration of electrons on p-side of the junction and voltage across the junction. It can be shown that the two concentrations are related to each other as given below

$$\frac{n(o)}{p(o)} = \frac{n_{po}}{p_{no}} \qquad (1.33)$$

This means that within the limits of validity of Jhockley boundary condition (i.e. low injection level), concentrations of minority carriers on the two sides of the junction are related by a constant (whose value depends on the doping concentrations of the p and n sides of the junction). We shall refer to this as p-n coupling. The concentrations on both sides of the junction are also coupled by the relation (1.15).

In the usual calculations, the contribution of diffuse layer and hence the p-n coupling is neglected. In many cases $n_{po} << p_{no}$ (for a p^+n diode) and $\tau_n << \tau_p$. Hence, contribution of diffuse layer to the saturation current is negligible compared to that of the base.

However, it has been shown recently (7) - (15), that in modern diodes, heavy doping in diffuse layer causes gap shrinkage which increases the thermal minority carrier concentration in the diffuse layer so much that it becomes comparable to or even exceeds that in the base. Since the ratio of the two minority carrier concentrations is constant, the concentrations of excess carriers will adjust themselves to maintain the ratio, which is an effect of coupling.

It has been reported recently (15) that p-n coupling affects open circuit voltage and short circuit current of a solar cell(with a heavily doped diffuse layer) in steady state.

Lindholm and Sah (17) have reported that p-n coupling can substantially affect the transient behaviour of a diode, so that it depends upon excess carrier life-time andi other material parameters of the emitter as well as the base. However their theory is based on too

simplified assumptions i.e. quasi state approximation and single lump charge control model.

As we shall see later (chapter 3), through a more rigorous theory that the effect of p—n coupling is to introduce a sharp, almost vertical drop in voltage in the initial stages of open circuit voltage decay. This drop is added to the vertical drop due to series resistance of the device. Hence to determine series resistance of a diode using OCVD data* one has to first separate the two drops. (A method is suggested in chapter 3* which also explains the anomalous dependence of series resistance on current as interpreted in (5)). It is also shown (in chapter 3) that an increase in the contribution from the diffuse layer to the reverse saturation current and decrease in diffuse layer minority carrier lifetime increases p-n coupling (i.e. Increases the initial vertical drop).

In case of reverse recovery transients also effect of P-n coupling is there. Kingston's (18) formulation* which neglects the diffuse layer contribution* predicts that calculated base minority carrier lifetime is independent of the reverse to forward current ratio at which the experiment 1B done. It is shown in chapter 4 through a rigorous theory that if p-n coupling

is substantial then Kingston*s formulation would give minority carrier lifetime dependent on the reverse to forward current ratio. Also the minority carrier lifetime calculated from Kingston's formulation will be less than the actual lifetime (i.e. the one calculated when p-n coupling effect is included). It is found that higher the coupling effect, more is the difference between the lifetimes thus calculated. In modern diodes and solar cells in which the diffuse layer is heavily doped, and p-n coupling is substantial, the calculated lifetimes may be different by almost an order of magnitude .

The effect of p-n coupling on the photo voltage decay (when the source of light is abruptly switched off) of a solar cell has not yet been fully analysed, because with the boundary conditions of solar cell it becomes difficult to handle the equations (15). However, the low time behaviour of photo voltage decay has been reported in (15) and it is shown that the p-n coupling can substantially affect the decay at small values of time. At large times the decay may not be substantially affected by p-n coupling (15).

Thus, it may be concluded that in modern diodes, (with heavily doped diffuse layer) because of gap shrinkage, the p-n coupling can substantially affect

steady state characteristics and transient response* However, when contribution from diffuse layer to the reverse saturation current is small, p-n coupling may be neglected.

4. Objective and Scope of the Present Investigation

The work reported in this thesis mainly deals with the measurement and analysis of solar cell properties. The aim is to analyse the existing methods with rigorous theories and introduce new interpretations wherever it is found necessary and also introduce new methods of measurement wherever it is suggested by theoretical analysis.

Apart from the studies of solar cells when exposed to various kinds of illuminations, it is also of interest to study the dark properties of solar cell3, since material parameters are the same; although the processes which are responsible for various phenomena may be different (as in case of OCVD and PVD). Comparison of the results obtained from two or more different methods may thus prove to be a starting point for further investigations and deeper understanding of the processes and phenomena involved. As discussed in the last section p-n coupling may substantially affect the response of

a solar cell or diode* whenever the contribution of diffuse layer is significant. A rigorous analysis of experimental data may in that case give some information about the diffuse layer. If the diffuse layer contribution is negligible then it may not be possible to extract much information about it from the experimental data. At the same time it may not be of much consequence because the contribution of diffuse layer is negligible.

In the present work transient response of p-n junction diode (OCVD and Reverse Recovery) has been analysed which includes the effect of p-n coupling. In case of solar cells the mathematics of transient response (photo voltage dec y) is quite complicated and no analytical solution has been reported in literature. Hence while studying the photo voltage decay we have neglected the diffuse layer contribution as given by the theory of Jain (20). The objective of studying photo voltage in this case is to compare it with the results of OCVD at moderately large (of the order of minority carrier lifetime in base) and large (more than the minority carrier lifetime in base) values of time. In a study conducted recently (19) the tiro methods are reported to have given different results

In all these investigations* we have neglected the saturation effects (arising at high injection for

junction voltage >/0.7 for silicon cell) and space charge effects which dominate at low junction voltages, viz. 0.4V (20).

Series resistance and shunt resistance of a solar cell directly affect its characteristics (13). An understanding of the dependence of these parameters on intensity is important for application purposes. In the present investigation, the studies have been made on low and moderate (about one suA) illumination level. Another objective is to compare the results obtained by steady state with those of (5) and our own analysis of OCVD (to determine the value of series resistance). Space charge effects have been neglected in this investigation also.

5. Summary of the work reported in this thesis

In this thesis we present theoretical and experimental investigations and analysis of p-n junction diodes and solar cells.

In chapter 1 a general introduction to this thesis is presented.

In chapter 2, we present experimental results and analysis of steady state measurements. The method

applied here makes use of the fact that when current passes through a forward biased diode, there is a linear region in the I-V characteristic, whose slope gives series resistance (4) and the intercept with I«0 axis of the (extrapolated) straight line gives the value of diffusion potential (4)• In the reverse bias condition, slope of the linear region determines shunt resistance of the device,

Mainly the effect of illumination level on series resistance and shunt resistance has been investigated. It is found that (within the experimental limits) series resistance and diffusion potential do not change when the illumination is changed from low to moderate (about 1 sun) levels, whereas shunt resistance of solar cell decreases with increase in the illumination level (for the same limits).

Chapter III presents a detailed theoretical analysis of a formula given by North (3) which describes the open circuit voltage decay of a p-n diode within low injection limits and includes the effect of p-n coupling. It is shown that the effect of p-n coupling is to introduce sharp, almost vertical initial drop in the open circuit voltage decay of a p-n junction diode. This drop is added to the vertical drop due to series resistance of the

device. In modern diodes (with heavily doped diffuse layer) this effect is particularly significant.

A method is suggested to separate the coupling drop from the total initial drop which exploits the fact that the drop due to series resistance is proportional to the current flowing through the device before it is switched off. When series resistance is determined by this method it is of the same order as obtained by steady state analysis. The analysis in this chapter also shows that the anomalous dependence of series resistance on current reported in (5) is due to misinterpretation.

A simpler form of North's formula (3) is also suggested in the same chapter which describes the open circuit voltage decay o[4] a p-n diode by a single representation prameter 'a' but is applicable in most cases. The method to fit this with experimental data to extract the value of minority carrier lifetime is described. However, it has not been possible to find a unique value of the representation parameter 'a* for a given experimental data.

Reverse recovery transients are discussed in chapter 4. The effect of p-n coupling is included in the theoretical calculation of the storage time by appropriately modifying the North's formula (3). It has been

brought to our attention that a similar formula has been recently derived by Jain (21). It is also shov.n/when that coupling is neglected, the formulation developed in this chapter reduces to that of Kinston (18). The effect of coupling is to change the dependence of reverse to forward current ratio on the storage time. It is shown that if the effect of coupling is not included, the calculated minority carrier lifetime (by Kingston's formulation (18)) may be much less than the correct value (calculated when the effect of p-n couplin is considered). Reverse Recovery experiments have been performed on some devices and the fitting of theory with the experimental results is shown.

In chapter 5. results of experimental studies on photo voltage decay are reported. Since it has not been possible to analyse fully the photo voltage decay of solar cell when the diffuse layer contribution is taken into account, the effect of p-n coupling is not considered here. It has been reported (15) that at large values of time, the PVD of a solar cell may not be strongly affected by p-n coupling. At small values of time it has not been possible for us to study PVD because of experimental limitations. It is shown that at moderate values of time, slope of PVD and OCVD is same for the same device, unlike the results reported in (19). We

also find by mathematical analysis that at large value of time, slope of PVD is almost independent of the wavelength of light which is also confirmed by our
J
experimental results. At moerate values of time, our experimental results of spectral dependence qualitatively agree with the theory proposed in (20). It is also shown that at moderate values of time, the slope of PVD is independent of the initial value of voltage (i.e. illumination level) except when space charge effects are dominant or saturation effects (due to high intensity) come in.

References

1. J.J. Loferski, "Photovoltaics IV;aAdvanced Materials", IEEE Spectrum, Vol. 17, No.2, p.37, 1980.

2. J.J. Loferski, "Photovoltaic I, Solar Cell Arrays", IEEE Spectrum, Vol. 17, No.2, p.26, 1980.

3. S.R. Lederhandler and L.J. Giacoletto, "Measurement of Minority Carrier Lifetime and Surface Effects in Junction Devices", Proc. IRE, Vol. 43, p.477, 1955.

4. B.R. Gossick, "On the Transient Behaviour of Semiconductor Rectifiers", J. Appl. Phys., Vol. 26, p.1356, 1955.

5. L.P. Hunter, Handbook of Semiconductor Electronics, New Yorki McGraw Hill# 1970.

6. Lindholm et. al "A methodology for experimentally based determination of gap shrinkage and effective lifetimes in the emitter and base of p-n junction solar cells and other p-n junction devices", IEEE Trans. Electron. Devices Vol. ED—24, p.402, 1977.

7. M.A. Shibib et. al., "Heavy Doped Transparent Emitter Regions in Junction Solar cells, Diodes, and Transistors", IEEE Trans. Electron Devices, Vol. ED-26, p.959, 1979.

References

1. J.J, Loferski, "Photovoltaics IV:aAdvanced Materials*, IEEE Spectrum, Vol. 17, No.2, p.37, 1980.

2. J.J. Loferski, "Photovoltaic I, Solar Cell Arrays", IEEE Spectrum, Vol. 17, No.2, p.26, 1980.

3. S.R. Lederhandler and L.J. Giacoletto, "Measurement of Minority Carrier Lifetime and Surface Effects in Junction Devices", Proc. IRE, Vol. 43, p.477, 1955.

4. B.R. Gossick, "On the Transient Behaviour of Semiconductor Rectifiers", J. Appl, Phys., Vol. 26, p.1356, 1955.

5. L.P. Hunter, Handbook of Semiconductor Electronics, New Yorki McGraw Hill, 1970.

6. Lindholm et. al "A methodology for experimentally based determination of gap shrinkage and effective lifetimes in the emitter and base of p-n junction solar cells and other p~n junction devices", IEEE Trans. Electron. Devices Vol. ED—24, p.402, 1977.

7. M.A. Shibib et. al., "Heavy Doped Transparent Emitter Regions in Junction Dolar cells, Diodes, and Transistors", IEEE Trans. Electron Devices, Vol. ED-26, p.959, 1979.

8. M.A. Shibib et. al., *Auger Recombination in Heavily Doped Shallow Emitter p-n Junction Solar Cells, Diodes, and Transistors, IEEE Trane. Electrons. Devices, Vol. ED—26, p.1104, 1979.

9. J.G. Fossum et. al., "The Importance of Surface Recombination and Energy Bandgap Narrowing in p-n Junction Silicon Solar Cells", IEEE Trans. Electron. Devices, Vol. ED-26, p.1294, 1979.

10. J.P. McKelvey, Solid state and Semiconductor Physics, New York i Harper & Row, 1966.

11. S.M. Sze, Physics of Semiconductor Devices, New York: John Wiley & Sons, 1969.

12. Yu. R. Nosov, Switching in Semiconductor Diodes, New York : Plenum Press, 1969.

13. H.J* Hovel, Solar Cells (Semiconductors and Semimetals Vol.ll)* New York : Academic Press, 1975.

14. Yu. R. Tkhorik, Transients in Pulsed Semiconductor Diodes, Jerusalem : Israel Program for Scientific Translations, 1968.

15. S.K. Sharma, A. Agarwala and V.K. Tewary, "Effect of p-n Coupling on Steady State and Transient Characteristics of a p-n Junction Solar Cells", To be published in J. Phys. E. (Appl. Phys.)

16. V.K. Tewary and S.C. Jain, J. Phys. D. (Appl. Phys.), Vol. 13, p.835, 1980.

17. F.A. Lindholm and C.T. Sah, "Normal Modes of Semiconductor p-n Junction Devices for Material Parameter Determination", J. Appl. Phys. Vol.47, p.4203, 1976.

18. R.H. Kingston, "Switching time in Junction Diodes and Junction Transistors", Proc. IRE, Vol. 42, p.829, 1955.

19. J.E. Mahan et. al., "Measurement of Minority carrier Lifetime in Solar Cells from Photo Induced Open Circuit Voltage Decay", IEEE Trans. Electron Devices, Vol.ED-26, p.733, 1979.

20. S.C. Jain, "Theory of Photo Induced Open Circuit Voltage Decay in a Solar Cell", Technical Report (1980), Solid Stat Physics Laboratory, Delhi.

21. S.C. Jain, Private Communication .

TA9LS 1.1

Photovoltaic solar cells with efficiency of 5% or more

Type of Cell	Semiconductor Constituents	Highest Efficiency (Air yass 1 Condition). Percent
Homojunction	Silicon	18
Homojunction	Gallium arsenide	22
Homojunction	Indium phosphide	6
Heterojunction	pCu_2S/nSi	5
Heteroj unction	plnP/nCdS	14
Homojunction heterostructure	Al Ga As GaAs	18
MIS*.	Silicon	12
MIS	Gallium Arsenide	15
SIS+	Indium tin oxide/silicon	12
SIS	Tin oxide/silicon	12
Heterojunction	pCdTe/nCdS	8
Schottky barrier	wse_2	5
Polycrystalline	Silicon	8
Th in-f iln/thin-f ilm Heterojunction	pCu, S/nCds	9
Thin-rilm heterojunction	pCUgTe/nCdS	6
Thin-film amprphous semiconductor, Schottky Barrie i"	Silicon	6

*Metal-insulator semiconductor cell

Semiconductor-insulator semiconductor cell

Figure Captions

Fig. 1.1 Percentage theoretical maximum efficiency shown as a function of energy gap (eV).

Fig. 1.2 Geometry and notational usage for the p-n junction photo-voltaic cell (10).

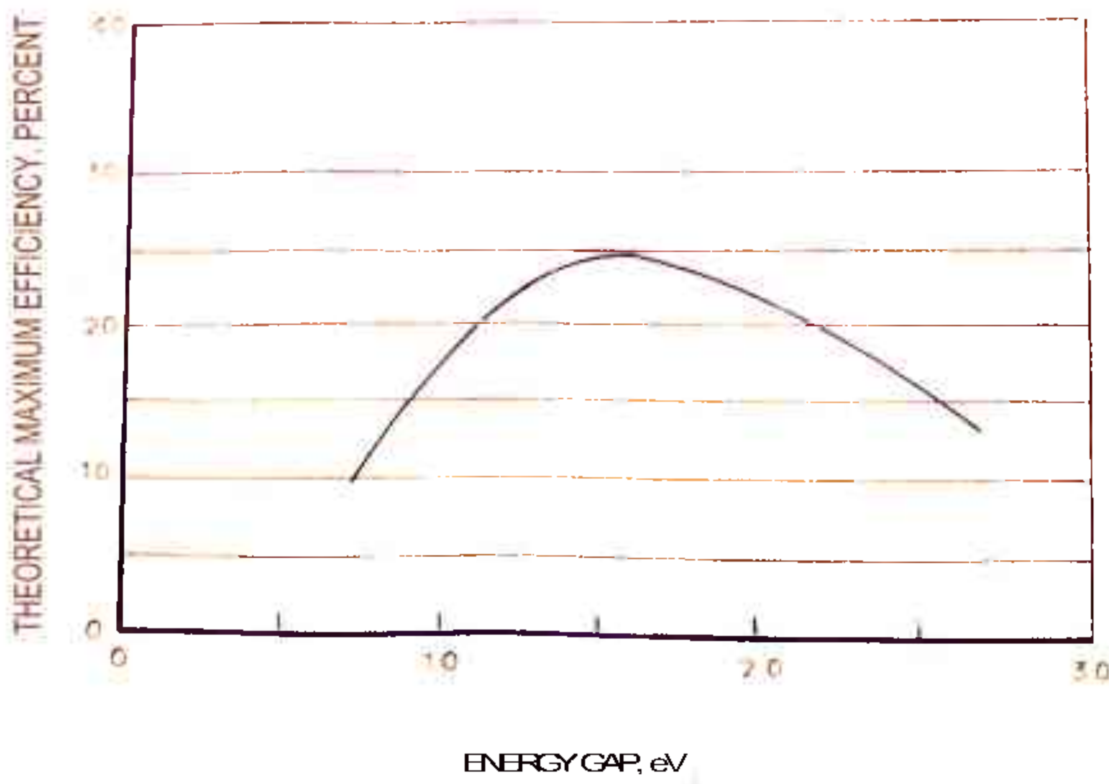

FIG. 1.1

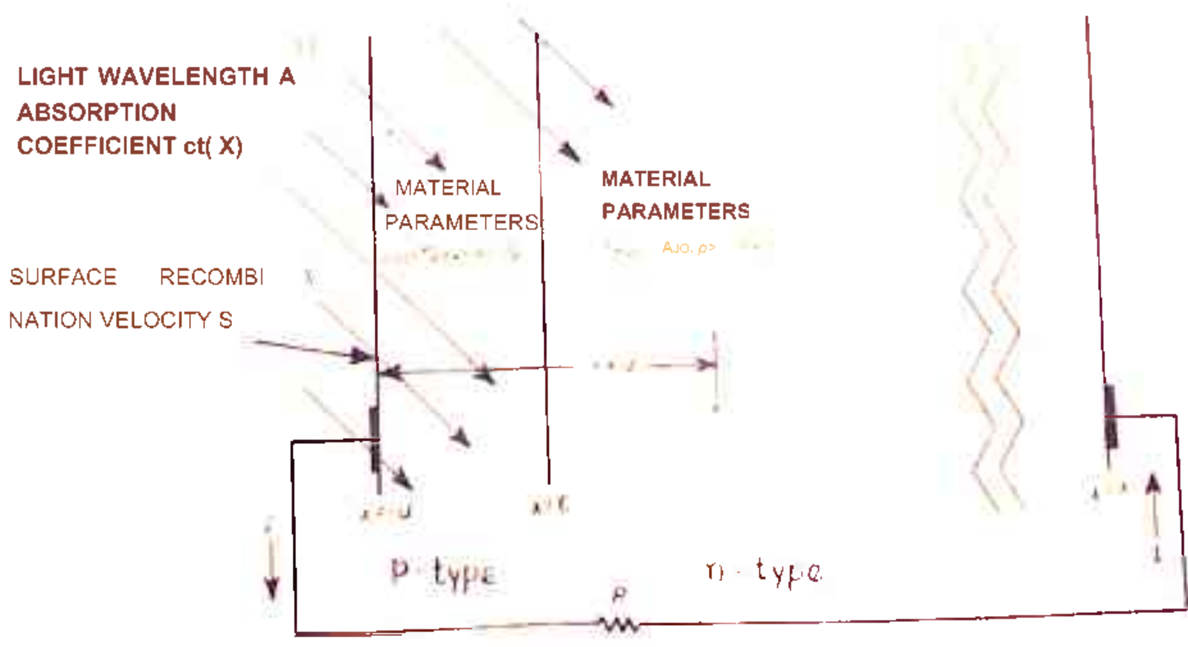

FIG.1.2

CHAPTER II

STEADY STATE MEASUREMENTS AND ANALYSIS

CHAPTER II

STEADY STATE MEASUREMENT AND ANALYSIS

1. Introduction

Direct current methods have been used very widely (1) - (6) to determine the parameters like series resistance, shunt resistance, diffusion length, efficiency etc., of a solar cell. These are perhaps the simplest methods (compared to OCVD, reverse recovery, etc.) to determine the properties of solar cells.

A method, based on I-V characteristic of a solar cell, has been developed in our laboratory, to measure series resistance, shunt resistance, diffusion potential and in principle saturation current also. The advantage of this method is that it can be used to study the dependence of these parameters on intensity level and wavelength of the light. This method makes use of the fact that when current passes through a forward biased diode, there is a linear region in the I-V characteristic, whose slope gives the series resistance (7)• The intercept on I = 0 axis of the (extrapolated) straight line gives the value of diffusion potential (7), Similarly, in the reverse biased condition the slope of the linear region can be used to determine shunt resistance and intercept on V = 0 axis gives saturation current.

It has been experimentally observed (7) that there is a linear region in forward characteristic of a diode; however this result is yet to be understood theoretically.

In the next chapter wd shall show that series resistance can also be determineitby open circuit voltage decay method. An analysis of the theory and experimental results of the OCVD is also given there and it is shown that series resistance of a diode does not seem to have the kind of dependence as reported in (8). The results of the method given in this chapter corroborate our analysis of OCVD.

In the next section of this chapter, a theoretical analysis of the I-V chatacteristic of solar cells based on the boundary condition given by Dhariwal et. al. (9) is presented.

Details of experimental measurements and results are given in sec. 3. In sec. 4 an analysis of these results has been presented.

2. Theory

2.1 I-v Characteristic of an Ideal Diode

Consider a diode with its junction at x = 0, p-side extending from $x = -\infty$ to x = 0 and n-side from x « 0 to $x = \infty$.

The transport equations in the linear approximation in steady state are as follows:

$$D_n \frac{d^2 n(x)}{dx^2} - \frac{n(x)}{\tau_n} = 0 \qquad (-\infty < x \leq 0) \qquad (2.1)$$

$$D_p \frac{d^2 p(x)}{dx^2} - \frac{p(x)}{\tau_p} = 0 \qquad (0 \leq x < \infty) \qquad (2.2)$$

where n(x) and p(x) are carrier concentrations, as function of excess minority carriers, D_n and D_p are diffusion coefficients, τ_n and τ_p lifetimes of minority carriers on p-side and n-side respectively.

The boundary conditions (9) for the above differential equations are as follows:

$$n(-\infty) = p(\infty) = 0 \qquad (2.3)$$

which corresponds to ohmic contact at the front and back surface, and

$$n(0) = \frac{n_{po} + p_{no} \exp[-q(V_D - V)/kT] \, [\exp(qV/kT) - 1]}{1 - \exp[-2q(V_D - V)/kT]} \qquad (2.4)$$

$$p(0) = \frac{p_{no} + n_{po} \exp[-q(V_D - V)/kT] \, [\exp(qV/kT) - 1]}{1 - \exp[-2q(V_D - V)/kT]} \qquad (2.5)$$

where n(o) and p(o) are excess minority carrier concentrations on the p and n-side of the junction respectively, V_D is the diffusion potential, v is the applied voltage.

n_{po} and p_{no} are the thermal equilibrium values of minority carriers on p and n-side respectively, k is the Boltzman constant and T is the temperature in Kelvins.

The solutions of eq.(2,1) and (2.2) are then, as given below (1)

$$n(x) = n(o) \exp (x/L_n) \qquad (2.6)$$

$$p(n) = p(o) \exp (-x/L_p) \qquad (2.7)$$

where $$L_n^2 = D_n C_n \text{ and } L_p^2 = D_p C_p \qquad (2.8)$$

L_n and L_p are diffusion lengths of minority carriers,

The flux through the junction is given by(1)

$$J = -D_n \frac{dn(o)}{dx} - D_p \frac{dp(o)}{dx} \qquad (2.9)$$

or $$J = (D_n/L_n)\, n(o) - (D_p/L_p)\, p(o) \qquad (2.10)$$

or $$J = \frac{(J_{no}^* + J_{po}^*)\,[\exp(qV/kT)-1]}{1-\exp\{-2q(V_D-V)/kT\}} \qquad (2.11)$$

where J_{no}^* and J_{po}^* are the effective saturation currents given by

$$J_{no}^* = J_{no}\left[1+(p_{no}/n_{po}) \exp \{-q(V_D-V)/kT\}\right] \qquad (2.12)$$

$$J_{po}^* = J_{po}\left[1+(n_{po}/p_{no}) \exp \{-q(V_D-V)/kT\}\right] \qquad (2.13)$$

where J_{no} and J_{po} are the conventional (Shockley) saturation currents (1), defined as

$$J_{no} = \frac{D_n \, n_{po}}{L_n} ; \quad J_{po} = \frac{D_p \, p_{no}}{L_p} \tag{2.14}$$

The total effective and Shockley saturation currents are defined as

$$J_o^* = J_{no}^* + J_{po}^* \text{ and } J_o = J_{no} + J_{po} \tag{2.15}$$

Eq. (2.11) gives the value of currents for an applied voltage V. To obtain the value of V for a given current we note that Eq.(2.11) is a quadratic equation in exp(qV/kT). The solution of this equation is as follows:

$$\exp\left[-q(V_D-V)/kT\right] = \frac{2(J+J_o)}{\left[(J_oC - J_o)^2 + 4(J_oC + J)(J+J_o^*)\right]^{\frac{1}{2}} + (J_oC-J_o^*)} \tag{2.16}$$

where $C = \exp(qV_D/kT)$ and $J_o^* = J_{no}(n_{no}/n_{po}) + J_{po}(p_{po}/p_{no})$ (2.17)

since C is quite large (about exp(40), a good approximation for Eq.(2.16) is the following:

$$\exp\left[-q(V_D-V)/kT\right] \simeq \frac{2(J+J_o)}{\left[J_o^2C^2+4J(J+J_o^*)C\right]^{\frac{1}{2}} + J_oC} \tag{2.18}$$

Eq. (2.18) gives the general I-V characteristic of a p-n

junction diode which is valid at all injection levels.

In the low injection limit J is much less than $J_Q C$ and $J'C_o$. In this limit eq.(2.18) reduces to conventional Shockley I-V characteristic as given below:

$$\exp\left[-q(V_D - V)/kT\right] = \frac{2(J+J_Q)}{2J_o C} \tag{2.19}$$

$$\text{or } V = \ln\left(\frac{kT}{q} J/J_o\right) \tag{2.20}$$

In the high injection limit when J tends to infinity, we notice that the right hand side of eq.(2.18) becomes unity. Hence

$$V = V_D \quad (\text{ for J tending to infinity}) \tag{2.21}$$

Thus we see that at low injection levels, V depends logarithmically on J as in eq.(2.20) in accordance with Shockley formula. At very high injection levels, V saturates and becomes equal to. the diffusion potential as shown by eq. (2.21)•

2.2 Effect of R_s and R_{sh} on the I-V characteristic of a diode

In the analysis given above it is assumed that the whole of the applied voltage acts at the junction which implies that the resistance of the material is zero everywhere except at the junction where it is infinite. But in

real cases this idealisation cannot be achieved. This is because the carriers in the material are not totally free and the region close to the junction is not totally devoid of free charges. The resistance of the material away from the junction manifests as series resistance R_s of the device whereas the finite resistance of the material in the region close to the junction (space charge layer) is called the shunt resistance R_{sh}. An ideal p-n device has $R_s = 0$ and $R_{sn} = \infty$. A real device is modelled (1), (10) as shown in Fig. 2.1 in which V_1 and V_2 are external terminals of the device.

If a current I flows in the forward direction, the total voltage across the device will be that across the resistance R_s and that across the ideal diode. The later is given by the ideal diode law as derived in eq. (2.18). If V_T is the applied voltage, then

$$V_{rf} = I + VR_s \tag{2.22}$$

where V is the voltage drop across the ideal diode D. In the forward bias case the current I through the device is quite large so that the effect of the high parallel resistance R_{sh} is negligible. In the high injection case V will approach V_D in accordance with eq.(2.21), but the IR_s term will keep increasing linearly with I. Thus the curve of V_T plotted with respect to I will show some initial curvature and will then become a straight line. The slope

of the straight line, i.e., the linear portion of the curve will give R_s and its intercept with I=0 axis will give V^, the diffusion potential.

In case of reverse bias since J is very small. eq.(2.18) reduces to the Shockley equation (2.20)

$$J = J_o \left[\exp (qV/kT) - 1 \right] \qquad (2.23)$$

where V is negative. For large negative values of V, the exponential term is negligible and

$$J \approx -J_o \qquad (2.24)$$

which shows that maximum current which can flow in the reverse direction under a reverse bias voltage in an ideal diode (R_{sh} = ∞) is equal to the saturation current. This current is independent of the applied voltage.

However in a real diode R_{sh} , is not infinite and therefore some current will flow through R_{sh}. If a large reverse bias voltage V is applied then the current flowing through the circuit I is given by

$$I = I_o + V/R_{sh} \qquad (2.25)$$

where I_o ($=qJ_o$) is the saturation current. Since R_{sh} is large, the effect of R_s in this case is negligible. We see from eq.(2.25) that for large reverse bias voltage, I increases linearly with V (after an initial curvature). The

slop<of the linear portion is given by $1/R_{gh}$ and its intercept with V = 0 axis gives I_Q.

2.3 I-V characteristic of a solar cell

It has been described (1), (10) that in case of solar cells, the diode I-V characteristic will be shifted down by I_g (generation current which is directly proportional to the light intensity falling on the cell). Hence the slope in the forward charactefistic and reverse characteristic would still determine R_S and a R_{sh} respectively. But the advantage here is that the effect of radiation intensity and wavelength on R_g and R_{gh} can be studied by taking solar cell I-V characteristic under such conditions.

3. Experimental Study

An SC4yl cm x 1 cm solar cell supplied by Plessey (England) was used for the experimental studies. A KEIC, japan, 1000W, 250V projector lamp was used as a light source. This is expected to give good uniformity in intensity throughout the exposed area of solar cell (used in present investigations) even when the lamp is very close to the cell# because of the filament shape.

The cell was fixed on a mount made of brass. The mount was designed to allow water circulation (at a high rate) to dissipate heat so that temperature of the cell

could be kept constant. A cover with a square opening, to expose only the required area has been placed between the lamp and the cell. With this simple care, it was possible to avoid heating of the mount. The rise in temperature thus has been controlled to less than 1°C throughout the experiment.

To keep the voltage across the lamp constant, a NELCO (India) servo control voltage stablizer has been used, which regulates the voltage within + 1% of the set voltage.

Since wires longer than 1 meter have been used to take connections from solar cell to rest of the circuit (measurement set up), a four terminal network was used to ensure accurate measurement of voltage across the cell. This is illustrated in fig. 2.2 where the terminals V_1 and V_2 are used to measure voltage across the cell. Voltage across 1standard resistor (0.005*4)« supplied by OSAW (India) was measured to determine the current passing through the cell. All voltages were measured by an APLAB (India) Digital Multimeter (4>; digits, + 0.05% for de voltage measurements + 1 digit) Model 1005, which has a resolution of 10 Al V on the lovzest range of DC voltage measurements and has an input impedence of 11.1 M ohms on all dc voltage measurement ranges. To apply dc voltage, externally, on cell, an APLAB Regulated DC Power Supply Model 7211 was used.

To make measurements at various intensities Neutral Density filters were used and/or distance of the light source from the cell was varied to adjust the short circuit current. All measurements were made at room temperature ($\sim$20°C) •

Fig. 2.3 and 2.4 give the Dark forward and reverse I-V characteristics respectively of the cell. Since in the dark reverse characteristic current is very small a known high resistance was put in the circuit and voltage across the high resistance was measured to find the value of current in the circuit. Fig. 2.5 to 2.16 give the characteristics of the same cell at different intensities of light.

To study the effect of wavelength on characteristics, interference filters were used to get monochromatic light. Two filters (max at 590 and 690 nm) have been employed in the present study, other filters could not be used due to experimental difficulties. Fig. 2.17 to 2.22 present the results of these studies.

In later part of this thesis we shall be using a silicon diode BY127 and a Germanium Diode DR25, both made by BEL (India), for some studies. Fig. 2.23 and 2.24 present there forward characteristics and fig.- 2.25 and 2.26 show their reverse characteristic respectively. In case of these two devices, however no attempt was made to keep the temperature constant.

A discussion of the above results is presented in the next section.

4. Analysis of Results

Table 2.1 summarises the results obtained from the analysis of dark characteristics and white light characteristics of solar cell.

Table 2.2 summarises the results of steady state analysis of the Plessey solar cell when used with interference filters.

It can be seen that the measured value of diffusion potential (v^) remains constant (within the experimental errors)• Similarly no consistent variation is seen in the measured value of R_s either with the change in light intensity or with the wavelength of light^ R_s may change with intensity and wavelength because of the following reasons t

1. Because of the change in carrier concentration (due to light intensity) conductivity of bulk material is affected.

2. Since there is a finite value of R_s , there will be voltage drop in bulk giving rise to electric field which may accelerate or deccelerate carriers, which in turn will change the current flowing through the device and hence the effective value of R_s.

3. With the change in the wavelength of light, absorption coefficient of the material changes, which will change the spatial distribution of the carriers in cell. This in turn may change the current passing through the device and hence a change in the effective value of R_s may be there.

However, the experimental and analytical errors may over take these effects (as outlined above) and thus no consistent changes in R_s have been observed.

The value of R_{sh} is found to decrease with increase in the light intensity.

5. Conclusion

1. The diode current voltage relation, valid at all injection levels is given by eq. (2.18) which reduces to the Shockley equation at low injection levels. In high injection case, the voltage across the junction will saturate at the value of diffusion potential. Hence in this region, slope of the I-V characteristics will determine the series resistance of the diode and the intercept of the straight line with I » 0 will give the value of diffusion potential. Similarly in case of reverse bias, the slope will determine the shunt resistance and the intercept at V « 0 will give the value of reverse saturation current.

2. The values of series resistance and diffusion potential thus determined# when the solar cell is exposed to light also# are found to remain same (in the experimental limits) in the present investigation when the light intensity is varied. The shunt resistance of solar cell is found to decrease with increase in light intensity. A summary of results is presented in Table 2.1 and 2.2.

The results of the series resistance measurements reported in this chapter show that the large variation of series resistance with current reported in (8) may be due to misinterpretation. In the next chapter we show that the same results when interpreted including the p-n coupling effect, give a more acceptable value of series resistance.

References

1. J.P. Mckelvey, Solid State and Semiconductor Physics, New York* Harper & Row, 1966,

2. V.M. Evdokimov, "Calculation of Series and Shunt Resistances on the Basis of the Volt Ampere Characteristics of a Solar Cell", Applied Solar Energy, Vol. 8, p.63, 1971.

3. M. wolf and H. Ra.'schenbach, "Series Resistance Effects on Solar Cell Measurements", Applied Energy Conversion, Vol. 3, p.455, 1963.

4. M.B. Prince, "Silicon Solar Energy Converters", Journal of Applied Physics, Vol. 25, p.676, 1954.

5. M.S. Imamura and J.I. Port scheller, "An evaluation of the methods of determining solar cell series resistance". The conference record of the eigth IEEE Photovoltaic Specialists Conference, p.102, 1970.

6. Loferski, J. J.# and J.J. Wysocki, "Spectral Response of Photovoltaic Cells", RCA Rev., Vol.22, p.38, 1961.

7. B.R. Gossick, "On the Transient Behaviour of Semiconductor Rectifiers", J. Appl. Phys, Vol.26, p.1356, 1955.

8. L.P. Hunter, Handbook of Semiconductor Electronics, New York i McGraw Hill, 1970.

9. S.R. Dhariwal et. al. "Saturation of Photovoltage and Photocurrent in p-n junction solar cells", IEEE Trans. Electron Devices, Vol. ED-23, p.5O4, 1976.

10. S.M. Sze, Physics of Semiconductor Devices, New York i Wiley-Interscience, 1969.

Table 2.1

Summary of results obtained by steady state analysis using white light

S. No.	Fig. No.	Device	I_{sc} (mA)	R_s (ohms)	R_{sh} (K.ohms)	V_D (Volts)	I_o (μA)
1.	2.3	Solar Cell (SC4)	-	0.78	•	0.72	*
2.	2.4	"	-	-	172	-	1.0
3.	2.5	"	2.00	0.75	-	0.72	-
4.	2.6	"	2.05	-	74	-	-
5.	2.8	"	4.97	0.74	-	0.72	-
6.	2.9	"	4.97	-	57	-	-
7.	2.11	"	10.10	0.78	-	0.70	-
8.	2.12	"	10.20	-	34	-	-
9.	2.14	"	25.70	0.72	-	0.71	-
10.	2.15	"	25.70	-	18	-	•
11.	2.23	Silicon Diode (BY 127)	-	0.10	-	0.79	•
12.	2.24	Germanium Diode (DR25)	-	0.38	-	0.33	-
13.	2.25	Silicon Diode (BY 127)	-	-	3.3×10^{6}	-	1.5×10^{-3}
14.	2.26	Germanium Diode (DR 25)	-	-	2.2×10^{5}	-	0.64

Table 2.2

Summary of results of steady state analysis of the solar cell when used with interference filters.

S. NO.	Fig. No.	Filter A max (nm)	I_{sc} (mA)	R_s (ohms)	R_{sh} (K. ohms)	V_O (Volts
1.	2.17	590	2.03	0.75		0.72
2.	2.18	590	2.02	-	75	-
3.	2.20	690	2.02	0,76	c	0.72
4.	2.21	690	2.02	-	79	-

Figure captions

Fig. 2.1 Circuit model of a practical diode. D is an ideal diode, R_s is the series resistance and R_{sh} is the shunt resistance of the practical diode.

Fig. 2.2 The circuit for I-V characteristic measurements. To measure voltage across the cell terminals and V_1 are used. Current through the cell is measured by measuring voltage appearing on 1 ohm standard resistor.

Fig. 2.3 Dark forward I-V characteristic of the SC4 (Plessey) Solar Cell. Intercept with I=0 axis is 0.72V and slope of the linear region is 0.78 ohms.

Fig. 2.4 Dark reverse I-V characteristic of SC4 (Plessey) Solar Cell. Intercept with V = 0 axis is 1 microampere and slope of the linear region gives R_{sh} = 172 K ohm.

Fig. 2.5 Forward I-V characteristic of SC4 under white light (adjusted for I_{sc} » 2.00 mA) Intercept with I=0 axis gives 0.72V and slope of the linear region gives 0.75 ohm.

Fig. 2.6 Reverse I-V characteristic of SC4 under white light (adjusted for I_{sc} » 2.05 mA). R_{sh} ^eterm;*_n®3 from the linear region is 74 K ohms.

Fig. 2.7 I-V characteristic of SC4 solar cell under white light (adjusted for I_{sc} = 2.03 mA)

Fig. 2.8 Forward I-V characteristic of SC4 under white light (adjusted for I_{sc} ■ 4.97 mA) sl-op c. of the linear region is 0.74 ohm and the interdept of the straight line with 1=0 axis is 0.72 V.

Fig. 2.9 Reverse I-V characteristic of SC4 under white light (adjusted for I_{sc} = 4.97 mA) R_{sh} determined from slope of the linear region is 57 K ohms.

Fig. 2.10 I-V characteristic of SC4 under white light (adjusted for I_{sc} « 4.97 mA).

Fig. 2.11 Forward I-V characteristic of SC4 under white light (adjusted for I_{sc} =10.1 mA) slope of the linear region is 0.78 ohms and intercept of the straight line with 1 = 0 axis is 0.70V.

Fig. :2.12 Reverse I-V characteristic of SC4 under white light (adjusted for I_{sc} =10.1 mA) R_{sh} determined from the linear region is 34 K ohms.

Fig. :?.13 I-V characteristic of SC4 under white light (adjusted for I « 8 0 10.1 mA)

Fig. 2.14 Forward I-V characteristic of SC4 under white light (adjusted for I_{sc} = 25.7 mA) Slope of the linear region is 0.72 ohms and intercept of the straight line with I=0 axis is 0.71 Volts.

Fig. 2.15 Reverse I-V characteristic of SC4 under white light (adjusted for I_{sc} » 25.7 mA) R_{sh} determined from the slope of the linear region is 18 K ohms.

Fig. 2.16 I-V characteristic of SC4 under white light (adjusted for I_{sc} « 25.7 mA).

Fig. 2.17 Forward I-V characteristic of SC4 under light of max « 590 nm, (adjusted for I_{sc} = 2.03 mA). Slope of the linear region is 0.75 ohms and intercept of the straight line with I=0 axis is 0.72 Volts.

Fig. 2.18 Reverse I-V characteristic of SC4 under light of X max «= 590 nm (adjusted for I_{sc} « 2.02 mA). R_{sh} determined from the slope of the linear region is 75 K ohms.

Fig. 2.19 I-V characteristic of SC4 under light of X max e 590 nm (adjusted for I_{sc} « 2.03 mA).

Fig. 2.20 Forward I-V characteristic of SC4 under light of A max « 690 nm (adjusted for I_{sc} « 2.02 mA),

Slope of the linear region is 0.76 ohms and intercept of the straight line with I=0 axis is 0.72V.

Fig. 2.21 Reverse I-V characteristic of SC4 under light of λ max = 690 nm (adjusted for I_{sc}=2.02 mA). R_{sh} determined from the slope of the linear region is 79 K ohms.

Fig. 2.22 I-V characteristic of SC4 under light of λ max = 690 nm (adjusted for I_{sc} = 2.10 mA).

Fig. 2.23 Dark forward I-V characteristic of BY 127 (silicon diode). Slope of the linear region is 0.1 ohm and intercept with I=0 axis is 0.79 Volt.

Fig. 2.24 Dark forward I-V characteristic of DR25 (Germanium Diode). Slope of the linear region is 0.38 ohms and intercept with I=0 axis is 0.33 Volts.

Fig. 2.25 Dark reverse I-V characteristic of BY 127 (silicon diode). R_{sh} determined from the slope of the linear region is 3.3×10^{9} ohms and intercept with V = 0 axis is 1.5 nA.

Fig. 2.26 Dark reverse characteristic of DR 25 (Germanium diode). R_{sh} determined from the slope of the linear region is 2.2×10^{6} ohms and intercept with V=0 axis is 0.64 microamperes.

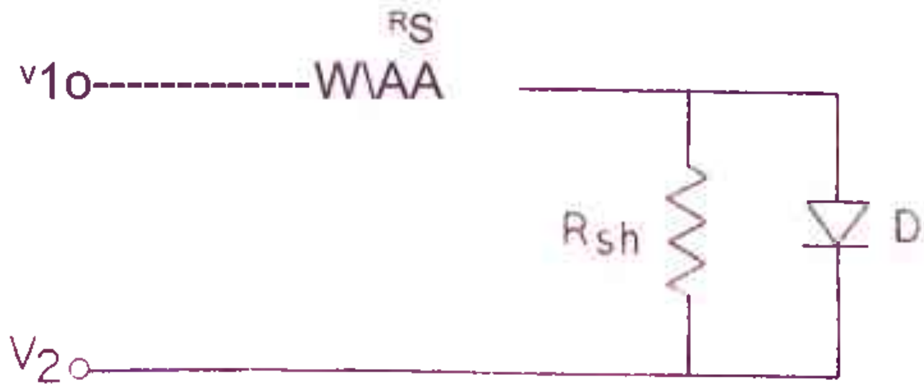

FIG. 2.1

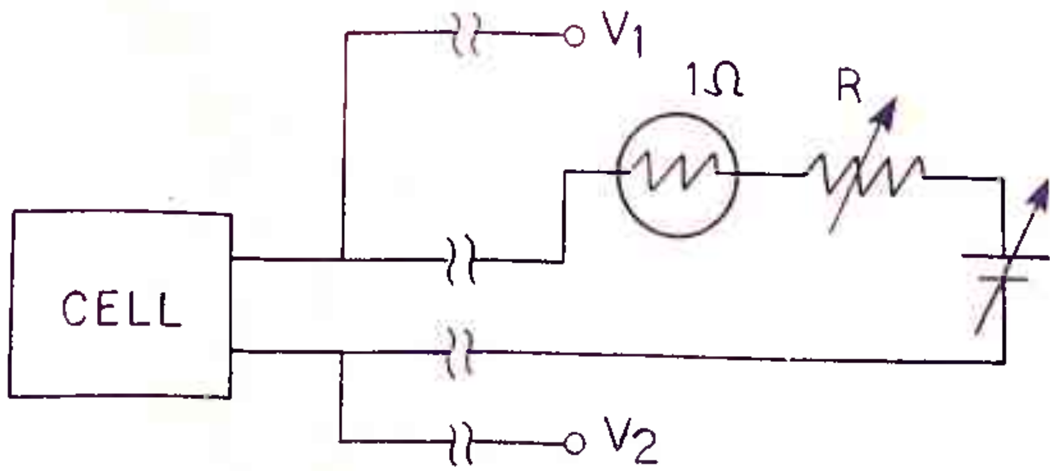

FIG. 2.2

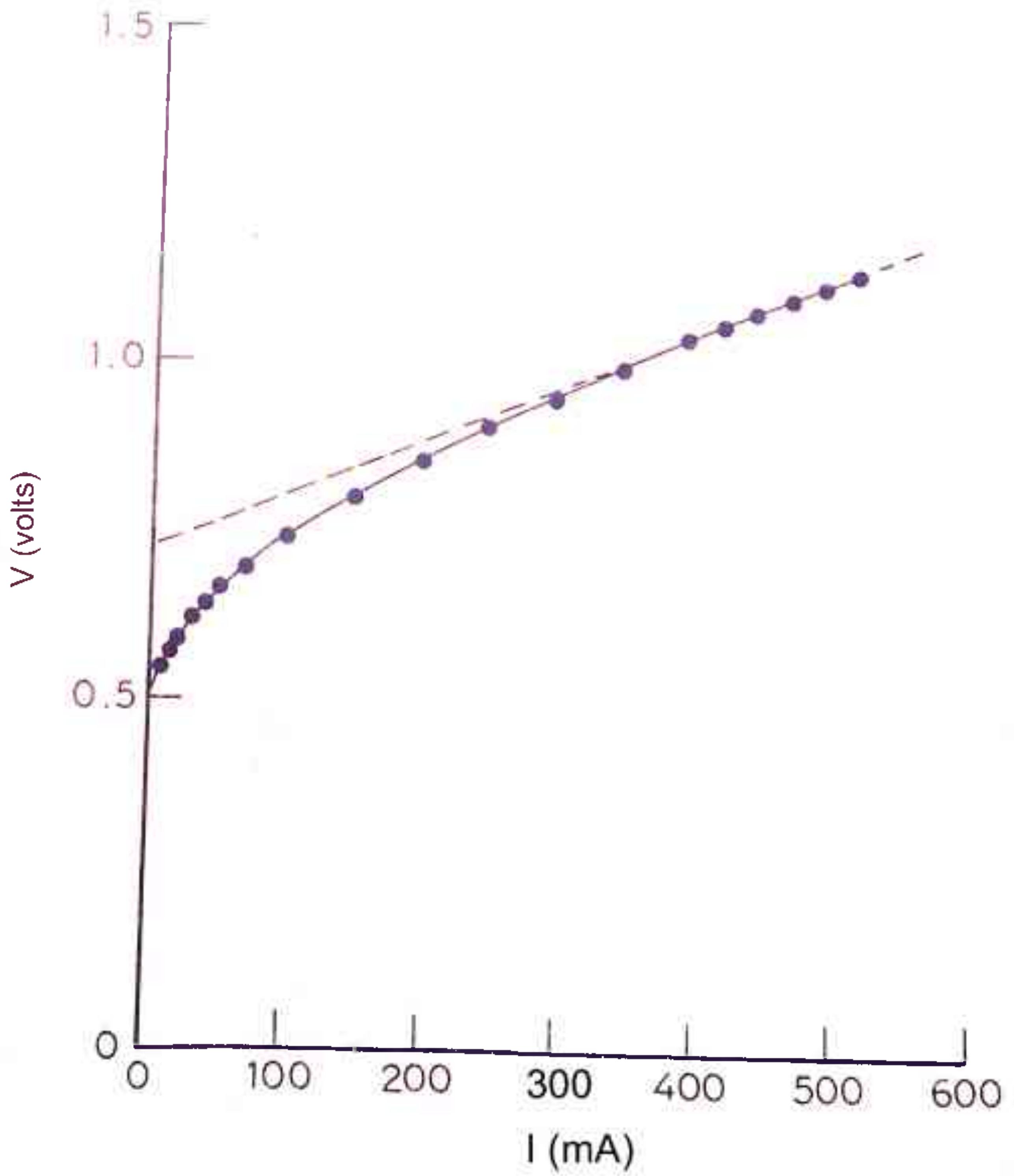

FIG. 2.3

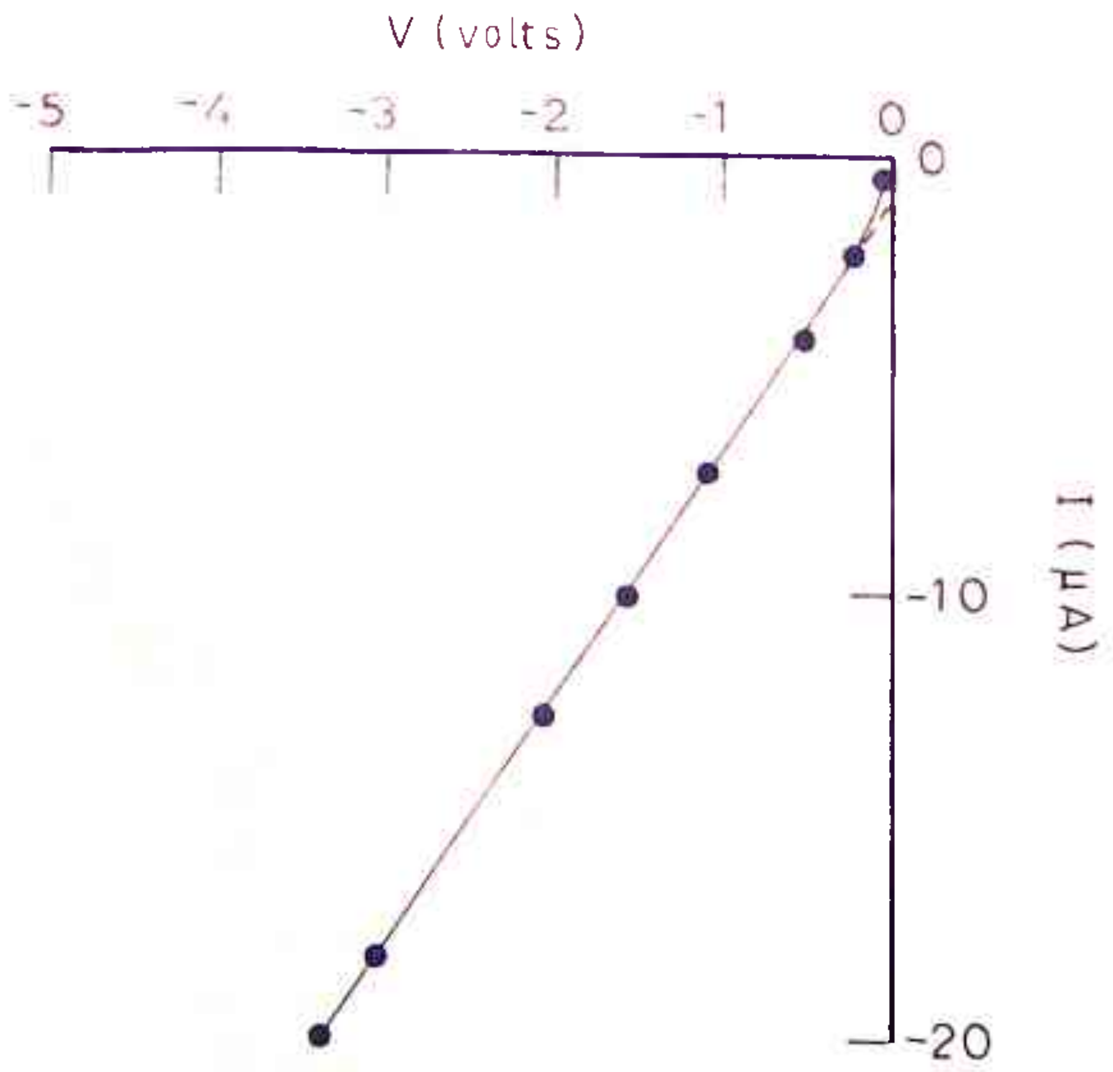

FIG. 2.4

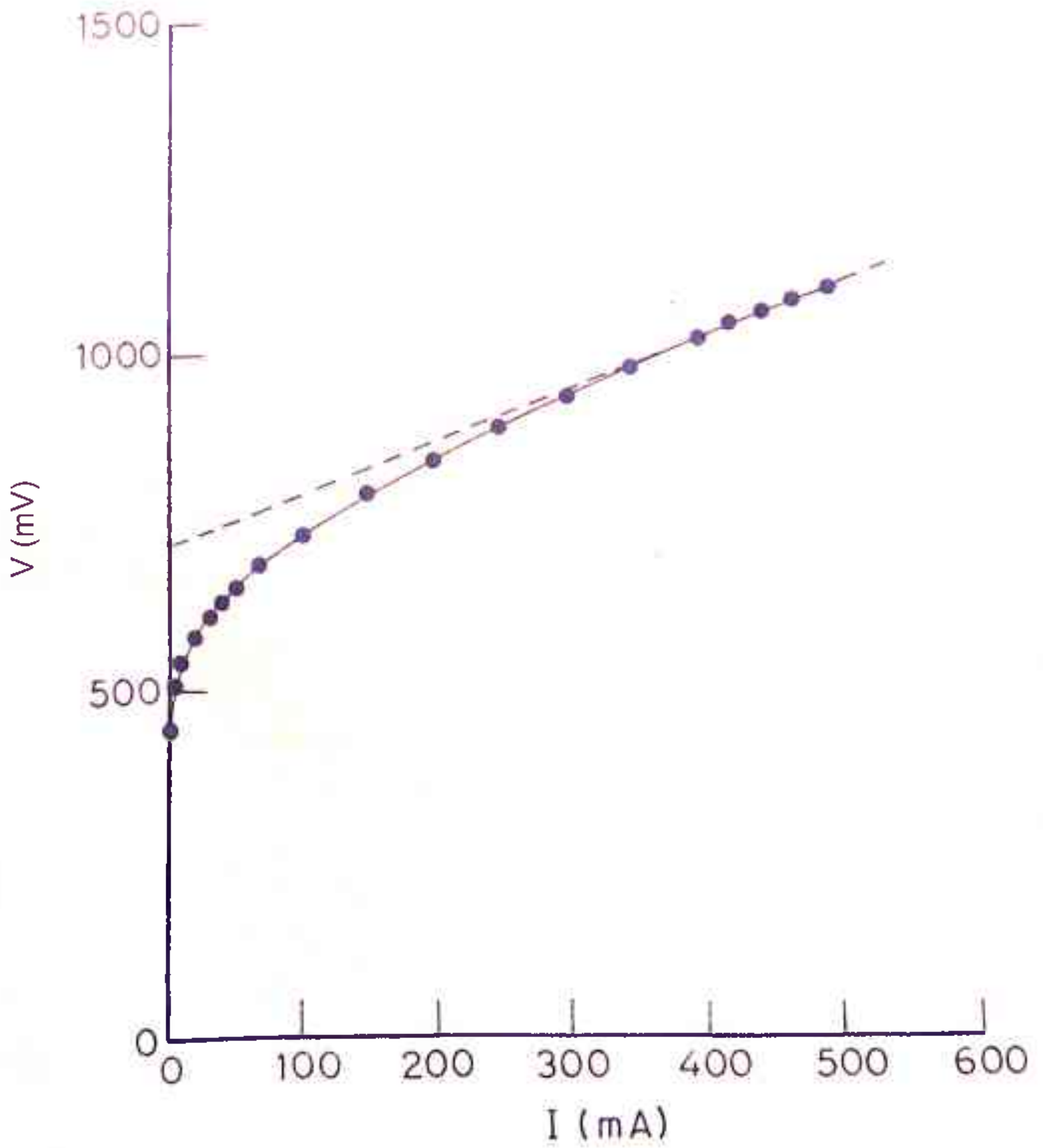

FIG.2.5

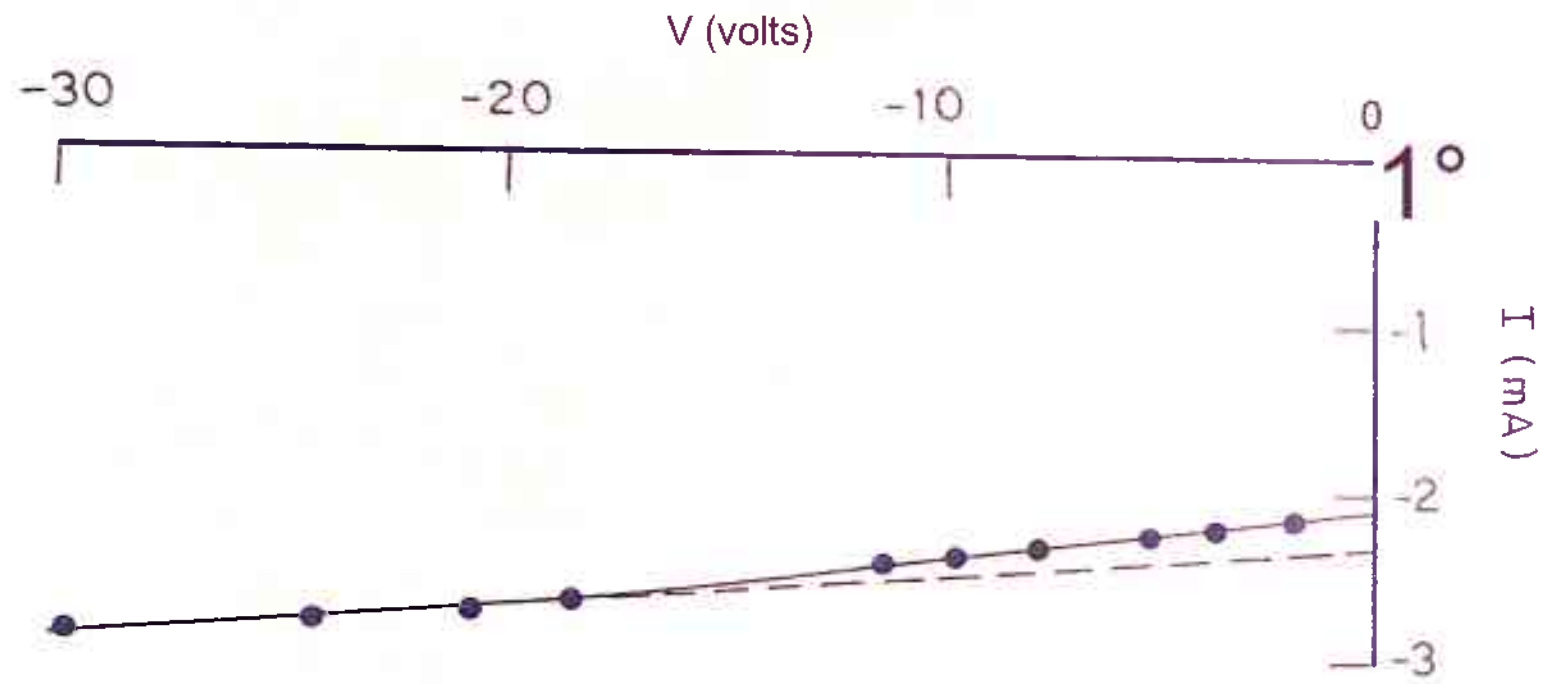

FIG.2.6

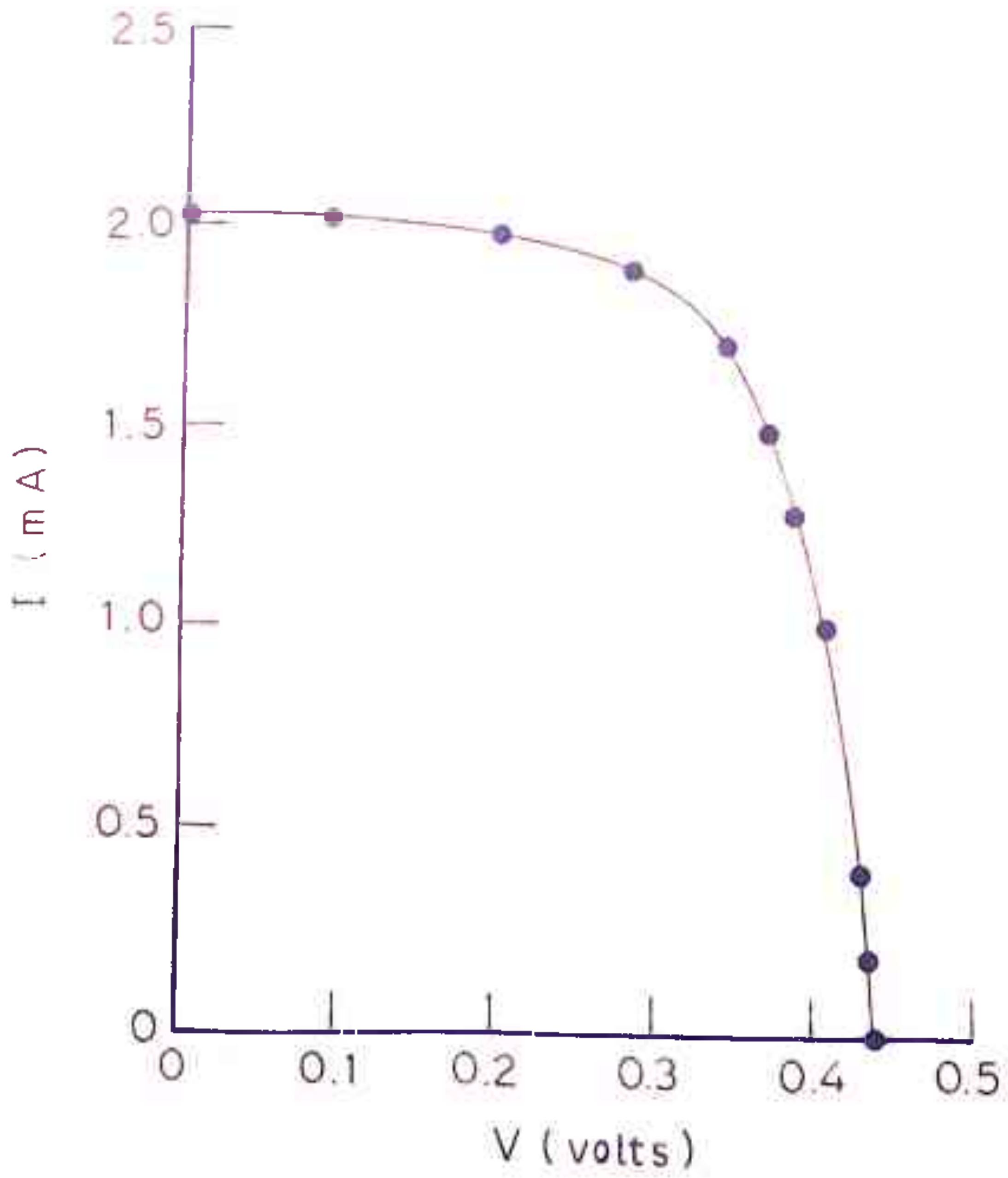

FIG. 2.7

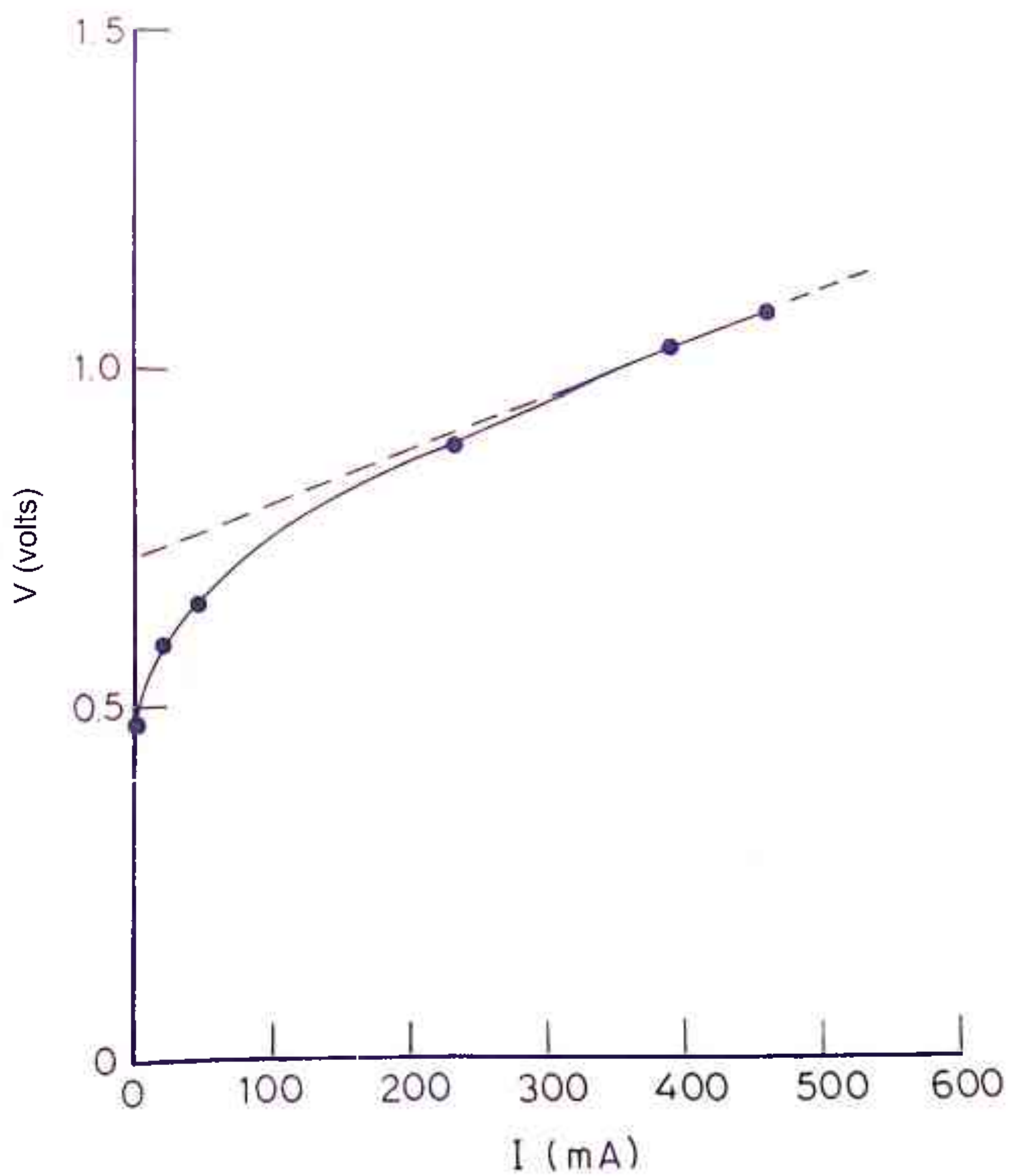

FIG. 2.8

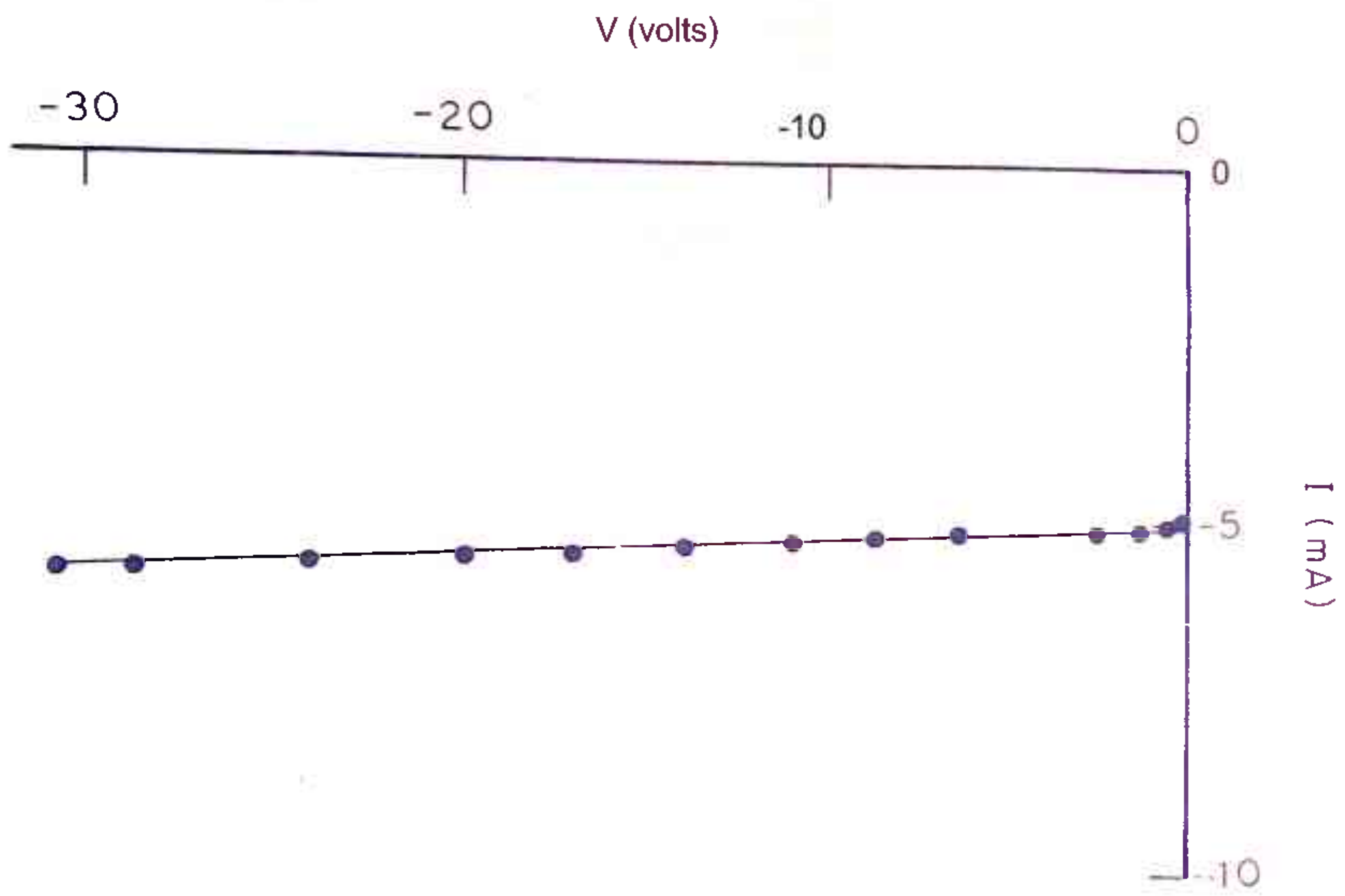

FIG. 2.9

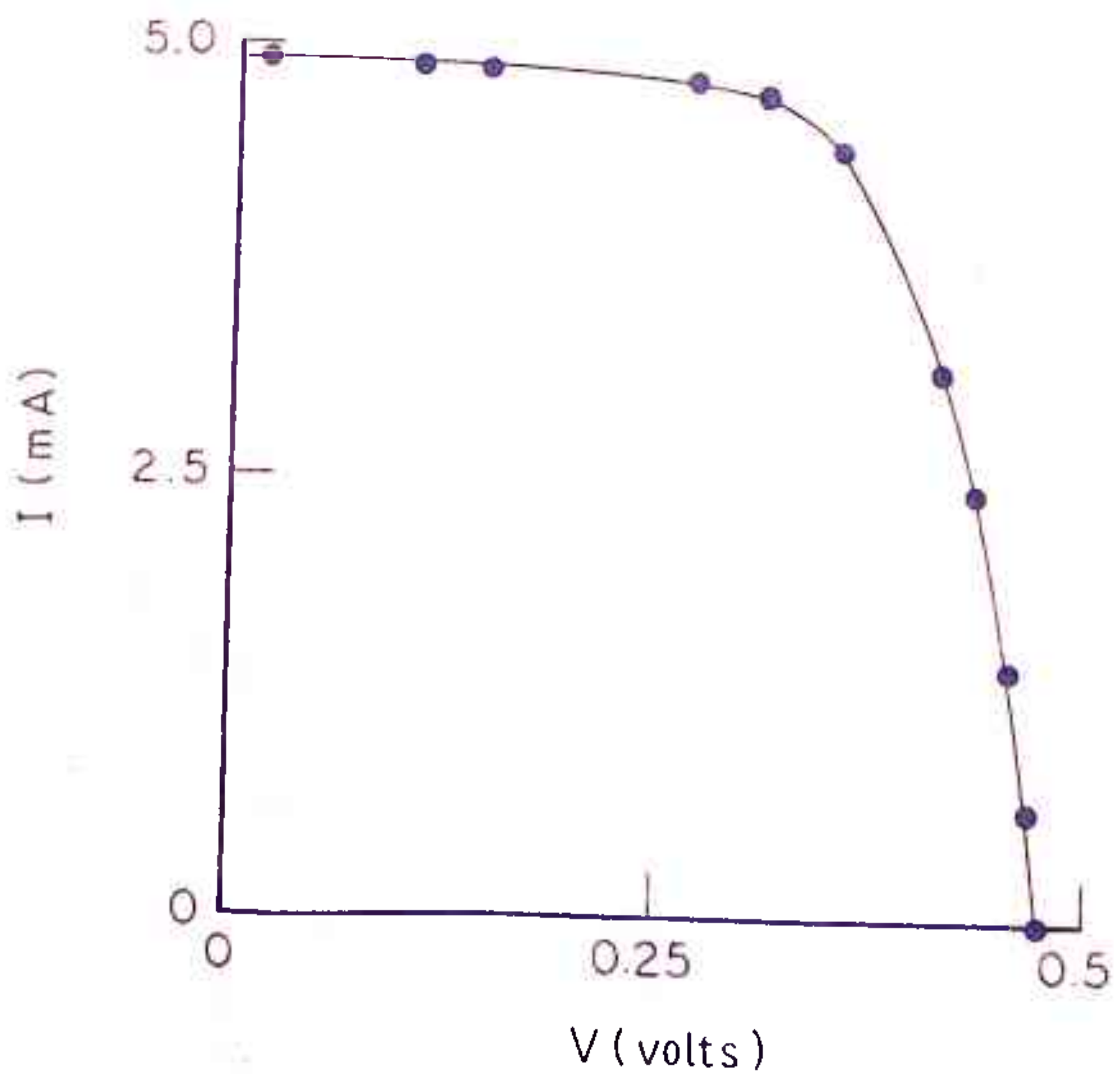

FIG. 2.10

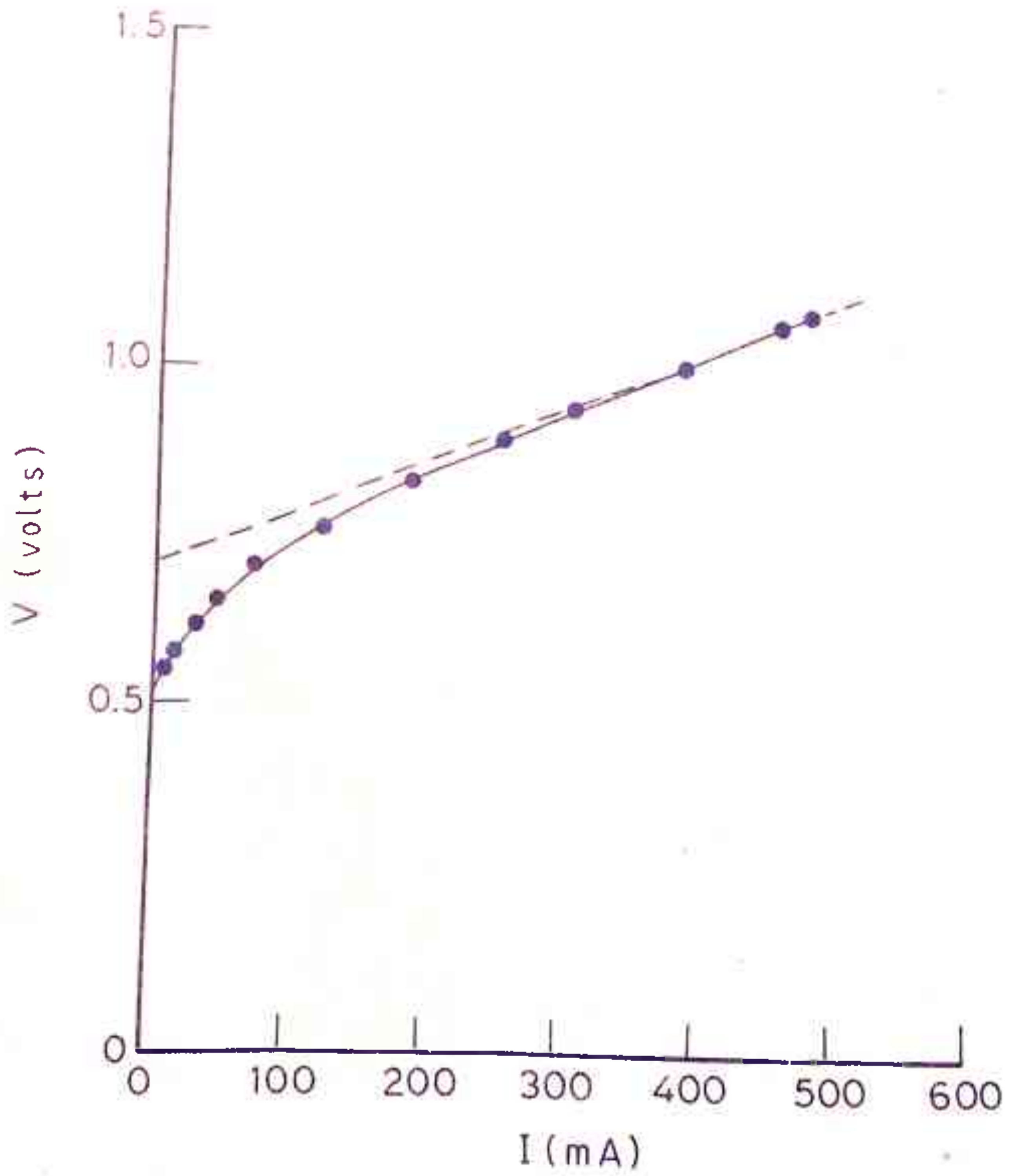

FIG. 2.11

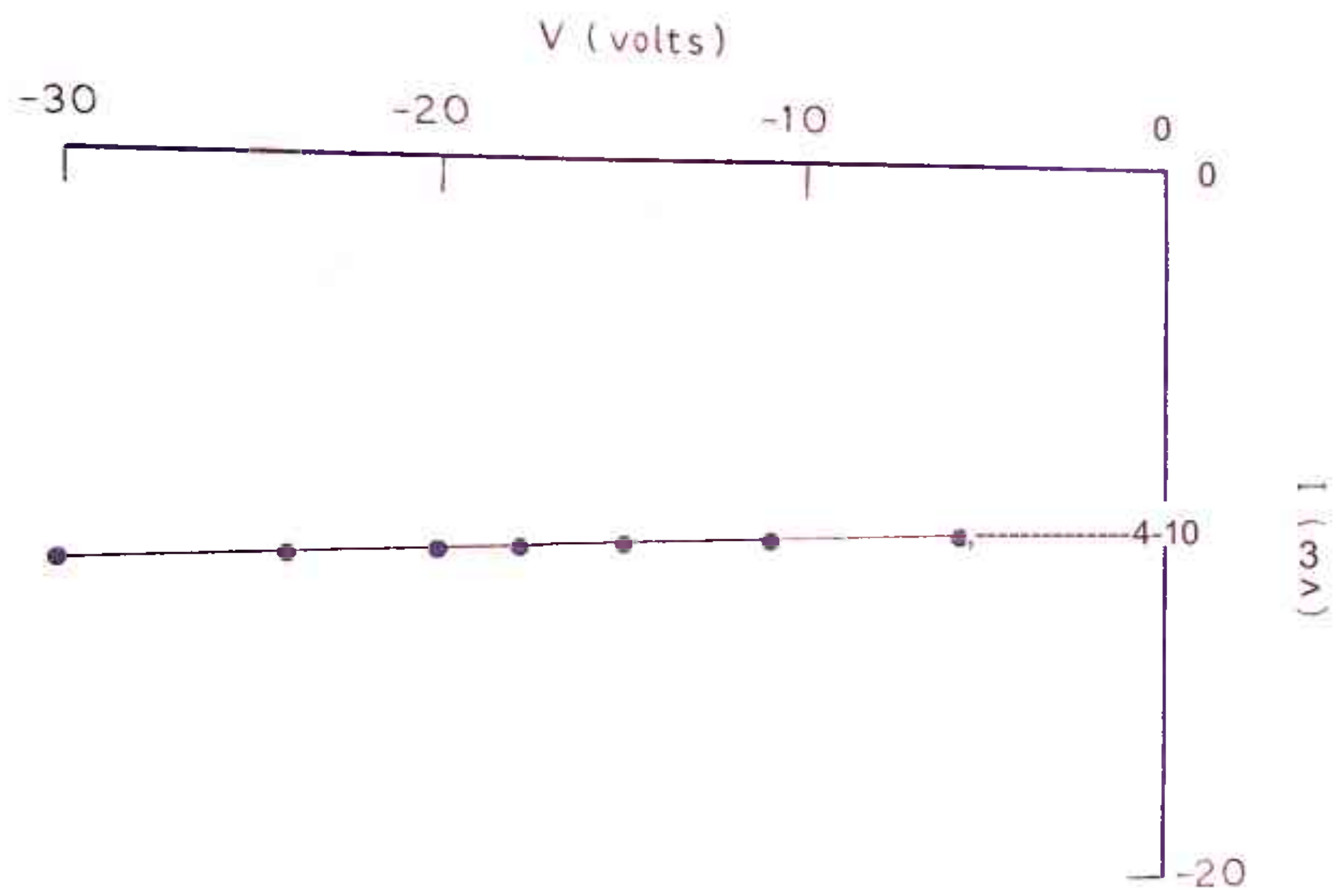

FIG.2.12

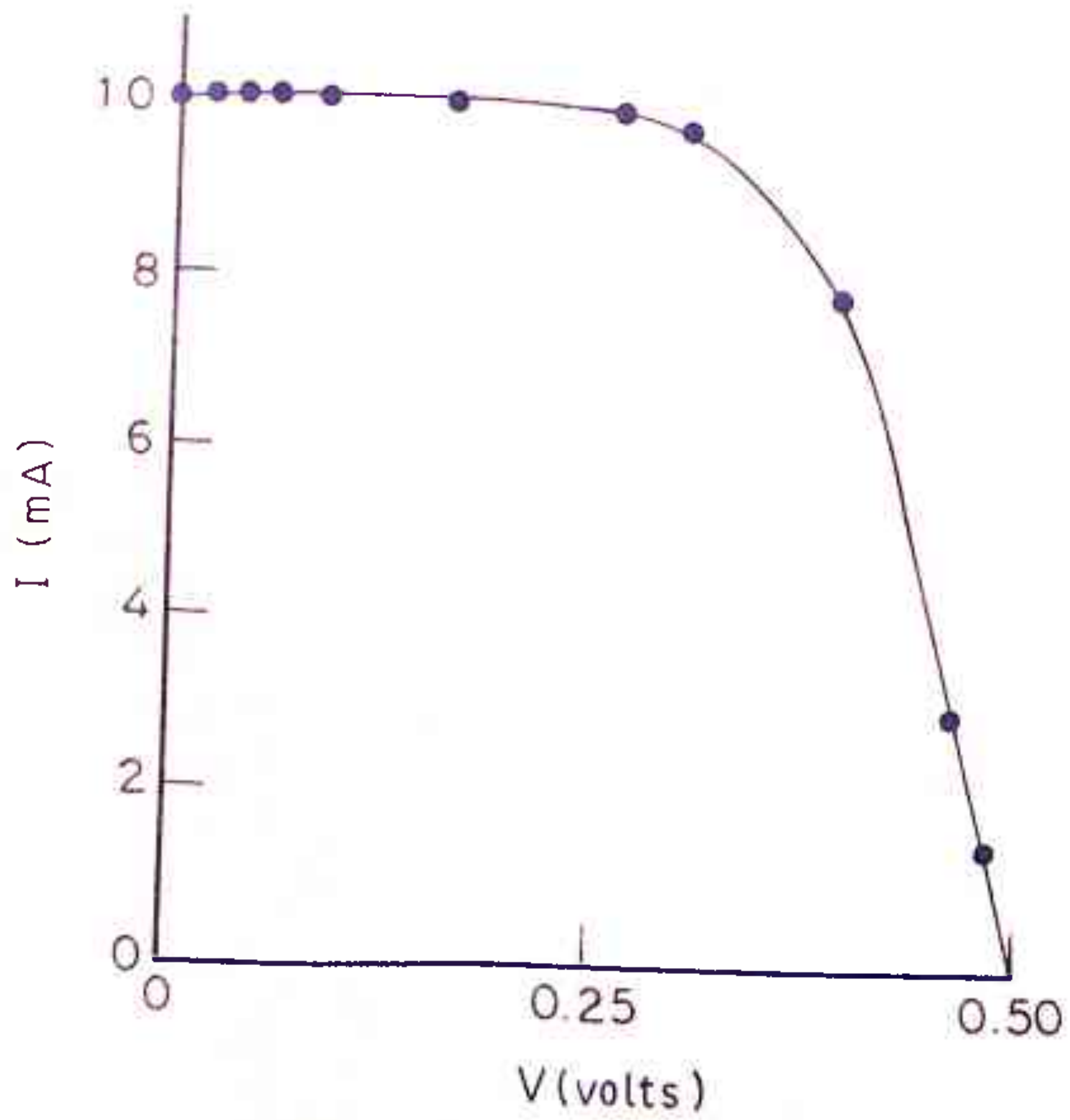

FIG. 2.13

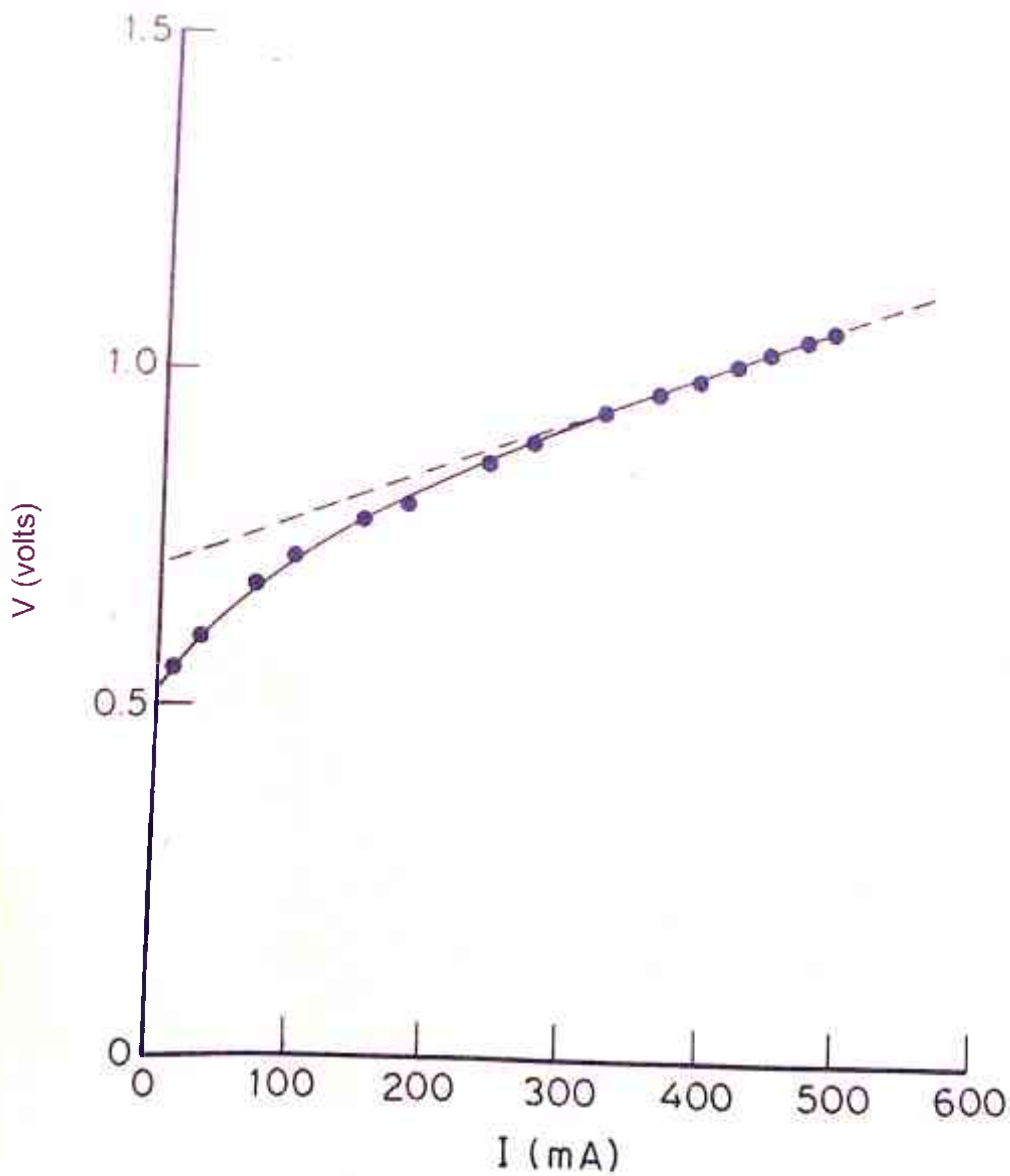

FIG. 2.14

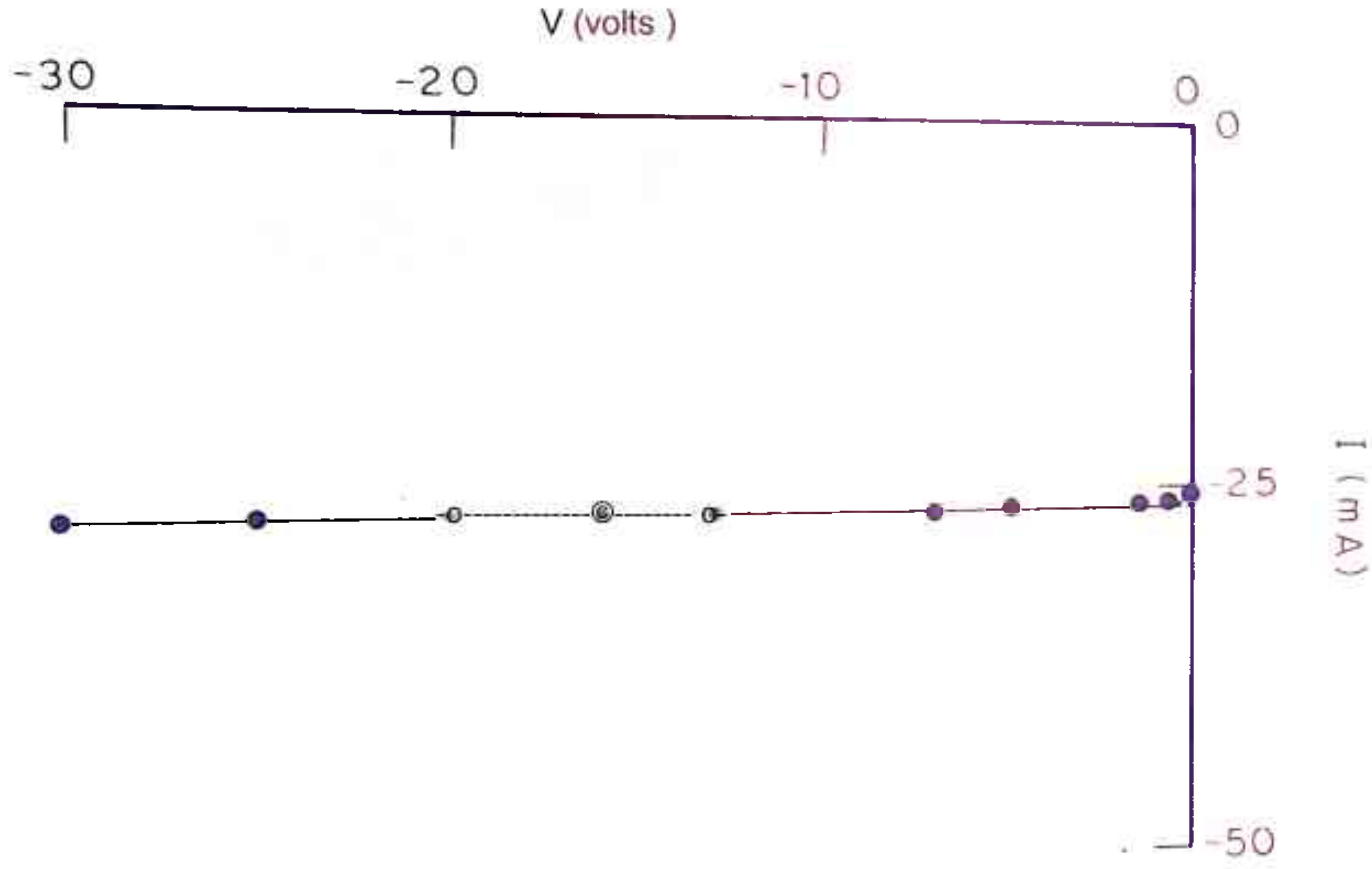

FIG.2.15

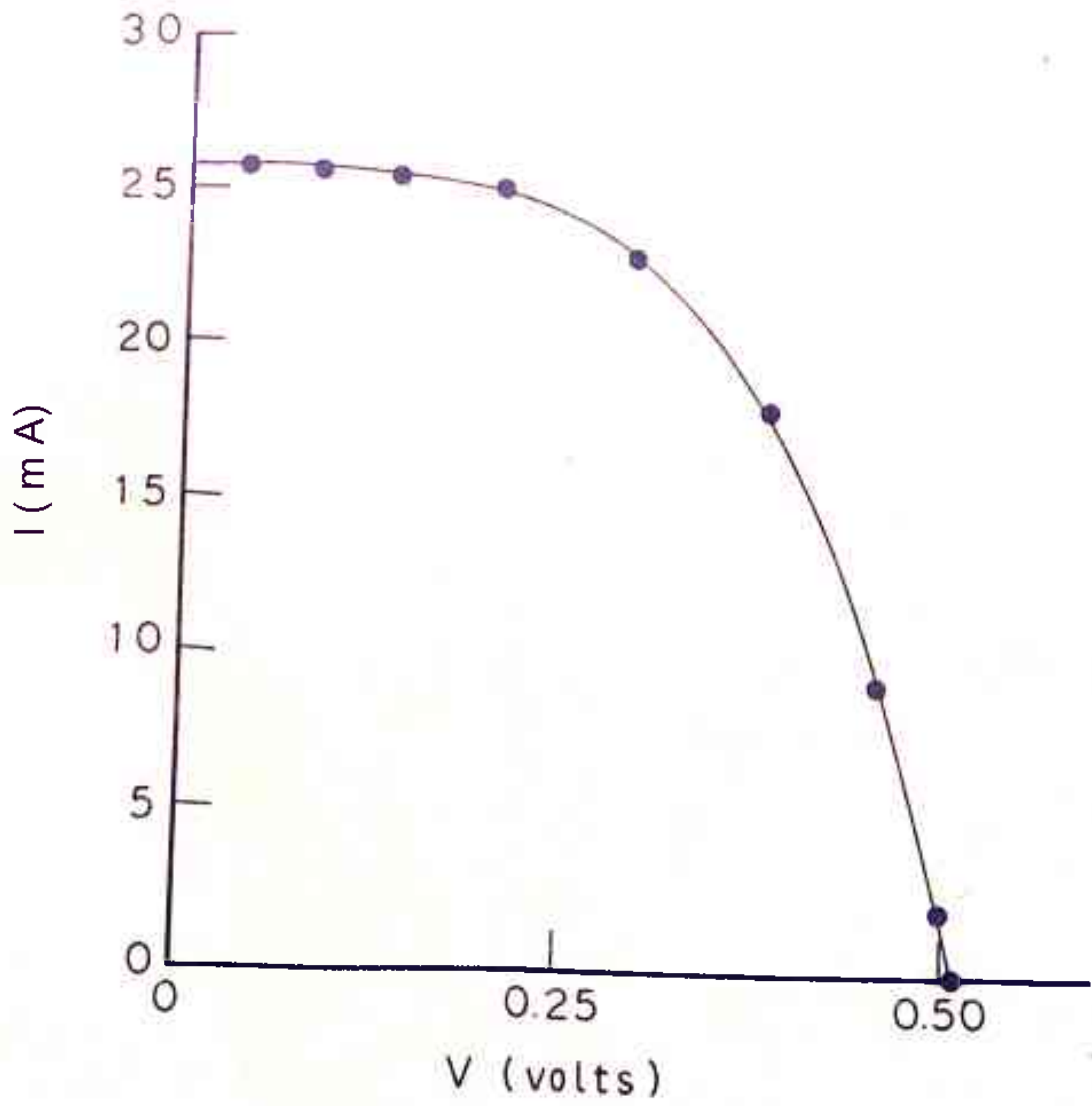

FIG. 2.16

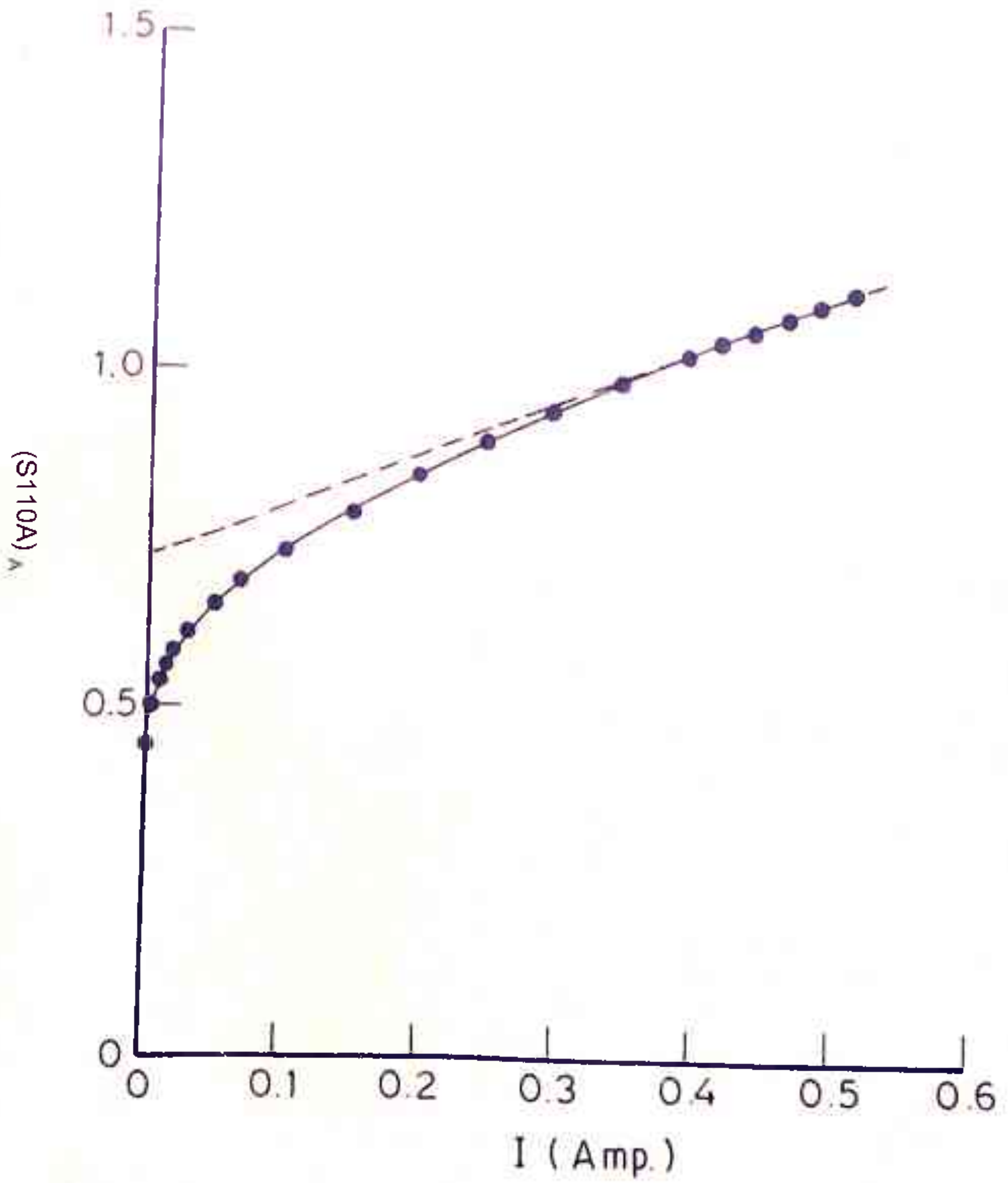

FIG. 2.17

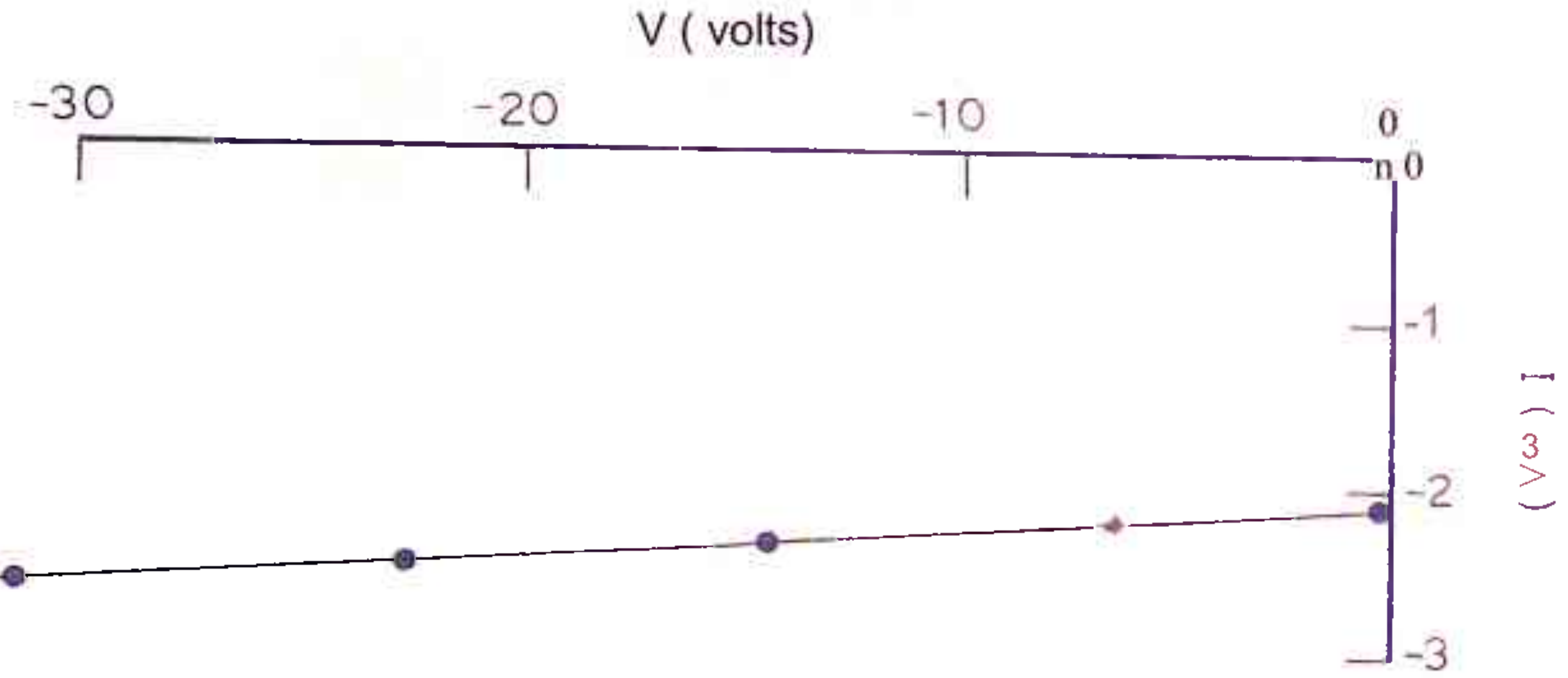

FIG.2.18

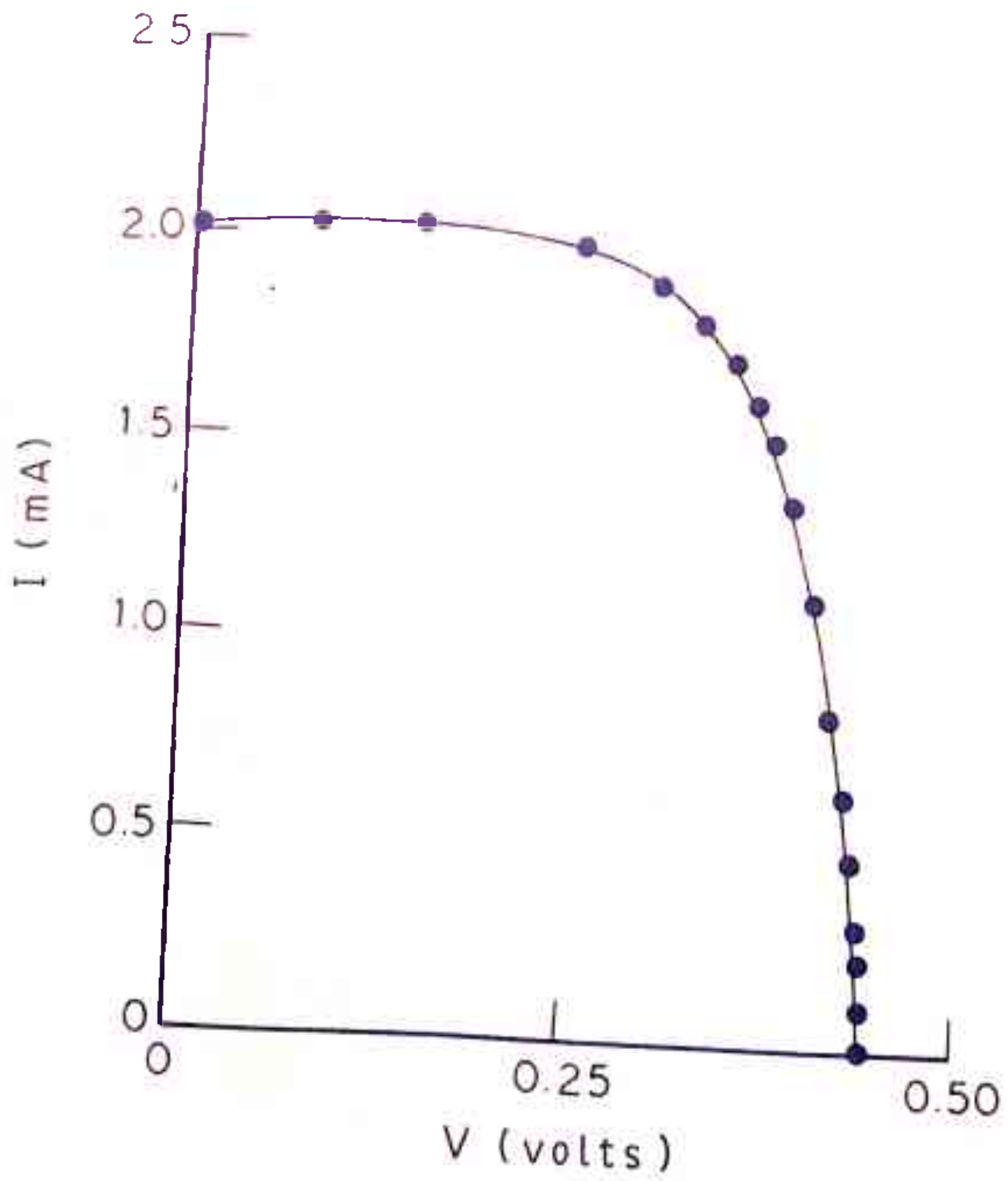

FIG. 2.19

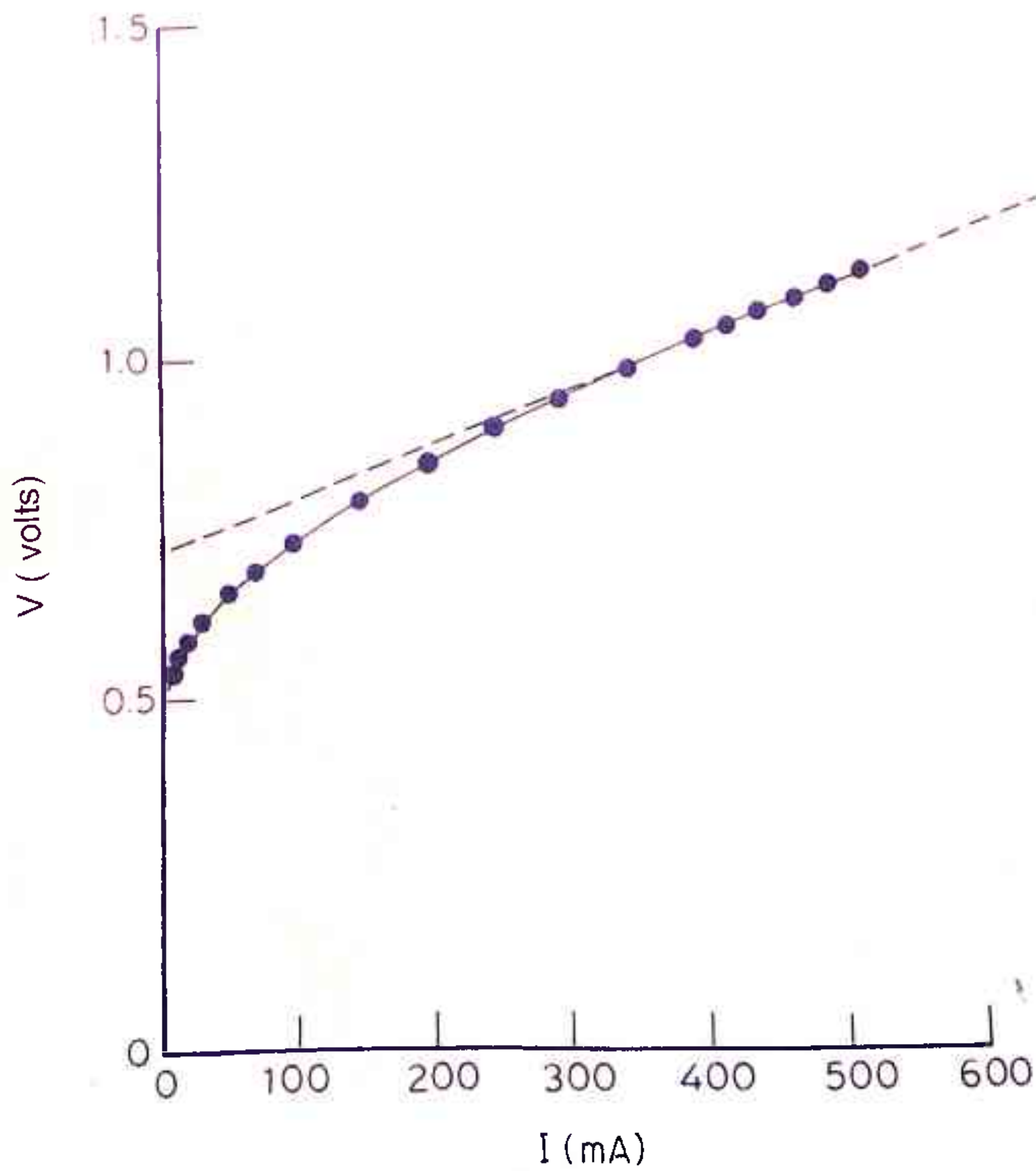

FIG. 2.20

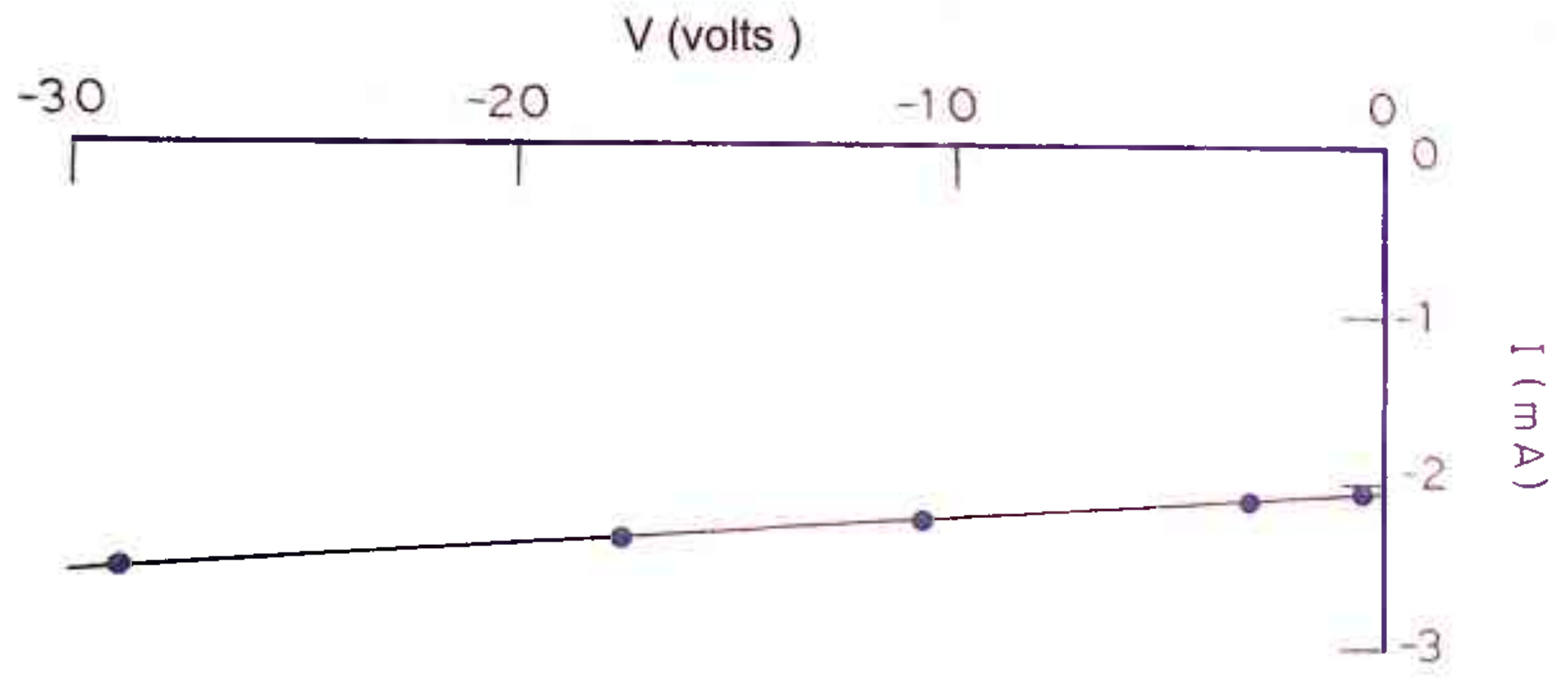

FIG.2.21

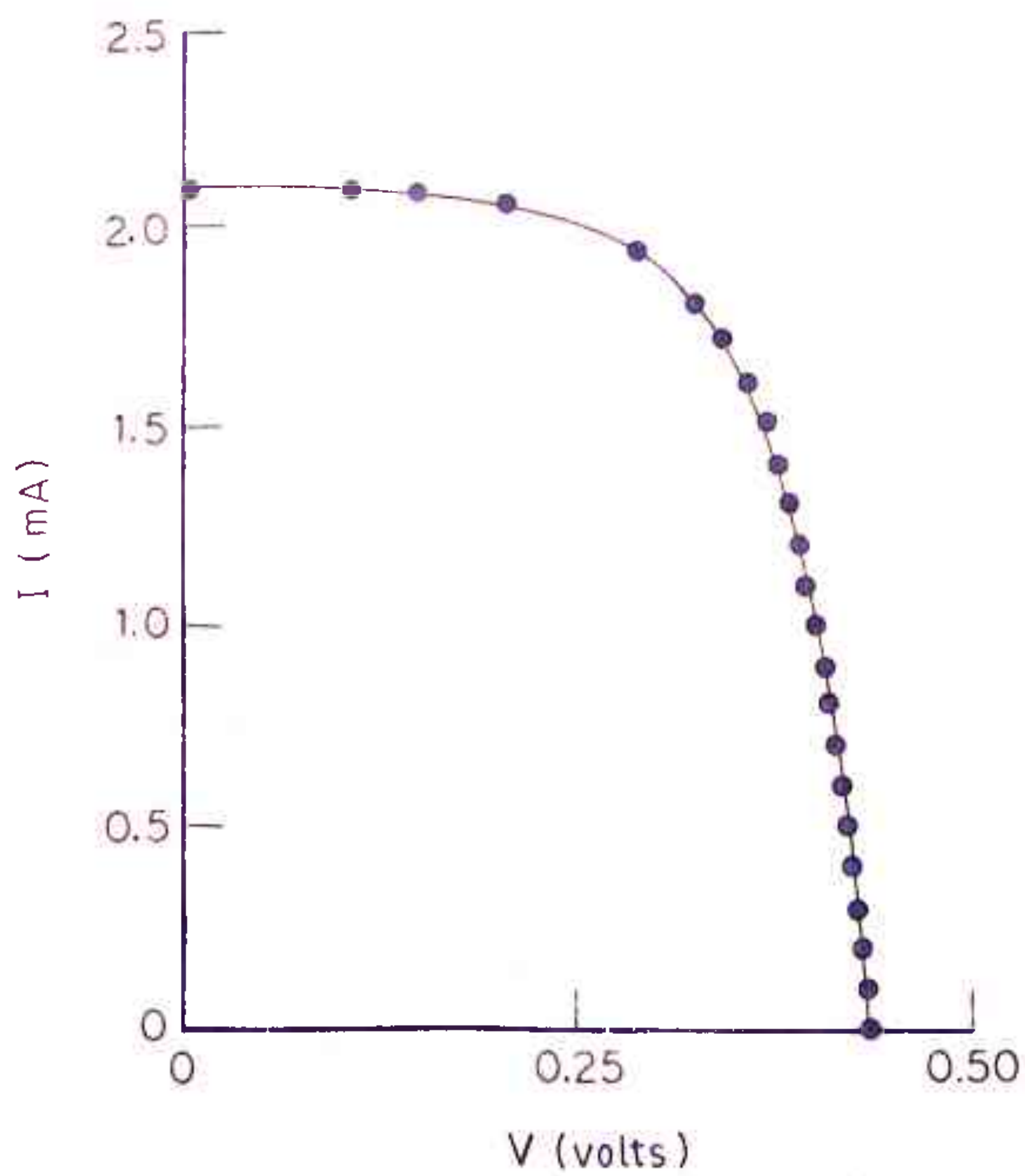

FIG.2.22

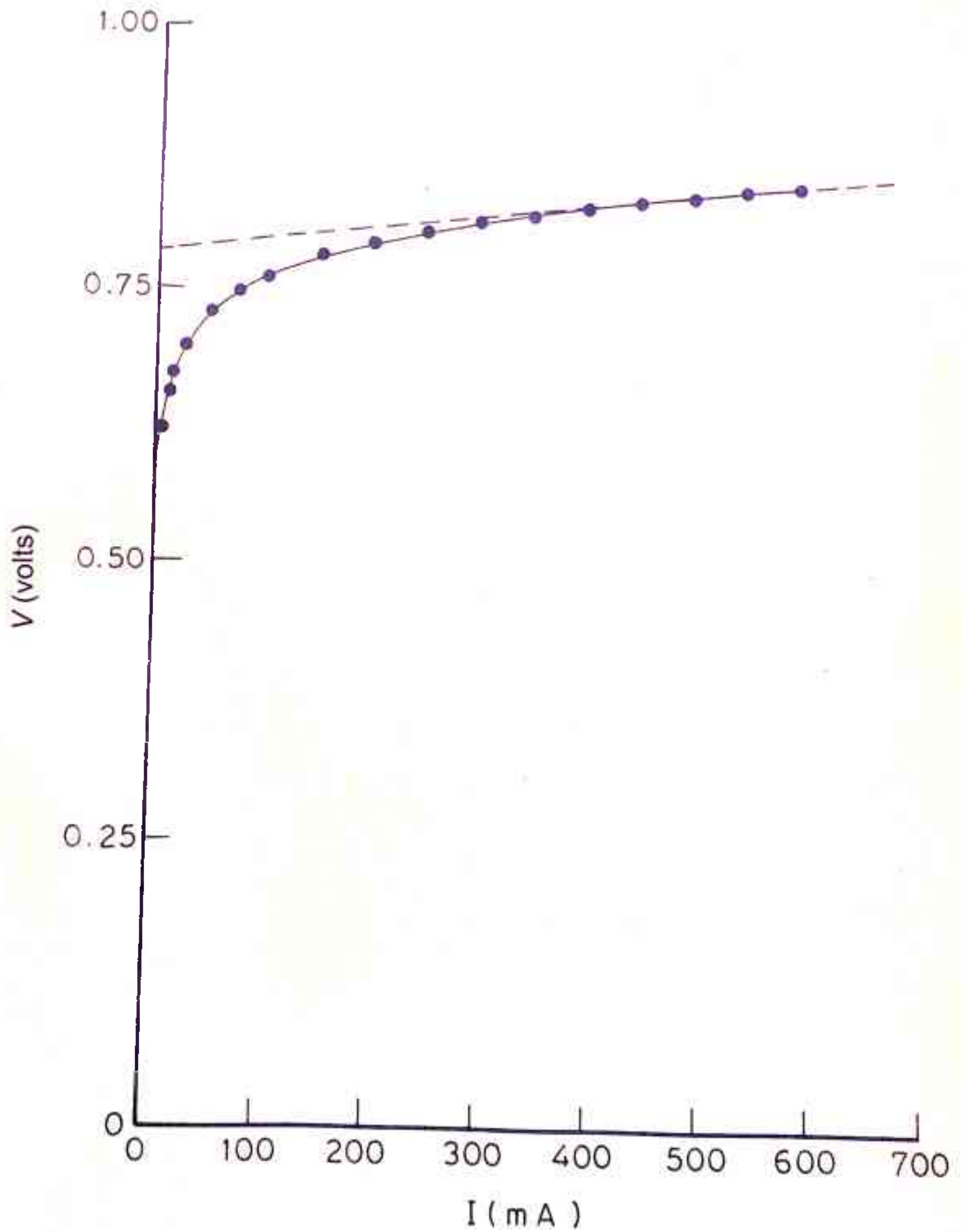

FIG.2.23

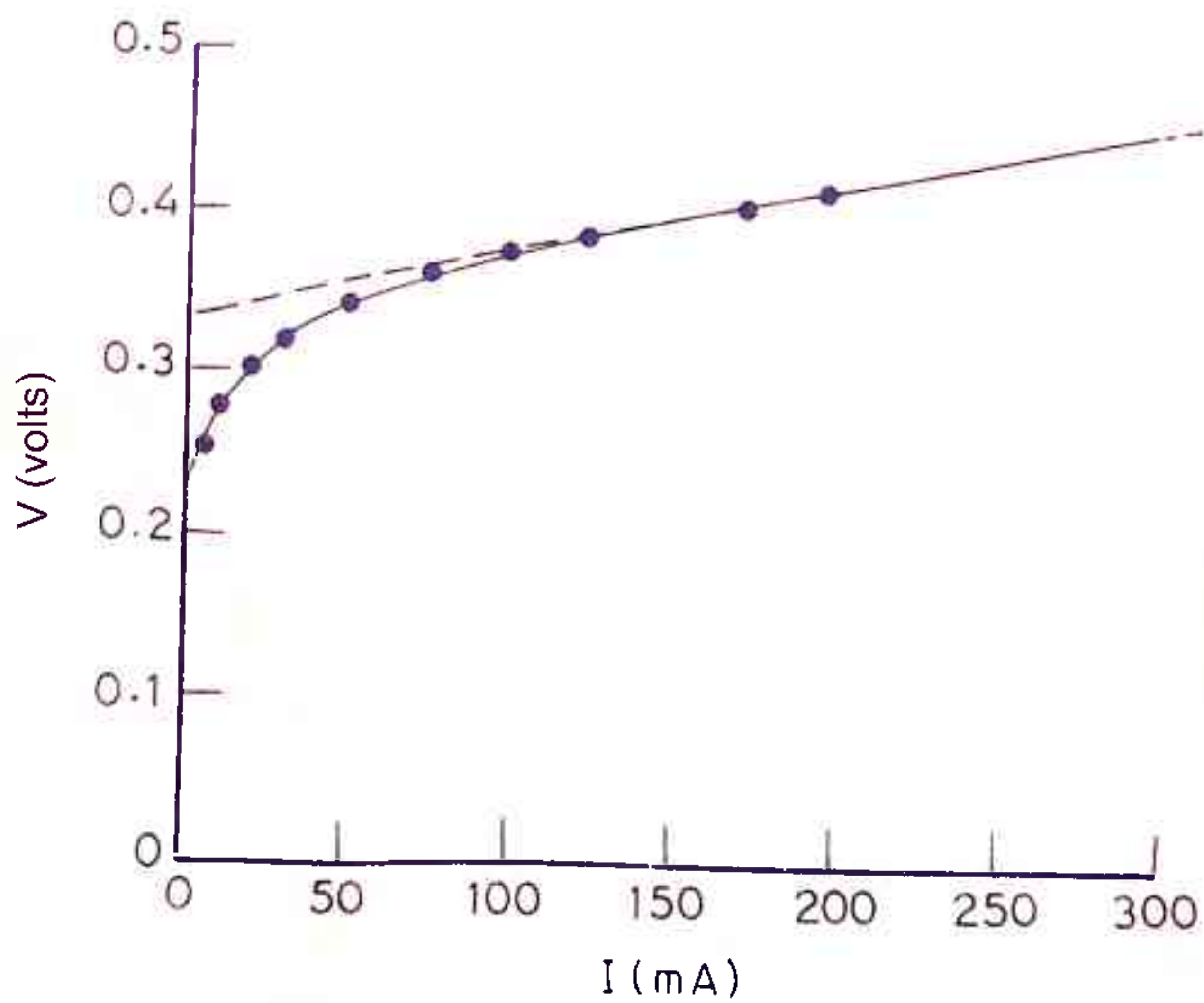

FIG. 2.24

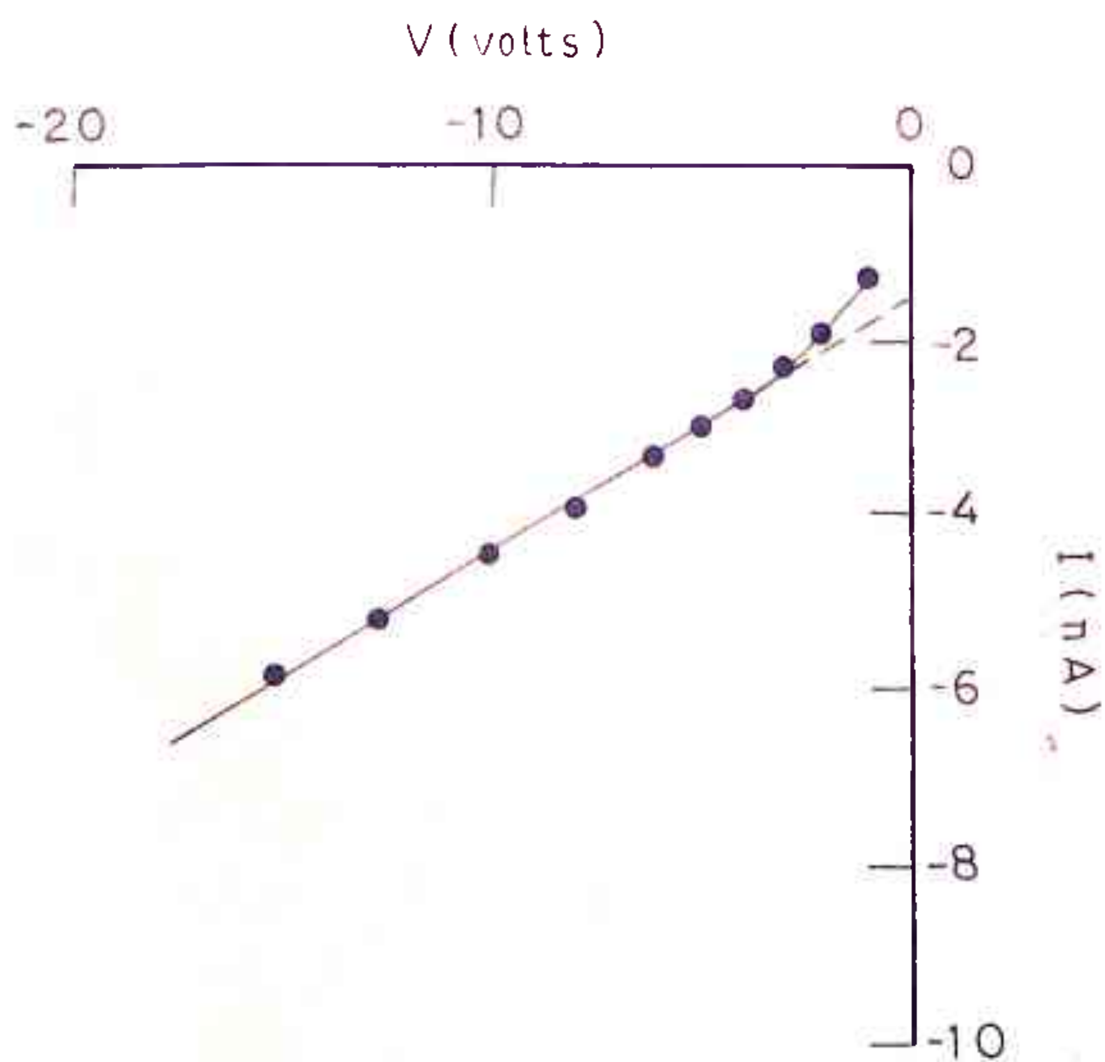

FIG. 2.25

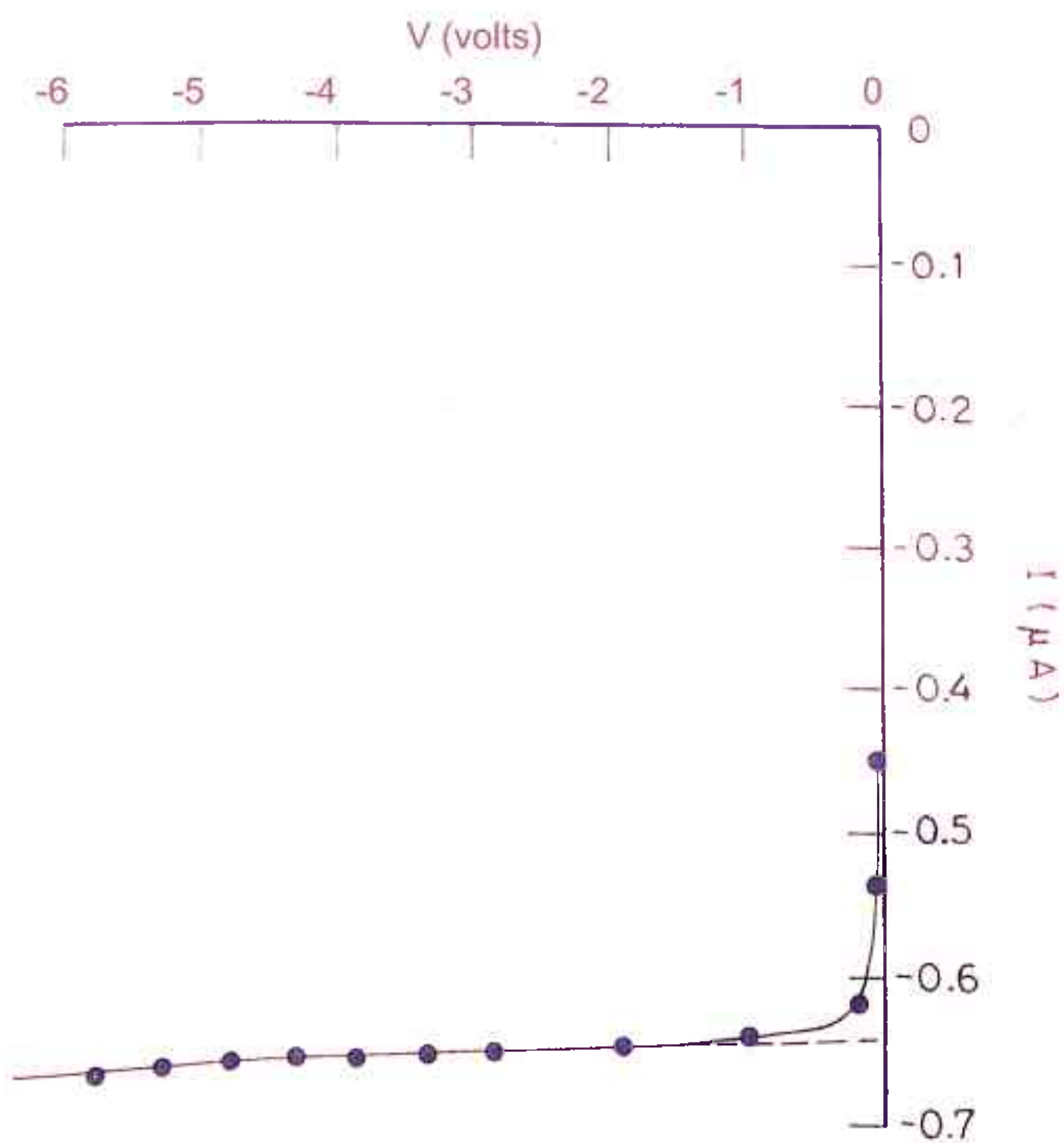

FIG.226

CHAPTER III

OPEN CIRCUIT VOLTAGE DECAY

CHAPTER III

OPEN CIRCUIT VOLTAGE DECAY

1. Introduction

Minority carrier lifetime of a junction device is one of the most important parameters and directly affects its characteristics and suitability for a particular application. Open circuit voltage decay (OCVD) is a very conventient and widely used method to determine the minority carrier lifetime (1)-(10). OCVD has also been used to study surface effects (1) and to determine series resistance (1), (2) of junction devices.

Since no current flows in the external circuit in case of OCVD, it is purely a junction property. The effect of shunt resistance (11) is significant at low voltages only, when studied at high injection levels, this method yields the value of diffusion potential (2), (3)• Unlike the case of d.c. measurements, the problem of heating of the device is almost eliminated in the OCVD experiment because current from the external circuit flows only for a small part of the cycle. This simplifies to a great extent the whole set up.

When a diode is forward biased, it offers low

resistance and current flows through it. If the current is now suddenly switched off, an emf across the diode appears due to nonequilibrium carrier concentration at the junction barrier. Since the excess carrier concentration at the junction barrier is related to the voltage by Shockley relation, by monitoring the voltage across the diode, we can find out how the excess carrier concentration at the junction is varying. The decay of voltage across a diode after the forward current has been switched off is referred to as Open Circuit Voltage Decay.

In chapter 5, we shall discuss photo voltage decay (PVD) of a solar cell in which case carriers are generated by a flash of light and then decay of voltage across the junction in open circuit condition is studied. To distinguish open circuit voltage decay studied after injection carriers, from PVD, we shall call it OCVD (dark). However, in this chapter it shall be simply referred to as OCVD.

Fig. 3.1 gives a representative circuit for doing the OCVD experiment and Fig.3.2 gives a typical OCVD of a diode.

As soon as the current is switched off, there is a sharp almost vertical drop in the voltage across the

diode. This has been referred to as initial drop V_1 in Fig. 2. This has been normally attributed to series resistance (1), (2). After the initial drop there are mainly two processes (8) governing the decay, i.e. diffusion and recombination of excess carriers. It is found that for first part of the decay diffusion component dominates and then the decay s(*ows down which signifies the domination of recombination (S). Later space charge effects set in and in some diodes, depending on the geometry and processing there is a faster decay (11).

Studies on OCVD were first reported in early fifties. In the earlier work (1), (2) an asymmetric diode was considered and the contribution due to emitter was neglected because of the low saturation current and concentration of excess minority carriers in emitter side, although it has been mentioned that there is- coupling of excess minority carriers concentrations across the junction because of Boltzman relation (2)• It was also assumed that the excess carrier concentration decays exponentially according to a single effective lifetime, which at low times would lead to a linear decay. By measuring the slope of this line it was shown (1), (2) that the value of effective lifetime can be determined.

According to the formulations given by Lederhandler and Giacoletto (1) and Gossick (2) the voltage decay is given by

$$\left(e^{qV(t)/kT} - 1\right) = \left(e^{qV_o/kT} - 1\right) e^{-t/\tau_e}$$

$$\text{or } V(t) = \frac{kT}{q} \ln \left[1 + \left(e^{qV_o/kT} - 1 \right) e^{-t/\tau_e} \right] \qquad (3.2)$$

where V(t) is the voltage across diode terminals at time t, q is the fundamental unit of charge k is Boltzman constant, T is temperature in Kelvins V_o is the voltage across diode terminals when current is shut off i.e. at t = 0 and τ_e is the single effective lifetime.

In (1) as long as $V(t) \geq \frac{kT}{q}$

$$V(t) \simeq V_o - \frac{kT}{q} \frac{t}{\tau_e} \qquad (3.3)$$

$$\text{so } \tau_e = \frac{kT}{q} \cdot \frac{1}{\text{slop of the linear decay}} \qquad (3.4)$$

and in the range $V(t) \leq \frac{kT}{q}$

$$V = \frac{kT}{q} \left(e^{qV_o/kT} - 1 \right) e^{-t/\tau_e} \qquad (3.5)$$

Whole of the initial sharp drop has been attributed to series resistance assuming that voltage

across an ohmic resistor decays almost instantaneously (compared to recombination times in semiconductors) (1), (2), (14). In (14) a plot of sexies resistance, thus calculated, has been given with respect to current, it is shown that series resistance thus calculated by this method first decreases rapidly and then approaches an asymptotic value. Such a variation in series resistance with respect to current has not yet been observed, when determined by other methods. This means, there may be some additional voltage drop apart from that due to series resistance. At high value of currents when IR_s is much larger than this drop, the series resistance thus calculated is of the same order as determined by other methods.

Recently there has been a renewed interest in OCVD (6) - (10), (13). It has been reported in (10) and observed in our laboratory also that for small values of time OCVD plots are not straight lines even for Germanium diode in which space charge effects are negligible* it has also been shown that coupling between the excess minority carrier concentrations across the junction due to Boltzman's condition (henceforth called p-n coupling) can substantially affect OCVD so that it depeds upon the excess carrier lifetimes and other material parameters of the emitter as well as

the base (6) - (8), The effect of coupling is particularly important in modern diodes (or solar cells) with a heavily doped diffuse layer in which, due to gap shrinkage, the thermal equilibrium value of the minority carrier concentration becomes comparable to or even exceed that in the base (7). The theory of Lindholm & Sah (6) which includes p-n coupling, is based upon a simplified charge control model and provides a simple and useful methodology for analysing the OCVD data in diodes. However, in the present thesis a more rigorous theory has been attempted.

A formula for OCVD was given by North as quoted in (1). Recently Tewary and Jain (10) have shown that this formula includes the effect of p-n coupling and is an exact result based upon a simplified but realistic model of a diode within low injection approximation. In this chapter, the derivation of this formula is given with the details of boundary conditions and the limits of its validity are defined. Then a method for analysing OCVD data using North's expression is developed. The effect of various parameters entering the formula on the final OCVD is also discussed and it is compared with earlier experimental data (13), and a good fit between the theoretical and experimental results is obtained*

It has been reported (10) that p-n coupling introduces a sharp, almost vertical, fall of voltage in the initial stages of the decay. This drop is added to the vertical drop due to series resistance of the device. A method to separate the p-n coupling drop is given here which exploits the fact that the drop due to series resistance is proportional to the initial current whereas the drop due to p-n coupling is independent of the current, flowing through the junction for moderate currents. Thus the observed anomalous dependence of series resistance on injection current (14) at moderately low injection currents i^Hen determined by OCVD method is explained taking into account that a current independent initial voltage drop due to p-n coupling is added to the voltage drop due to series resistance. The series resistance determined in this way after separating the contribution due to the p-n coupling is found to be quite independent of the injection current for our experimental results as well as those reported in (14).

The space charge effects which dominate at very low Injection currents and also the saturation effects associated with high injection currents have been neglected so that the present theory is valid for moderate injection levels, in present work, OCVD

experiments on silicon and germanium p-n diodes and a silicen solar cell were conducted. The experimental results are found to be in good agreement with the theory. The expression of OCVD is derived in sec. 2. In sec. 3 a theoretical analysis of the expression derived in sec. 2 and its application to interpret the experimental results of Neugroschel et. al. (13) is given. The OCVD experiments on silicon and germanium p-n diodes and a silicon solar cell and the measurements of their series resistance by separating the initial voltage drop due to p-n coupling and an analysis of these experimental results in terms of the present theory are described in sec. 4. A summary of the main results is presented in sec. 5.

2. Theory of OCVD

-V

Consider a forward biased p n diode as shown in Fig* 3.3 whose base and emitter widths are much larger than the diffusion length of the minority carriers of the respective regions.

When the current from external circuit is switched off at t = 0, the following equation will govern the decay of excess minority carriers on p side.

$$D_n \frac{\partial^2 n}{\partial x^2} - \frac{n}{\tau_n} = \frac{\partial n}{\partial t} \tag{3.6}$$

where n is the excess electron concentration on p side D_n and τ_n are diffusion length and lifetime respectively of electrons in the same region, n is a variable of x and t and D_n and τ_n are taken as constants.

Following are the boundary conditions

1. $n(-\infty, t) = 0$ (3.7)

2. $n(x,0) = F_n(0)\, e^{x/L_n}$ (3.8)

   where $F_n(0) = n_{p0}\left(e^{\frac{qV_o}{kT}} - 1\right)$ (3.9)

3. $n(0,t) = F_n(t) = n_{p0}\left(e^{\frac{qV(t)}{kT}} - 1\right)$ (3.10)

where V_0 is the junction voltage at $t = 0-$ i.e. before the current is switched off, n_{p0} is thermal equilibrium electron concentration on p side, $V(t)$ is the junction voltage at time t.

Similarly for n-side the equation would be

$$D_p \frac{\partial^2 p}{\partial x^2} - \frac{p}{\tau_p} = \frac{\partial p}{\partial t} \qquad (3.11)$$

with the following boundary conditions

1. $p(\infty, t) = 0$ (3.12)

2. $p(x, 0) = F_p(0)\, e^{-x/L_p}$ (3.13)

   where $F_p(0) = p_{no}\left(e^{qV_o/kT} - 1\right)$ (3.14)

3. $p(0,t) = F_p(t) = p_{no}(e^{qV(t)/kT} - 1)$ (3.15)

where p is the excess hole concentration on n-side which is a function of x and t, D_p and τ_p are diffusion coefficient and minority carrier lifetime respectively which are taken as constants, p_{no} is the thermal equilibrium hole concentration on n-side.

The first boundary condition of both sides means, that excess carrier concentration is zero at the ohmic contact. Second boundary condition is the excess carrier profile of both sides before the current is switched off.

Third boundary condition explains how the excess carrier concentration at the junction ($x = 0$) is related to the junction voltage at time t. This is also called the Shockley condition and is valid at low injection levels. The exact boundary condition valid for all injection levels is given by Dhariwal et. al. (15). For p side it will be

$$n(0,t) = \frac{n_{po} + p_{no} \exp\left\{-(q/kT)\,(V_D - V(t))\right\}}{1 - \exp\left\{\dfrac{-2q\,(V_D - V(t))}{kT}\right\}} \left(e^{\frac{qV(t)}{kT}} - 1\right) \quad (3.16)$$

where V_D is the diffusion potential. A similar relation can be written for n-side. When $V(t)$ is less than V_D

such that

$$p_{no}\, e^{\frac{-q}{kT}(V_D - V)} << n_{po}$$

and $e^{\frac{-2q}{kT}(V_D - V(t))} << $ [illegible]

eq. (3.16) reduces to Shockley condition. This sets the limit of validity of the Shockley condition and hence that of the formulation developed below.

Since excess carrier concentration at $x = 0$ of both side is related to same variable $V(t)$, they can not decay independently. From eq.(3.10) and eq.(3.15)

$$\frac{n(0,\ t)}{p(0,\ t)} = \frac{n_{po}}{p_{no}} \tag{3.17}$$

v/hich means the ratio of the excess carrier concentrations of both sides of the junction is constant for all times. This is called Boltzman condition.

Now consider the diode as shown in Fig. 3.3 p side is heavily doped so the minority carrier lifetime may be of the order of nanoseconds in that region as compared to that of the order of microseconds in n region. If the minority carriers on both sides were to decay independently electrons in p side will try to recombine

in nanoseconds according to their natural lifetime which would according to eq.(3.10) mean that the junction voltage becomes zero within nanoseconds, on the other hand there is a negligible reduction in the concentration of minority carriers (holes) on n side which would according to eq. (3.15) lead to a negligible reduction in voltage across junction. However, the two concentrations are related to the same voltage and one out of them can not go to zero while other one still retaining its same value. This may lead to the conclusion that the decay of concentration on any side of the junction affects the decay on other side.

This, in the present case means, somehow or other electron concentration on p side will not be allowed to go down that fast as it will independently tend to be. The only way to allow the electrons to recombine and still retain their cortcentration in this case (open circuit) is to supply some electrons from n side which are majority carriers on this side, since the charge neutrality is to be maintained, and there is no current flowing in the external circuit, same number of holes will also have to cross from n side to p side. This means at the cost of minority carriers on n side, concentration of minority carriers/at the junction on p side is

being maintained to keep the ratio constant described by eq.(3.17).

In a general case, the above discussion can be summarised as follows

I. The minority carrier concentrations at the junction on its eithex side are related to the junction voltage by the Boltzmann factor in accordance with the Shockley boundary condition. At low injection levels it can be shown that the ratio of the two concentrations remains constant during the decay.

II. The total current through the junction is the sum of the minority carrier currents from the emitter and the base. In the open circuit condition the total current has to be zero and not the base and emitter currents separately.

The condition II will lead to the mathematical boundsxy condition

$$-D_p \left.\frac{\partial p_1}{\partial x}\right|_{x=0} + D_n \left.\frac{\partial n_1}{\partial x}\right|_{x=0} = 0 \qquad (3.18)$$

The Laplace transform of eq. (3.6) with respect to t would give

$$\frac{\partial^2 \hat{n}}{\partial x^2} - \frac{\hat{n}}{L_n^2}(1+s\,\tau_n) = -\frac{\tau_n}{L_n^2}\, n(x,0) \qquad (3.19)$$

where L_n is the diffusion length given by

$$L_n^2 = D_n \tau_n \tag{3.20}$$

Solution of eq.(3.19) with the mentioned boundary conditions for p-side is

$$\hat{n}(x, s) = \left(\hat{F}_n(s) - \frac{F_n(0)}{s}\right) e^{\sqrt{1+s\tau_n}\,\frac{x}{L_n}} + \frac{F_n(0)}{s} e^{x/L_n} \tag{3.21}$$

and hence

$$\frac{\partial \hat{n}}{\partial x} = \left(\hat{F}_n(s) - \frac{F_n(0)}{s}\right)\left(e^{\sqrt{1+s\tau_n}\,\frac{x}{L_n}}\right)\left(\frac{\sqrt{1+s\tau_n}}{L_n}\right) + \frac{F_n(0)}{s}\cdot\frac{1}{L_n}\, e^{x/L_n} \tag{3.22}$$

or

$$\left.\frac{\partial \hat{n}}{\partial x}\right|_{x=0} = \left(\hat{F}_n(s) - \frac{F_n(0)}{s}\right)\frac{\sqrt{1+s\tau_n}}{L_n} + \frac{F_n(0)}{sL_n} \tag{3.23}$$

We now define, (based on boundary conditions 1 and 2

$$\hat{F}_n(s) = n_{po}\hat{f}(s) \text{ and } F_n(0) = n_{po} f(0) \tag{3.24}$$

Putting eq.(3.24) in eq. (3.23) we get

$$\left.\frac{\partial \hat{n}}{\partial x}\right|_{x=0} = n_{po}\left[\left(\hat{f}(s) - \frac{f(0)}{s}\right)\frac{\sqrt{1+s\tau_n}}{L_n} + \frac{f(0)}{sL_n}\right] \tag{3.25}$$

Similarly for n-side

$$\hat{p}(x,s) = \left(\hat{F}_p(s) - \frac{F_p(0)}{s}\right) e^{-\sqrt{(1+s\tau_p)}\,\frac{x}{L_p}} + \frac{F_p(0)}{s} e^{-x/L_p}$$

(3.26)

$$\frac{\partial \hat{p}}{\partial x} = -\left(\hat{F}_p(s) - \frac{F_p(0)}{s}\right)\left(-\frac{\sqrt{1+s\tau_p}}{L_p}\right) - \frac{F_p(0)}{s}\left(\frac{1}{L_p}\right) e^{-x/L_p}$$

(3.27)

$$-D_p \frac{\partial \hat{p}}{\partial x}\Big|_{x=0} = D_p p_{no}\left[\left(\hat{f}(s) - \frac{f(0)}{s}\right)\frac{\sqrt{1+s\tau_p}}{L_p} + \frac{f(0)}{sL_p}\right] \quad (3.28)$$

where

$$\hat{F}_p(s) = p_{no}\hat{f}(s) \text{ and } F_p(0) = p_{no} f(0) \qquad (3.29)$$

Putting eq.(3.25) and eq.(3.29) in eq.(3.18) we get

$$\frac{n_{po} D_n}{L_n}\left[\sqrt{1+s\tau_n}\left(\hat{f}(s) - \frac{f(0)}{s}\right) + \frac{f(0)}{s}\right]$$

$$+ \frac{p_{no} D_p}{L_p}\left[\sqrt{1+s\tau_p}\left(\hat{f}(s) - \frac{f(0)}{s}\right) + \frac{f(0)}{s}\right] = 0$$

(3.30)

$$\text{or } \hat{f}(s)\left[\frac{n_{po} D_n}{L_n}\sqrt{1+s\tau_n} + \frac{p_{no} D_p}{L_p}\sqrt{1+s\tau_p}\right]$$

$$+ \frac{f(0)}{s}\left[\frac{n_o D_n}{L_n}\left(1 - \sqrt{1+s\tau_n}\right) + \frac{p_{no} D_p}{L_p}\left(1 - \sqrt{1+s\tau_p}\right)\right] = 0$$

(3.31)

Let $J_n =$ [illegible: n D … τ_n] and $J_p =$ [illegible: P D … τ_p]

Then eq. (3.31) can be written as

$$\hat{f}(s)\left[J_n\sqrt{1+s\tau_n} + J_p\sqrt{1+s\tau_p}\right] + \frac{f(0)}{s}\left[J_n\left(1-\sqrt{1+s\tau_n}\right) + J_p\left(1-\sqrt{1+s\tau_p}\right)\right] = 0 \qquad (3.32)$$

or

$$\frac{\hat{f}(s)}{f(0)} = \frac{1}{s} - \frac{J_n + J_p}{s\left(J_n\sqrt{1+s\tau_n} + J_p\sqrt{1+s\tau_p}\right)} \qquad (3.33)$$

where J_n is thermally generated electron current density in p type semiconductor and J_p is thermally generated hole current density in n type semiconductor. They are also called saturation currents. By multiplying the numerator [illegible] denominator [illegible] of eq. (3.33) [illegible] by rearranging eq. (3.33) and taking the Inverse Laplace Transform we get

$$\frac{f(t)}{f(0)} = \frac{J_p}{J_p - J_n}\left[1-\mathrm{erf}\sqrt{\frac{t}{\tau_p}}\right] - \frac{J_n}{J_p - J_n}\left[1-\mathrm{erf}\sqrt{\frac{t}{\tau_n}}\right]$$

$$+ \frac{\sqrt{J_n J_p}}{J_p - J_n}\sqrt{A}\; e^{-Bt}\left[\mathrm{erf}\sqrt{\frac{J_n}{J_p}A\frac{t}{\tau_p}} - \mathrm{erf}\sqrt{\frac{J_p}{J_n}A\frac{t}{\tau_n}}\right]$$

(3.34)

where

$$A = \frac{J_p J_n (\tau_p - \tau_n)}{J_p^2 \tau_p - J_n^2 \tau_n},$$

$$B = \frac{J_p^2 - J_n^2}{J_p^2 \tau_p - J_n^2 \tau_n},$$

$$f(t) = e^{\frac{qV(t)}{kT}} - 1, \quad f(0) = e^{\frac{qV_o}{kT}} - 1$$

$$\text{and } \operatorname{erf}(y) = \frac{2}{\sqrt{\pi}} \int_0^y e^{-x^2} dx.$$

which is the same expression as given by North in the appendix of (1).

Using the following relations

$$\operatorname{erf}(x) = 1 - \operatorname{erfc}(x)$$

$$\text{and } S(x) = e^{x^2} \operatorname{erfc}(x)$$

The expression (3.34) can be put in the following form

$$\phi(t) = \frac{e^{\beta V(t)} - 1}{e^{\beta V_o} - 1} = \frac{1}{b-a} \Big[b e^{-z^2} \{ S(z) - a S(az) \} - a e^{-y^2} \{ S(y) - b S(by) \} \Big] \qquad (3.35)$$

where

$$b^2 = \frac{J_p^2 (\tau_p - \tau_n)}{J_p^2 \tau_p - J_n^2 \tau_n} \qquad (3.36)$$

$$a^2 = \frac{J_n^2 (\tau_p - \tau_n)}{J_p^2 \tau_p - J_n^2 \tau_n} \qquad (3.37)$$

$$z^2 = \frac{t}{\tau_p}, \; y^2 = t/\tau_n \qquad (3.38)$$

and $\beta = \frac{q}{kT}$

In a general case eq. (3.36) (3.37) and (3.38) can be written as

$$b^2 = \frac{J_B^2 (\tau_B - \tau_E)}{J_B^2 \tau_B - J_E^2 \tau_E} \qquad (3.39)$$

$$a^2 = \frac{J_E^2 (\tau_B - \tau_E)}{J_B^2 \tau_B - J_E^2 \tau_E} \qquad (3.40)$$

$$z^2 = \frac{t}{\tau_B}, \; y^2 = t/\tau_E \qquad (3.41)$$

where suffixes B and E refer to the base and emitter respectively.

We shall use expression (3.35) for theoretical analysis in sec. 3.

3• Theoretical Analysis of OCVD and Measurement of Device Parameters

3.1 Theoretical Behaviour of OCVD

In this section an analysis of the expression (3.35) is presented. Mathematical expression for small and large times are found and analysed. Then a simpler expression for OCVD is presented which is an approximation of (35) but is practically applicable. A method of fitting is given at the end of this section.

In most cases $\beta V_o >> 1$. As long as the following inequality is also satisfied

$$e^{\beta V(t)} >> 1 \qquad (3.42)$$

from eq.(3.35) voltage decay is given by

$$\Delta v(t) \equiv (V(t) - V_o) = \left(\frac{1}{\beta}\right) \ln W(t) \qquad (3.43)$$

and is independnt of V_o.

To examine the low 't' behaviour of V(t), we expand W(t) using the McLaurin's expansion for the error function and expanding ln W(t) we obtain for $t << \tau_B, \tau_E$

AvCt) = - IT 4- (1) 7 JBJTB+JEJ>B (3.44)

we notice from eq.(3.44) that Av(t) is linear in Jt for small values of t. Its derivation with respect to t would therefore be very large near t « 0. Usually A V(t) is observed as a function of t rather than Jt on a CRO. The observed Av(t) curve would therefore show a kink at t ® 0.

For a typical diode the emitter is more heavily doped and T_B << τ_B. For example τ_r is usually of the order of 10 - 100 ns whereas τ_B « 1 - 50 microseconds. The terms containing y» i.e. the second curly bracket on the right of eq.(3.35) therefore fall off much more raoidly than the terms in the first curly bracket. This combined with the large derivative of Av(t) with respect to t, for low values of t shows that the voltage drop will be very fast within a time period of the order of Y_E. If it is observed on a CRO on which the time scale is set to the order of τ_B, it would appear to be almost vertical and may be confused with the vertical drop due to the series resistance; this drop has been referred as the coupling drop. It may be resolved on a CRO set to the time scale of τ_E. An alternate method has been

described in the present work to separate the two drops by analysis.

It can be easily verified that the magnitude of the coupling drop depends upon the relative value of J_E and J_B. The drop would be more for $J_E > J_B$ and be small for $J_E \leq J_B$. In a diode with heavily doped emitter the value of J_E estimated in terms of the doping density is much smaller than J_B. However it has been found (7) that due to gap shrinkage the effective value of J_E may be larger than J_B and therefore in real cases the coupling drop would be quite substantial. This drop would be added to the drop due to series resistance and has to be separated out for a measurement of series resistance of the device using OCVD.

The origin of the coupling drop can be physically understood as follows. The minority carrier concentrations at the junction are related to the voltage across the junction. As mentioned in 1 in sec. 2. the ratio of their concentrations at the Junction on its either side remains constant, i.e. does not depend upon t during the decay at low injection levels. The minority carriers on either side of the junction cannot therefore decay independently. The minority carriers on the emitter side of the junction would be annihilated more rapidly than those in the base because of low value of τ_E.

The base therefore has to supply some carriers to the emitter in order to keep the aforementioned ratio constant. Thus the minority carrier concentration on the base side would reduce at a faster rate than required by their own life-time. The voltage decay across the junction due to p-n coupling would therefore be faster than that determined by the base only.

The number of carriers which has to be supplied by the base to the emitter to keep the ratio constant would of course depend upon the number already in the emitter. If the number on the emitter side is already small, the extra carriers it would need from the base would also be small. Hence if τ_E is much smaller than τ_{B-E} is either comparable to or more than τ_E; the coupling drop for $t \lesssim \tau_E$ would be quite substantial. For large values of t the number on the emitter side would have substantially decayed and the effect of coupling would be reduced; then the voltage decay would be largely determined by the base.

Now we consider large t behaviour of $\Delta V(t)$. For $t \gg \tau_B \gg \tau_E$ the contribution of the second curly bracket in eq.(3.35) becomes very small and can be neglected. Using the asymptotic expansion (16) of $S(z)$ in powers of $1/z$ which is reliable for $z \geq 2$, we obtain

$$W(t) = \frac{b}{b-a} \exp(-z^2) \left[\left(\frac{1}{a} - 1\right) \frac{1}{z^3} + o\left(\frac{1}{z^5}\right) \right] \quad (3.45)$$

If the inequality (3.42) is still satisfied for such values of t $(\frac{t}{\tau_B} > 4)$ we get from eq.(3.43)

$$\beta \Delta V(t) = -\frac{t}{\tau_B} + \ln\left(\frac{t}{\tau_B}\right)^{-3/2} + \ln\left[\frac{b(1-a)}{a(b-a)}\right] \quad (3.46)$$

Since for $t \gg \tau_B$ the contribution of the logarithmic term is really small, we find that $\Delta V(t)$ has a linear dependence on t with its slope equal to $1/\tau_B$. If the inequality (3.42) is violated by the time (3.45) becomes valid $(\frac{t}{\tau_B} > 4)$, then, as can be seen from the definition of W(t), $\Delta V(t)$ will not have a linear dependence on t and will depend upon V_0.

To findthe exact $\Delta V(t)$ within the limits set by eq.(3.42), ln W(t) was numerically computed using eq.(3.35). It was found that for calculating erfc (z), Chebyshev series works well for $z \leq 4$. For $z > 4$ first three terms of the asymptotic expansion (16) give the most optimum results which can be written as

$$\text{erfc}(z) = \frac{e^{-z^2}}{\sqrt{\pi}} \left[\frac{1}{z} - \frac{1}{2z^3} + \frac{3}{4z^5} \right] \quad (3.47)$$

For the purpose of calculations we have taken a and as the basic variables where

$$\tau = \tau_B / \tau_E \qquad (3.48)$$

b is calculated using

$$b^2 = \frac{\tau^2 + \tau(a^2-2) - a^2+1}{\tau(\tau-1)} \qquad (3.19)$$

which can be derived using eq.(3.39) and eq.(3.40) . Again using eqns. (3.41) and (3.48) y can be written as

$$y = z \sqrt{\tau} \qquad (3.50)$$

A summary of these results is presented in Tables 3.1 to 3.5, which give ln W(t) with respect to z for various values of a and τ . Fig. 3.4 gives for τ = 2, the variation of ln W(t) with respect to z for a = 0.1, 1 and 10. Fig. 3.5 and 3.6 give similar curves for τ = 50 and 1000 respectively. Figs. 3.7, 3.8 and 3.9 give ln W(t) with respect to z^2 (= t/τ_E) for the same values of τ and a used in Figs. 3.4 to 3.6 respectively.

Some observations on these figures are presented here:

(1) As mentioned earlier, when ln w(t) is plotted with respect to t/τ_E, a kink is found at 11.0, in the beginning there is a sharp fall.

(2) For a fixed value of τ_B, coupling drop increases with increase in a. When a is large (10), the coupling drop is so sharp that it may mix up with that due to series resistance, if observed in the time scale of τ_B. Hence, in such cases, series resistance should be measured independently or by a method given in sec. 4 of this chapter and its contribution to the initial decay (1), (2) should be calculated and subtracted from the initial drop to determine experimentally the true shape of the curve for small values of time.

(3) For a value of a, the coupling drop increases with increase in τ.

(4) At large times ($\frac{t}{\tau_B} \gg 1$), for a value of C_* the slope is essentially same for any value of a. in this region recombination process is dominant and the slope is $1/\tau_B$.

(5) At $\frac{t}{\tau_B} \lesssim 1$, decay is slower than that found at t = 0 but is faster than when $\frac{t}{\tau_B} \gg 1$. This is the region where diffusion terms is dominant. There is a movement of carriers outwards from the junction because of the concentration gradiant.

From a practical point of view for analysing OCVD data on a typical diode, eq.(3.35) can be simplified by

neglecting the y dependent terms and taking b = 1 and $a = J_E/J_Q$. These approximation are valid provided

$\tau_B \gg \tau_E$ and $\tau_B \tau_B \gg J_E^2 \tau_E^2$. The former inequality will generally hold in a typical p-n diode with heavily doped emitter which also implies the latter inequality if gap shrinkage is neglected in which case $J_s \gg J_E$. Even if gap shrinkage effects are included such that J_E may be comparable to or more than J_B, τ_0 would be, in general, so much larger than τ_E that $J_B^2 \tau_B$ may still remain much larger than $J_E^2 \tau_E$.

Subject to above assumptions, we can write eq.(3.35) in the following form

$$W(z) = \frac{1}{1-a} e^{-z^2} \left[S(z) - a\, S(az) \right] \tag{3.51}$$

and provided inequality eq.(3.42) is satisfied

$$\Sigma\, V(z) = \left(\frac{1}{\beta}\right) W(z) \tag{3.52}$$

The advantage of eq.(3.52) is that it describes the theoretical behaviour of W(z) in terms of a single representation parameter 'a'. The values of In W(t) for several z and some values of 'a' have been given in Table 3.6. Fig. 3.10 gives In W(z) plotted against z for

a = 0.1, 1 and10. Fig. 3.11 given ln W(z) against $z^{\frac{9}{}}$ for the same values of a.

3.2 Method to determine Solar Cell Parameters using OCVD

We shall now describe the use of eq.(3.51) and eq.(3.52) for the purpose of analysing experimental OCVD data. The experimental OCVD data in general contains a vertical drop which is usually attributed to the series resistance. As discussed earlier, this drop will also contain the coupling drop. It is therefore important to separate out the series resistance dop by an independent measurement or using the OCVD data as follows: initial sharp drop is plotted with respect to current; slope of the linear region in this plot determines series resistance and intercept at I = 0 would give the value of coupling drop. (For a detailed discussion on this point, see next section)• After subtracting the series resistance contribution from the initial drop, we determine the value of V_o and experimental V(t).

If the experimental Δ v(t) vs. t curve contains a linear region for large values of t, its slope gives an estimate of T_2 in accordance with eq.(3.46). Then from Table 3.6 (or more extensive tables of ln W(z) as defined by eq. (3.51) an estimate of 'a* can be obtained

which gives a good fit between the theory and the experimental result • If the aforementioned linear region is not found in the experimental ZSv(t) curve, both ' T_{n}'$_{o}$ and 'a' have to be obtained by comparing the experimental values with the theoretical values in Table 3.6. For this purpose we find it more convenient to plot the experimental values of A V(t) as a function of jt~ rather than t. A crude fit can be usually obtained by a visual inspection, then a more refined fit can be obtained by using the least square or some other method.

The value of 'a' can give some information about gap shrinkage by using the arguments similar to that given in (7). For example if a>l it indicates gap shrinkages. However, to find reliable information about T_E. it would be necessary to resolve the low t (0 – 'T„) & behaviour of ^V(t) on the CRO. A point to be noted is that none of the above mentioned fitting procedure gives a unique value of a, as will be shown in the next section.

in those cases where 'G, and j| '(may be comparable to '(and J_g^2 respectively, eq. (3.51) may not be reliable andthe whole of eq.(3.35) has to be used. It may be noted that this equation contains three

independent parameters (τ_B, τ_E and J_B/J_E or 'a* which can be determined by a suitable fitting procedure such as the least square analysis. Once having determined these parameters, we can calculate the value of gap shrinkage using the methodology described in (7).

In certain special cases $J_B^2 \tau_B$ may be less than $J_E^2 \tau_E$ while $\tau_B > \tau_E$. In these cases a and b will become imaginary and the nature of eq.(3.35) will become quite different.

3.3 comparison with earlier Experimental Data

As an example we use the present theory to analyse the experimental results of Neugroschel et. al (13) on OCVD of a silicon p-n diode at 376°K. In their results the initial vertical drop about 0.05 V which, as discussed earlier, should be partly due to series resistance and partly due to p-n coupling. In the absence of any information about the series resistance and since our objective is only to illustrate the present theoretical method, it may be assumed that the series resistance of the device is zero. Thus the vertical voltage drop at $t \approx t_0$ can be attributed entirely to p-n coupling. We take V_0 as 0.4V which is the starting value of the voltage.

Fig. 3.12 shows the theoretical V(t) as calculated from eq.(3.51) by taking a = 5 and τ_0 » 27 microseconds along with the' experimental results of Neugroschel et. al (13). We see that the fit between the theoretical and the experimental results is reasonably good. The values of a and τ_0 are realistic* the larger than unity value of a indicates gap shrinkage. However it ts not quite justifiable to attach any quantative significance to the values of a and τ_0 because of two main uncertainties one arising from the lack of information about the series resistance and the other from the fact that the experimental values given in Fig. 3.12 were read from the printed figures of (13) which may have introduced a substantial numerical error. It is not therefore worthwhile to compare this value of τ_0 with that obtained by other methods reported in (13). It may be mentioned, however, that the authors of (13) have reported that it was not possible to fit those experimental results with a simple linear formula for voltage decay.

To demonstrate the application of the present theory and to extract more quantitative information, we have done OCVD experiments on a silicon diode and on a solar cell. Since we have neglected space charge effects and Germanium diode are found to have less space charge

effects than silicon diodes, we did similar experiments on a Germanium diode also. All these experimental results and their analysis is reported in the next section.

4. Experimental study and Analysis

4.1 Experimental Arrangements

he conducted some simple experiments on OCVD in p-n diodes and a solar cell with the objectives of experimentally verifying the existance of the coupling drop by separating the contribution of the series resistance of the diode to the initial voltage drop.

Fig. 3.13 gives the circuit we have used to study OCVD of diodes. A Yamuna Digital Electronics (India) Model 108 pulse generator which gives pulse rise and fall times of approximately 50 nanoseconds was used. S D is a switching diode. Switching diodes like IN914 or SD40 can be used,Ufe did not get any difference in experimental data while using any of these two in the present investigation. The voltage decay was observed on a Philips (India) PM3231 CRO which has a

rise time of 23 nanoseconds.

All the experiments were done in ambiant conditions. The minimum time over which the voltage drop could be resolved is about 1 microsecond • We could not <jet any data for the devices we studied from manufacturers regarding the carrier lifetime, doping concentrations etc. The OCVD data was read from CRO and the plots were made later. We expect that the experimental error in the measurements is less than 10% except when the magnitude of voltage measured by CRO is of the order of the least count of the scale on the screen for the particular setting (which sometimes is the case when initial drop is measured). Such limitations will provide only a qualitative verification of the basic physical phenomena involved in the theory of OCVD as discussed in the preceding section.

The circuit operation and the experimental procedure are as follows! The pulse generator generates pulses whose repetition rate and width can be adjusted independently. A 50 ohms termination is provided to match the characteristic impedence of the coaxial cable used which reduces overshoot and ringing. As soon as there is a positive pulse from the pulse generator, switching diode offers a low resistance path and the

diode under test gets forward biased, and current flows through it. Pulse width is so adjusted that the whole system attains equilibrium before the pulse gets terminated. When the pulse is being terminated, voltage across the pulse generator goes to zero within a very short time (fall time of the pulse), but the device under test will have some voltage across it because of the presence of excess minority carriers at the junction. If there is no switching diode in the circuit the current from the device under test will flow through R and 50 ohms termination of the pulse generator and it u;ould not be possible to study OCVD of the device. Hence a switching diode is employed. The selection of switching diode depends upon two factors. One is the time constant of the device under study. The switching diode should have a much less time constant than the device under test, at least less than 1/10 for reasons of reliability. The second factor is the peak forward current at which it is proposed to study the device. Table 7 provides a guide to such a selection. There ar many such commercial diodes available. The injection current X in the device under test can be adjusted by controlling the amptitude of the pulse and/or by varying resistance R. The initial i.e., steady state voltage across the diode can be controlled by adjusting the current I. The repetition rate of the pulse generator should be so adjusted that

the open circuit voltage across the device under test comes down to zero before the next pulse starts. Pulse generator and CRO also have to be selected carefully so that there rise and fall times ar much less than the time constant of the device under test. CRO should be used only in DC coupled mode. Pulse generator should be checked for de bias to the pulses being generated. If there is any de bias in the pulses, it should be removed. The final de bias should be negligible compared to the open circuit voltage across the device under study. The circuit described in Fig. 3.13 would give reliable open circuit voltage decay till $v(t) > v_{de}$ where V(t) is the open circuit voltage across the diode and V_{dc} is the de bias in the pulses available from the pulse generator.

The initial voltage drop can be easily discerned from the other decay on CRO because this being a sharp vertical drop, is very faint compared to the other part. The electron beam spends the same time for the same horizontal length. In case of initial drop it travels a large vertical distance so the time spent by the beam on screen is much less per unit distance in this case than in the case of the slow decay. Hence the vertical drop is less bright than the other decay. In

fact it was found, on the CRO used in our laboratory, than any phenomena about two to three orders of magnitude faster than the other one can be easily discerned because of the large difference in intensity of the display on the CRO screen.

Since both series resistance drop and coupling drop are more than about 3 orders of magnitude faster than the other decay part, they will get mixed and whole initial drop will be much faint compared to the voltage decay of diode, provided the fall times of pulses generator and CRO are of the order of a few nanoseconds.

4,2 Experimental Results of OCVD

In th/s subsection, we present the results of OCVD experiments of three devices i.e., a silicon diode BY127 made by BEL (India), a silicon solar cell SC4 m?de by Plessey (England) and a germanium diode DR25 made by BEL (India).

Fig. 3.14 to Fig. 3.19 give the OCVD observed across BY127 (silicon diode) at different injection levels. W® observe that except at very low currents (Fig. 3.14 and 3.15), shape of the curve essentially remains the same.

Similar experimental results for SC4 (silicon solar cell) are given in Fig. 3.20 to 3.23. Fig. 3.24 gives the dimensional details of silicon solar cell SC4 used in the present study. w« see that at moderate injection levels the shape of OCVD is different from that observed on 3Y127. This may be attributed to space charge effects (j.1). Moreover from the Fig, 3.24 it is clear that the carrier distribution will be highly nonunirorm in the diffuse layer when solar cell is forward biased. Hence even where current is switchel off there will be movement of carriers parallel to the junction also which may introduce changes in the OCVD.

Since germanium diodes are observed to have much less space charge effects (7), (8), (13) than found in silicon diodes, this will give a good estimate of the minority carrier lifetime even at low voltage and large times l.e. it is expected that linear decay in the region where recombination dominates may be more apparent*

Results of OCVD experiments done on DR25 (germanium diode) are presented in Fig. 3,25 to Fig.3 27.

4.3 Measurements of Initial Drop

in the last subsection, we observed in OCVD figures that there is a sharp initial drop irmedlately

after the current is switched off. m this subsection we present results of the measurements of initial drop, in Fig. 3.28 curve 'a' represents the sharp initial drop with respect to the injection current for BY127. if we ado a small resistance -the dioce and measure the whole drop, the drop will be that due to the added resistance and the diode. Fig. 3.29 gives for different added resistance values, the variation in sharp drop with respect to the Injection current for BY127. Fig.3.30 and 3.31 give sharp drop with respect to current for SC4 and DR25 respectively.

The analysis and discussion of these data are presented in the next subsection.

4.4 Analysis of Experimental Results

As pointed out earlier, the Initial sharp drop contains the drop due to series resistance andthe coupling drop. If we want to extract the value of series resistance, we should first separate the two drops by analysis.

We note that the coupling drop is independent of V_o (the voltage before the current is switched off) and therefore the current I; whereas the drop due to

series resistance? is equal to I R_s, where R_s is the series resistance.

Thus if Δv_o represents the total initial (vertical) voltage drop, we write

$$\Delta v_o = \Delta V_c + IR_s \qquad (3.53)$$

where ΔV_c is the coupling drop.

We see from eq. (3.53) that if Δv_c, which can be measured on CRO, is plotted against I, it would be a straight line with slope R_f and intercept ΔV_c at I = 0.

Our measured values, for BY127 of ΔV_o as a function of I are shown in curve 'a' of Fig. 3.28. We see from this figure that our experimental results follow the linear law given by eq.(3.53) reasonably well except at very low values of current. The descrepancy at such low values of current is not surprising partly because it was difficult to read the drop accurately on CRO for such low currents and, what is perhaps more important is the space charge effects which become prominent at low injection levels which are not accounted for in the present theory.

By measuring the slope of the line (curve 'a') and its intercept on the Y-axis in Fig. 3.28, we obtain the following result in accordance with eq.(3.53);

R_s = 0.24 ohms and ΔV_c = 0.027 V. These are obviously realistic values. Though the value of R_s thus found is different from that found by DC analysis for the same sample. This may be so because R_s by DC method was calculated at much higher currents and R_{fl} is known to have current dependence (17) - (19). Secondly in the DC method current flows continuously which may heat the device, we did not make any effects to control the temperature of the device. It has been already reported that a change in temperature affects the value of R_b (19).

To obtain a further verification of the above result we adoed an extra known resistance R_{a} in series to the diode and measured the voltage across the combination. The extra resistance has the effect of increasing the series resistance of the diode from R_s to $R_s + R_a$. We again measured the voltage drop ΔV_o across this combination and plotted with respect to I. As expected from eq.(3.53) we found a linear dependence of ΔV_{on} I with no change (within experimental limits) in the intercept ΔV_c. This experiment was repeated for various values of R_a. Fig. 3.29 gives the plot of ΔV_o with respect to I for various R_a.

To verify it further we plotted the slope of each line in fig. 3.29 with respect to R_a. The intercept at $r_a = 0$ would give $\dot{s}$. This is shown in Fig. 3.32.

When initial drop V is observed across a diode with a resistance padded to it, the following equation may hold

$$\Delta V = IR_s + IR \qquad \Delta V \qquad (3.54)$$

For a current I, if we put R* =» -R in eq. (3.54) we get AV « v « In Fig. 3.33 we give a plot of Z^V with respect to R_{f1} at I = mA. We find that at

R_a ' $-R_s$ on x-axis At gives the coupling drop on y-axis and its slope is I. The points for this were read from Fig. 3.29 at I = 8 mA. We believe all this provides adequate verification for the existence of the coupling drop and gives a reliable value of R .B

A more direct study of coupling drop may be done by usin a more sophisticated CRO by expanding the time scale, This would at least partly resolve the *voltage drop* , Such a study should be quite interesting and may be able to provide an estimate of '^,. *Although* there are experimental limitations to such a study, because of the constraints described earlier.

i.e. rise and fall times of pulse generator and CRO should be at least an order of magnitude better than the times for which wc want to study the phenomena. Switching diode will also impose limitations on the study at low times because of its reverse recovery time of the order of nanoseconds. As described earlier, this also should be at least an order of magnitude better. At such high frequencies, capacitances and inductances introduced due to circuit layout and lead lengths of the components and their connections may introduce time constants comparable to τ_{B}. Hence there art chances of misinterpreting a decay pattern obtained for such low times. Such a study will have to be done with extreme care.

In the theoretical analysis (1), (4) the p-n coupling and therefore the coupling drop ΔV_C in eq. (3.53) is neglected and the whole of the initial drop is assumed to be due to the series resistance. On this assumption series resistance is calculated by dividing ΔV_0 by i. We refer to it as the apparent series resistance R^*_S defined by

$$R^*_S = \frac{\Delta V_0}{I} = R_S + \frac{\Delta V_C}{I} \tag{3.55}$$

The dependence of R_s^* on I for our experimental results of curve -a- in Fig. 3.28 is shown as curve -b- in the same figure. As expected from eq. (35.5) this shows a nonlinear dependence of R_s^* on I. For low I the second term on the right of eq. (3.54) dominates which gives the sharp rise in R_s^* as I decreases. For large I, this term makes a small contribution and $R_s^* \approx R_s$ is approximately independent of I. It is therefore clear that the usual analysis gives only R_s^* which is approximately equal to R_s only if the measurement was made at moderately high value of the initial injection current. If the value of the current is too high, then the high injection effects would set in, which have not been accounted for in the present theory.

Our observed dependence of R_s^* on I is quite similar to that reported in literature (14). In the usual analysis this is interpreted as the dependence of the series resistance on the injection current (14). whereas a weak dependence of the series resistance on injection current can be expected on physical grounds, no really satisfactory explanation of such a strong dependnce of series resistance on I has been reported in literature. We have shown here that the usual method of determining the series resistance actually yields

R_s^* and not R_{ti}. The dependence of R'_s on I is correctly explained by present theory which also gives a method for extracting R_c by plotting ΔV_o as a function of I.

As an additional verification of the existence of the coupling drop we have analysed the experimental results on series resistance reported in (14) by using the present theory. In the light of the above discussion, we identified these values as and plotted yAV . IR o s as a function of I. We have found a linear dependence of ΔV_o on I with a finite intercept for I = o which gives the magnitude of the coupling drop. This is shown in Fig. 3.34. Thus we infer that the experimental results on series resistance as reported in (14) are consistent with the present theory.

The resulting CCVD curve after separating out the series resistance contribution is shown in Fig. 3.35. It may be noted that the initial voltage drop, the non-linear dependence on t for low values of t and a linear dependence on t for large values of t are in qualitative agreement with the present theory. The theoretical $\Delta V(t)$ calculated from eq.(3.51) and (3.52) by taking a « 1.1 and T_B • 11 microseconds is also shown in Fig. 3.35 we see from this figure that the curve OL y agreement between the theory and experimental results

of OCVD Is quite satisfactory. We could of course fit different values of a by taking a suitable T_B as shown in curve 'B* of same figure for a = 0.1 and t_B * 8 microseconds. Hence there is no unique value of a available from this fitting procedure.

We did similar experiments for a germanium diode DR25 made by BEL India. Fig. 3.31 gives the initial drop vs. I for DR25 from which we get R_s « 1.06 ohms and AV_c - 0.013 V. Fig. 3.36 gives the final OCVD curve after subtracting the series resistance contribution. We get a = 1.1 and T_B = 16 for curve 'A' and a «= 0.1 and T_B " 11 for curve 'B' of Fig. 3.36.

We also did similar experiments on a silicon solan cell SC4 supplied by Plessey (England). Fig. 3.30 shows the $/IV_o$ versu I plot for SC4. In this we could not find a good straight line as was the case with BY127 and DR25. This we feel, may be because of the nonuniform injection of carriers and taeir/jniform non-concentration at the junction. • Secondly eq. (3.ul) is valid for a diode having infinite emitter and base widths whereas in case of solar tcells the emitter width is much smaller of the order of 100-200 & (20). So just to demonstrate we have taken an approximate straight line in Fig. 3.3C which gives «<- R_s -1.55 ohms, and ΔV_c » 0.024V.Fig. 3.37

gives the OCVD curve after subtracting the contribution due to R_S calculated above, which gives a = 1.1 and τ_B = 30 microseconds for curve 'A' and a = 0,1 and τ_B = 20 microseconds for curve ' B'. in this case we find that space charge effects set in at comparatively higher voltages which indicates a low leakage resistance (11) .of this device compared to BY127 and DR25. This also confirms qualitatively the results obtained in chapter 2.

5. Conclusions

To summarise, the main results of this chapter are following:

1. OCVD in a p-n diode or solar cell is affected by the p-n coupling.

2. The experimental data on OCVD can be represented in most cases by eq. (3.51) which is valid for $\tau_D \gg \tau_E$ and $J_B^2 \tau_B \gg J_E^2 \tau_E$. If these inequalities are not *valid eq. (3.35) has to* be used.

3. The decaying voltag. has a sharp faU near t = 0 *which may be* confused with the initial drop due to series resistance. Th. magnitud. of the coupling drop will be more for $J_E > J_B$ which implies gap shrinkage. The coupling drop can be separated from th -ne drop due to

series resistance by measuring the current dependence of the total initial drop and exploiting the fact that the coupling drop is independent of the current whereas the drop due to series resistance is proportional to the current.

4. The usually reported values of the series resistance obtained from OCVD actually give an apparent series resistance which has $\frac{1}{I}$ dependence on I for low values of I and is approximately constant for moderately high values of I. It is only in the latter region when the apparent series resistance is approximately equal to the actual series resistance which is independent of I (apart from a possible weak dependence on I which was not resolved in our experiment (due to experimental limitations) and which has not been accounted for in our theory).

5. The decaying voltage, has a nonlinear dependence on t for low values of t which, if accurately measured can yield information about gap shrinkage and possibly τ_{E^*}. For $\frac{t}{\tau_B} \geq 4$ the decaying voltage has a linear dependence on t with slope $\frac{1}{\tau_B}$ provided exp.(ρ v) remains much larger than unity.

6. A summary of results obtained using the analysis described in this chapter is presented in Table 3.8.

References

1. J.R. Lederhandler and L.J. Giacoletto, "Measurement of Minority Carrier Lifetime and Surface Effects in Junction Devices", Proc. IRE, Vol. 43 p.477, 1955,

2. B.R. Gossick, "On the Transient Behaviour of Semiconductor Rectifiers", J, Appl. Phys., Vol. 26, p.1356, 1955.

3. Yu. A. Tkhorik, Transients in Pulsed Semiconductor Diodes, Jerusalem* Israel Program for Scientific Translation, 1968.

4. Y.R. Nosov, Switching in Semiconductor Diodes, New York : Plenum Press, 1969.

5. S.C. Choo and R.G. Mazur, "Open Circuit Voltage Decay Behaviour of Junction Devices", Solid-State Electronics, Vol. 13, p.553, 1970.

6. ;?.A. Lindholm and C.T. Sah, "Normal Modes of Semiconductor p-n Junction Devices for Material Parameter Determination", J. Appl. Phys., Vol. 47, p.4203, 1976.

7. F.A. Lindholm et. al., «A Methodology for Experimentally Based Determination of Gap Shrinkage and Effective Lifetime in the Emitter and Base of the p-n Junction Solar Cells and other p-n junction Devices", IEEE Trans. Electron Devices, Vol. ED-24, p.402, 1977.

8. A. Neugroschel et. al., "A Wethod for Determining the Emitter and Base Lifetimes in p-n Junction Diodes'*, IEEE Trans. Electron Devices, Vol. ED-24, p.662, 1977.

9. J.E. Mahan et. al, "Measurement of Minority Carrier Lifetime in Solar Cells from Photoindced Open Circuit Voltage Decay", IEEE Trans. Electron Devices, Vol.ED-26, p.733, 1979.

10. V.K. Tewary and S.C. Jain, "Open Circuit Voltage Decay Method of Measuring Lifetime in a p-n Junction Diode", Solid-State Physics Laboratory, Delhi, Tech. Report (1980) i to be published.

11. R.J. Bassett, "Observations on a Method of Determining the Carrier Lifetime in p^+-ν -n^+ diodes", Solid-State Electron., Vol. 12, p.385, 1969,

12. J.P. *McKelvey, Solid* State and Semiconductor Physics New York s Harper and Row, 1966.

13. A. Neugroschel et. al, "Diffusion Length and Lifetime Determination in p-n Junction Solar Cells and Diodes by Forward Biased Capacitance Measurements", IEEE Trans. Electron Devices, Vol. ED-25, p.485, 1978.

14. L.P. Hunter, Handbook of Semiconductor Electronics, New York s McGraw Hill, 1970.

15. S.R. Dhariwal et. al., "Saturation of Photovoltage and Photocurrent in p-n Junction Solar Cells", IEEE Trans. Electron Devices, Vol. ED-23, p.5O4, 1976.

16. M.Abramowitz and I.A. Stegun, (Ed.), Handbook of Mathematical Functions, New York s Dover Publications, 1965.

17. M.S. Imamura andJ.I. Portscheller, "An Evaluation of the Methods of Determining Solar Cell Series Resistance", The Conference Record of the Eigth IEEE Photovoltaic Specialists Conference, p.102, 1970.

L8. A. Agarwala, Response of Solar Cells to High Intensity, Concentrated Radiation, Ph.D Thesis, Birla Institute of Technology andScience, Pilani, India, 1979.

19. N.K. Swami, Studies on Efficiency Considerations in Conventional and Schottky Barrier Solar Cells, Ph.D Thesis, Birla Institute of Technology and Science, Pilani, India, 1979.

20. S.c. Jain, Private Com-unication .

TABLE 3.1

In W(t) for HC « 2 and different values of a as calculated from eq.(3*35).

z	a 0.10	0.50	1.00	5.00	10.00
0.00	-0.00	-0.00	-0.00	-0.00	-0.00
0.10	-0.12	-0.14	-0.14	-0.14	-0.15
0.20	-0.26	-0.29	-0.30	-0.31	-0.31
0.30	-0.42	-0.46	-0.48	-0.49	-0.49
0.40	-0.58	-0.65	-0.68	-0.70	•0. 69
C.50	-0.77	-0.85	-0.89	-0.93	-0.93
0.60	-0.97	-1.08	-1.13	-1.17	-1.18
0.70	-1.19	-1.32	-1.39	-1* 44	-1.44
0.80	-1.42	-1.58	-1.67	-1.72	-1.74
0.90	-1.67	-1.86	-1.96	-2.04	-2.05
1.00	-1.94	-2.16	-2.28	-2.38	-2.38
1.20	-2.53	-2.82	-2.98	-3.10	-3.11
1.40	—3 • 18	-3.55	-3.74	-3.90	-3.91
1.60	-3.91	-4.36	-4.59	-4.78	-4.79
1.80	-4.72	-5.23	-5.50	-5.72	-5.73
2.00	-5.59	-6.18	-6.48	-6.74	-6.75
2.50	-8.11	-8 * 86	-9.24	-9.56	-9.58
3.00	-11.09	-11.99	-12.40	-12.81	-12.81
3.50	-•14.55	-15.58	-15.99	-16.51	-16.53

TABLE 3.2

in W(t) for C « 20 and different values of a as calculated from eq.(3.35).

z \ a	0.10	0.50	1.00	5.00	10.00
0.00	-0.00	-0.00	-0.00	-0.00	-0.00
0.10	-0.13	-0.16	-0.20	-0.32	-0.34
0.20	-0.27	-0.35	-0.43	-0.70	-0.76
0.30	-0.43	-0.55	-0.68	-1.11	-1.20
0.40	-0.60	-0.77	-0.94	-1.53	-1.65
0.50	-0.79	-1.SO	-1.22	-1.94	-2.10
0.60	1.00	-1.25	-1.51	-2.34	-2.51
0.70	1.22	-1.52	-1.82	-2.73	-2.92
0.80	1.45	-1.80	-2.14	-3.12	-3.33
0.90	1.71	-2 • 10	-2.47	-3.53	-3.73
1.00	1.98	-2.41	-2.82	-3.93	-4.14
1.20	2.57	-3.08	-3.55	-4.76	-4.93
1.40	3.23	-3.83	-4.35	-5.63	-5.85
1.60	3.96	-4.64	-5.21	-6.55	-6.77
1.80	4.76	-5.52	-6.13	-7.51	-7.74
2.00	5.64	-6.47	-7.12	-8.54	-8.77
2.50	8.15	-9.15	-9.88	-11.37	-11.60
3.00	11.13	-12.28	-13.04	-14.62	-14.85
3.50	14.60	-15.87	-16.63	-18.33	-18.56

TABLE 3.3

ln W(t) for « 50 and different values of a as calculated from eq.(3.35)

z \ a	0.10	0.50	1.00	5.00	10.00
0.00	0.00	0.00	0.00	0.00	0.00
0.10	-0.13	-0.17	-0.22	-0.42	-0.50
0.20	-0.27	-0.36	-0.45	-0.90	-1.07
0.30	-0.43	-0.56	-0.71	-1.36	-1.60
0.40	-0.61	-0.78	-0.98	-1.80	-2.08
0.50	-0.80	-1.02	-1.25	-2.21	-2.53
0.60	-1.00	-1.27	-1.55	-2.61	-2.95
0.70	-1.22	-1.53	-1.85	-3.00	-3.36
0.80	-1.46	-1.81	-2.17	-3.40	-3.76
0.90	-1.71	-2.11	-2.50	-3.80	-4.17
1.00	-1.98	-2.42	-2.85	-4.21	-4.58
1.20	-2.57	-3.10	-3.59	-5.04	-5.42
1.40	-3.23	-3.84	-4.38	-5.90	-6.29
1.60	-3.96	-4.65	-5.24	-6.82	-7.21
1.80	-4.76	-5.53	-6.17	-7.79	-8.18
2.00	-5.64	-6.48	-7.15	-8.81	-9.20
2.50	-8.15	-9.16	-9.91	-11.64	-12.04
3.00	-11.14	-12.29	-13.08	-14.89	-15.29
3.50	-14.60	-15.88	-16.66	-18.60	-19.00

TABLE 3.4

ln W(t) for =»100 and different values of a as calculated from eq.(3.35)

z \ a	0.10	0.50	1.00	5.00	10.00
0.0	0.00	0.00	0.00	0.00	0.00
0.10	-0.13	-0.17	-0.22	-0.49	-0.64
0.20	-0.28	-0.36	-0.46	-1.01	-1.29
0.30	-0.43	-0.57	-0.72	-1.48	-1.84
0.40	-0.61	-0.79	-0.99	-1.91	-2.32
0.50	-0.80	-1.02	-1.26	-2.32	-2.77
0.60	-1.00	-1.27	-1.56	-2.73	-3.19
0.70	-1.22	-1.54	-1.86	-3.12	-3.60
0.80	-1.46	-1.82	-2.18	-3.51	-4.00
0.90	-1.71	-2.11	-2.51	-3.92	-4.41
1.00	-2.00	-2.43	-2.86	-4.32	-4.82
1.20	-2.57	-3.10	-3.60	-5.15	-5.65
1.40	-3.23	-3.84	-4.40	-6.02	-6.53
1.60	-3.96	-4.65	-5.25	-6.93	-7.45
1.80	-4.76	-5.53	-6.18	-7.90	-8.42
2.00	-5.64	-6.48	-7.10	-8.93	-9.44
2.50	-8.16	-9.17	-9.92	-11.76	-12.28
3.00	-11.14	-12.30	-13.09	-15.01	-15.53
3.50	-14.60	-15.89	-16.67	-18.71	-19.24

TABLE 3*5

ln W(t) for T = 1000 and different values of a as calculated from eq.(3.35)

z \ a	0.10	0.50	1.00	5.00	10.00
0.00	0.00	0.00	0.00	0.00	0.00
0.10	-0.13	-0.18	-0.23	-0.60	-0.94
0.20	-0.28	-0.37	-0.47	-1.13	-1.63
0.30	-0.43	-0.57	-0.73	-1.60	-2.18
0.40	-0.61	-0.79	-0.99	-2.03	-2.66
0.50	-0.80	-1.02	-1.27	-2.45	-3.10
0.60	-1.00	-1.27	-1.56	-2.85	-3.53
0.70	-1.22	-1.54	-1.87	-3.24	-3.94
0.80	-1.46	-1.82	-2.19	-3.63	-4.34
0.90	-1.71	-2.12	-2.52	-4.04	-4.75
1.00	-1.98	-2.43	-2.87	-4.44	-5.16
1.20	-2.57	-3.10	-3.61	-5.27	-5.99
1.40	-3.23	-3.85	-4.40	-6.14	-6.87
1.60	-3.96	-4.66	-5.26	-7.06	-7.78
1.80	-4.76	-5.54	-6.19	-8.02	-8.75
2.00	-5.64	-6.49	-7.17	-9.05	-9.78
2.50	-8.16	-9.17	-9.93	-11.88	-12.61
3.00	-11.14	-12.30	-13.09	-15.13	-15.87
3.50	-14.60	-15.89	-16.68	-18.84	-19.57

TABLE 3.6

In W(z) for different values of a as calculated from eq.(3.51)

z \ a	0.01	0.10	0.30	L.50	0.80
0.00	-0.00	-0.00	-0.00	-0.00	-0.00
0.10	-0.12	-0.13	-0.15	-0.18	-0.21
0.20	-0.25	••Oc 27	-0.32	-0.37	-0.43
0.30	-0.40	-0.43	-0.50	-0.57	-0.67
0.40	-0.56	-0.61	-0.70	-0.79	-0.92
0.50	-C.7 4	-0.80	-0.91	-1.02	-1.18
0.60	-0.93	-1.00	-1.14	-1.27	-1.45
0.70	-1.14	-1.22	-1.39	-1.54	-1.74
0.80	-1.36	-1.46	-1.65	-1.82	-2.05
0.90	-1.61	-1.71	-1.92	-2.12	-2.37
1.00	-1.86	-1.98	—2.22	-2.43	-2.71
1.20	-2.43	-2.57	-2.85	—3 • 10	-3.42
1.40	-3.06	-3« 23	-3.56	-3.85	-4.20
1.60	-3.77	-3.96	-4.34	-4.66	-5.05
1.80	-4.54	-4.76	-5.19	-5.54	-5.96
2.00	-5.39	-5.64	-6.11	-6.49	-6.93
2.50	-7.84	-8.16	-8.13	-9.17	-9.67
3.00	-10.76	-11.14	-11.81	-12.31	-12.84
3.50	-14.16	-14.60	-15.36	-15.90	-16.44

Conte!....

TABLE 3.6 contd.

z \ a	1.00	3.00	5.00	8.00	10.00
0.00	-0.00	-0.00	-0.00	-0.00	-0.00
0.10	-0.23	-0.43	-0.62	-0.85	-0.99
0.20	-0.47	-0.84	-1.14	-1.49	-1.68
0.30	-0.73	-1.24	-1.61	-2.02	-2.23
0.40	-1.00	-1.62	-2.05	-2.49	-2.71
0.50	-1.27	-2.00	-2.46	-2.92	-3.16
0.60	-1.57	-2.37	<2 • 86	-3.35	-3.58
0.70	-1.87	-2.75	-3.26	-3.75	-3.99
0.80	-2.19	-3.13	-3.65	-4.16	-4.39
0.90	-2.52	-3.51	«-4* 05	-4.56	-4.80
1.00	-2.87	-3.90	-4.46	-4.97	-5.21
1.20	-3.60	-4.71	-5.29	-5.80	-6.05
1.40	-4.40	-5.58	-6.15	-6.68	-6.92
1.60	-5.26	-6.48	-7.07	-7.59	-7.84
1.80	-6.19	-7.45	-8.04	-8.56	-8.81
2.00	-7.17	-8 • 47	-9.06	-9.59	-9.83
2.50	-9.93	-11.90	-11.90	-12.42	-12.67
3.00	-13.10	-14.55	-15.15	-15.68	-15.93
3.50	-16.69	-18.25	-18.86	-19.39	-19.63

TABLE 3.7

Specifications of some switching diodes* available commercially

S.No.	Switching Diode	Manufacturer	trr (ns)	I_F (mA)	PIV (Volts)
1.	SD 40	BEL	20	100	40
2.	1N914	NGEF	2	10	100
3.	SHI 51	NGEF	2	10	30
4.	CD61	CDIL	20	15	12
5.	CDS 2	CDIL	20	15	12
6.	CD63	CDIL	20	10	20
7.	CA40 to CA79**	CDIL	4	10 to 100	25 to 100
e.	EA40 to EA59**	E.C.	4	10 to 20	25 to 100
9.	BA22O to BA222 and BA316 to BA318**	Philips	4	75 to 200	10 to 50
10.	BAW62	Philips	4	100	75
11.	1N4009 to 1N4448**	Philips	2 to 4	75 to 200	25 to 75

trr « Reverse Recovery Time

I_F - Forward Current (average)

PIV = Peak Inverse Voltage.

*This is only a representative list. There may be some more switching diodes in the list of the manufacturers mentioned Zlrr- There are many other manufacturers also offering s^Uar devices.

**For details of each diode, please see the manufacturers data sheet.

TABLE 3.8

A summary of results obtained by OCVD method

S.No.	Device	Series resistances R_s (ohms)	Coupling Drop ΔV_c (Volts)	a	Minority carrier lifetime τ_B (microseconds)
1.	Silicon Diode (BY127)	0.24	0.027	1.1	11
				0.1	8
2.	Germanium Diode (DR25)	1.06	0.013	1.1	16
				0.1	11
3.	Silicon Solar Cell (SC4)	1.55	0.024	1.1	30
				0.1	20

Figure Captions

Fig. 3.1 A representative circuit for OCVD experiment, S is a switch, R is a current limiting resistor, D is the diode under test and V is the voltage source.

Fig. 3.2 A typical OCVD of a p-n junction diode. Current is switched off at t = 0. $v_{\perp}$ is the initial sharp drop.

Fig. 3.3 Approximate profiles of excess carrier concentrations in a forward biased diode with base and emitter widths much larger than the diffusion length of minority carriers in the respective regions.

Fig. 3.4 In W(t) as a function of z for T - o - 2 *as* predicted by eq.(3.35). The three curves shown are for different values of *a' i.e. o.l, l.o, io.o.

Fig. 3.5 In h (t) as a function of z^'U 50 as predicted by eq.(3.35). The three curves shown are for different values of 'a' i.e. o.l, l.o, lo.O.

Fig. 3.6 ln v(t) as a function of z for ® 1000 as predicted by eq.(3.35). The three curves shown are for different values of 'a' i.e. 0.1, 1.0, 10.0

Fig. 3.7 In w(t) as a function of z (= 2 t/ τ_B) for

t> 2 as predicted by eq. (3.35) . The three

curves shown are for different values of ‘a’

!•€?• Oel; 1.0, lO.O.

Fig. 3.8 In WCt) as a function of z (= t/^$_B$) for T ^=50 2

as predicted by eq.(3.35). The three curves

shown are for different values of ’a’, i.e. 0.1,

1.0, 10.0.

Fig. 3.9 In w(t) as a function of z^2 (= t/^$_B$) for

T « 1000 as predicted by eq.(3.35). The three

curves shown are for different values of •a*

i«e« 0«l# 1*0/ lO.O.

Fig. 3.10 in w(t) as a function of z for three different

values of a (i.e. 0.1, l.o, 10.0) as predict^

by eq.(3.51).

Fig. 3.11 In W(t) as a function of z^2 ($_s$ +./_ , ' I for three$_B$'

different values of a (i,$_e$. o 1 i • -• 1*0 and lo.o)

as predicted by eq.(3.51),

Fig. 3.12 calculated open circuit voltage decay curve in

a p-n diode (for a . 5 and T_0 . $_{27}$ microseconds).

Points indicate experimental results of

Neugroschel et. al. (13).

x ig. 3.13 (a) Circuit to stucJvOCVD. V_p is a pulse generator, S.D. is a switching diode and R i_s the current limiting resistor.

(b) waveshape of the time varying voltage available at the output of pulse generator. On right side is shown the voltage observed across the diode terminals.

Fig. 3.14 Open circuit voltage decay of a silicon diode (BY127). Current passing through the device (before t = 0) is very low (of the order of microampere).

Fig. 3.15 Open circuit voltage decay of a silicon diode (BY127). Current passing through the device (before t « 0) is approximately 20 microamperes

Fig. 3.16 Open circuit voltage decay of a silicon diode (BY127). Current passing through the device (before t=0) is 0.5 mA.

Fig. 3.17 0Pen circuit: voltage decay of a silicon diode (BY127). Current passing through the device *(before* t»0) is 3 mA.

Fig. 3.18 *Open* circuit voltage decay of a silicon diode (BY127). Current passing through the device (befoi'e t=»0) is 9 mA.

Fig. 3.19 Open circuit voltage decay of a silicon diode (BY127). Current passing through the device (before t=o) is 21 mA.

Fig. 3.20 Open circuit voltage decay of a silicon solar cells (SC4). Current passing through the device (before t=0) is 0.4 mA.

Fig. 3.21 Open ciicult voltage decay of a silicon solar cell (SC4). Current passing through the device (before t«0) is 6.5 mA.

Fig. 3.22 Open circuit voltage decay of a silicon solar cell (SC4). Current passing through the device (before ts»O) is 17 mA,

Fig. 3.23 Open circuit voltage decay of a silicon solar cell (SC4). Current pacing through the device (before t»0) is 54 mA.

Fig. 3.24 Geome?r?.l details of the silicon solar cell (SC4) used m present investigation.

Fig. 3.25 Open circuit voltage decay of a geraanium diode (DR25). Current passing through the device (*before* t=0) is 3 mA.

Fig. 3.26 Open circuit voltage decay of a germanium diode (DR25). Current passing through the device (before t«0) is 23 mA.

Fig. 3.27 Open circuit voltage decay of a germanium diode *(DR25)*• Current passing through the device (before t=0) is 58 mA.

Fig. .J.28 Initial voltage drop (curve 'a') and apparent series resistance (curve 'b') of BY127 (silicon diode) as a function of injection current. Dotted portion of curve *a» indicates linear extrapolation to zero current.

Fig. 3. 29 Initial voltage drop of silicon diode (BY127) with a small resistance added to it. .Values of added resistors are 1.54, 3.27, 4.64 and 5.49 ohms respectively for curves a, b, c and d.

Fig. 3.30 *Initial voltage drop of silicon solar cell (SC4) with respect to* injection current.

Fig. 3.31 initial voltage drop of germanium diode (DR25) with respect to Injection current.

Fig. 3. *32 Slope of the curves shown in* *9• 3 • 29 *function of the* added added *resistance.* resistance *Inter*With *R* a r ® a =0 *a 3xis* represents *is 0,23 ohm,*

Fig. 3.33 Initial voltage drop (for forward current 8 mA) as a function of added series resistance (R_a). At R_a = 0.24, initial voltage drop is 0.265.

— 3.3. — -tage drop as a function of current for the results reported in (14).

Fig. 3.35 calculated open circuit voltage decay curves. Parameters for curve *A» are a - i 2 and T_{fi} = 11 *microseconds and those for* curve *B* are a = 0.1 and = 8 microseconds, Points indicate *experimental results of* W127 (silicon *diode)* after subtracting series resistance contribution.

fig. 3.36 *Calculated open* circuit voltage decay curves *for a 1,1 and* "B ' 16 "—seconds (curve ,A>) *and a e o,l and* T_a = 11 microseconds (curv. ,B'h *Points indicate experimental* results of DR25 *(germanium diode) after subtracting series resistance contribution.*

Fig. 3.37 Calculated open circuit voltage decay curves *for a* « 1*1 and (. B " 30 microseconds* (curve *A*) *and* a « 0.1 and *B ~ 20 microseconds* (curve 'B') *Points indicate experimental results of* silicon *golar cell (SC'4)* after subtracting series resistance *contribution.*

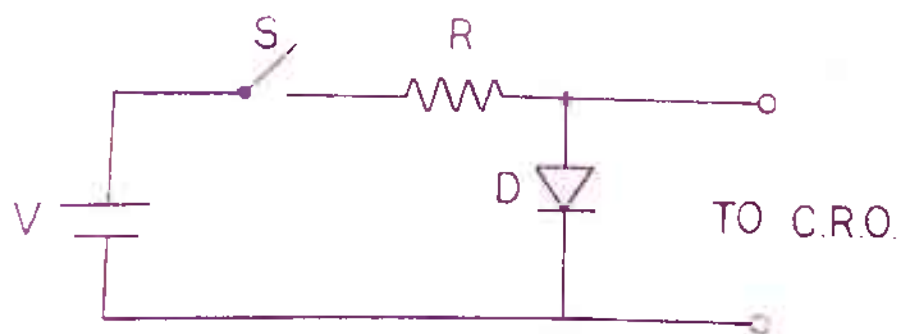

FIG. 3.1

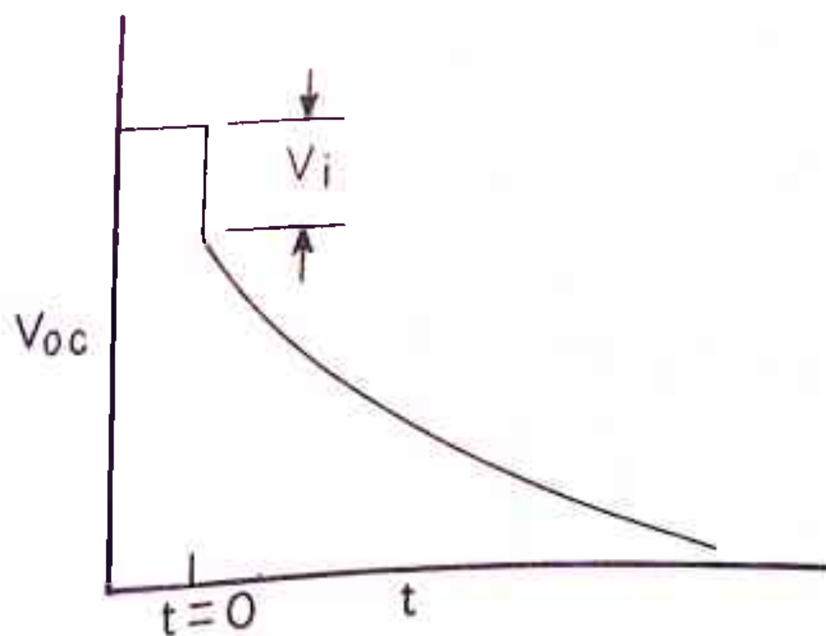

FIG.3.2

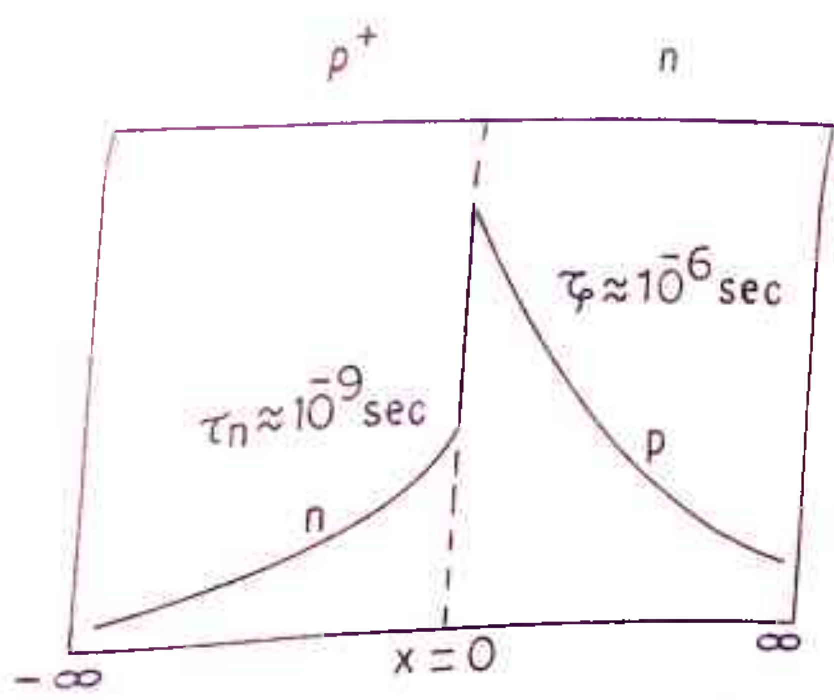

FIG.3-3

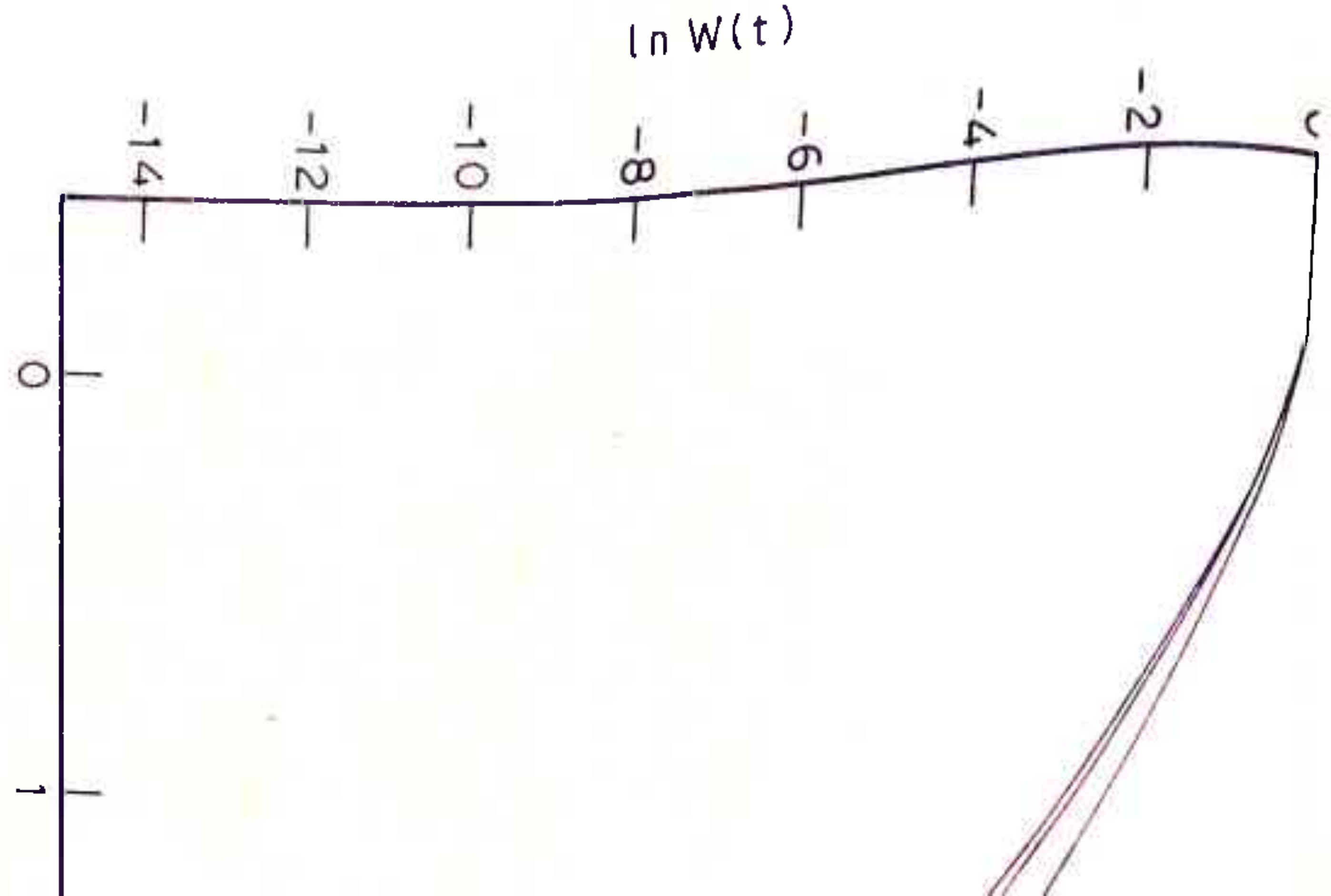
ln W(t)
-14
-12
-10
-8
-6
-4
-2
0
1

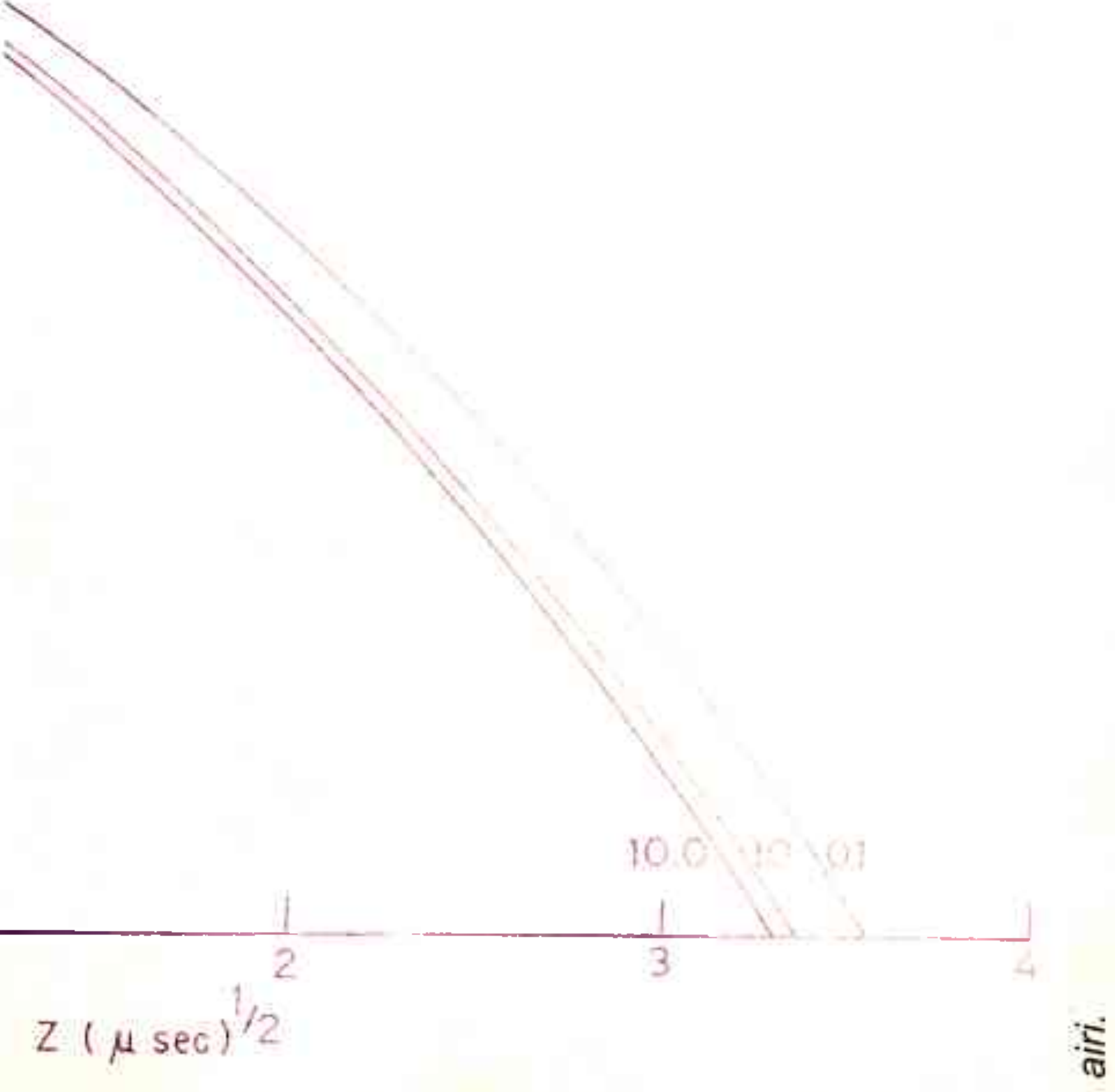

FIG.3.4

airi.

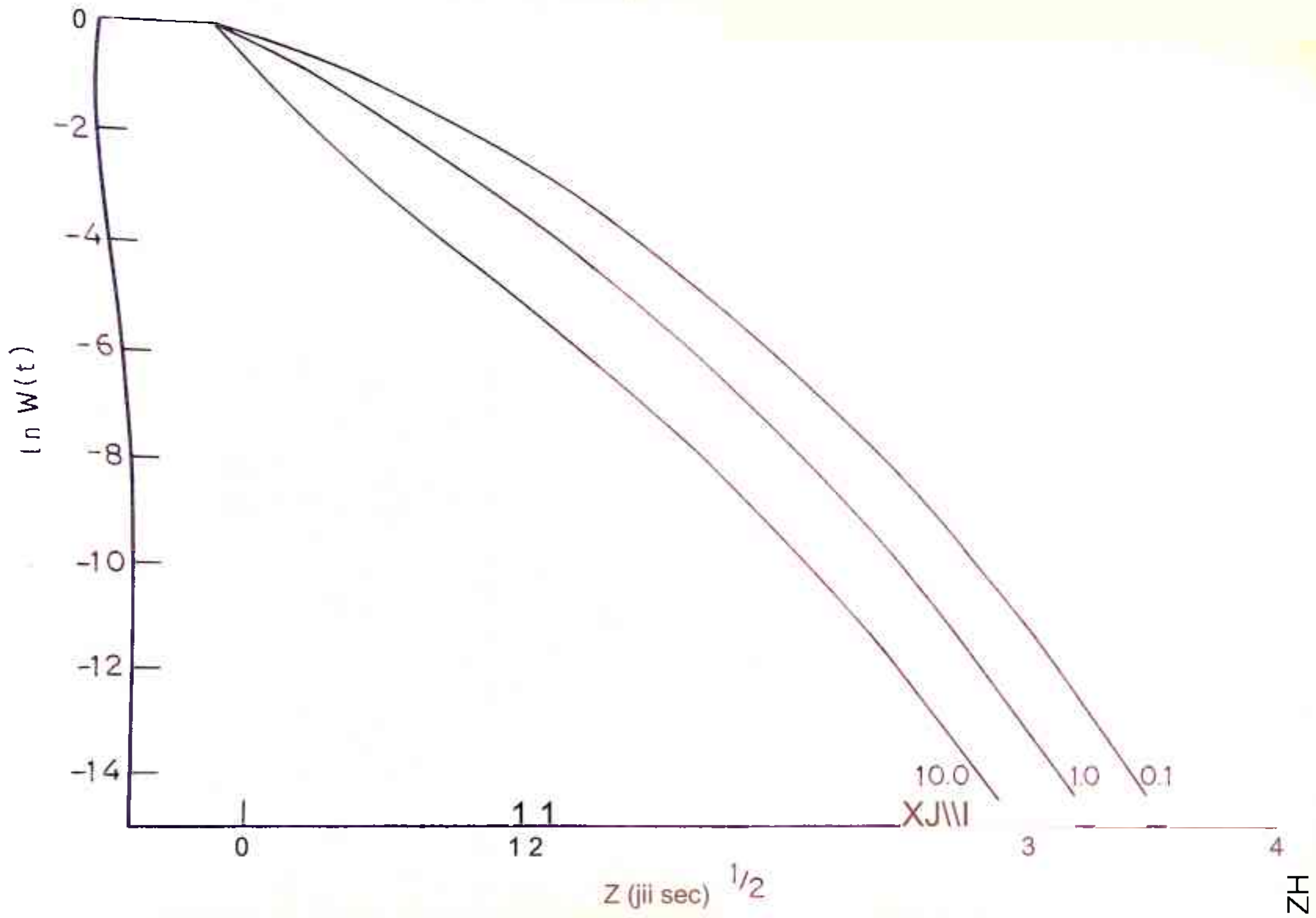

FIG. 3.5

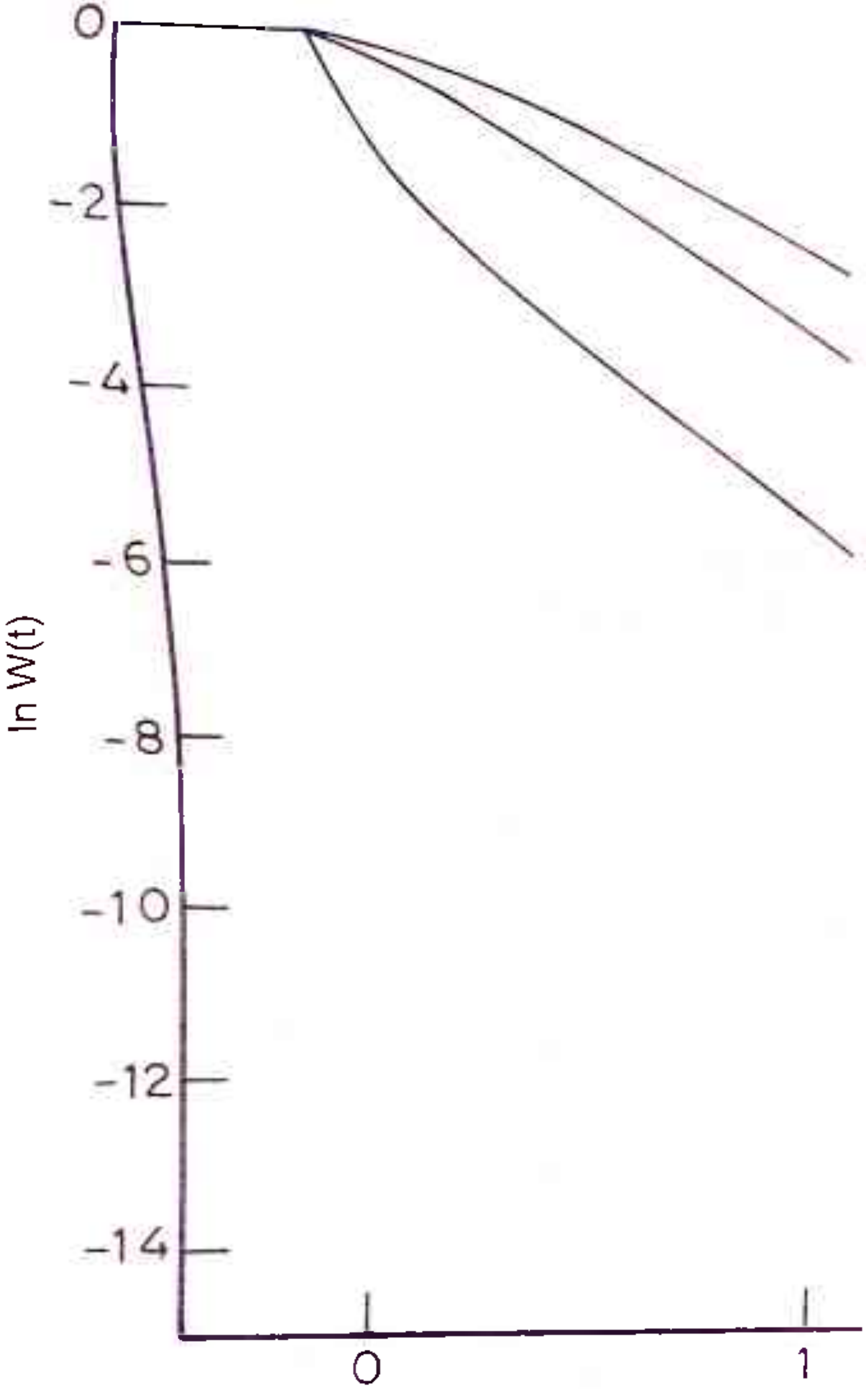
ln W(t)
0
-2
-4
-6
-8
-10
-12
-14
0
1

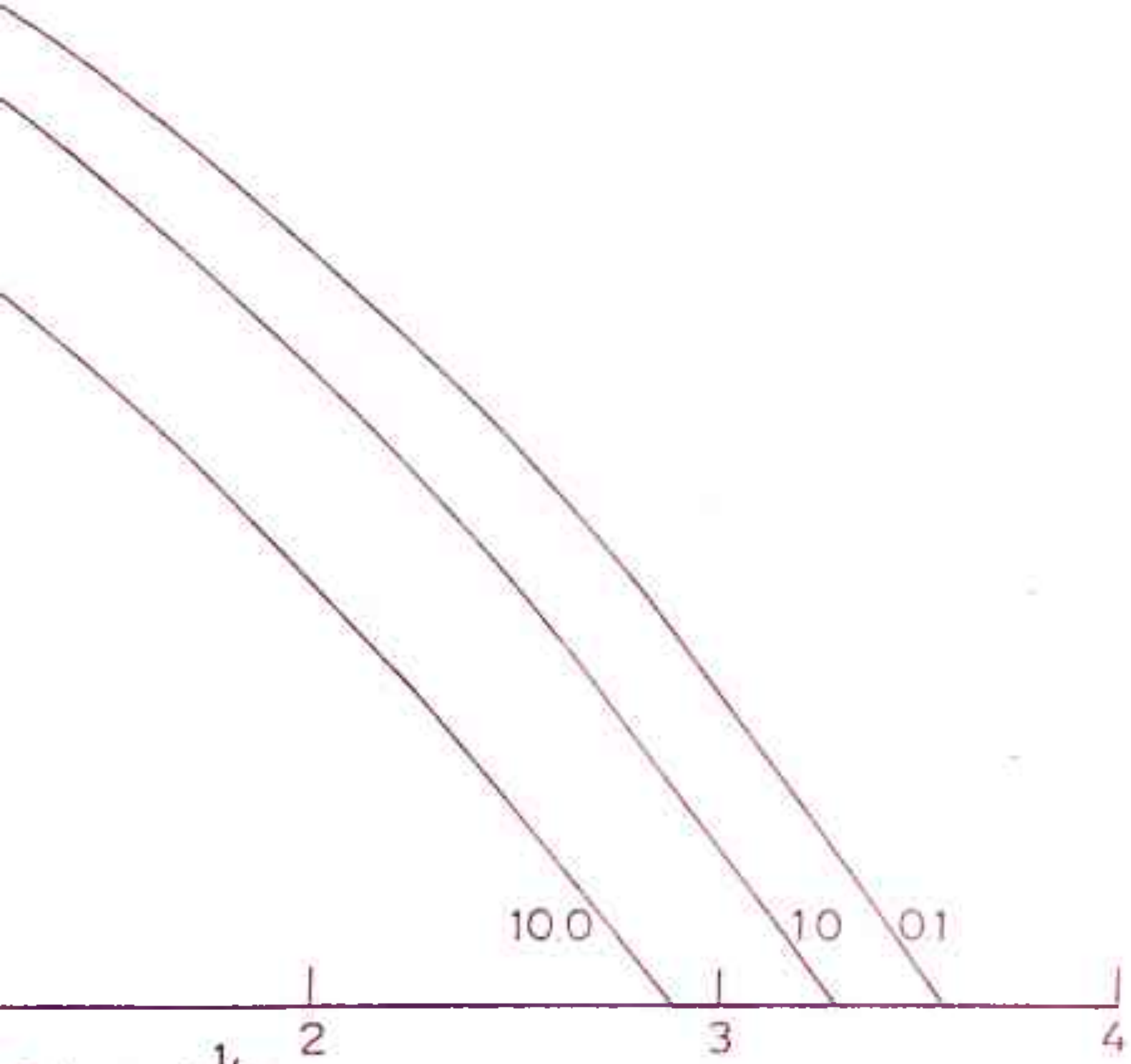

FIG. 3.6

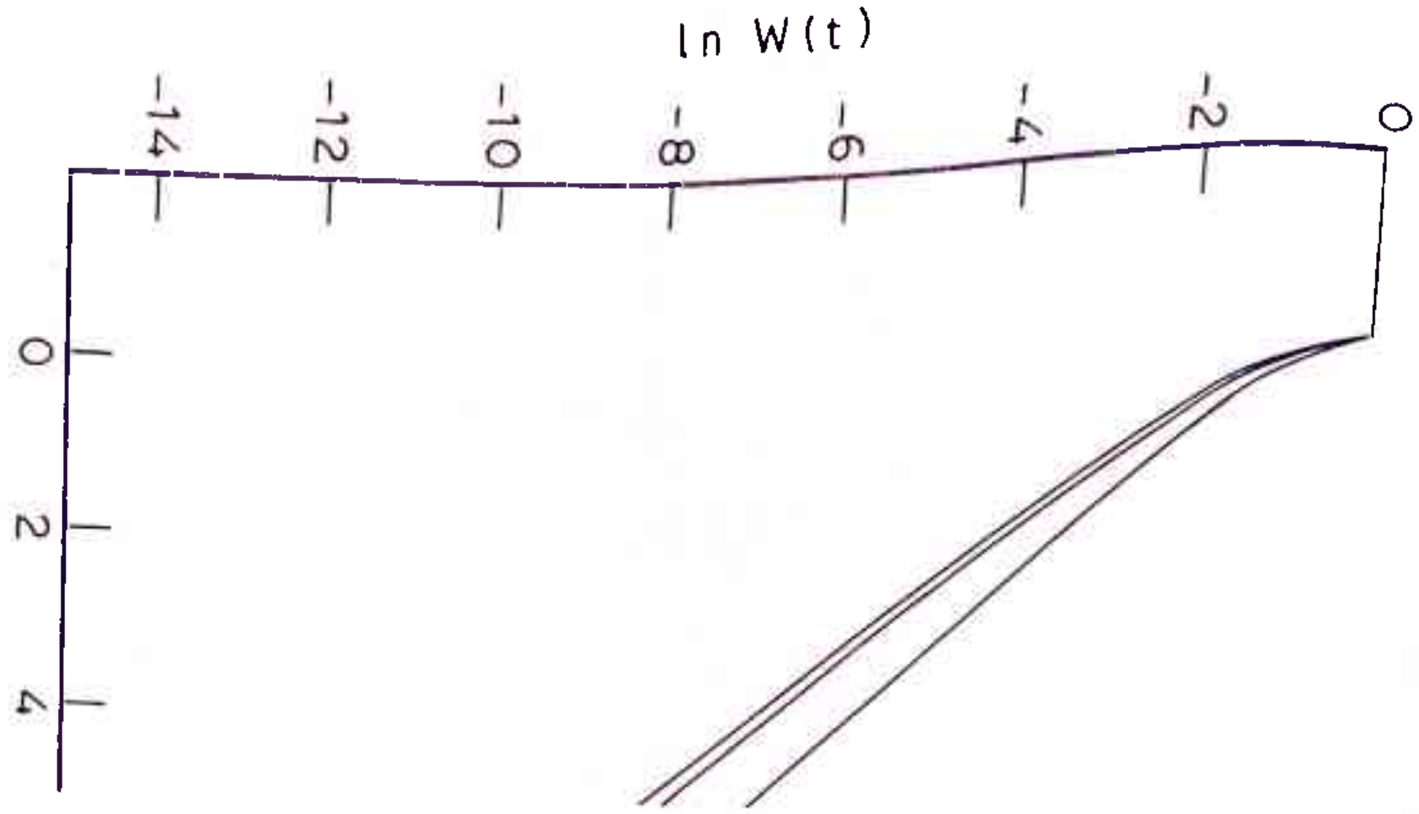

ln W(t)
-14
-12
-10
-8
-6
-4
-2
0
0
2
4

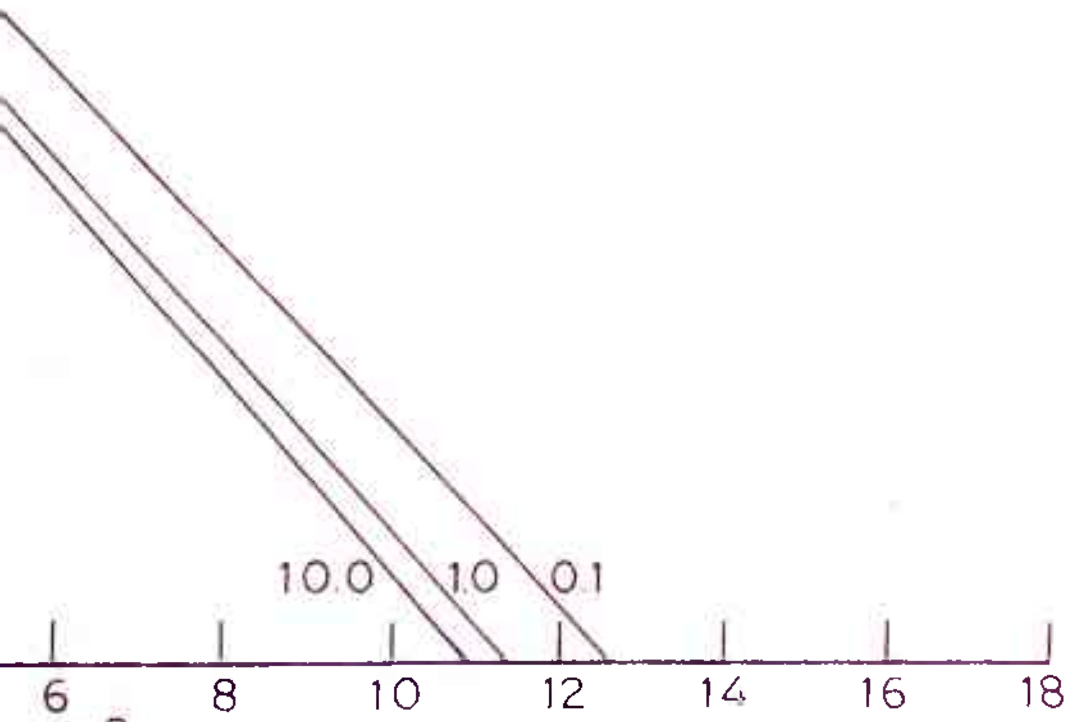

FIG. 3.7

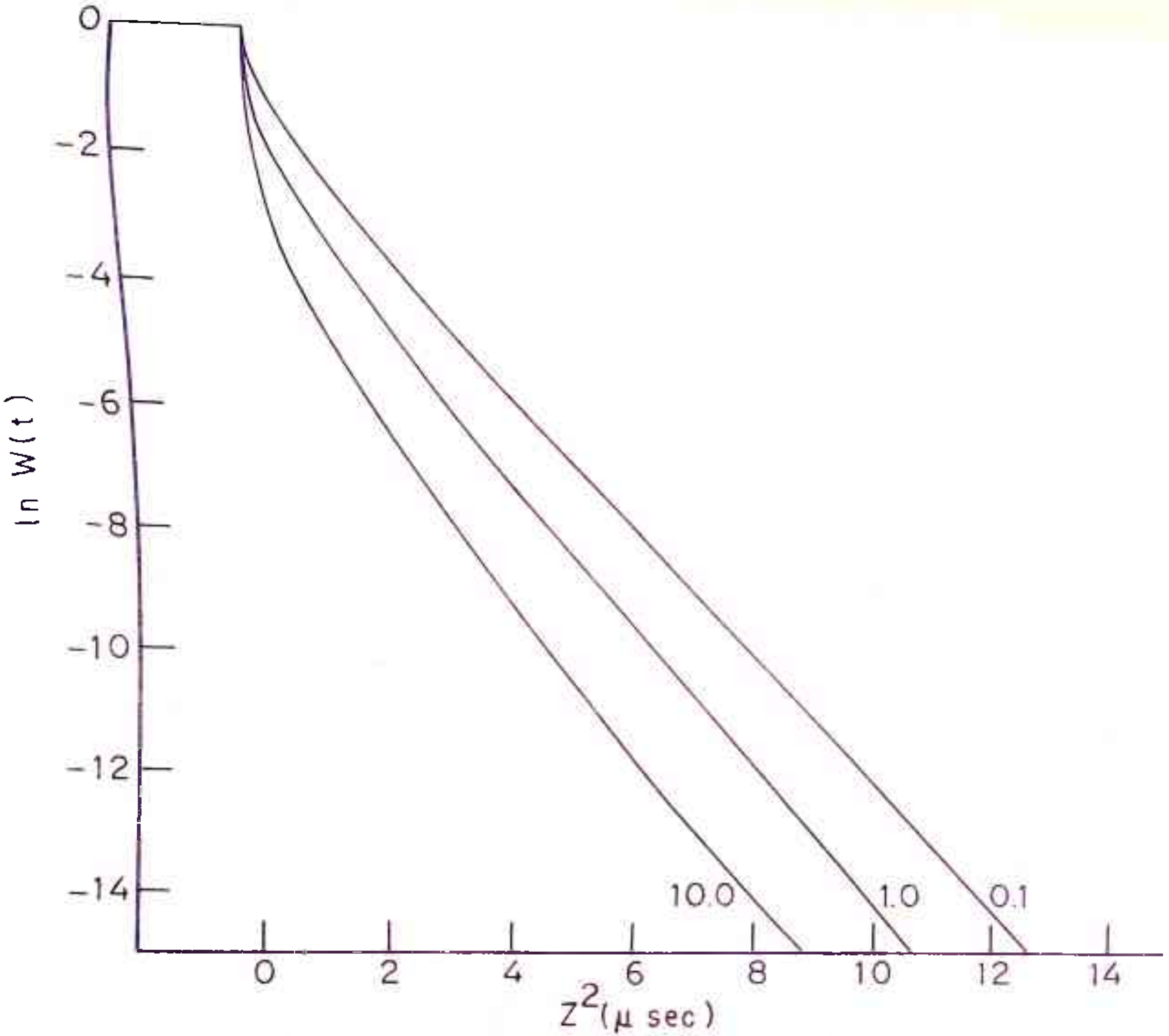

FIG.3.8

osr

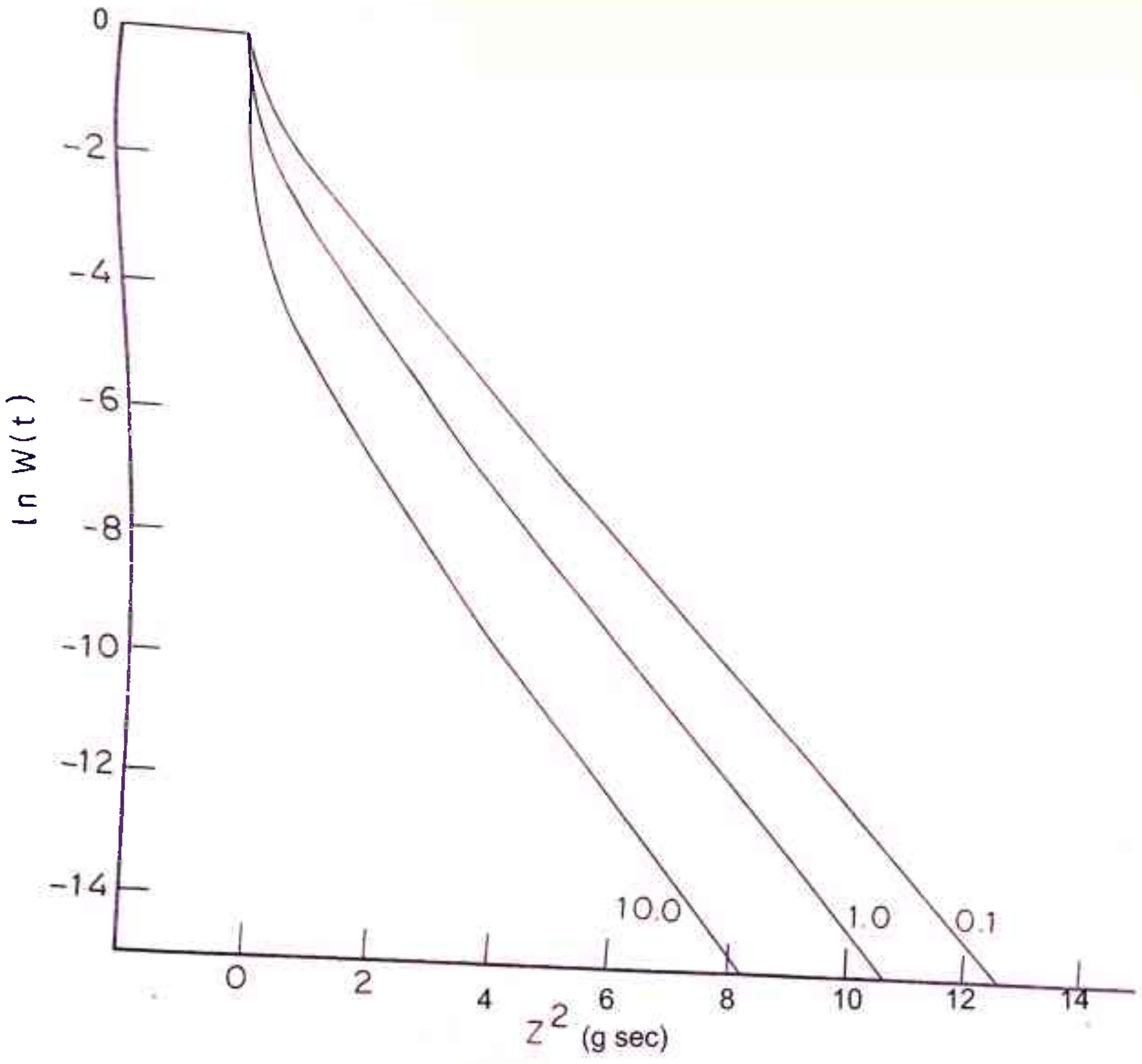

FIG.3.9

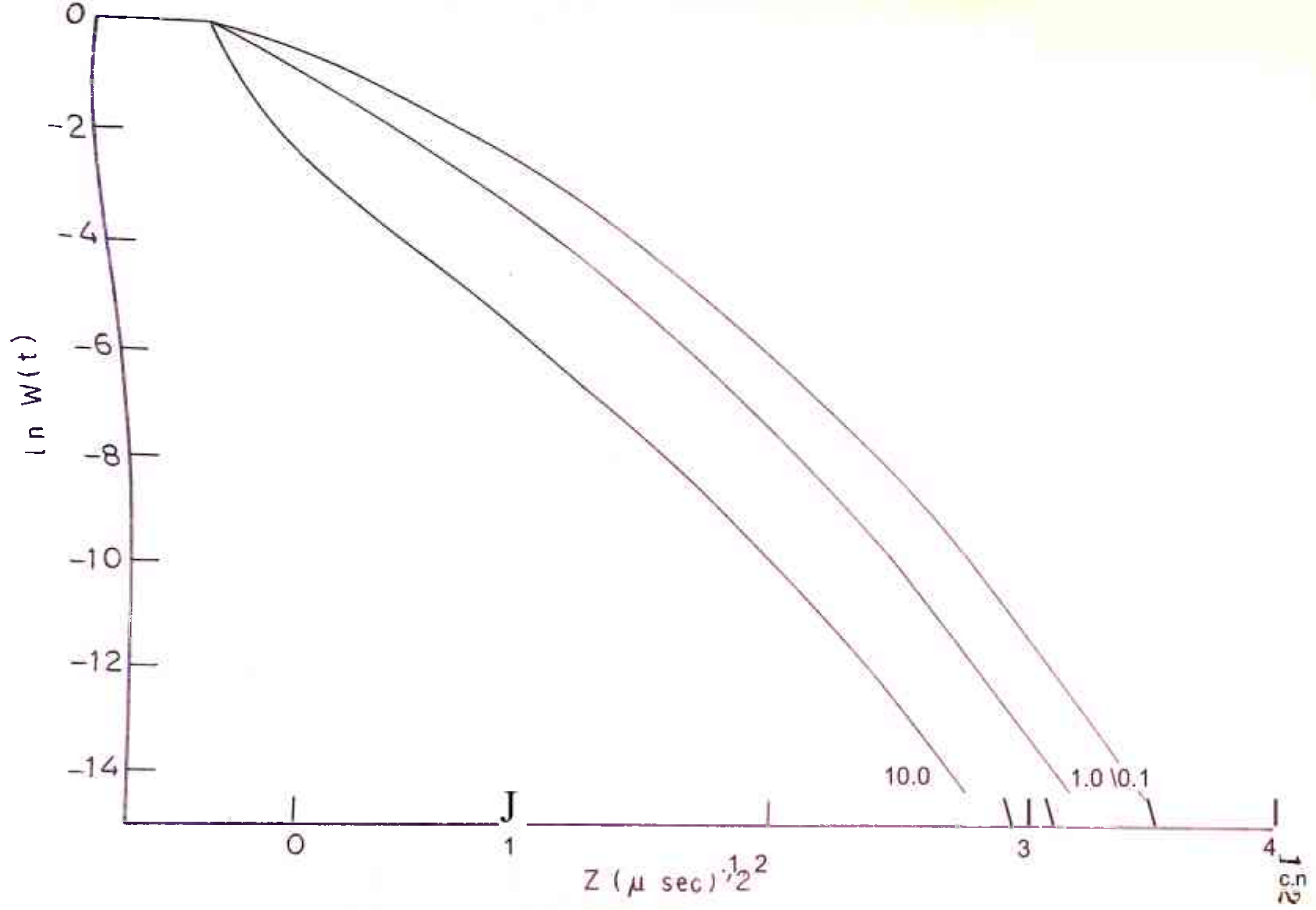

FIG. 3. 10

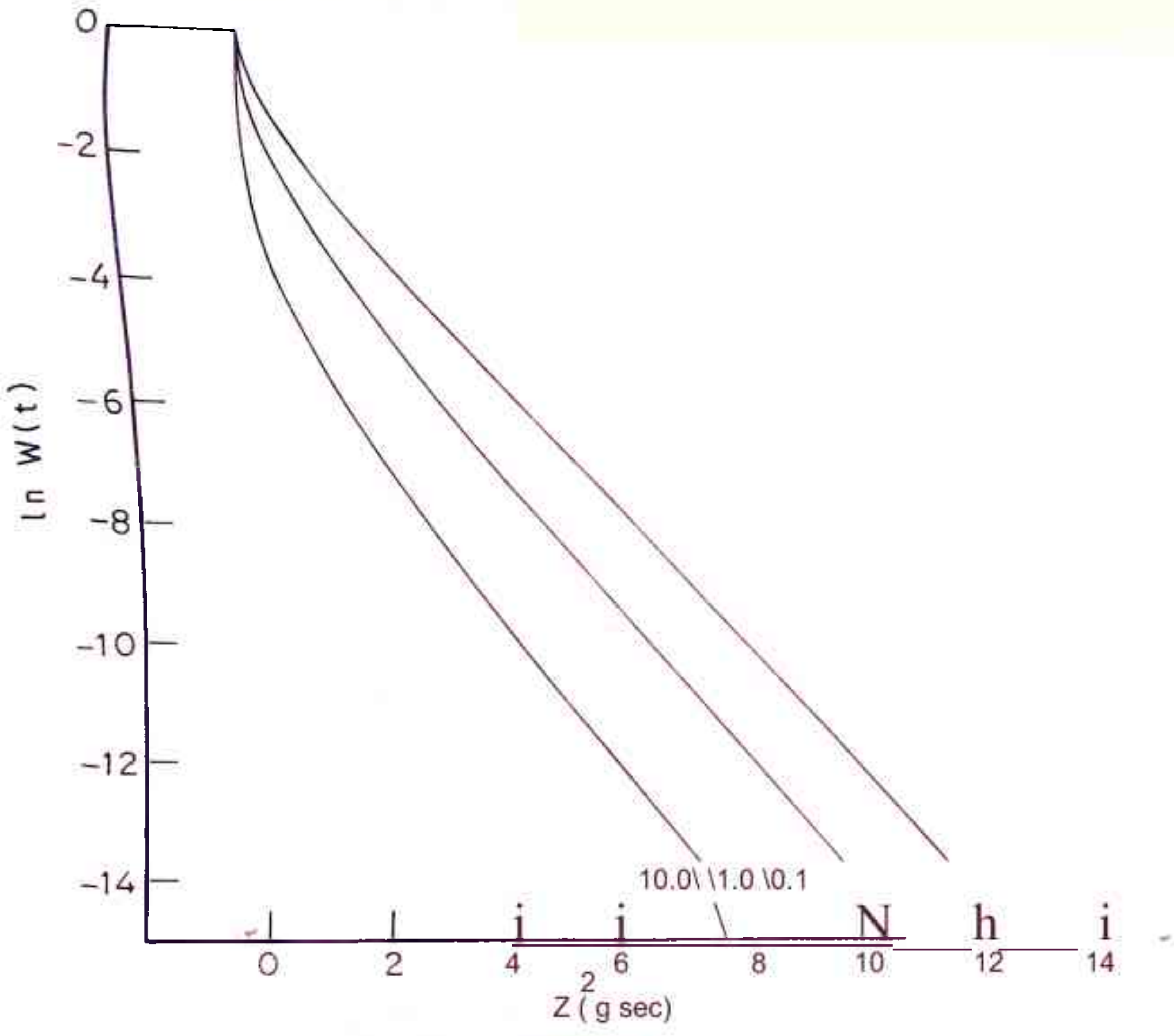

FIG. 3.11

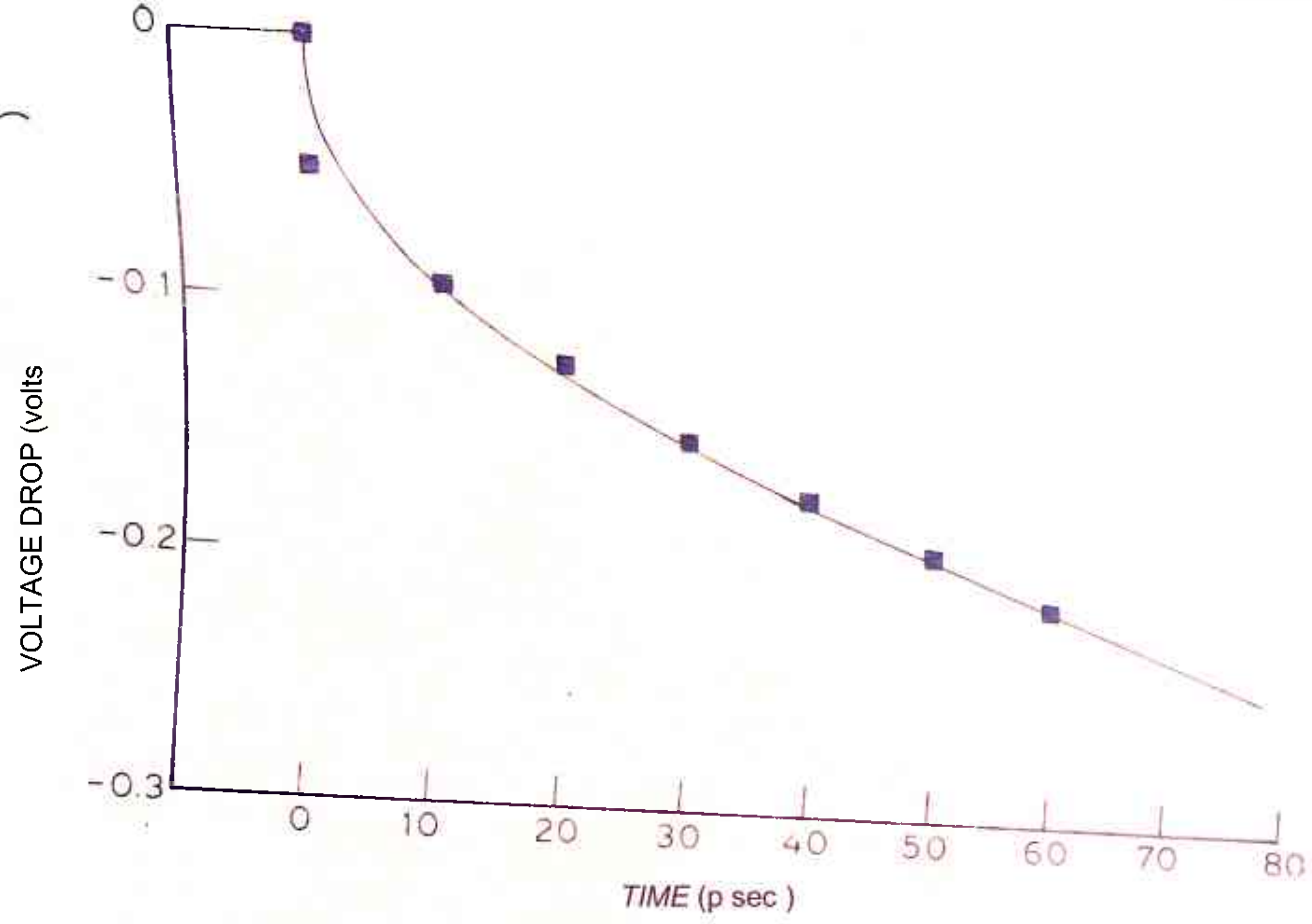

FIG. 3.12

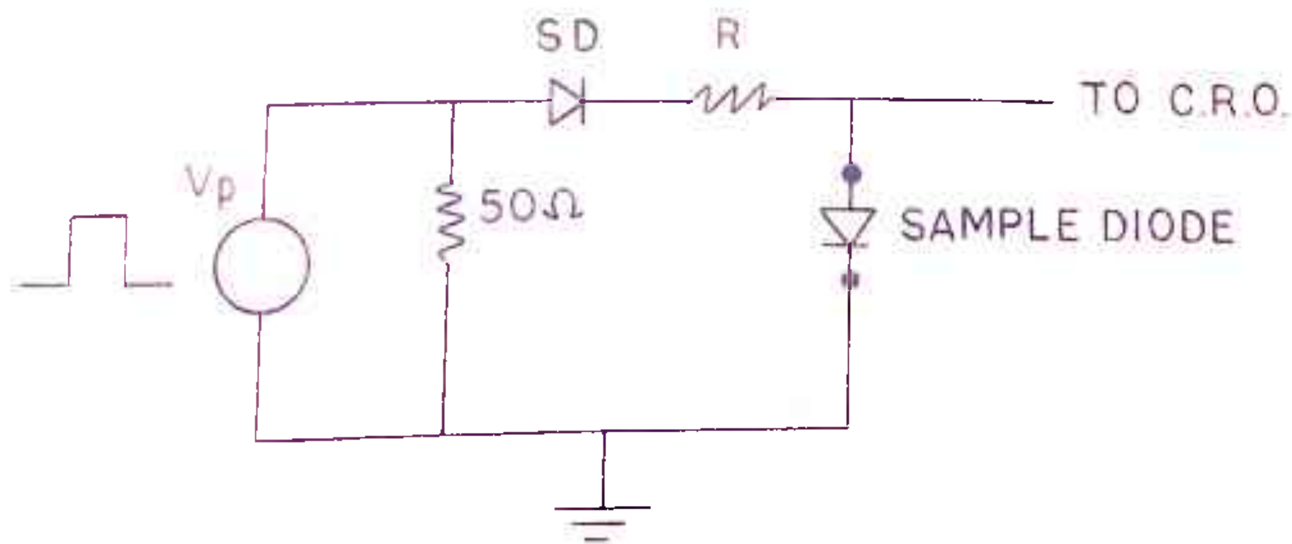

FIG5.13 (a)

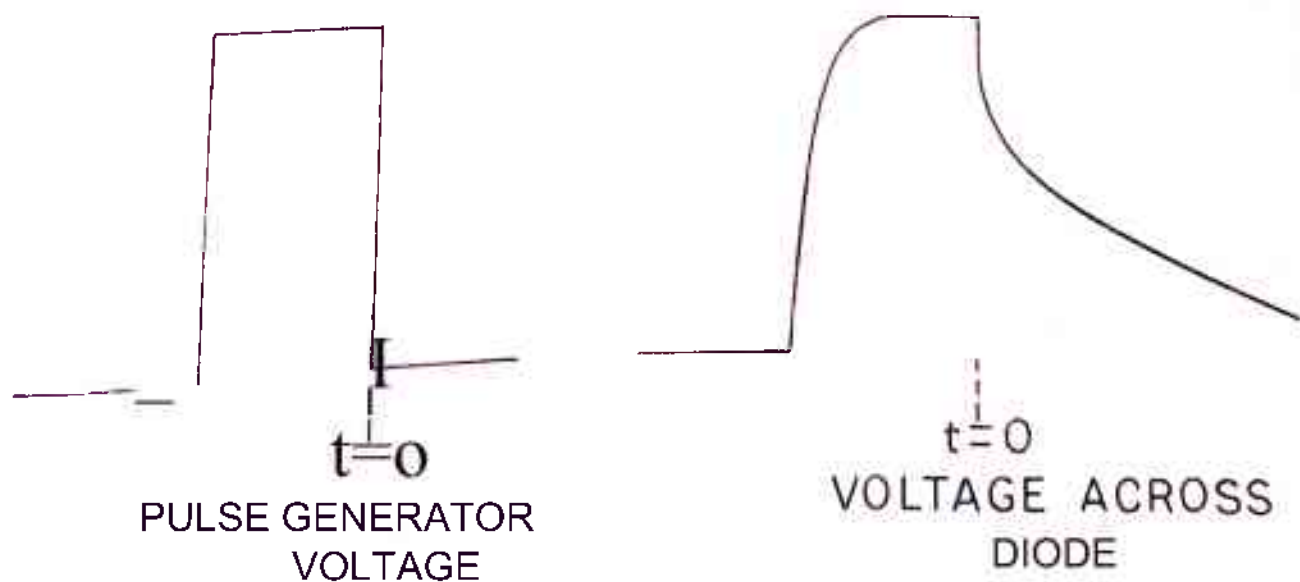

FIG3.13 (b)

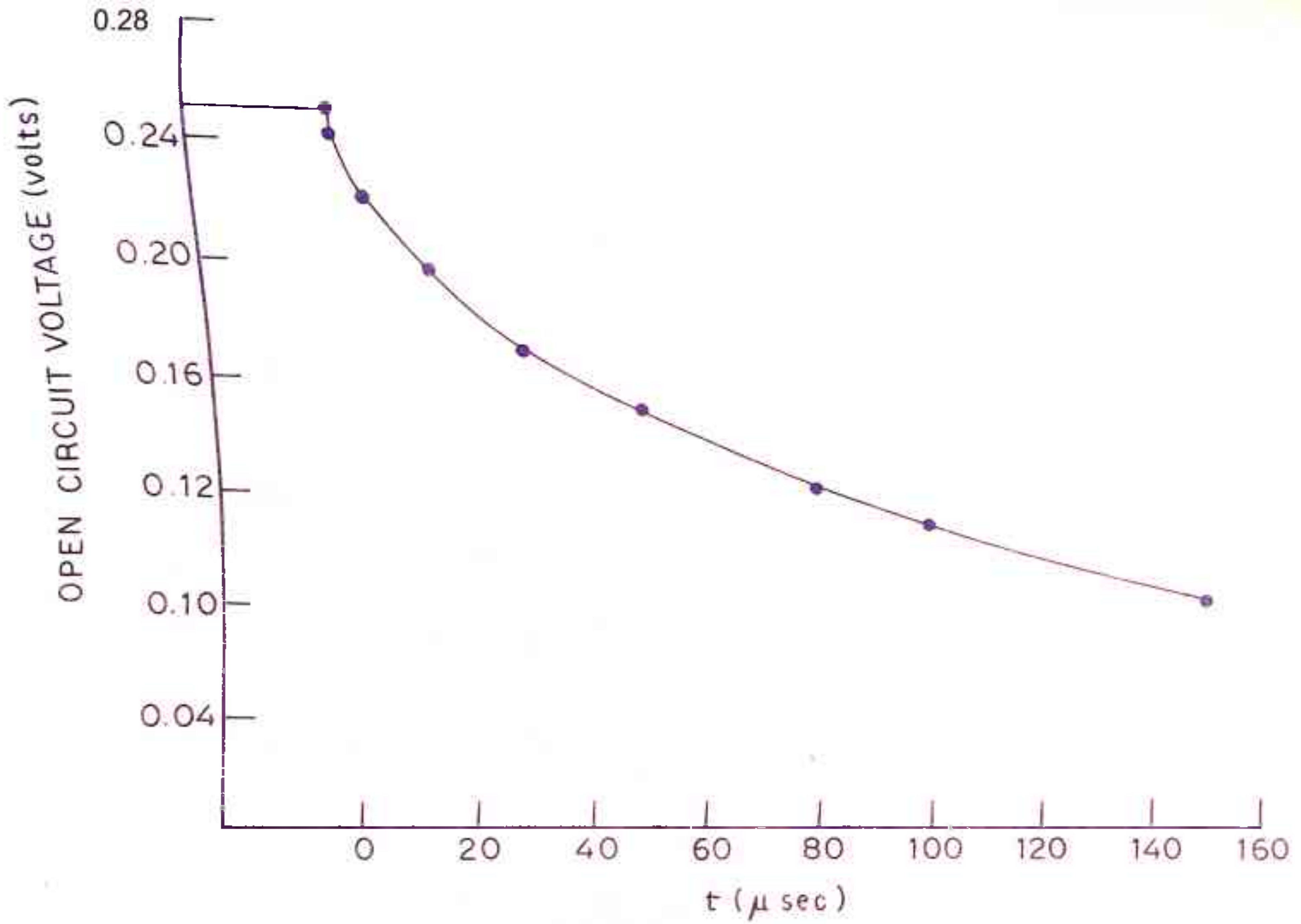

FIG. 3.14

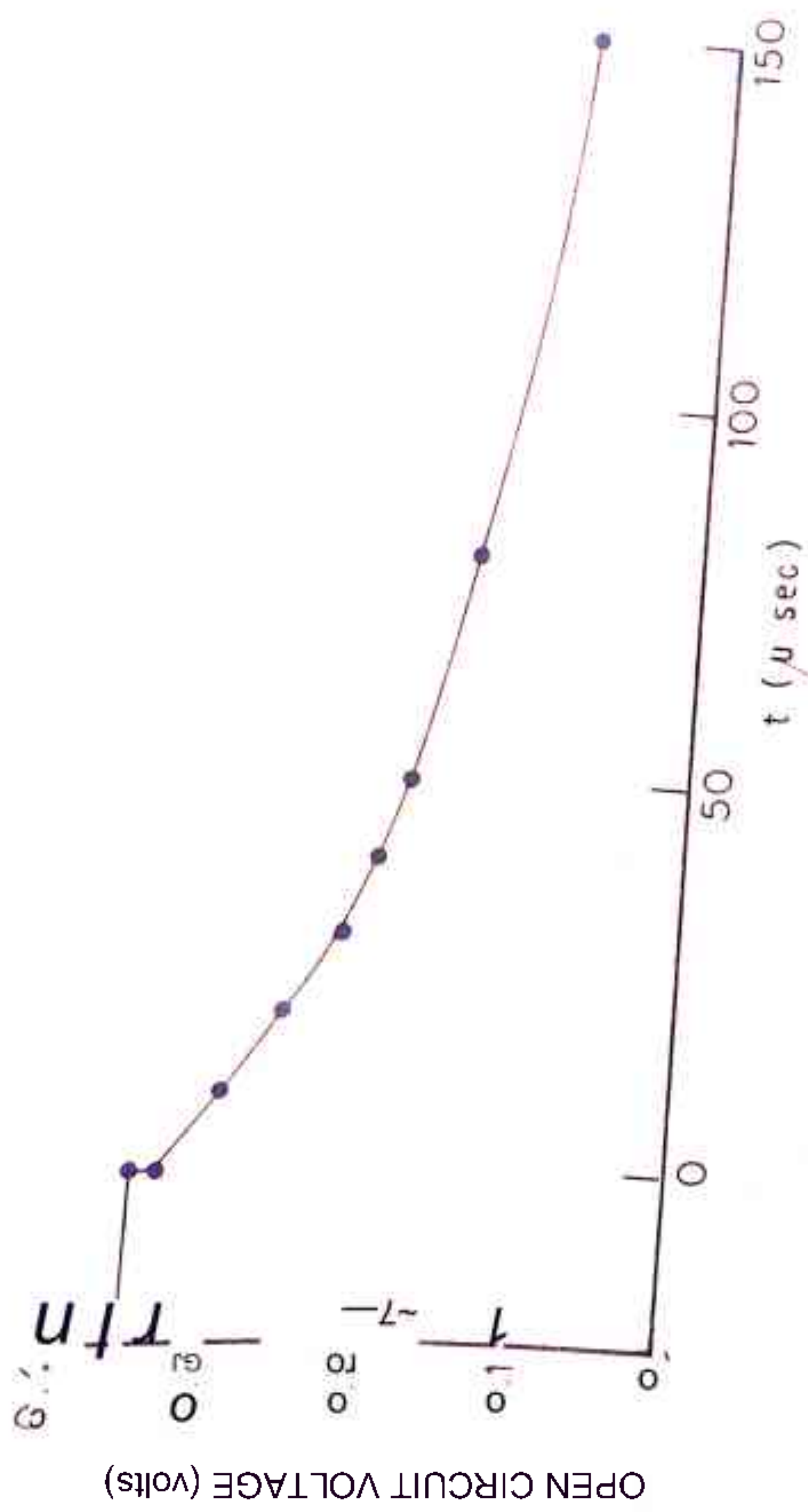

FIG. 3.15

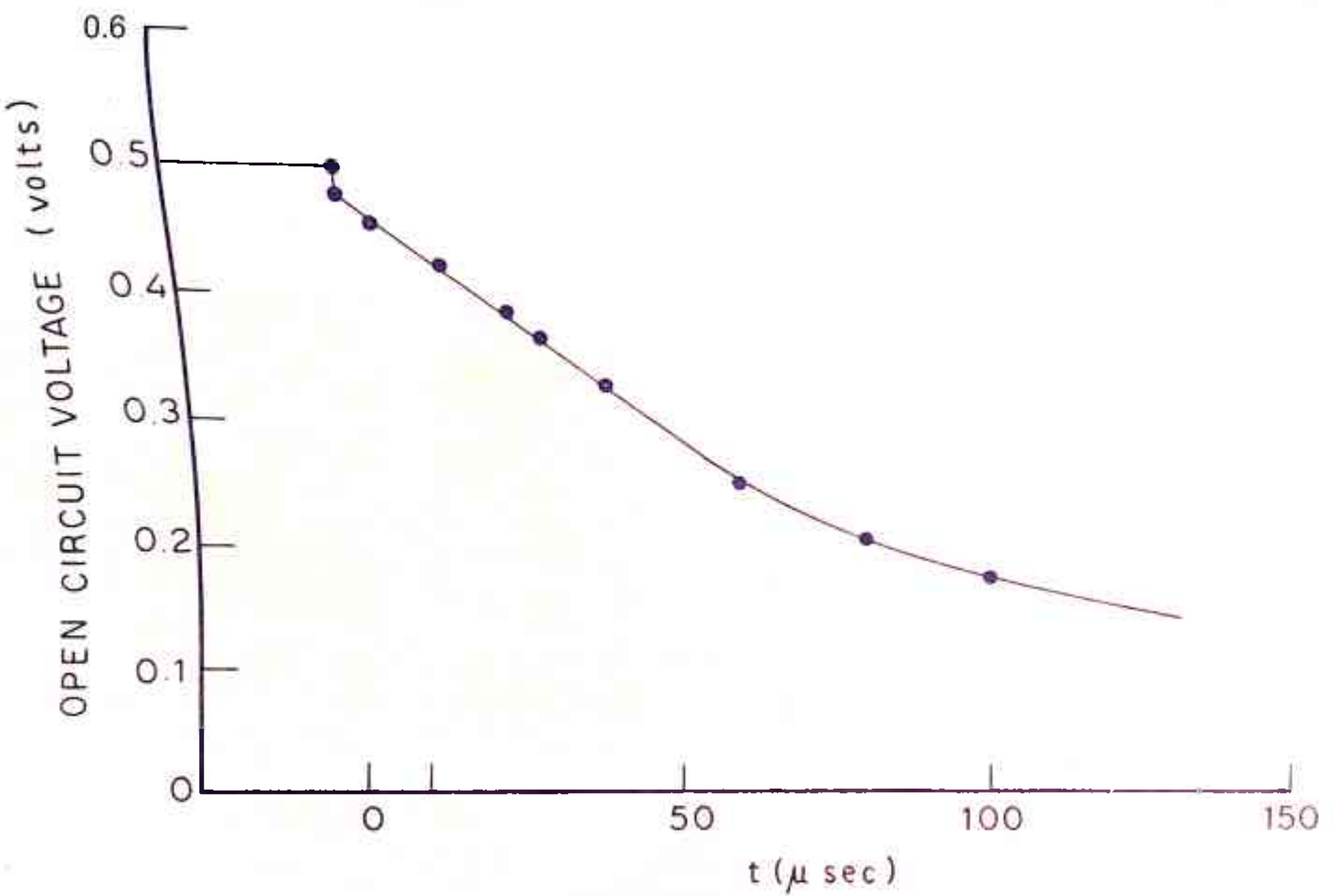

FIG. 3.16

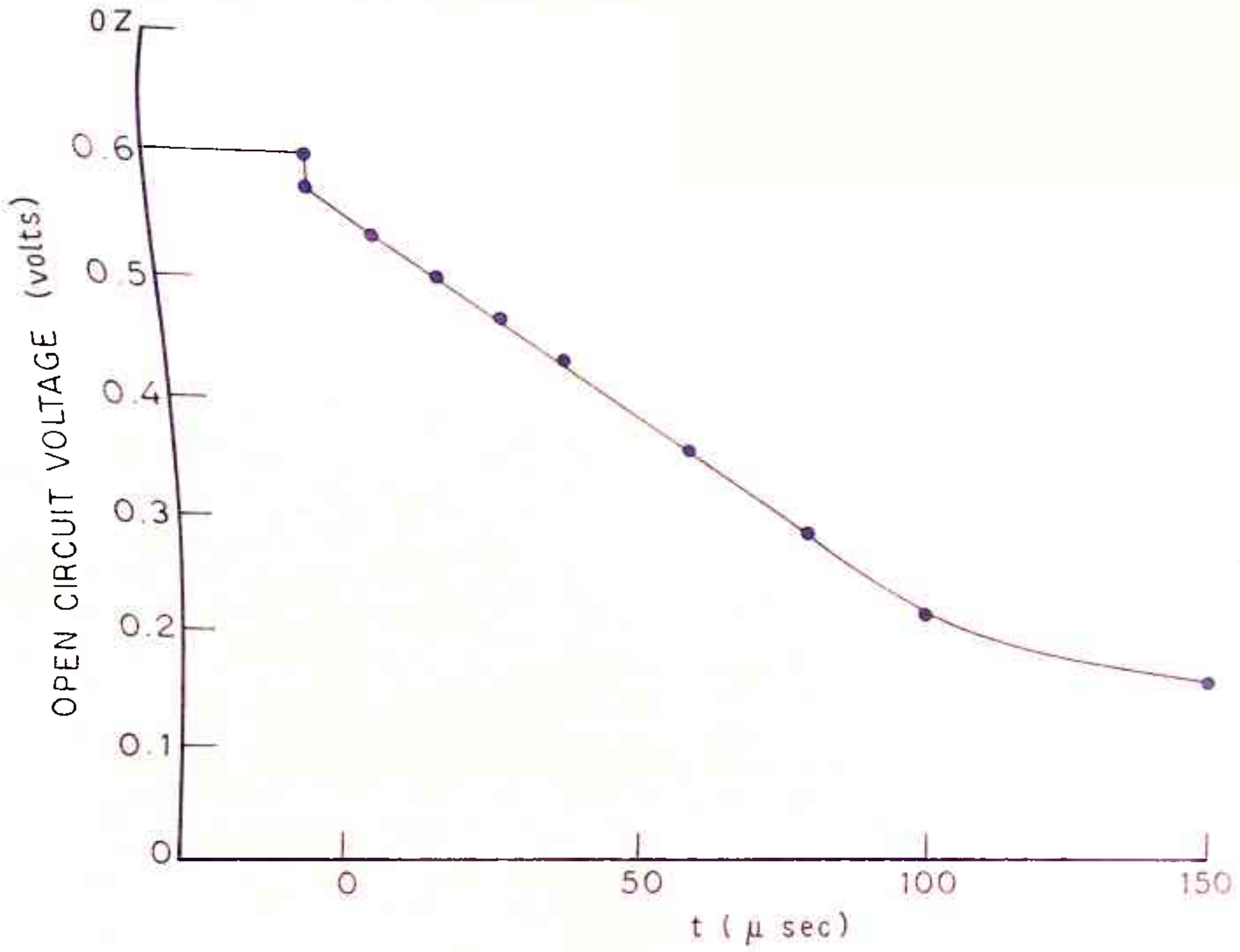

FIG. 3.17

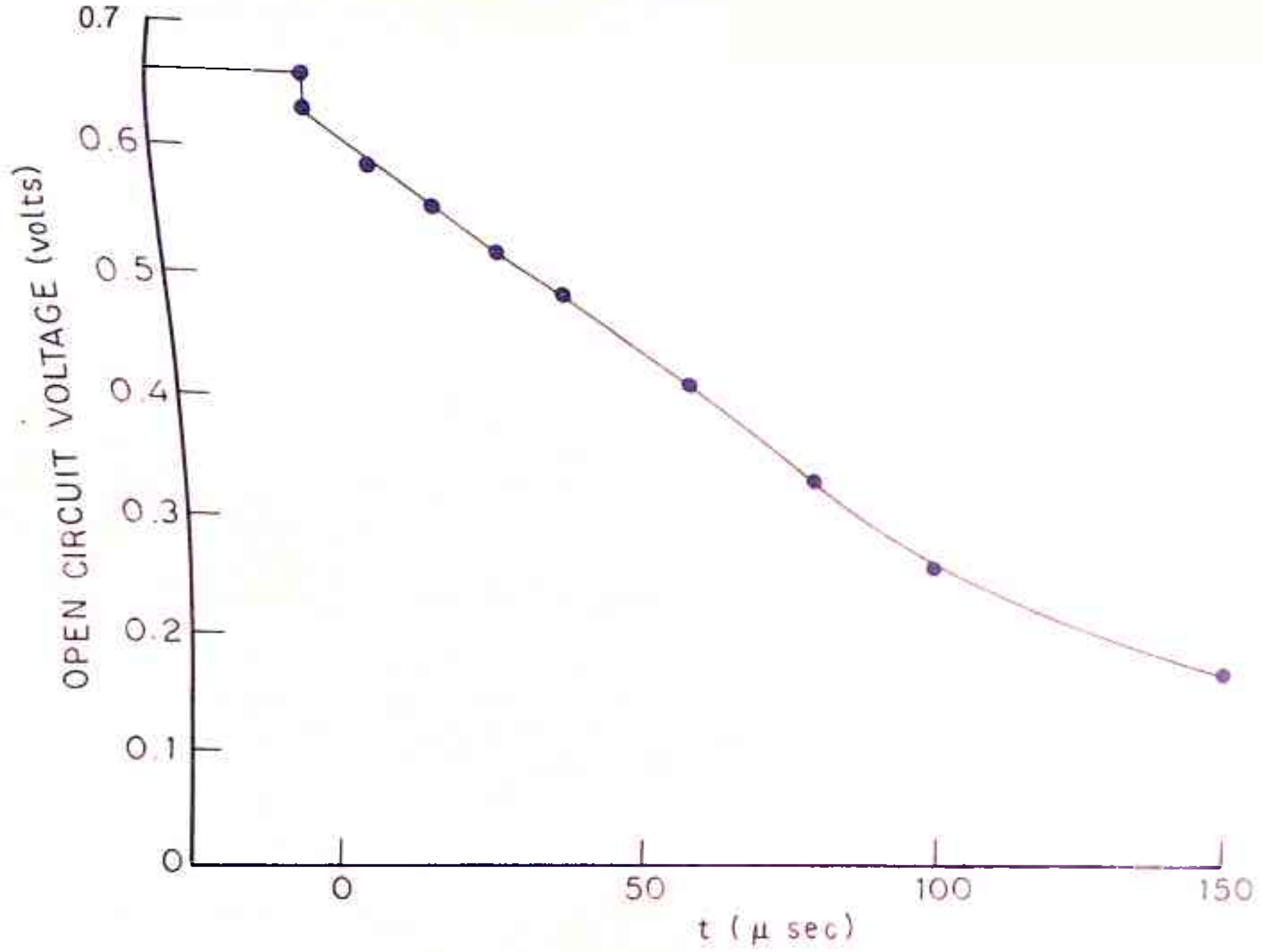

FIG. 3.18

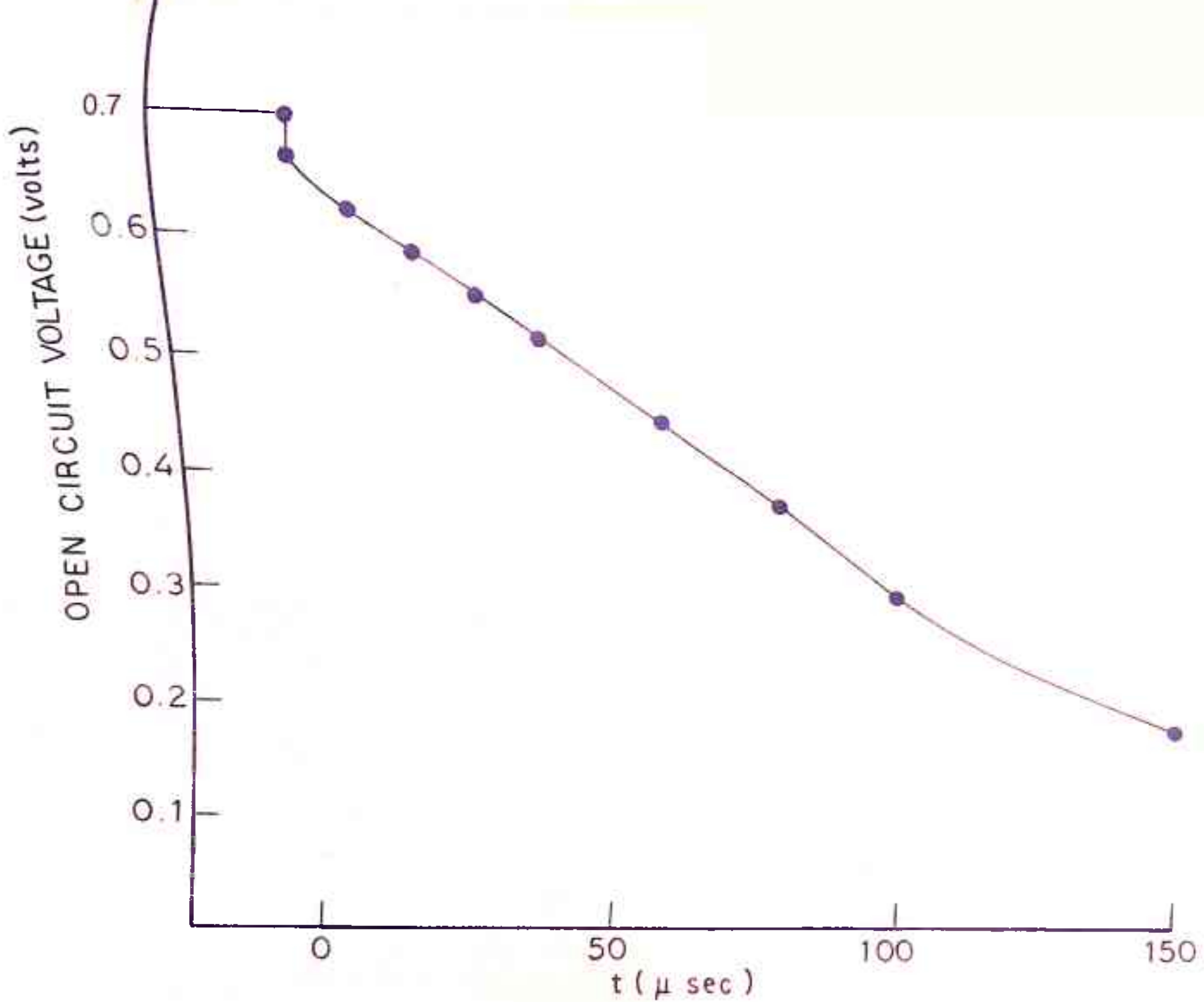

FIG.3.19

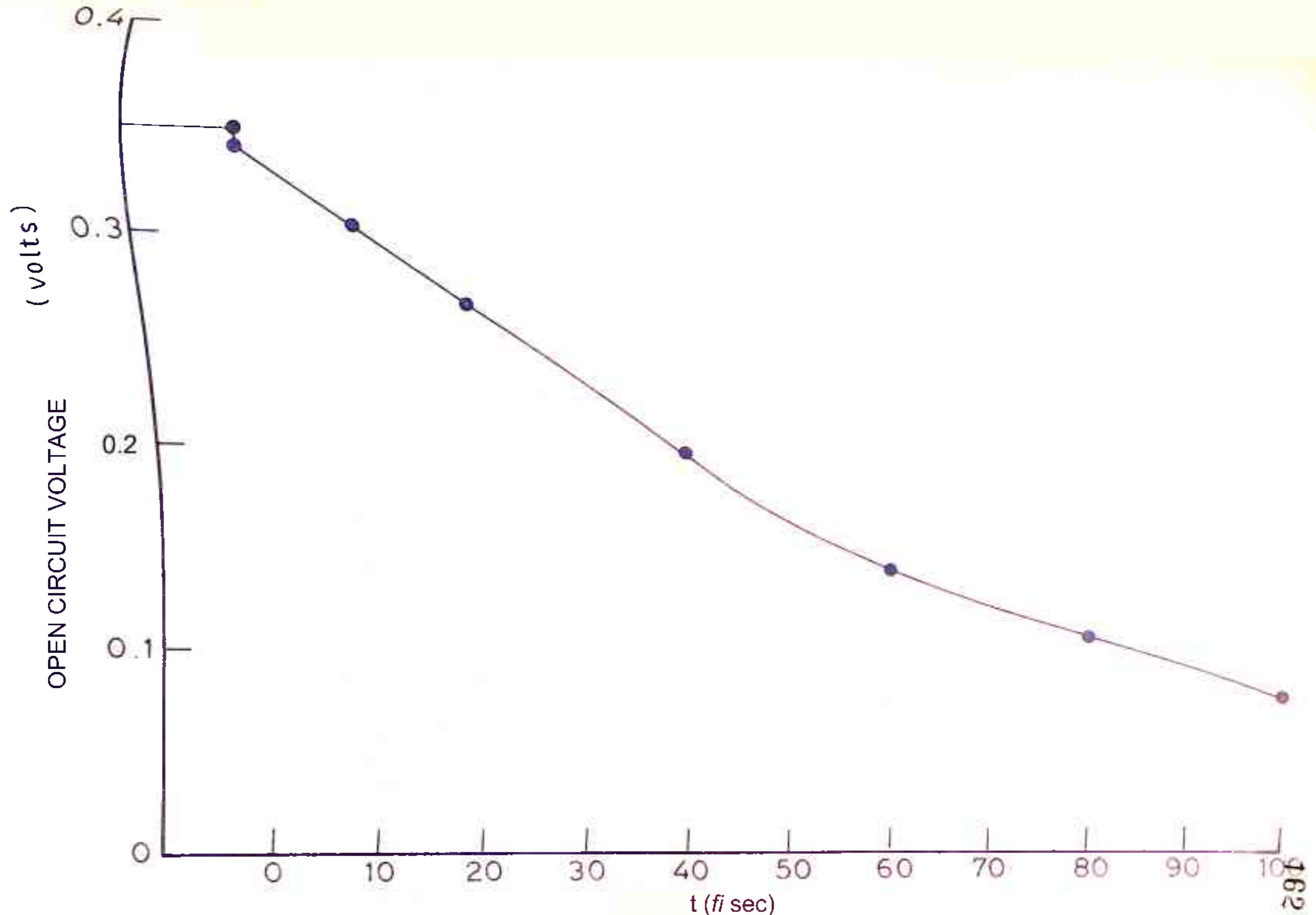

FIG.3.20

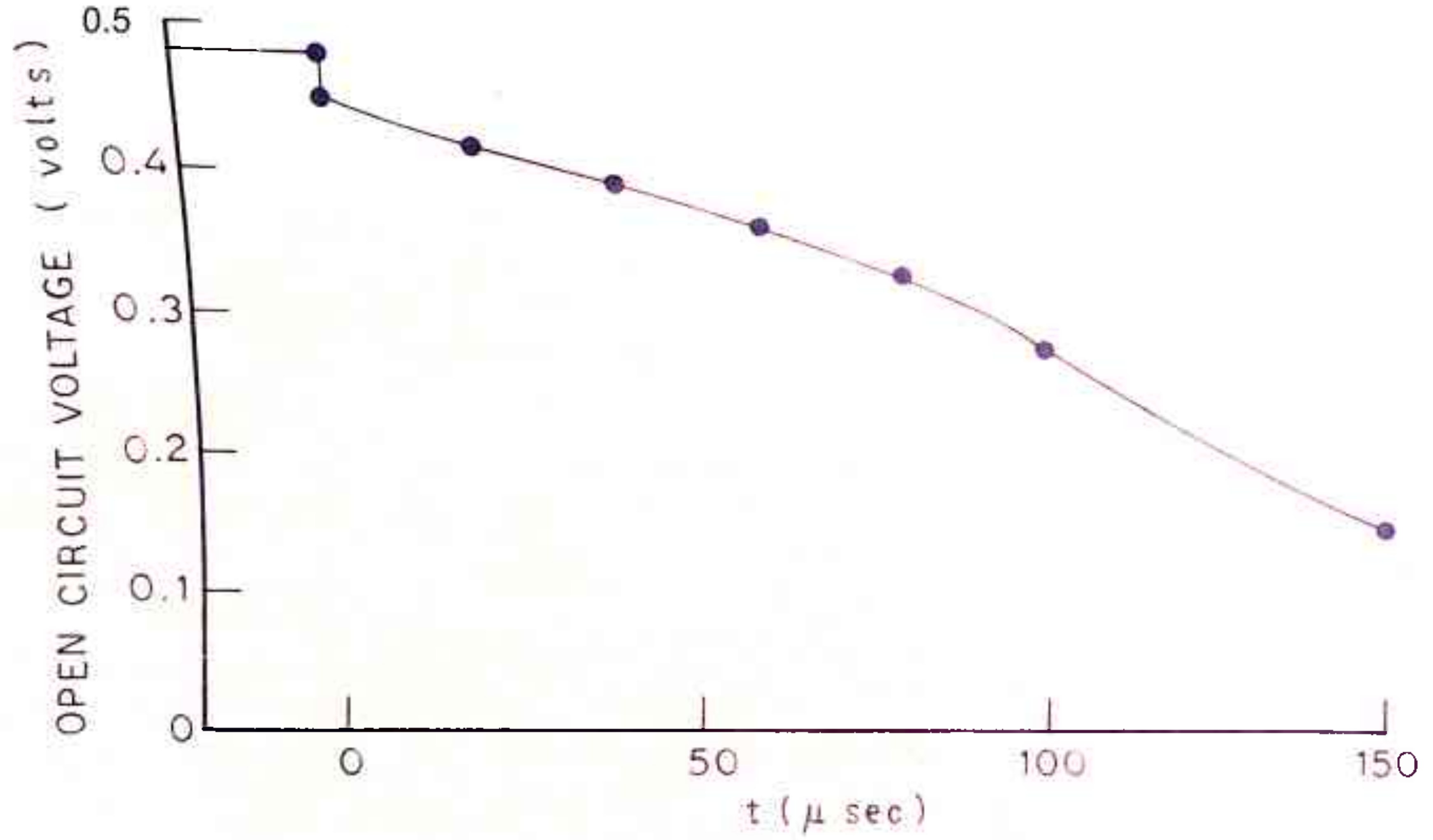

FIG. 3.21

E9C

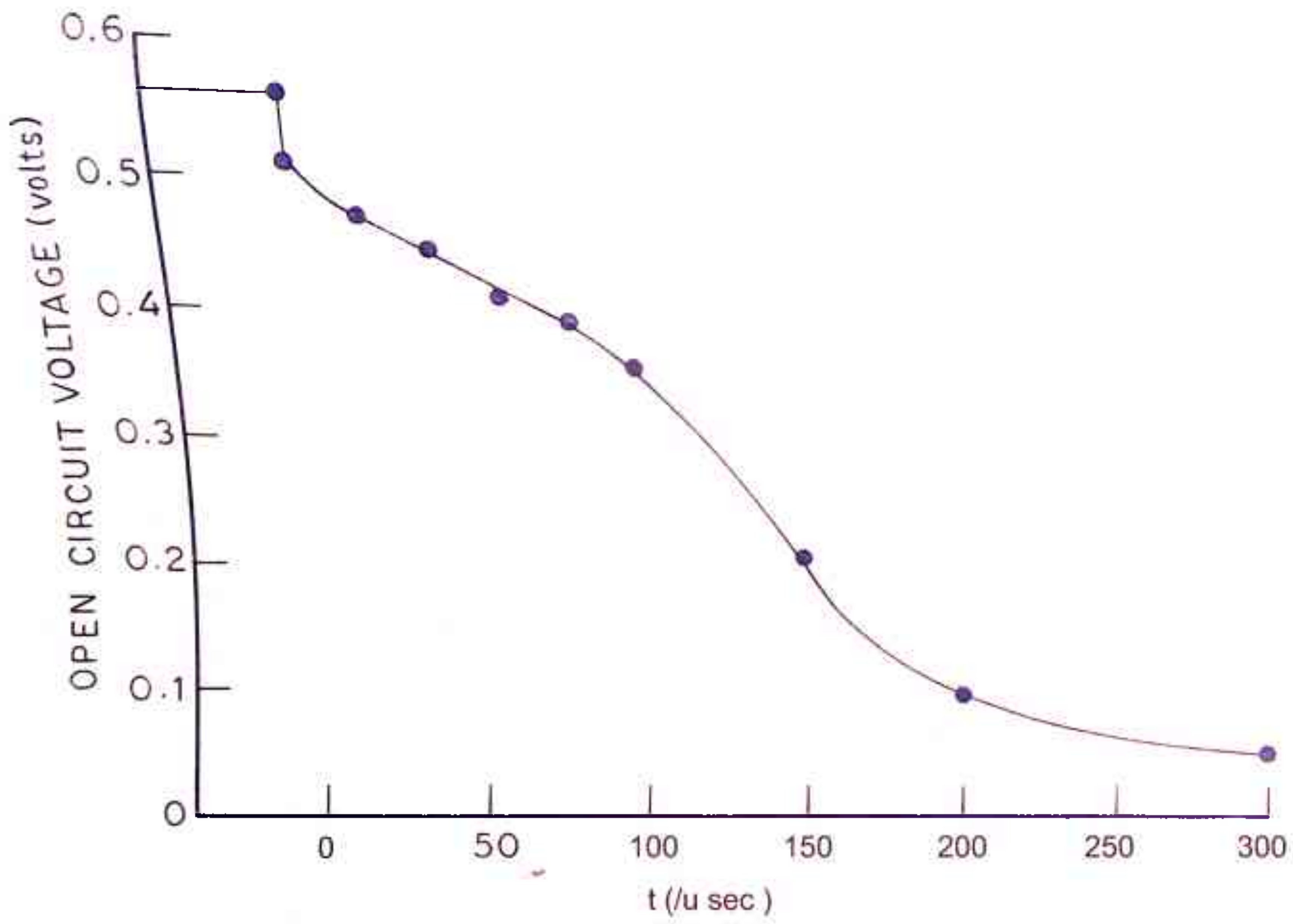

FIG.3.22

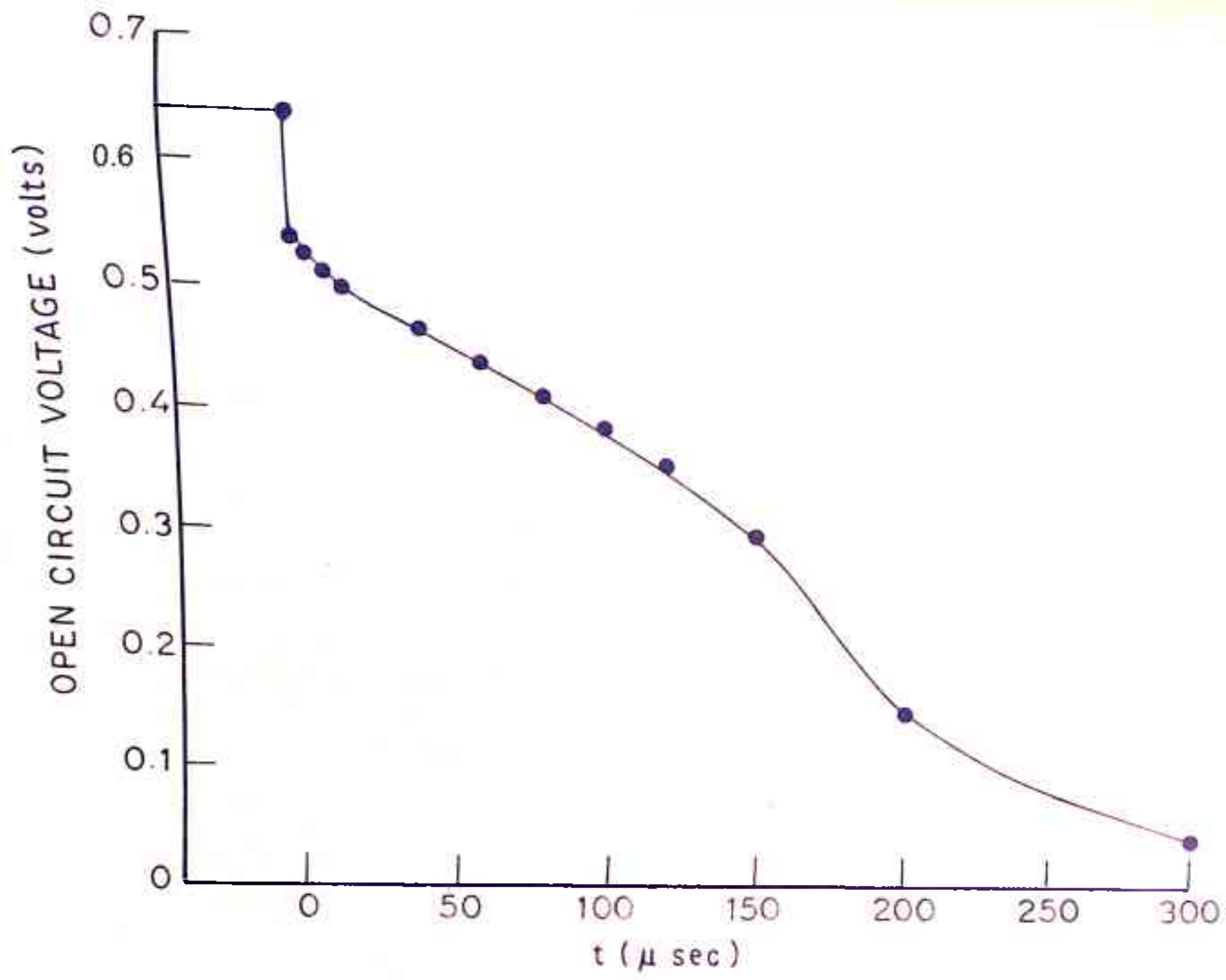

FIG. 3.23

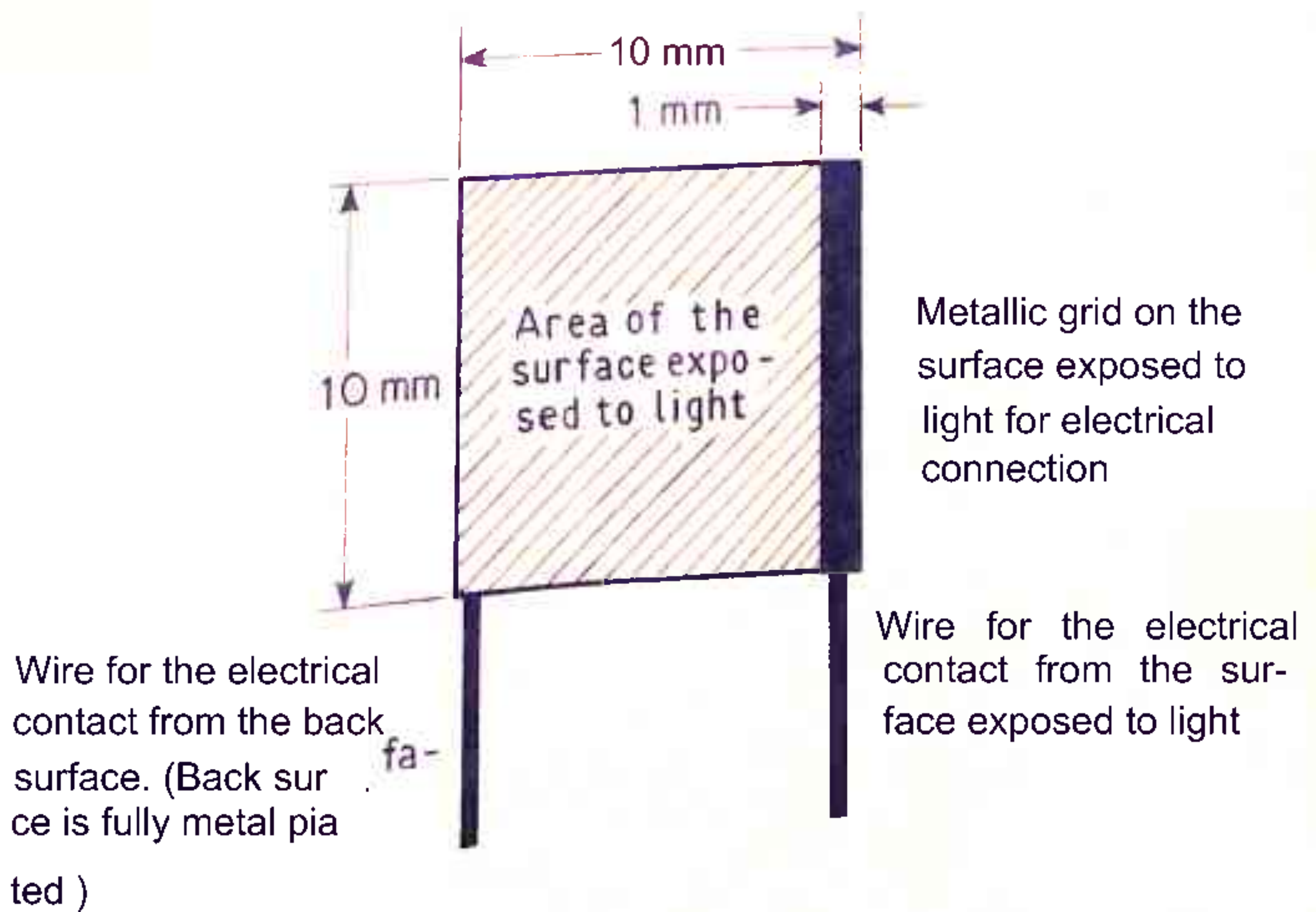

FIG.3.24 SC4 (PLESSEY)SOLAR CELL

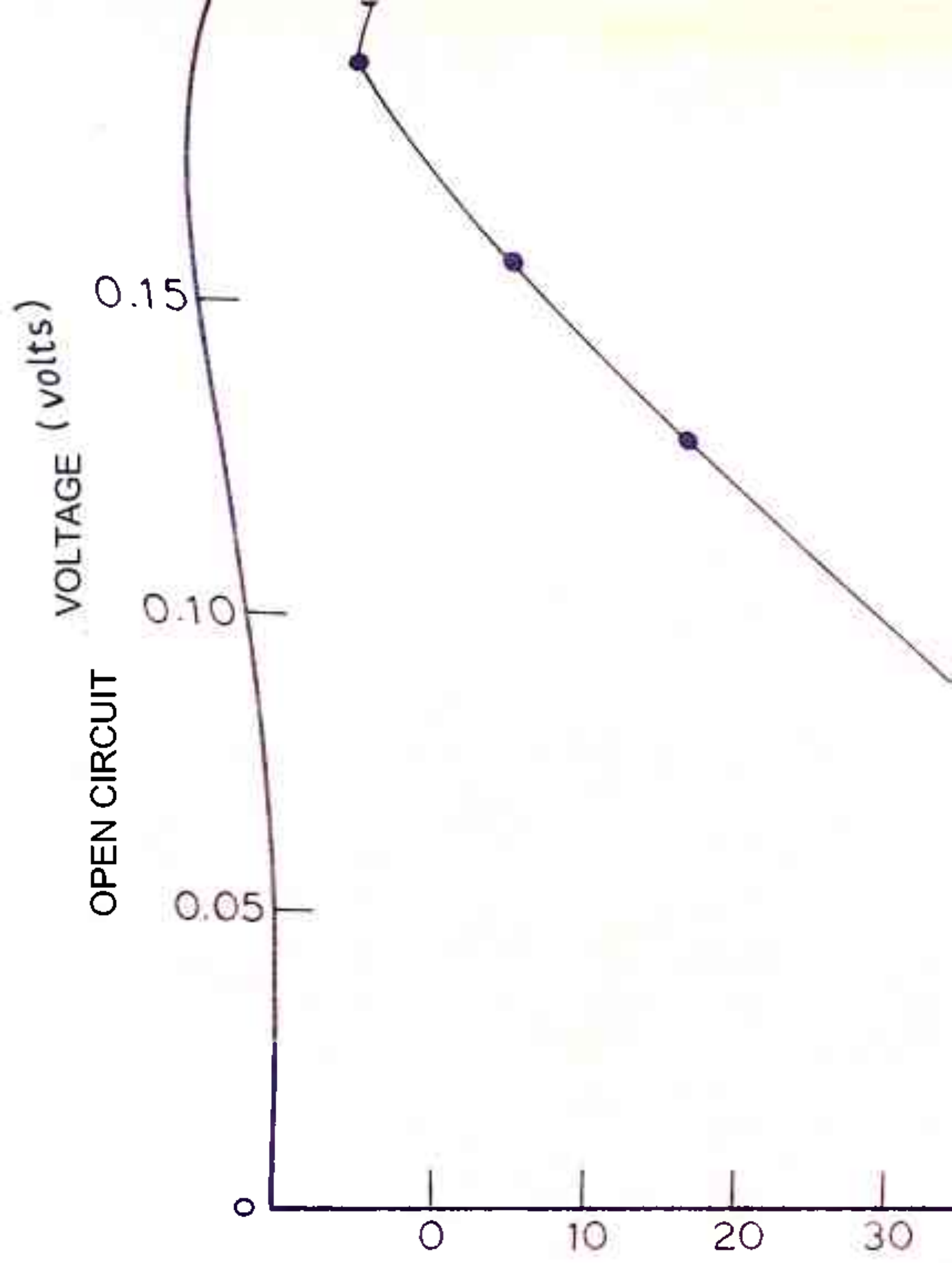

OPEN CIRCUIT
VOLTAGE (volts)
0.15
0.10
0.05
0
0
10
20
30

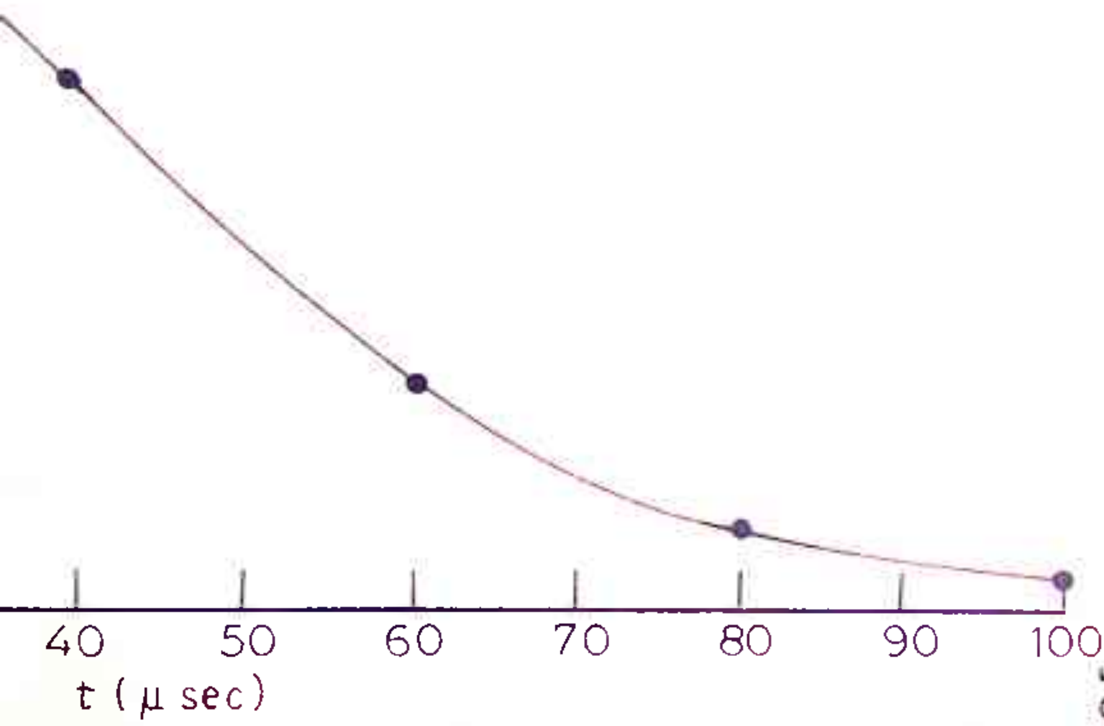

FIG. 3.25

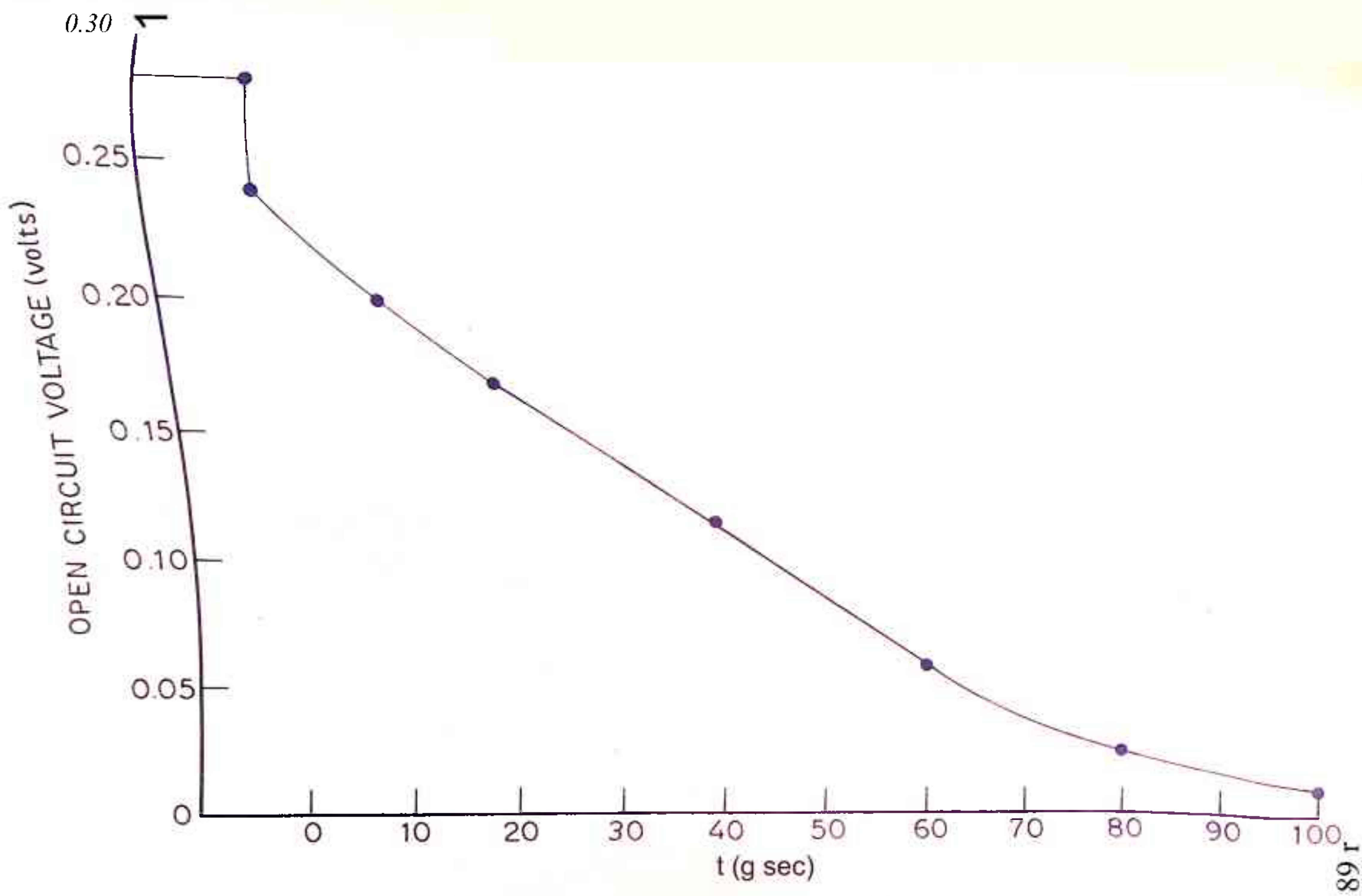

FIG. 3.26

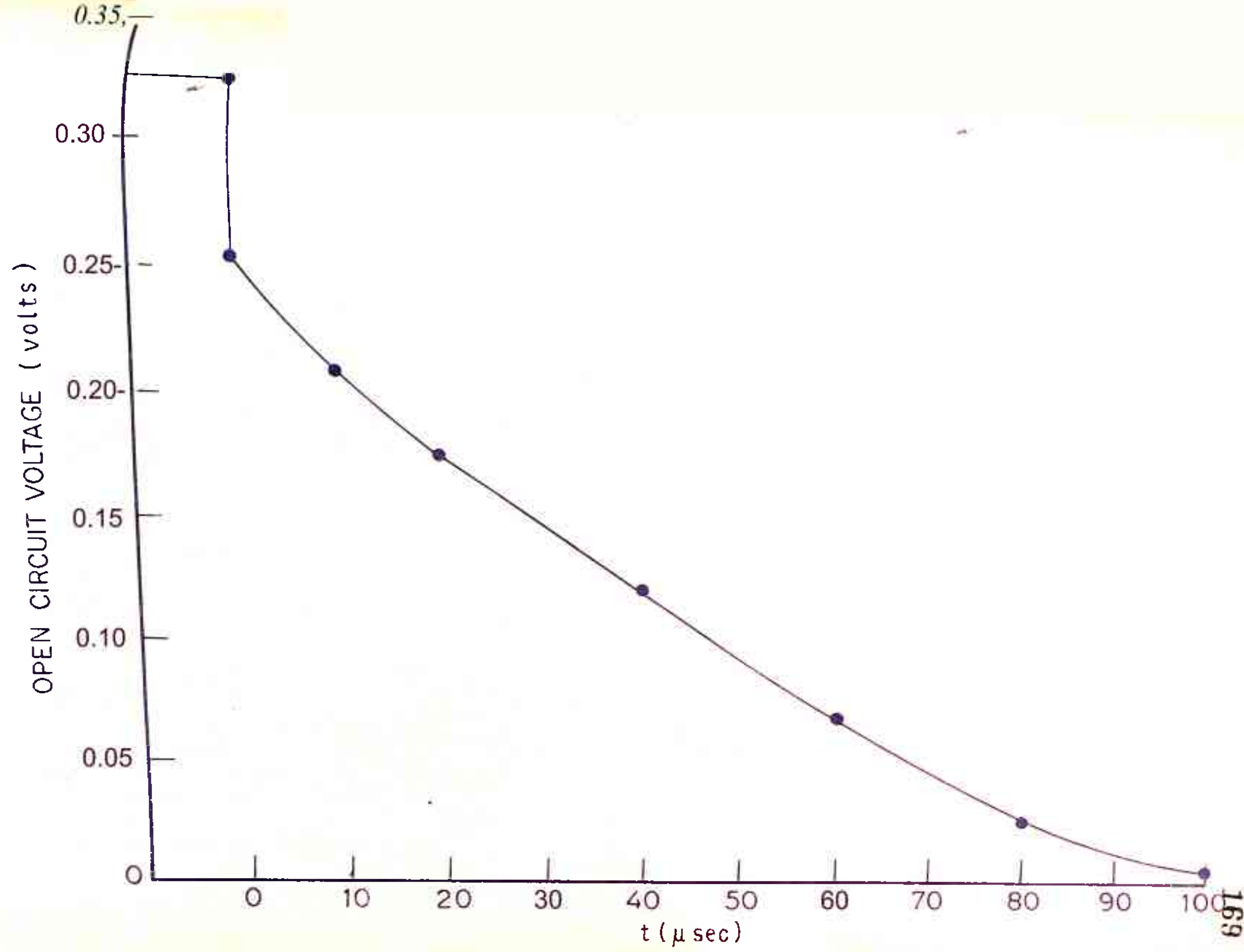

FIG. 3.27

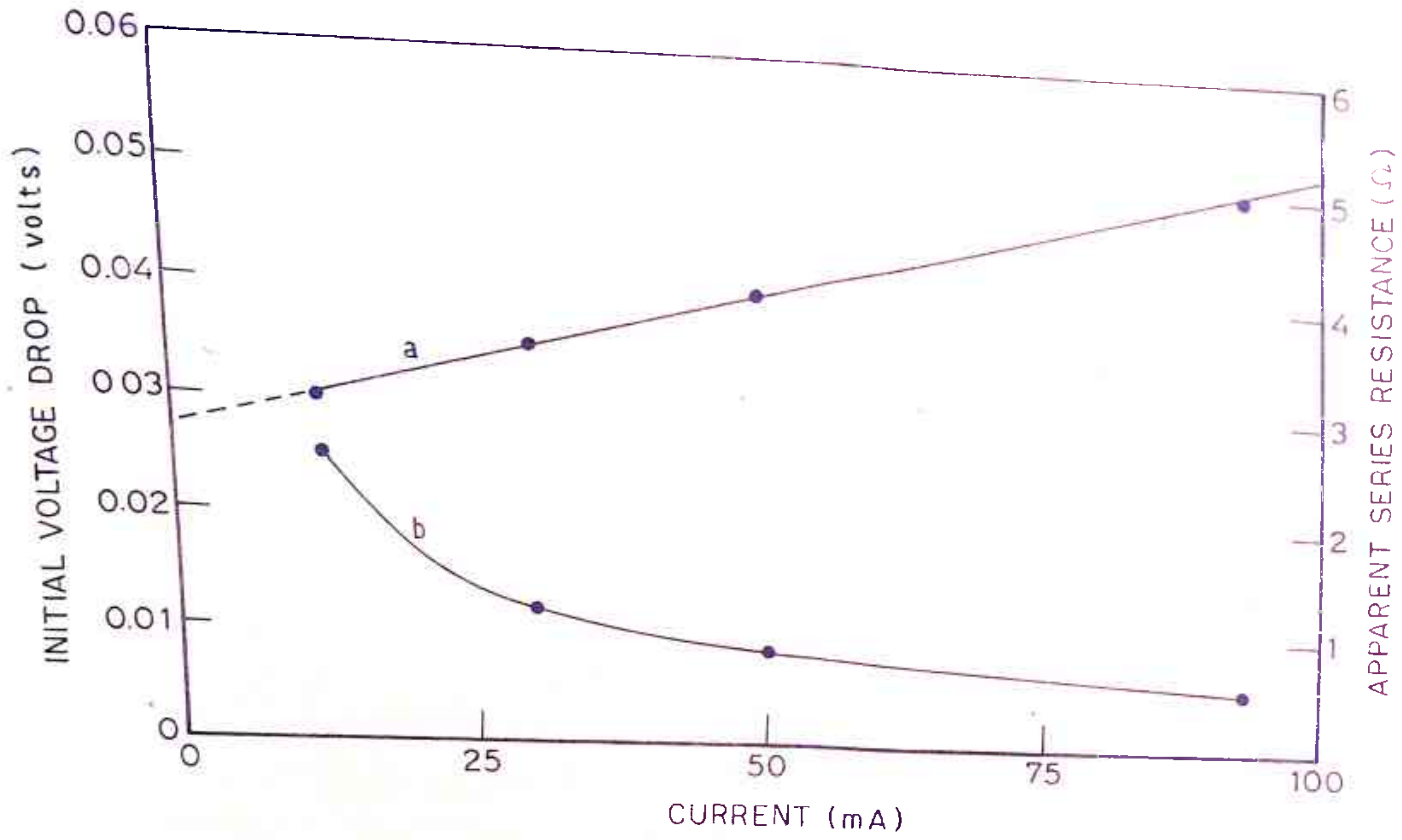

FIG. 3.28

Oil

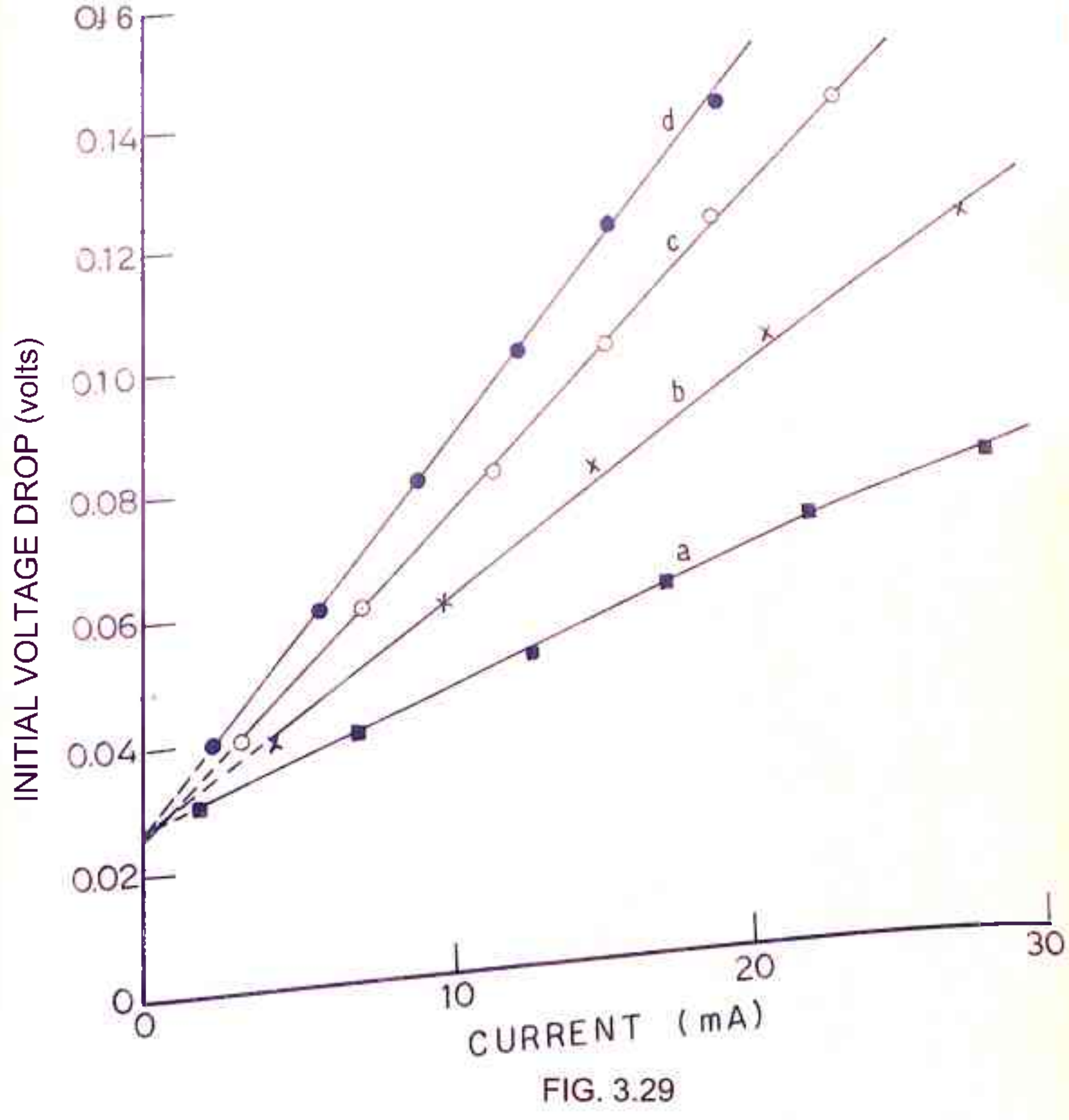

FIG. 3.29

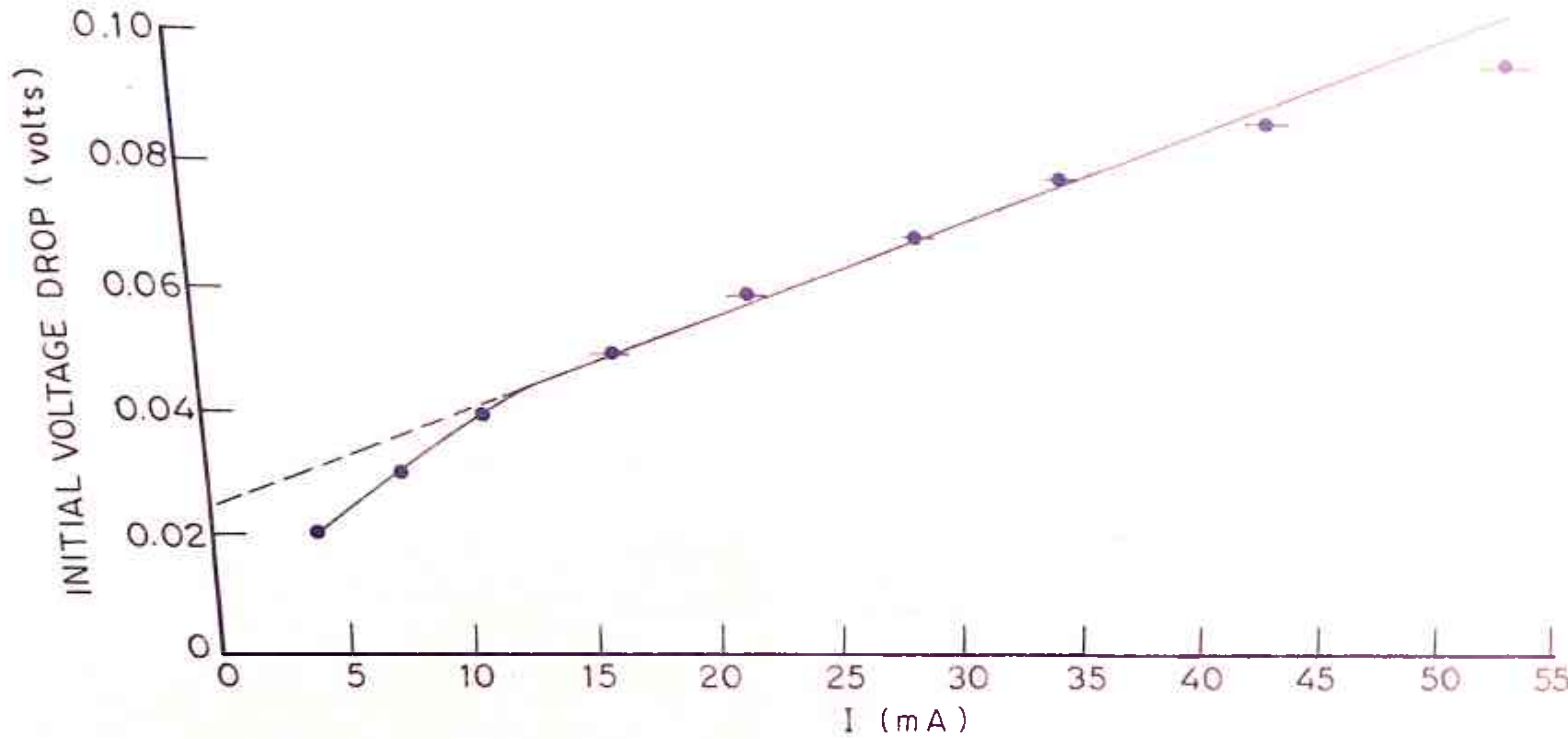

FIG. 3.30

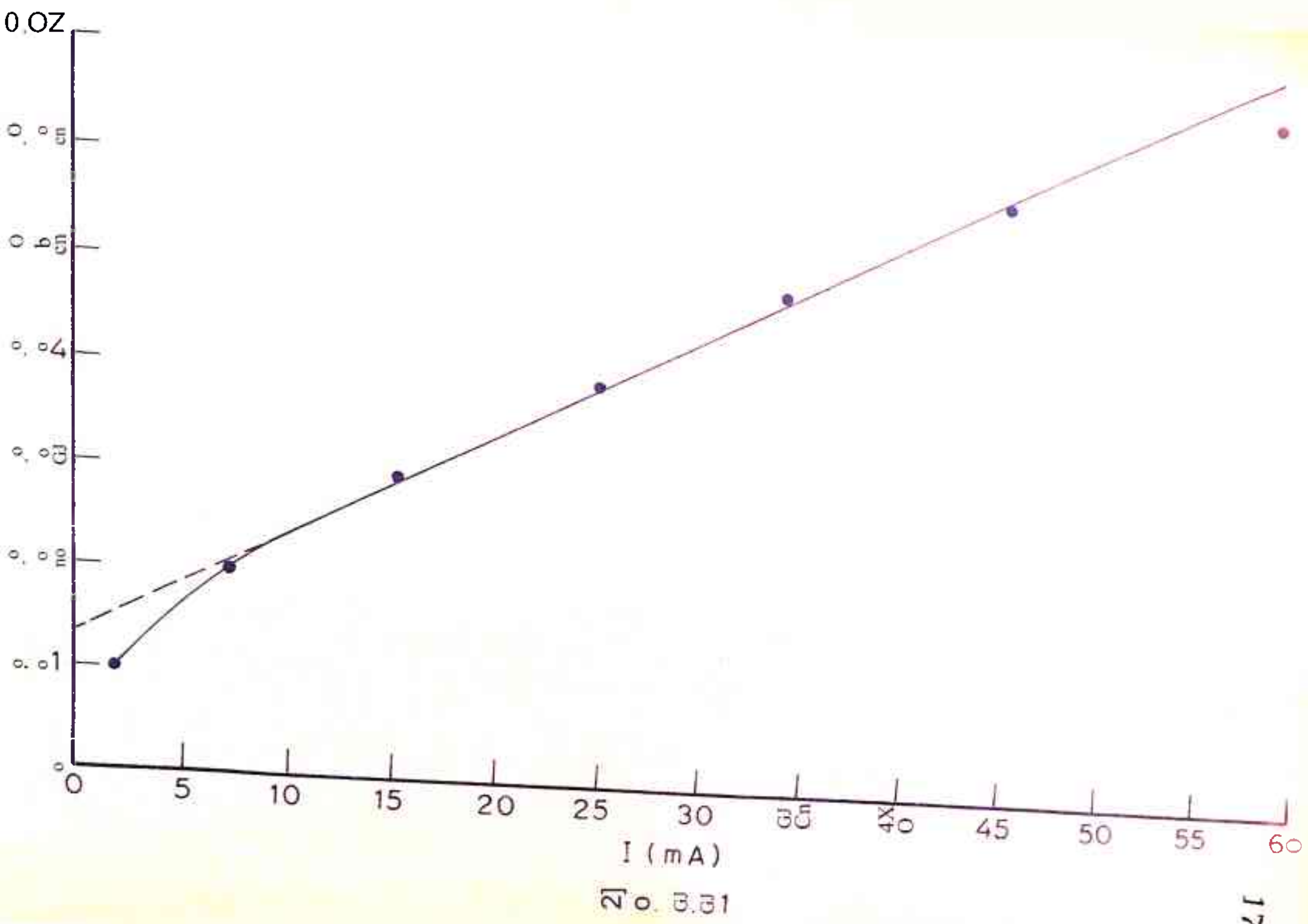
INITIAL VOLTAGE DROP (volts)
0
5
10
15
20
25
30
45
50
55
60
I (mA)

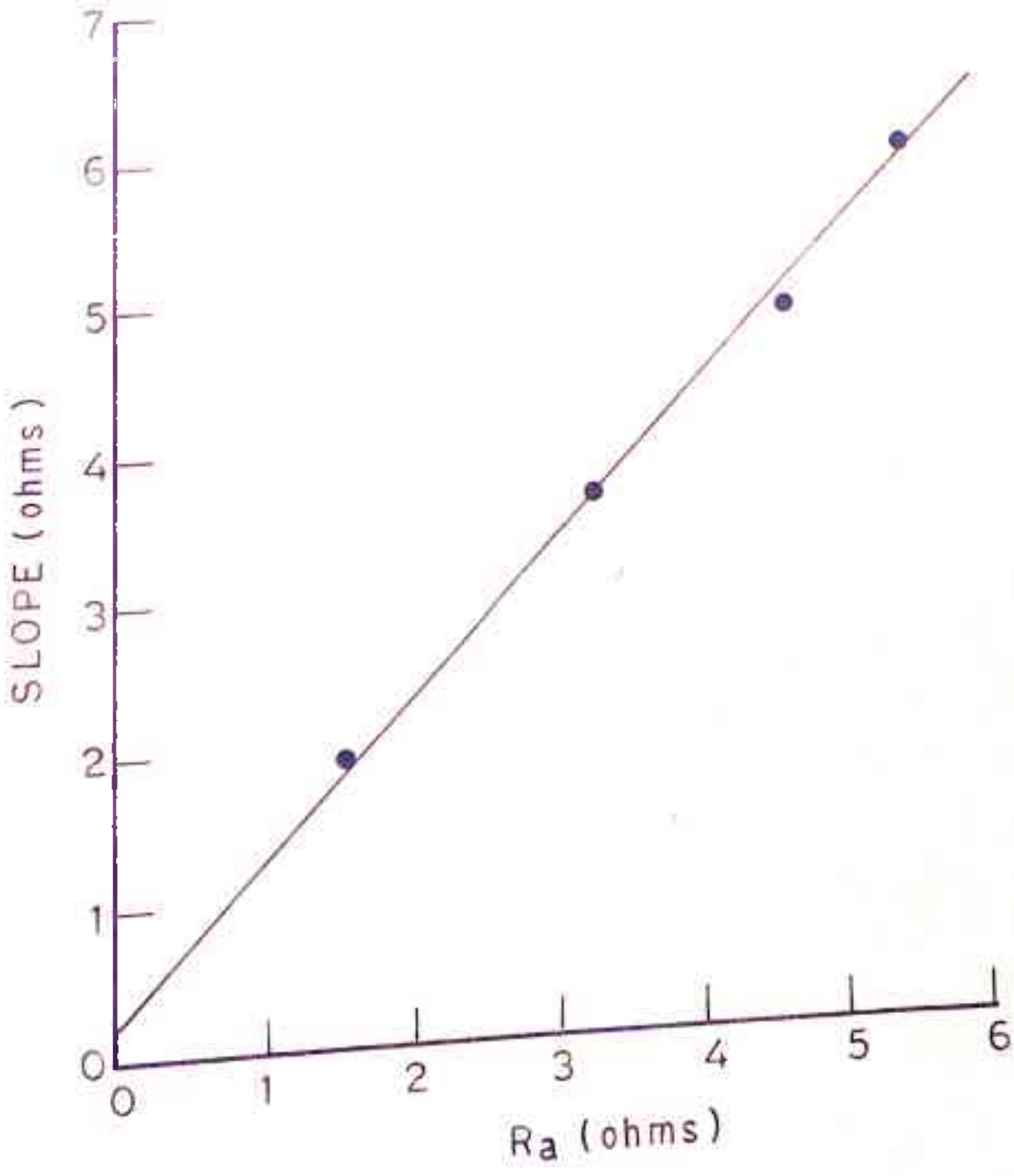

FIG. 3.32

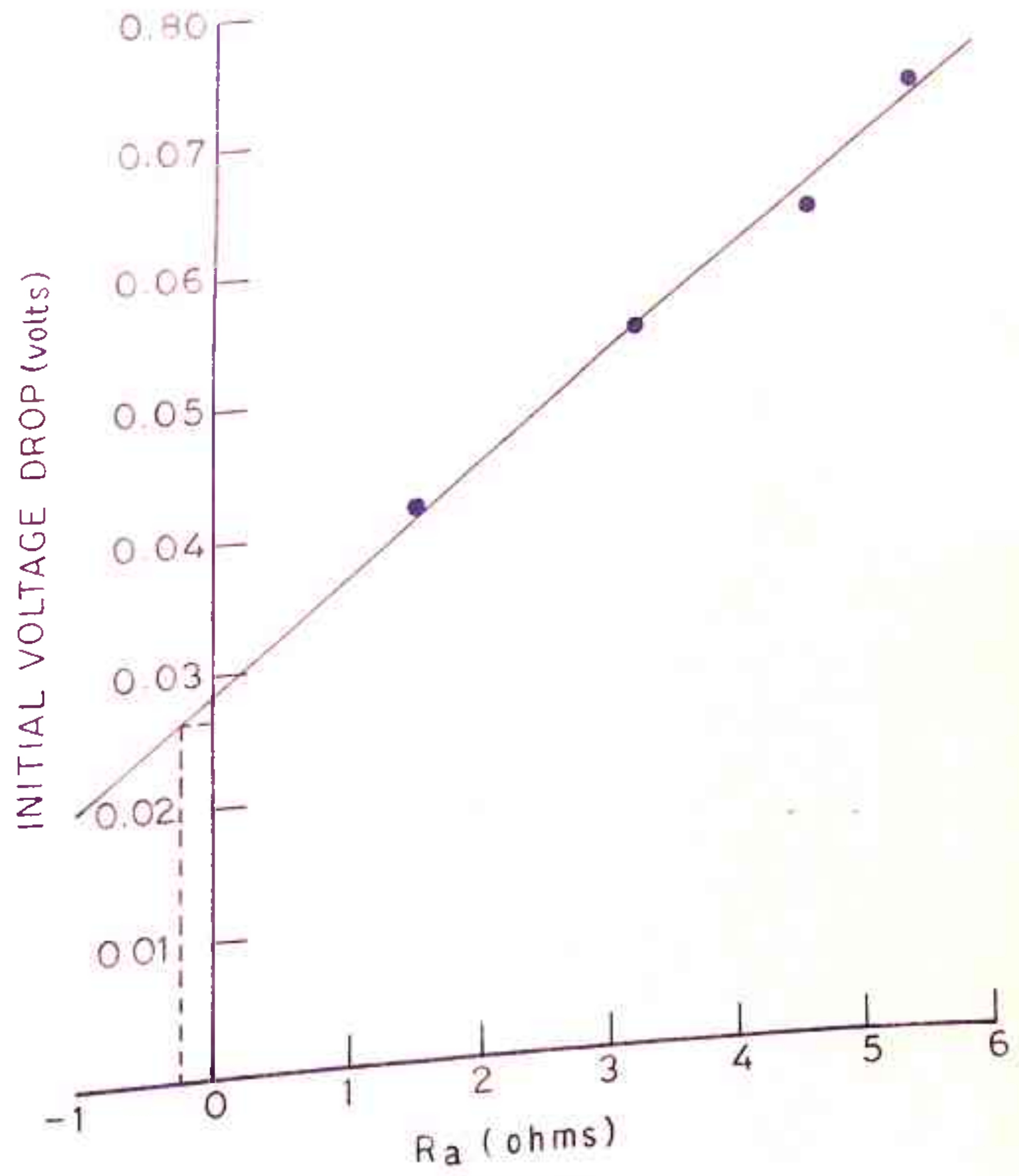

FIG.3.33

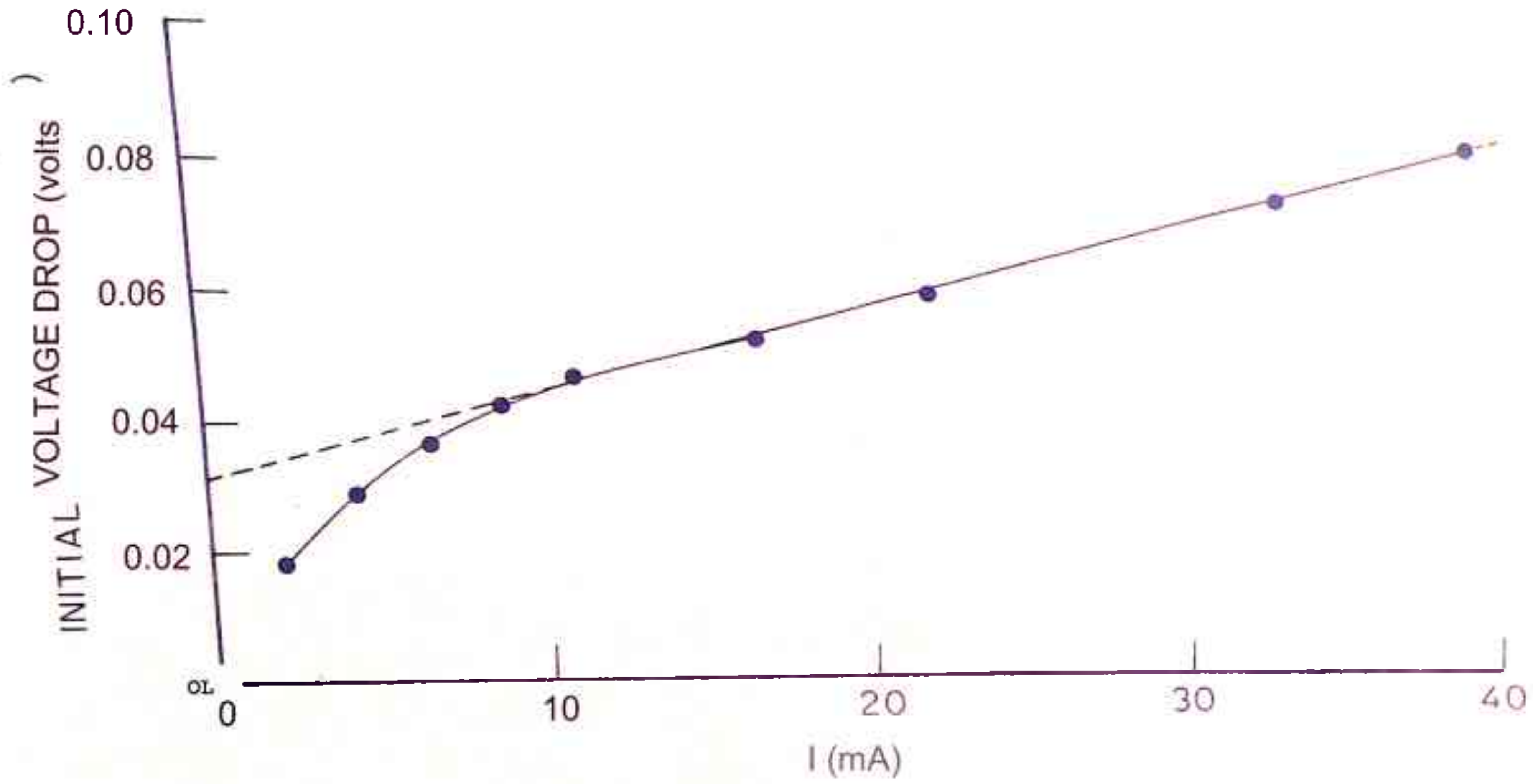

FIG. 3.34

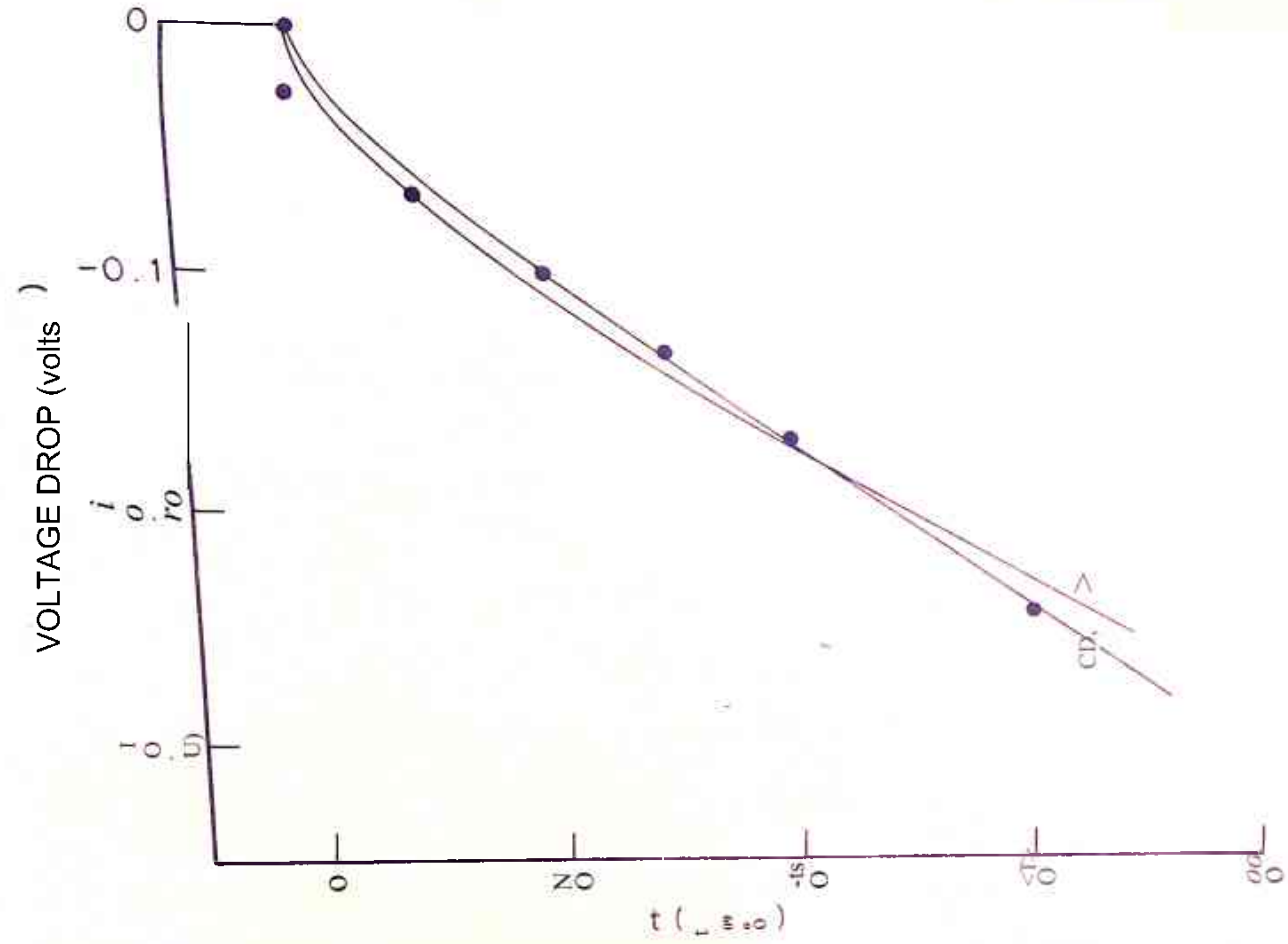

FIG.3.35

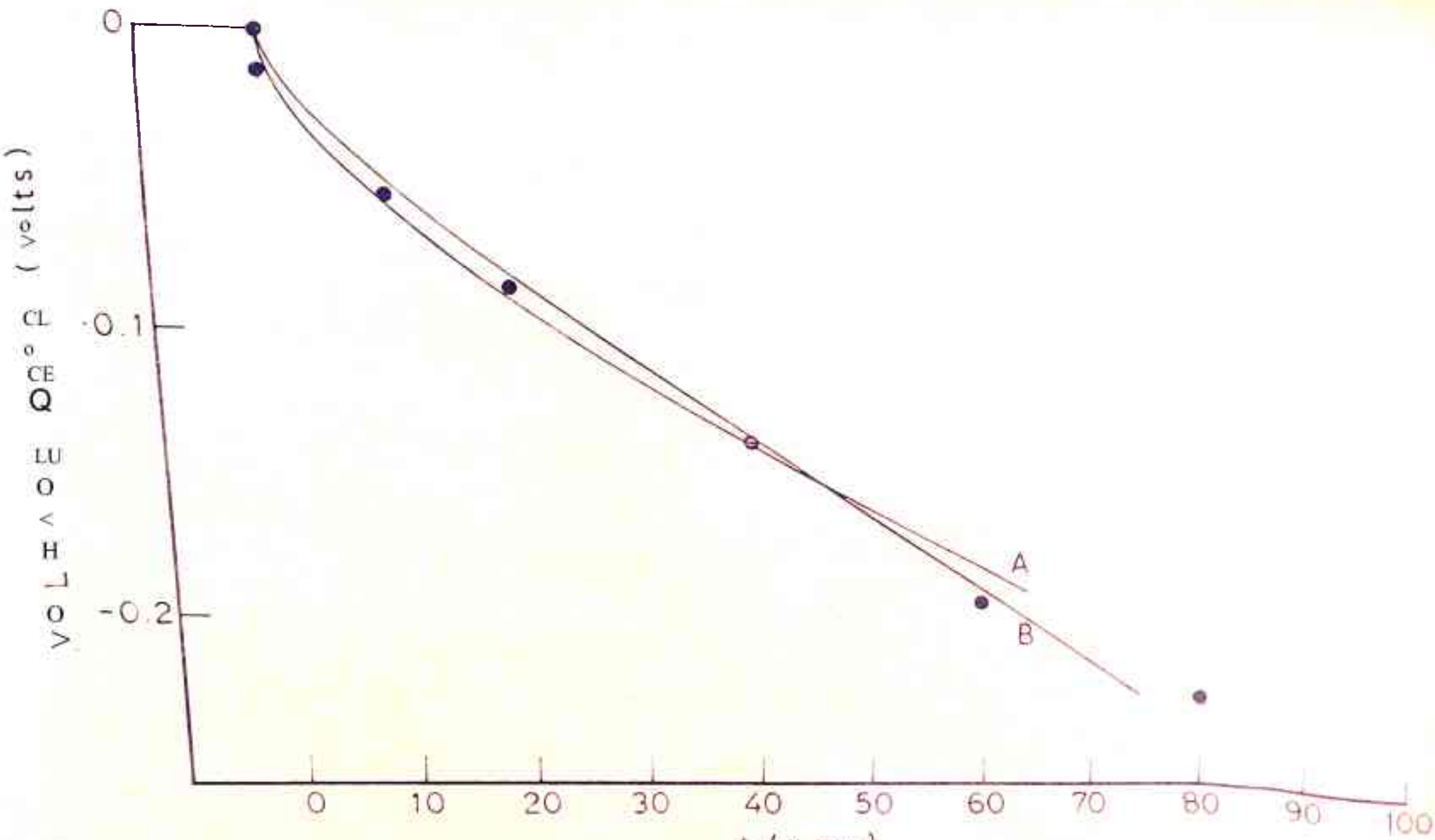

FIG. 3.36

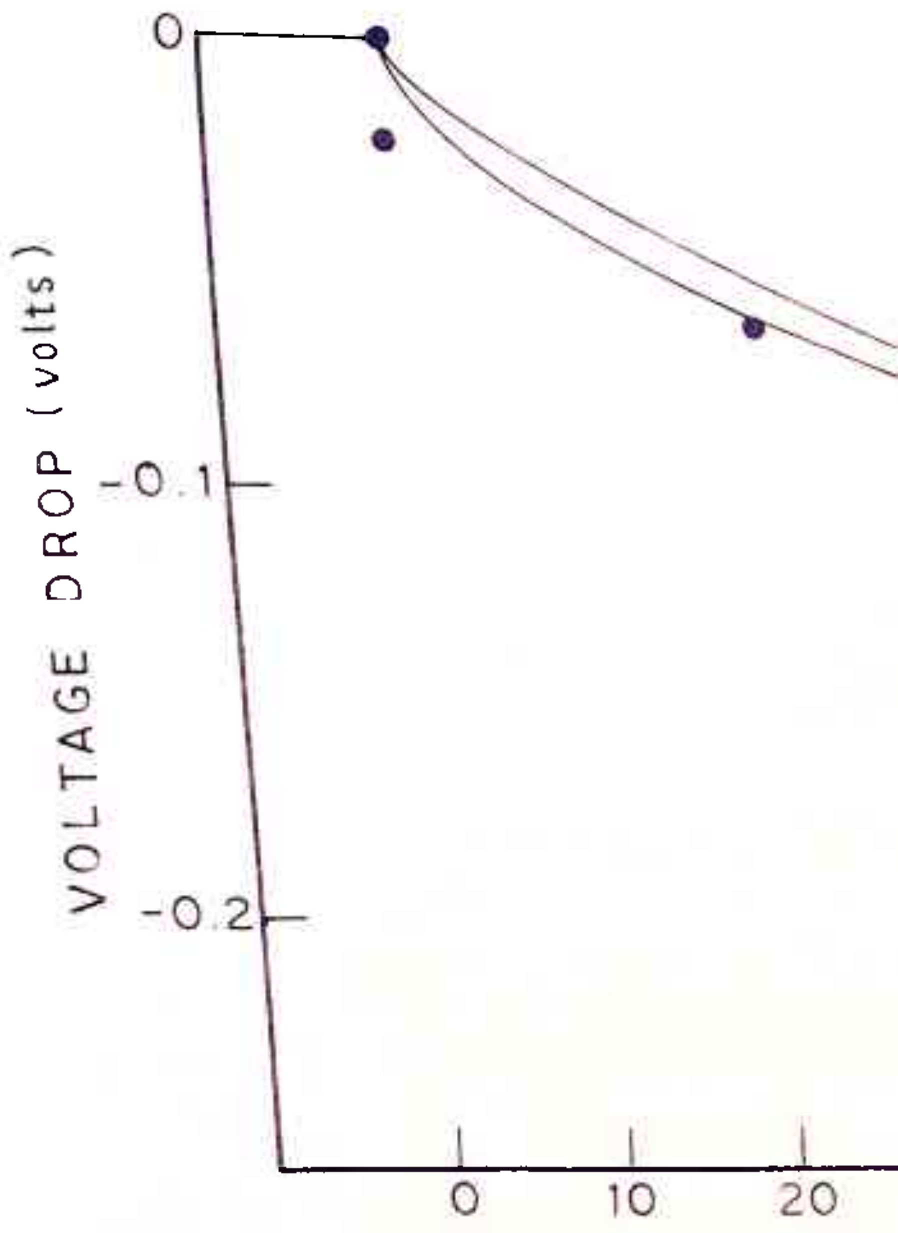
VOLTAGE DROP (volts)
0
-0.1
-0.2
0
10
20

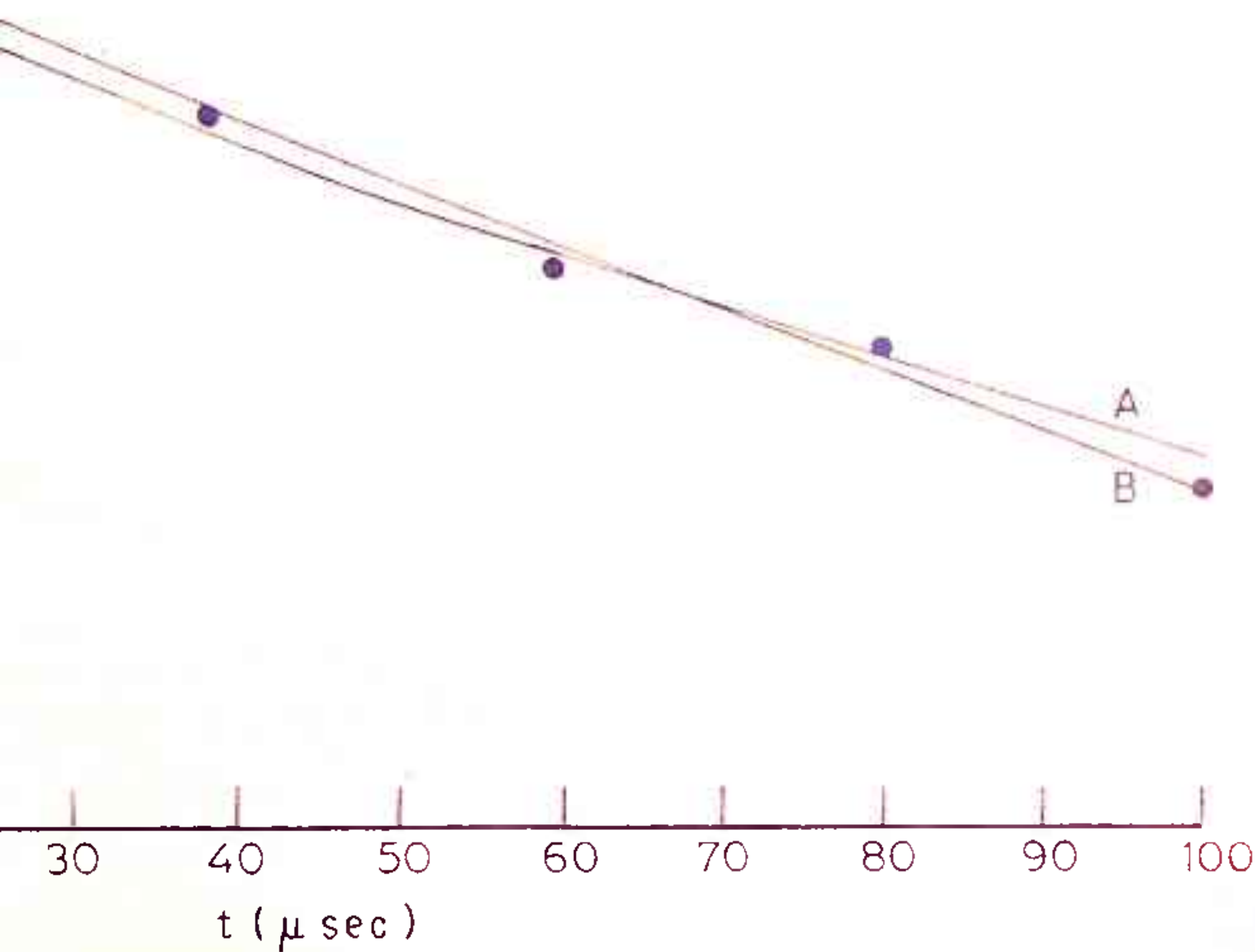

FIG.3.37

CHAPTER IV

REVERSE RECOVERY

CHAPTER IV

REVERSE RECOVERY

1. Introduction

It was found in the late 1940's that when point contact germanium diodes were used in circuits through which short (several tenths of a microsecond) electrical pulses were being passed, the effective reverse resistance of these diodes decreased considerably below the static value. Further studies (1) showed that when a diode was switched rapidly from the forward to the reverse direction, an anomalously large current, which often actually destroyed the diode, flowed briefly.

In view of the importance of this phenomenon in the efforts to reduce the response time of pulse circuits. Investigations of the phenomenon were carried out and many these *provided the basis of a theory* of transient processes in semiconductor diodes.

Since the phenomena of accumulation and dispersal of non-equilibrium *carriers govern this process,* such a study may be *effectively used to relate the physical and geometrical properties of the device* with the various parameters involved in the above mentioned phenomenon. Experimental and theoretical Investigations (1) - (9) have shown that the large current surge obtained as mention above.

is a consequence of the finite decay time of minority carriers which were stored in the base while the forward current was flowing.

The investigations into this phenomenon later led to many applications (2) - (6) and improvement of device designs. It has also stimulated the development of new devices such as charge storage diodes and some special types of varactor for frequency multiplication.

in chapter 3 we discussed the use of OCVD to determine the minority carriers lifetime. Study of reverse recovery as we shall see later, can also be used to determine minority carrier lifetime.

To study tne .. reverse transients, a p-n junction

rst forward biased and a current I_p is allowed to

18 fi

flow through it* As shown in Fig. 4.1(a), at t = 0,

the switc h s is suddenly thrown to the right and

. i reverse current I_{R} R fi ows (io) for a time

Initia

c] This is c a iled the constant current phase. Fig.4(b)

shows the con ant currents phase (also called the

storage P - hase^ decay P and nhase. Fig* 4.1(c) shows the

junction , « voltage aS a function of time and Fig. 4.1(d)

gives the minority carrier distribution for various

time in 4«tervals-

In the earlier papers (7), (8), only the base contribution was taken into account and the relation between the storage time t_s, minority carrier (in the base) lifetime τ and τ_F and τ_R were given as follows,

$$\text{Erf}\sqrt{\frac{t_s}{\tau}} = \frac{1}{1 + \frac{I_R}{I_F}} \qquad (4.1)$$

In the chapter 3 of this thesis, it has been shown that p-n coupling affects the decay of minority carriers. Although the current contribution of the emitter side is normally negligible, but in some cases, for the reasons described in chapter 3, the p-n coupling becomes important, which may substantially affect the decay of carriers and hence the determination of minority carrier lifetime may not be accurate if contribution due to p-n coupling is not taken into account. In the work reported by Smet and Overstraeten (in) the current contribution of both sides is considered but p-n coupling is not taken into account.

In this chapter we report our theoretical and experimental investigations of the Reverse Recovery Transients. In the next section we present theory of the constant current phase of reverse recovery transient

when p-n coupling is taken into account and its qualitative analysis, it is also shown that when contribution of the diffuse region is neglected, our results reduce to Kingston's formulation (8). in sec. 3 we report our measurement set up and analysis of the experimental results. Finally a summary of our findings is presented in sec.4.

2. Theory and Analysis

2,1 Theory of Constant Current Phase

consider a diode, in forward biased
.e
ascribed in chapter 3. Eqns. (3.6) to
condition, as oescrx
(3.19) to (3.29) describe the carrier
(3.17) and Eqns.
boundary conditions etc. which are applicable
profiles,
to the present ease also.

the OCVD case (chapter 3) the external supply
In
, - 0 and as described earlier
"" switched Off at ' "
boundary condition (3.16) which essen-
e
•his led to th
. total current through the junction
that tn©
tially means
is *zero*

in the reverse *recovery* constant current
Since
Unction i_s
phase, the total current through the
0.) - 0 1, we

constant and is in reverse direction

can write

$$D_n \frac{\partial n}{\partial x}\Big|_{x=0} - D_p \frac{\partial p}{\partial x}\Big|_{x=0} = -J_R \qquad (4.2)$$

where J_R is the reverse current flux. We shall use this boundary condition Instead of the boundary condition (3.18). Rest of the conditions remain same.

The Laplace Transform of eq.(4.2) can be written as

$$D_n \frac{\partial \hat{n}(x, s)}{\partial x}\Big|_{x=0} - D_p \frac{\partial \hat{p}(x, s)}{\partial x}\Big|_{x=0} = -\frac{J_R}{s} \qquad (4.3)$$

$\frac{\partial \hat{n}}{\partial x}$ and $\frac{\partial \hat{p}}{\partial x}$ are defined by equations (3.25) and (3.28) respectively.

Following this we can write

$$\hat{f}(s) = \frac{-\frac{J_R}{s} - \frac{f(o)}{s}\left[J_n\left(1-\sqrt{1+s\tau_n}\right) + J_p\left(1-\sqrt{1+s\tau_p}\right)\right]}{\left[J_n\sqrt{1+s\tau_n} + J_p\sqrt{1+s\tau_p}\right]} \qquad (4.4)$$

where all the symbols have the same meaning as in chapter 3.

Eq. (4.4) can be written as

$$\hat{f}(s) = \frac{-J_R\left(J_n\sqrt{1+s\tau_n} - J_p\sqrt{1+s\tau_p}\right)}{s\left[J_n^2(1+s\tau_n) - J_p^2(1+s\tau_p)\right]} - f(o)\left\{\frac{J_n + J_p}{s\left[J_n\sqrt{1+s\tau_n} + J_p\sqrt{1+s\tau_p}\right]} - \frac{1}{s}\right\} \qquad (4.5)$$

$$= -J_R(J_n\sqrt{1+s\tau_n} - J_p\sqrt{1+s\tau_p})\left[\frac{1}{s(J_n^2 - J_p^2)}\right.$$

$$\left. - \frac{(J_n^2\tau_n - J_p^2\tau_p)(J_n^2 - J_p^2)}{J_n^2 - J_p^2 + s(J_n^2\tau_n - J_p^2\tau_p)}\right]$$

$$-f(o)\left[(J_n + J_p)(J_n\sqrt{1+s\tau_n} - J_p\sqrt{1+s\tau_p})\left\{\frac{1}{(J_n^2 - J_p^2)s}\right.\right.$$

$$\left.\left. - \frac{(J_n^2\tau_n - J^2\tau_p)/(J_n^2 - J_p^2)}{J_n^2 - J_p^2 + s(J_n^2\tau_n - J_p^2\tau_p)}\right\} - \frac{1}{s}\right] \qquad (4.6)$$

By *taking Inverse Laplace transform* of both sides we get

$$f(t) = -\frac{J_R}{J_n^2 - J_p^2}\left[J_p \operatorname{erf}\sqrt{\frac{t}{\tau_p}} - J_n \operatorname{erf}\sqrt{\frac{t}{\tau_n}}\right.$$

$$-e^{-Bt}\left\{J_p\sqrt{\tau_p}\sqrt{\left(\frac{1}{\tau_p} - B\right)}\operatorname{erf}\sqrt{\left(\frac{1}{\tau_p} - B\right)t}\right.$$

$$\left.\left. - J_n\sqrt{\tau_n}\sqrt{\left(\frac{1}{\tau_n} - B\right)}\operatorname{erf}\sqrt{\left(\frac{1}{\tau_n} - B\right)t}\right\}\right]$$

$$+f(o)\left[(J_n + J_p)\left\{\frac{J_p\sqrt{\tau_p}}{J_n^2 - J_p^2}\left(\frac{1}{\sqrt{\tau_p}}\operatorname{erf}\sqrt{\frac{t}{\tau_p}}\right.\right.\right.$$

$$- \sqrt{\left(\frac{1}{\tau_p} - B\right)} \; e^{-Bt} \, \mathrm{erf} \sqrt{\left(\frac{1}{\tau_p} - B\right)t} - \frac{J_n \sqrt{\tau_n}}{J_n^2 - J_p^2}$$

$$\times \left(\frac{1}{\sqrt{\tau_n}} \, \mathrm{erf} \sqrt{\frac{t}{\tau_n}} - \sqrt{\left(\frac{1}{\tau_n} - B\right)} \; e^{-Bt} \, \mathrm{erf} \sqrt{\left(\frac{1}{\tau_n} - B\right)t} \right\} + 1 \Bigg] \qquad (4.7)$$

Using the relation

$$\mathrm{erf}(z) = 1 - \mathrm{erfc}(z) \qquad (4.8)$$

and $s(z) - /$ erf $\qquad$ (4.9)

Eq. (4.7) can be written as

$$f(t) = \frac{J_R}{J_o} \Bigg[\frac{b}{b-a} \, e^{-z^2} \left\{ s(z) - a\, S(az) \right\}$$

$$- \frac{a}{b-a} \, e^{-y^2} \left\{ s(y) - b\, S(by) \right\} - 1 \Bigg]$$

$$+ f(o) \Bigg[\frac{b}{b-a} \, e^{-z^2} \left\{ g(z) - a\, S(az) \right\}$$

$$- \frac{a}{b-a} \, e^{-y^2} \left\{ s(y) - b\, S(by) \right\} \Bigg] \qquad (4.10)$$

where

$$J_o = J_p + J_n \qquad (4.11)$$

and z, y, a and b have the same meanings as in chapter 3

Eq. (4.10) can also be written in the form

$$f(t) = \frac{J_R}{J_o}\left[W(t) - 1\right] + f(o)\,W(t) \qquad (4.12)$$

where $W(t)$ is defined by relation (3.35).

The constant current phase is retained till the voltage across the junction becomes zero (10). Let t_s be the time till the current in reverse direction remains constant then at $t = t_s$

$$V(t) = \phi f(t) = 0 \qquad (4.13)$$

eq.(4.13) in combination with eq.(4.12) would yield the result

$$W(t_s) = \frac{J_R/J_F}{1 + J_R/J_F} \qquad (4.14)$$

where $J_F = J_o f(o)$

which can also be written as

$$W(t_s) = \frac{I_R/I_F}{1 + I_R/I_F} \qquad (4.15)$$

Where I_F is the forward current before $t = 0$ and I_R is the *reverse* current during constant current phase through the junction.

It can be shown (12) that when $J_n \to 0$ (i.e. neglecting the contribution of diffuse region)

$$M(t) \approx 1 - \exp(\ldots) \sqrt{\frac{t}{\tau_B}} \quad (4.16)$$

using eqs. (4.15) and (4.16) we can write

$$\text{erf}\sqrt{\frac{t_s}{\tau_3}} = \frac{1}{1 + \frac{\ldots}{\tau_F}} \quad (4.17)$$

which is the same as reported in (8) and (9).

We shall be using eq.(4.15) for further theoretical analysis and fitting with experimental data.

2.2 Qualitative Analysis

Tables 4.1 to 4.5 present the value of W(t) for different values of a and T. Fig- *4.2* shows the functional dependence of W(t) on z, for three different values a (i.e. «•*. >. » - r-v 1- r/rp.

Fig. 4.3 and 4.4 show w(t) for X - SO and 1000 respectively*

It can be seen from the plots that with the increase In a# in a for the same value of X, W(t) goes down, which essentially means that the effect of coupling is to decrease the the value of the ratio I_R/I_F. Which means

if a X O for the device, eq. (4.17) would yield a lifetime lower than the actual value. As the value of I increases, this effect becomes very significant and at higher values of a and I, the determination of minority carrier lifetime by eq.(4.17) would yield a substantially low lifetime. Hence to determine the minority carrier lifetime. it would be better to do the experiment for various t_s and W Plot the ratio

$$\frac{I_R/I_F}{1+\frac{I_R}{I_F}}$$

with respect to \Tt and try to obtain the values of a. X and Tg by fitting a suitable theoretical curvo (Tsblc 4el to 4«5 can ba used fox en approximate estimate of these values).

From a practical point of view, for the reasons described in last chapter, W(t) can be simplified to

$$W(t) = \frac{1}{1-a} \quad e^{-z^2} \quad \hat{S}(z) - a\, s(azQ \qquad (4.18)$$

which is same os equation (3e51)»

The advantage with eq.(4.18), as described earlier. is that the shape of the curve now depends only on one parameter a. This simplifies the fitting procedure to a great extent. Fig. 4.5 shows w(t) as a function of z for various values of a.

If we put a « o in eq.(4.18) we again arrive at eq. (4.17), which is a case of no p-n coupling, if a / 0 for the device, and still if we neglect the second term in the right hand side bracket of eq. (4.18) we are taking a higher value of W(t) than its actual value, which means it will lead to the determination of a lower lifetime.

Table 4.6 gives a summary of the functional dependence of w(t) on a and s as predicted by eq. (4.18). This can be used for fitting with the experimental values plotted in a manner described earlier.

It can be seen that a unique value of a may not *be achieved because to fit* eq.(4.18) with experimental *data, a pair of values of a and* τ_B has to be chosen, which may not be unique.

To *start with, an approximate* value of $_Q$ can *be determined by eq.(4.17)* which iq <-w the re^tion f$_{or}$ *uncoupled case*. *To fit eq. (4.18)* with experimental data, τ_B *has* to be higher than the vai$_{ue}$ determine by eq. *(4.17).* Now *for a* τ_B higher than thia, one can obtain *a good fit between* the experimental data and eq.(*.18) *which will* g*ve the value of a •

in *those* cases as described in last chapter, *where eq.(4.18)* may not be reliable, the whole of the

eq. (3.35) may have to be used for a good fit. The analysis of this equation similar to the one presented in last chapter is applicable here.

3. Experimental study

3.1 Experimental Arrangements

The circuit shown in Fig. 4.6 has been used for the experimental studies ;----------------------- presented m this chapter. An *Aplab Model 7211 DC* Regulated Power —■ Supply was used as a d.c. source. The 600 ohms termination (rise time 0.1 microseconds) of a Hewlett Packard Model 21 n square wave generator was used to supply y negative pulses, A *Tektronix 'Type* 556 Oscilloscope with Type jAl D ual Trace Plug In *(rise time* 7 nanoseconds) was used t o study the *waveform.*

For the reasons described in the last chapter, risetime and r. dfMme of the pulses should be at least an order *o£* magnitude onde less than the time for which the -ujavefo Js tO be studied. Hence with this set up, it ible to do - w t-hls experimental study only beyond was P°®s cond storage time. To set the forward current 1 *micros-* d.c. voltage of the power supply was throng ^ode adjusted*

To do the experiment, first forward current was adjusted and then the pulse height (within the limits defined in (8) and other references) was varied to get a required l/Ip. % was read by noting the point when the voltage across the diode goes to zero.

in the next subsection we present the results of this experimental and their analysis on three samples.

3.2 Results and Analysis

Fig. 4.7 shows the ratio $\frac{I_p/I_p}{1 + \frac{I_R}{I_F}}$ plotted

against^ *>r three different forward currents for *BY127 (silicon* diode). Curve 'a' is for 6 mA and curve • b' and c are for U"* and 22 mA. This shows that there io * small varl , i variation of lifetime with the forward current.

in Fig- 4,u 4 0 curve 'b' *of* Fig. 4.7 is shown and by the fittl g fotained by fitting with eq.(4.1Q) are of parameters □ procedure described earlier. the values

a « 1 1 and * τ_B 85 microseconds. As discussed earlier, It was possible to fit the same results for other sets of · aod t_B valu- Two of them are a « 0.1, τ_B = 33 micro - seconds an a . a - 0<01' τ_B « 29 microseconds.

Fig* 4 9 shows the $\frac{I_R/I_F}{1 + \frac{I_R}{I_F}}$ with respect to

$t_{\&}$ for DR25 (Germanium Diode) at IS mA forward current. A similar analysis gives three sets of values, a* 1.1, 7\= 45 microseconds; a » 0.1, Z = 18 microseconds; and a » 0.01, T_B = 16 microseconds.

Fig. 4.10 shows a similar curve for SC4 (silicon solar cell). The sets of values obtained by analysis are a * I.A, tg i l -7 s* 160 microseconds; a = 0.1, T = 60 microseconds; and a = 0.01, Z_0 - 52 microseconds.

Table 4.7 presents a comparative study of the results obtained oy - bv OCVD and Reverse Recovery Methods, It can D& ...n that, for all the three samples Reverse Recovery Hethod has yielded a higher lifetime than the OCVD method. As the value of a increases, the matching value of lifetime for the best fit increases much more in case of reverse recovery than in case of OCVD. This might mean that Reverse Recovery is more sens- Itiv. to P-n COUP than OCVD.

The po«sible r 'hlc reasons for difference in the results m3" be the follow^*

!. Space charge effects have been neglected in both the theories. m case of OCVD, if the initial voltage (across the diode) is high enough (13), space charge efieote can be neglected for the OCVD curve at low ti^s- Whereas in case of Reverse Recovery, it

necessarily involves an excursion over the entire range of forward voltages, including the range for which the space charge region will dominate in producing the response (14).

2. In both the theories the junction is assumed to be abrupt and of zero width. In practical cases, it may never be so, and hence the theories may give different results. It has been reported (9) that a non-abrupt junction would Introduce some changes in results.

3. in case or nrvo. there is no external electric field after t = 0• but in case of reverse recovery, there is a large e lectric field after t = 0, which may affect the movement of carriers and hence the results obtained may differ.

4. mease of OCVD the fitting has been done at large e times (normally > 10 microseconds) whereas reverse recovery has oe en studied for small times only (1 to !5 microseconds)•

5« rnhe theory aB oaeumes infinite length in both sides of junctio n whereas m of solar cells, diffuse y «nt be taxen as of infinite length. This may also introduce deviations.

from these, it was found that in case of OCVD, Higher value of AP would give a better fit at

small values of time whereas a lower value of a would give a better fit at large values of time* It was not possible to make such a study in case of reverse recovery because of experimental limitations.

4. Conclusions

The study presented in this chapter may be summarised in these points*i*

1. in general p-n coupling would affect the reverse *recovery* results. As the values of a and T (« τ_B/ τ_E) *increases, the effect increases.*

2. Results obtained for the samples under study, by the two- methods namely OCVD and reverse recovery are different as summarised in Table 4.7. Reverse *recovery is* found to give higher value of minority *carriers lifetime* than those obtained by OCVD

3. The *fitting procedure* used in this investigation does not give a unique value *of* the fitting parameter a, as is evident from the results hence a unique value *of In-* B is diff*cult to find*

References

1. L.A. Meacham and .... Mchaels' "Observatlons of the Rapid Withdrawal of Stored Holes from Germanium Transistors and varistors... Phys. Rev., Vol. 78 No. 2, 1950.

2. n.G. Shulman and M.E. McMohan, " Recovery Currents in Germanium p-n Junction Diodes", J. Appl. Phys. Vol. 24 p.1267, 1953.

3. w. Miller. "Arc Prevention Using p-n Junotlon Reverse Transient-, Proc, IRE, VOL 4T M • *3, NO.H, 1957.

4. K.C. Hu, "Improving Pulse Rise Time with sh ff Diodes ", Electronics, Vol. 36, No. 7, 1963.

5. Yu. A.Tkhorik, -Transients in Pulsed Semiconductor Diodes, Jerusalems Israel Program for Scientific Translations, 1968.

6. Y.R. Nosov, Switching in Semiconductor Diodes New Yorki Plenum Press, 1969.

7. B. Lax and S.P. Neustadter, "Transient Response of a p-n junction", J. Appl. Phys., vol. 25, p.li4B/ lg54

8. R.H. Kingston, "Switching time in Juncdlon Modes and Junction Transistors". Proc. IRE, Vol. 42, p. 829, 1955.

9. R.H. Dean and C.J. Nuese, "A refined Step Recovery Technique for Measuring Minority Carrier Lifetimes and Related Parameters in Asymetric p-n Junction Diodes., IEEE Trans. Electron Devices Vol. ED-18, p.151, 1971.

io. *S.M. Sze,* Physics of Semiconductor Devices, *New York t* John Wiley & Sons, 1969.

11. L. DE Smet and R. van Overstraeten, "Calculation of the Switching Time in Junction Diodes "* Solid state Electronics, Vol. *18, p.557, 1975.*

12. *J.R. Lederhandler* and L.J. Gia coletto, "Measurement of Minority Carrier Lifetime and Surface Effects 1 n junction Devices'[1], Proc, IRE, vol. 43, *p.47y, 1955* .

13. S.C. Jain,*'Theory of Photo Induced Open Circuit voltage Decay in a Solar cell". Technical Report, Solid State physICS Laboratory' Mareh 1980.

14. *F.A.* Lindholm et. al., "A MBthatfoloov « yy tor Experian tally *Based Determination of Gap* t-h rinkage and Eff *Lifetimes in the Emitter and Base.* of • sc P-n Junction Sol *Cells and other* p-n *Junction Devieoou* * IESE Trans. *Electron Devices, Vol. ED-24,* p.402, 1977

TABLE 4.1

W(t) as a function of a and z for (= 2 (eq. (3.35))

2»	0.10	0.50	1.00	5.00	10.00
0.00	1.00	1.00	1.00	1.00	1.00
0.05	0.94	0.94.	0.93	0.93	0.93
0.10	0.89	0.87	0.87	0.86	0.86
0.15	0.83	0.81	0.80	0.80	0.80
0.20	0.77	0.75	0.74	0.73	0.73
0.25	0.71	0.69	0.68	0.67	0.67
0.30	0.66	0.63	0.62	0.60	0.61
0.35	0.61	0.58	0.56	0.55	0.55
0.40	0.56	0.52	0.51	0.50	0.50
0.45	0.51	0.47	0.46	0.44	0.44
0.50	0.46	0.43	0.41	0.40	0.40
0.55	0.42	0.38	0.36	0.35	0.35
0.60	0.38	0.34	0.32	0.31	0.31
0.65	0.34	0.30	0.28	0.27	0.27
0.70	0.31	0.27	0.25	0.24	0.24
0.75	0.27	0.23	0.22	0.21	0.20
0.80	0.24	0.21	0.19	0.18	0.18
0.85	0.21	0.18	0.16	0.15	0.15
0.90	0.19	0.15	0.14	0.13	0.13
0.95	0.16	0.13	0.12	0.11	0.11
1.00	0.14	0.11	0.10	0.09	0.09
1.10	0.10	0.08	0.07	0.07	0.06
1.20	0.08	0.06	0.05	0.05	0.04

TABLE 4.2

W(t) as a function of a and z for T = 20 (eq. (3.35))

z 'x	0.10	0.50	1.00	5.00	10.00
0.00	1.00	1.00	1.00	1.00	1.00
0.05	0.94	0.92	0.91	0.86	0.85
0.10	0.88	0.85	0.82	0.73	0.71
0.15	0.82	0.78	0.78	0.60	0.58
0.20	0.76	0.71	0.65	0.50	0.50
0.25	0.70	0.64	0.58	0.41	0.38
0.30	0.65	0.58	0.51	0.33	0.30
0.35	0.60	0.52	0.44	0.27	0.24
0.40	0.55	0.46	0.39	0.22	0.19
0.45	0.50	0.41	0.34	0.18	0.15
0.50	0.45	0.37	0.29	0.14	0.12
0.55	0.41	0.32	0.25	0.12	0.10
0.60	0.37	0.29	0.22	0.10	0.08
0*65	0.33	0.25	0.19	0.09	0.07
0.70	0.30	0.22	0.16	0.08	0.05
0.75	0.26	0.19	0.14	0.07	0.04
0.80	0.23	0.17	0.12	0.05	0.04
0.85	0.21	0.14	0.10	0.04	0.03
0.90	o.i8	0.12	0.08	0.04	0.02
0.95	0.16	0.11	0.07	0.03	0.02
1.00	O.I4	0.09	0.06	0.02	0.02
1.10	0.1°	0.06	0.04	0.01	0.01
1.20	O.O0	0.05	0.03	0.01	0.01

TABLE 4.3

W(t) as a function of a and z for $T = 50$ (eq.(3.35))

z \ a	0.10	0.50	1.00	5.00	10.00
0.00	1.00	1.00	1.00	1.00	1.00
0.05	0.94	0.92	0.90	0.82	0.79
0.10	0.88	0.84	0.81	0.66	0.61
0.15	0.82	0.77	0.72	0.52	0.46
0.20	0.76	0.70	0.63	0.41	0.34
0.25	0.70	0.63	0.56	0.32	0.26
0.30	0.65	0.57	0.49	0.26	0.20
0.35	0.60	0.51	0.43	0.21	0.16
0.40	0.55	0.46	0.38	0.17	0.12
0.45	0.50	0.41	0.33	0.13	0.10
0.50	0.45	0.36	0.29	0.11	0.08
0.55	0.41	0.32	0.25	0.09	0.06
0.60	0.37	0.28	0.21	0.07	0.05
0.65	0.33	0.25	0.18	0.06	0.04
0.70	0.30	0.22	0.16	0.05	0.03
0.75	0.26	0.19	0.13	0.04	0.03
0.80	0.23	0.16	0.11	0.03	0.02
0.85	0.21	0.14	0.10	0.03	0.02
0.90	0.18	0.12	0.08	0.02	0.02
0.95	0.16	0.10	0.07	0.02	0.01
1.00	0.14	0.09	0.06	0.01	0.01
1.10	0.10	0.06	0.04	0.01	0.01
1.20	0.08	0.05	0.03	0.01	0.00

TABLE 4.4

W(t) as a function of a and z for (= 100 (eq. (3.35))

z \ a	0.10	0.50	1.00	5.00	10.00
0.00	1.00	1.00	1.00	1.00	1.00
0.05	0.94	0.92	0.90	0.79	0.74
0.10	0.88	0.84	0.80	0.61	0.53
0.15	0.82	0.77	0.71	0.47	0.38
0.20	0.76	0.70	0.68	0.37	0.28
0.25	0.70	0.63	0.55	0.29	0.21
0.30	0.65	0.57	0.49	0.23	0.16
0.35	0.60	0.51	0.43	0.18	0.12
0.40	0.54	0.46	0.37	0.15	0.10
0.45	0.50	0.41	0.33	0.12	0.08
0.50	0.45	0.36	0.28	0.10	0.06
0.55	0.41	0.32	0.24	0.08	0.05
0.60	0.37	0.28	0.21	0.07	0.04
0.65	0.33	0.25	0.18	0.05	0.03
0.70	0.30	0.22	0.16	0.04	0.03
0.75	0.26	0.19	0.13	0.04	0.02
0.80	0.23	0.16	0.11	0.03	0.02
0.85	0.21	0.14	0.10	0.02	0.01
0.90	0.16	0.12	0.08	0.02	0.01
0.95	0.16	0.10	0.07	0.02	0.01
1.00	0.14	0.09	0.06	0.01	0.01
1.10	0.10	0.06	0.04	0.01	0.01
1.20	0.08	0.05	0.03	0.01	0.00

TABLE 4.5

w(t) as a function of a and zfor » 1000 (eq. (3.35))

z \ a	0.10	0.50	1.00	5.00	10.00
0.00	1.00	1.00	1.00	1.00	1.00
0.05	0.94	0.92	0.89	0.74	0.61
0.10	0.88	0.84	0.79	0.55	0.39
0.15	0.82	0.76	0.70	0.42	0.27
0.20	0.76	0.69	0.62	0.32	0.20
0.25	0.70	0.63	0.55	0.25	0.15
0.30	0.65	0.57	0.48	0.20	0.11
0.35	0.60	0.51	0.42	0.16	0.09
0.40	0.54	0.45	0.37	0.13	0.07
0.45	0.50	0,40	0.32	0.11	0.06
0.50	0.45	0.36	0.28	0.09	0.04
0.55	0.41	0.32	0.24	0.07	0.04
0.60	0.37	0.28	0.21	0.06	0.03
0.65	0.33	0.25	0.18	0.05	0.02
0.70	0.30	0.21	0.15	0.04	0.02
0.75	0.26	0.19	0.13	0.03	0.02
0.80	0.23	0.16	0.11	0.03	0.01
0.85	0.21	0.14	0.10	0.02	0.01
0.90	0.18	0.12	0.08	0.02	0.01
0.95	0.15	0.10	0.07	0.01	0.01
1.00	0.1⁴	0.09	0.06	0.01	0.01
1.10	c.i°	0.06	0.04	0.01	0.00
1.20	C.08	n.04	0.03	0.01	0.00

TABLE 4.6

W(t) as a function of a and z (eq. (4.18))

z \ a	0.01	0.10	0.30	0.50	0.80
0.00	1.00	1.00	1.00	1.00	1.00
0.05	0.94	0.94	0.98	0.92	0.90
0.10	0.89	0.88	0.86	0.84	0.81
0.15	0.83	0.82	0.79	0.76	0.73
0.20	0.77	0.76	0.72	0.69	0.65
0.25	0.72	0.70	0.66	0.63	0.58
0.30	0.67	0.65	0.60	0.56	0.51
0.35	0.62	0.59	0.54	0.51	0.45
0.40	0.57	0.54	0.50	0.45	0.40
0.45	0.52	0.50	0.45	0.40	0.35
0.50	0.48	0.45	0.40	0.36	0.30
0.55	0.43	0.41	0.36	0.32	0.27
0.60	0.39	0.38	0.32	0.28	0.23
0.65	0.35	0.33	0.28	0.24	0.20
0.70	0.32	0.29	0.25	0.21	0.17
0.75	0.29	0.26	0.22	0.19	0.15
0.80	0.25	0.23	0.19	0.16	0.13
0.85	0.28	0.20	0.17	0.14	0.11
0.90	0.20	0.18	0.15	0.12	0.09
0.95	0.18	0.16	0.13	0.10	0.08
1.00	0.15	0.14	0.11	0.09	0.07
1.10	o.H	o.io	0.08	0.06	0.05
1.20	0.09	0.08	0.06	0.04	0.03

Contd ......

TABLE 4.6 (Contd.)

z \ a	1.00	3.00	5.00	8.00	10.00
0.00	1.00	1.00	1.00	1.00	1.00
0.05	0.89	0.80	0.72	0.63	0.58
0.10	0.80	0.65	0.54	0.43	0.40
0.15	0.71	0.52	0.41	0.30	0.26
0.20	0.63	0.43	0.32	0.22	0.19
0.25	0.55	0.35	0.25	0.17	0.14
0.30	0.48	0.29	0.20	0.13	0.11
0.35	0.42	0.24	0.16	0.10	0.08
0.40	0.37	0.20	0.13	0.08	0.07
0.45	0.32	0.16	0.10	0.07	0.05
0.50	0.28	0.13	0.08	0.05	0.04
0.55	0.24	o.n	0.07	0.04	0.03
0.60	0.21	O.C®	0.06	0.03	0.03
0.65	0.18	0.08	0.05	0.03	0.02
0.70	0.15	0.06	0.04	0.02	0.02
0.75	0.13	0.05	0.08	0.02	0.01
0.80	o.n	0.04	0.03	0.01	0.01
0.85	0.09	0.04	0.02	0.01	0.01
0.90	0.08	0.03	0.02	0.01	0.01
0.95	0.07	0.02	0.01	0.01	0.01
1.00	0.06	0.02	0.01	0.01	0.00
1.10	0.04	0.01	0.01	0.00	0.00
1.20	0.03	0.01	0.00	0.00	0.00

TABLE 4.7

A summary of the results obtained by reverse recovery and OCVD methods.

S.No.	Devices	Minority carrier lifetime in μ secs. Reverse recovery*		OCVD	
		3=0 • 1	a=l.l	a=0.1	a=l.l
1.	BY 127 (Silicon Diode)	33	85	8	11
2.	DR 25 (Germanium Diode)	18	45	11	16
3.	SC 4 (Silicon Solar Cell)	60	160	20	30

Figure Captions

Fig. 4.1 Reverse recovery transient behaviour of a

p— n junction

(a) basic switching circuit

(b) transient response, tj.is the time interval for constant current phase

(c) junction voltage as a function of time

(d) minority carrier distribution for various time intervals.

Fig. 4.2 w(t) as a function of z for T= 2. The three curves are for a - 0.1. 1.0 and 10.0 (eq.(3*35)).

Fig. 4.3 w(t) as a function of z for I = SO. The three curves shown are for a - 0.1. 1.0 and 10.0 (eq.(3.35)).

Fig. 4.4 w(t) as a function of z for t - 1000. The three curves shown are for a = 0.1. 1.0 and 10.0 (eq.(3.35)).

Fig* 4.5 W(t) as a function of z_t based Qn eq.(4.18), shown tor three values of a, i.e. 0.1, 1.0 and 10-°'

Fig* 4.6 Circuit ^<aaram for studying the reverse recovery tr transients of a p-n junction,

Fig. 4.7 Experimental result of reverse recovery
transients of BY 127 (silicon diode) plotted
as $(I_R/I_F)/(1 + I_R/I_F)$ versus (tp for three
different forward currents (a) 6 mA (b) 11 mA
(c) 22 mA.

Fig. 4.8 Calculated < $I_R/I_F)/(1+I_R/I_F)$ as a £unctl<jn
of £for a - o.l and . 33 mlcroseconds' τ_B
Points indicate the ejqjerimental results of
silicon diode (BY127) at I_p . li mA. These
points could also *be fitted* quite well with
calculated curves for a « 1,1, •£B› c5
microseconds and a = 0.01, 7;3› 2g micro-
seconds.

Fig* 4,9 calcuated *(W/(l* +IZ *as a function*
of *t*for* a ® 0.01 and *'r* *CB* micro-
seconds. *Points indicate* the experimental
results of germanium diode (DR 25) at
I_F = 18 mA. These points could also be
fitted quite well with calculated curves
for a = 0.1, Z_B - microseconds and

3 *S3 1.1/* Ljg *

Fig. 4.10 Calculated $(I_1/I_2)/(1+I_1/I_F)$ as a function

of t, for a = 0.1 and τ_B = 60 microseconds.

Points Indicate the experimental results

of silicon solar cell (SC4) at I_F = 13.5 mA

These points could also be fitted quite well

with calculated curves for a ® 0.01,

τ_B a 52 microseconds and a « 1.1, τ_B * 160

microseconds.

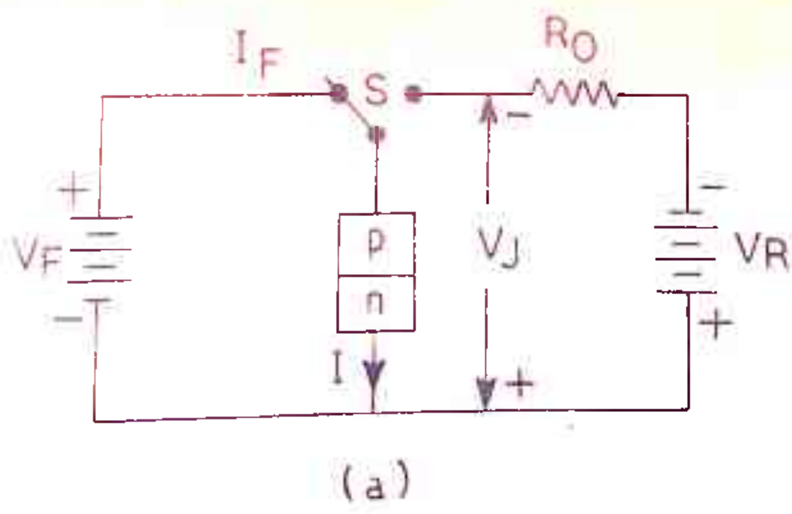

(a)

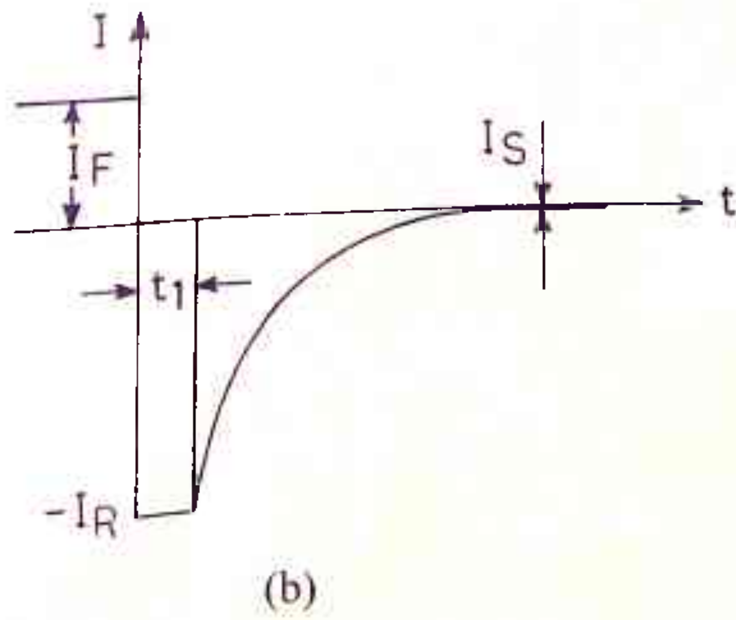

(b)

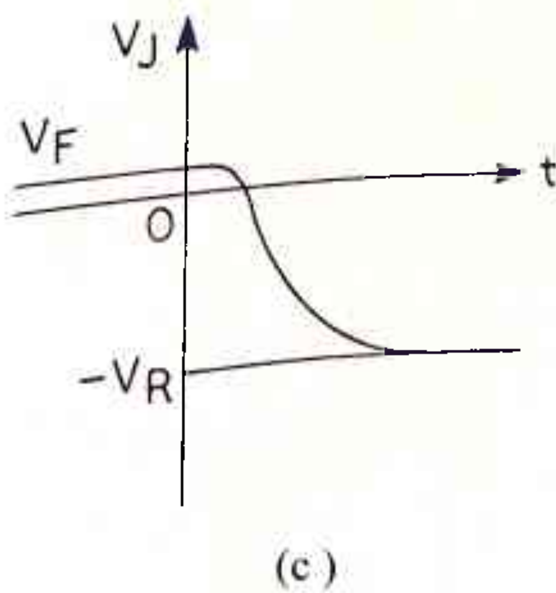

(c)

FIG. 4.1

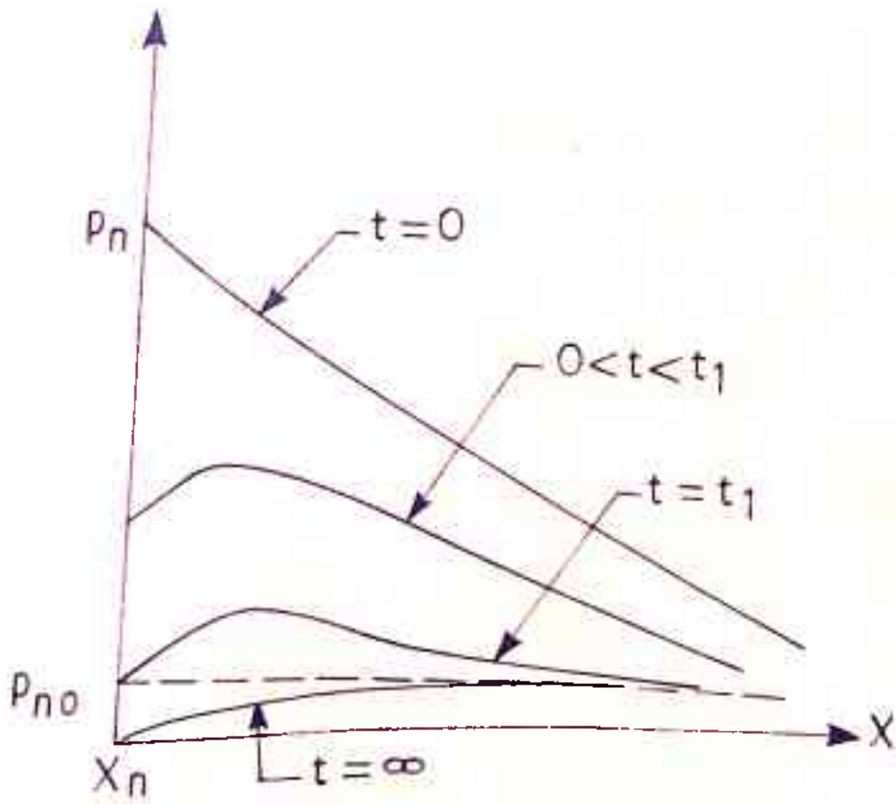

(d)

FIG. 4.1

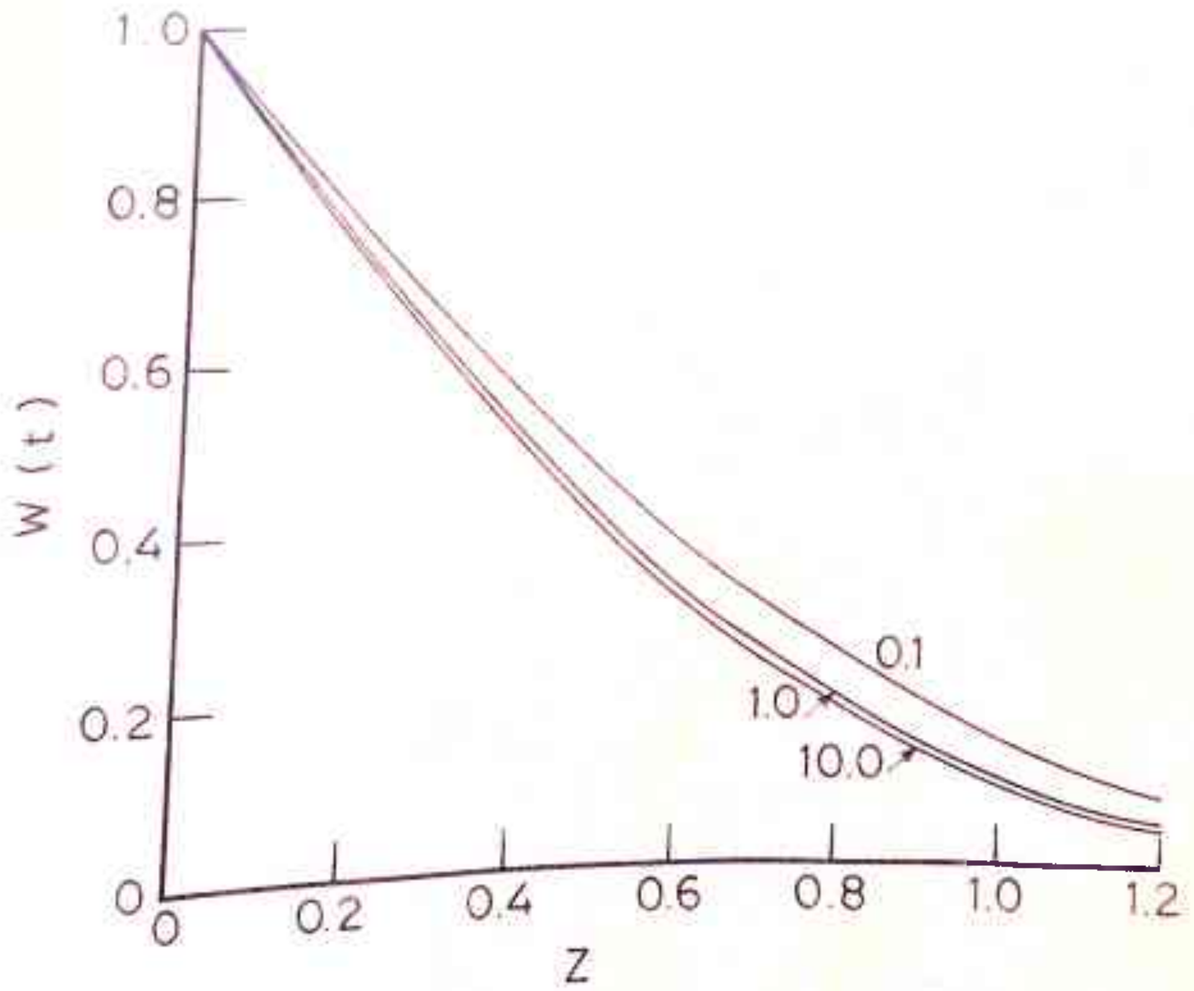

FIG. 4.2

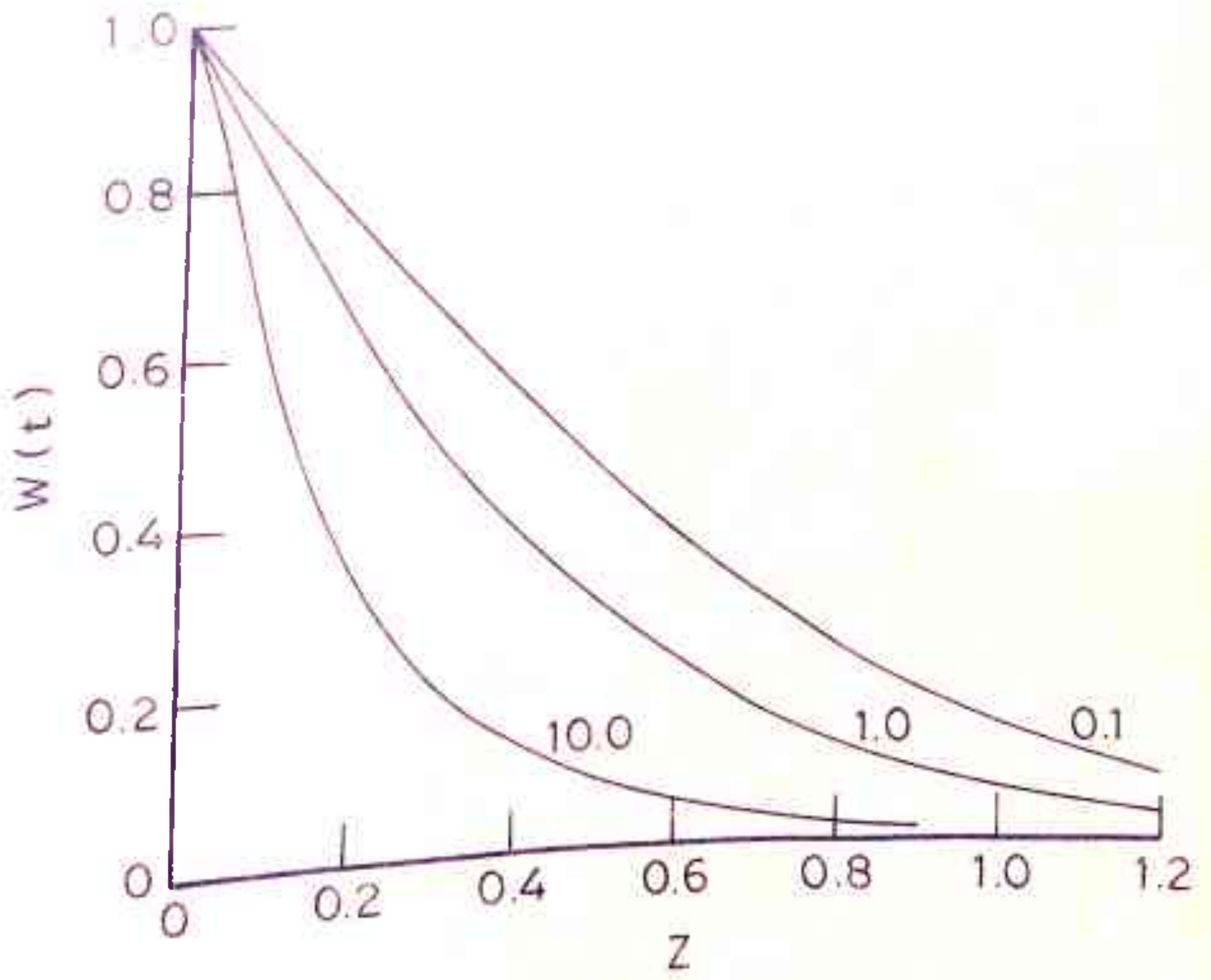

FIG.4.3

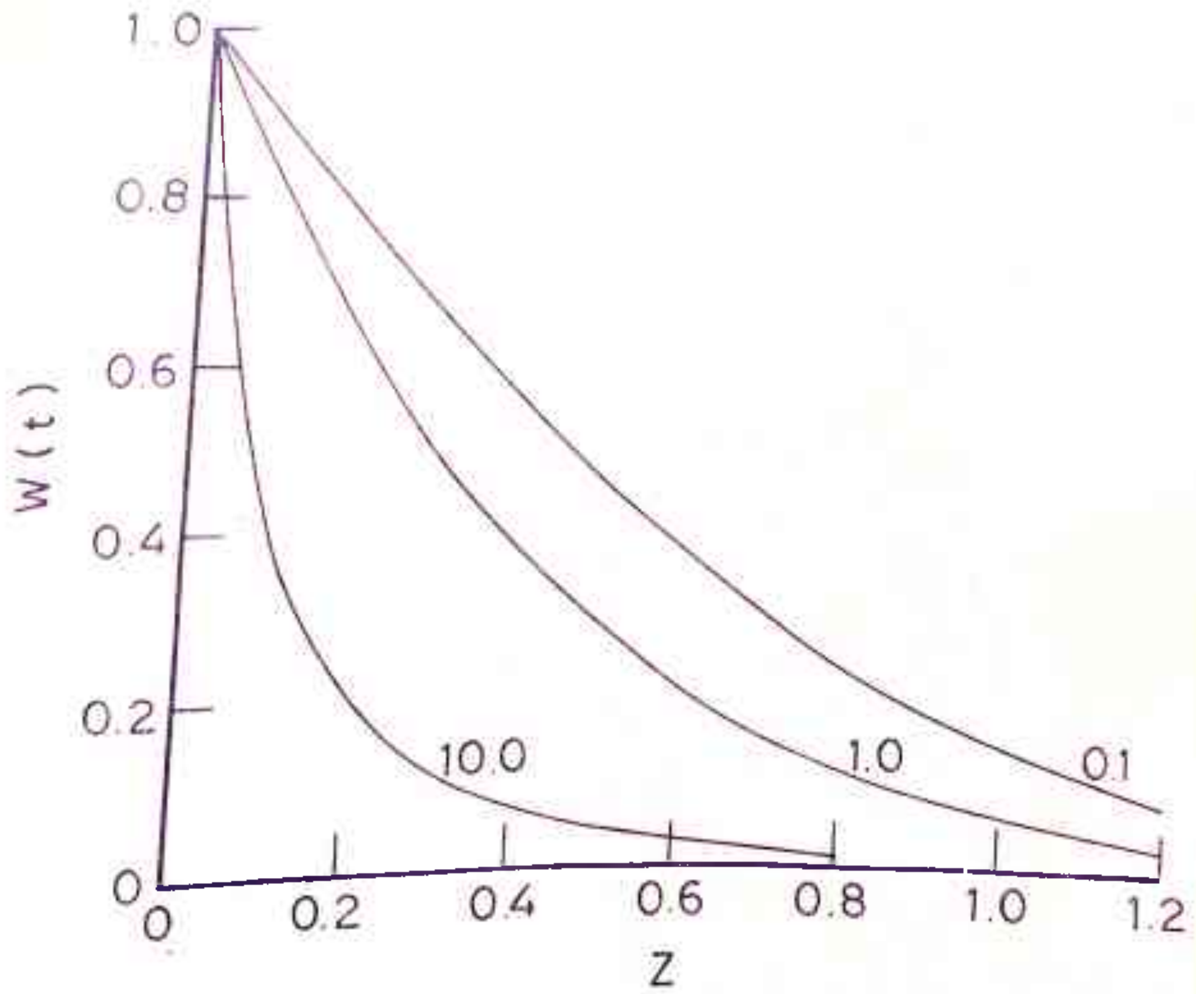

FIG. 4.4

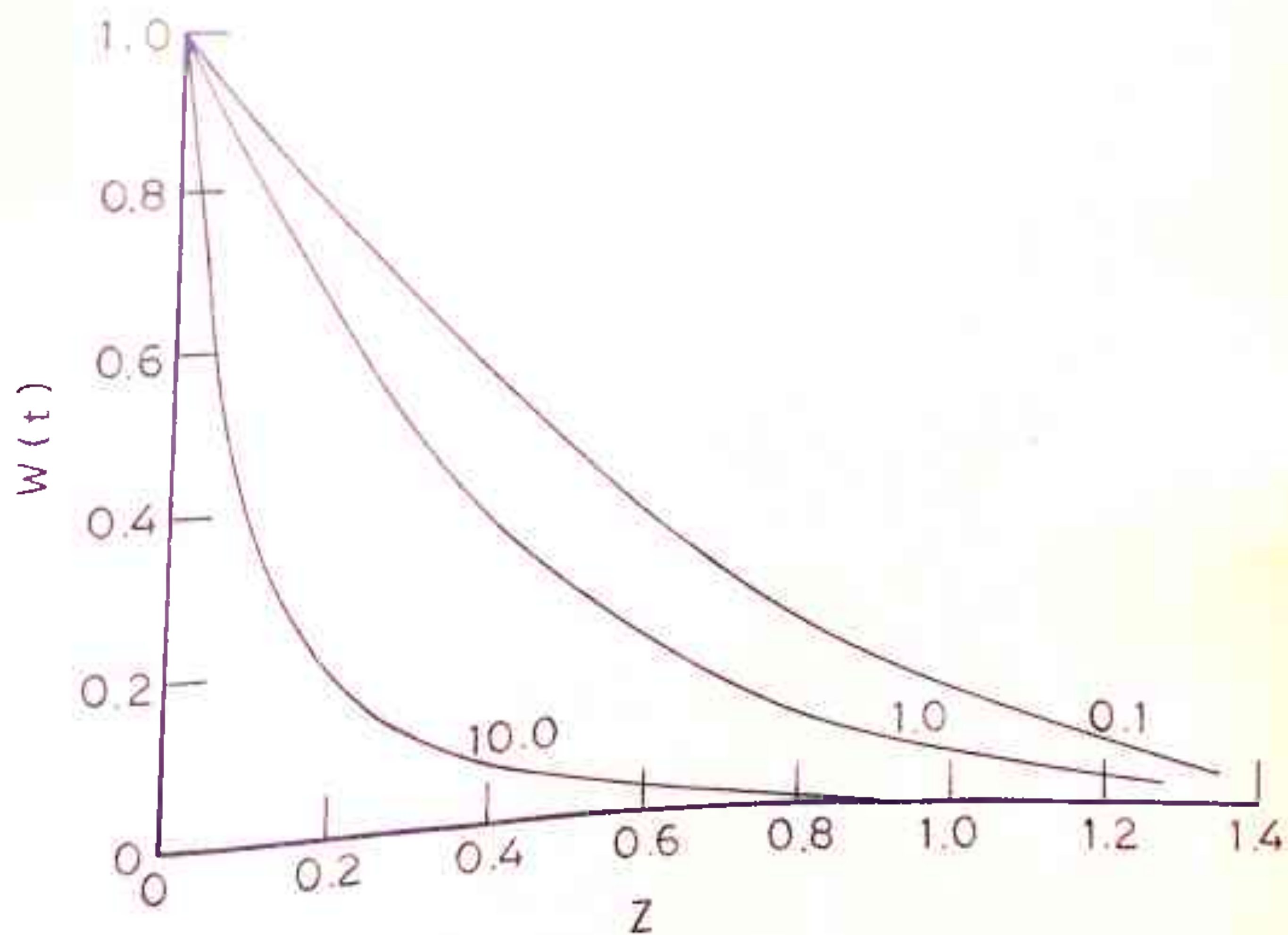

FIG. 4.5

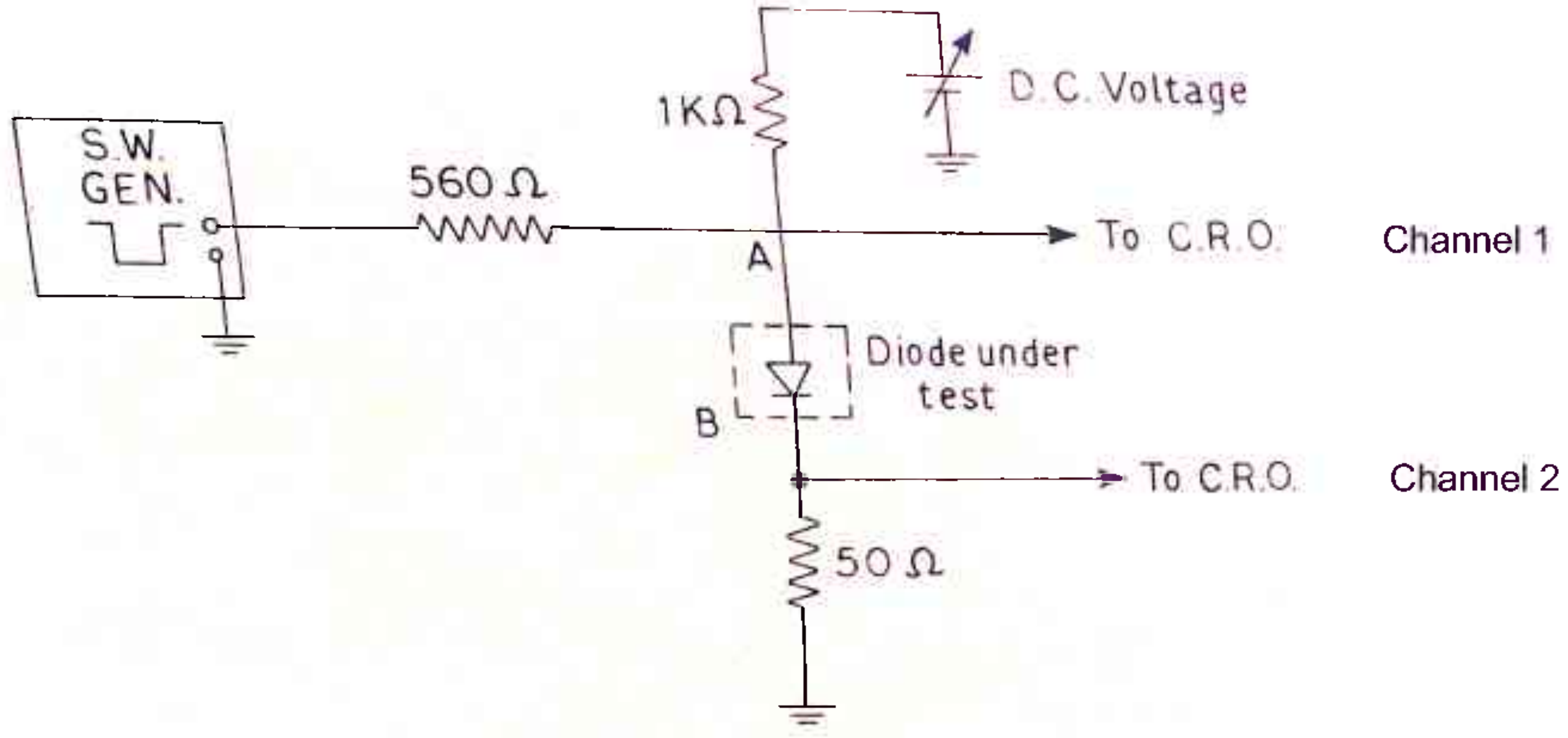

FIG.4.6

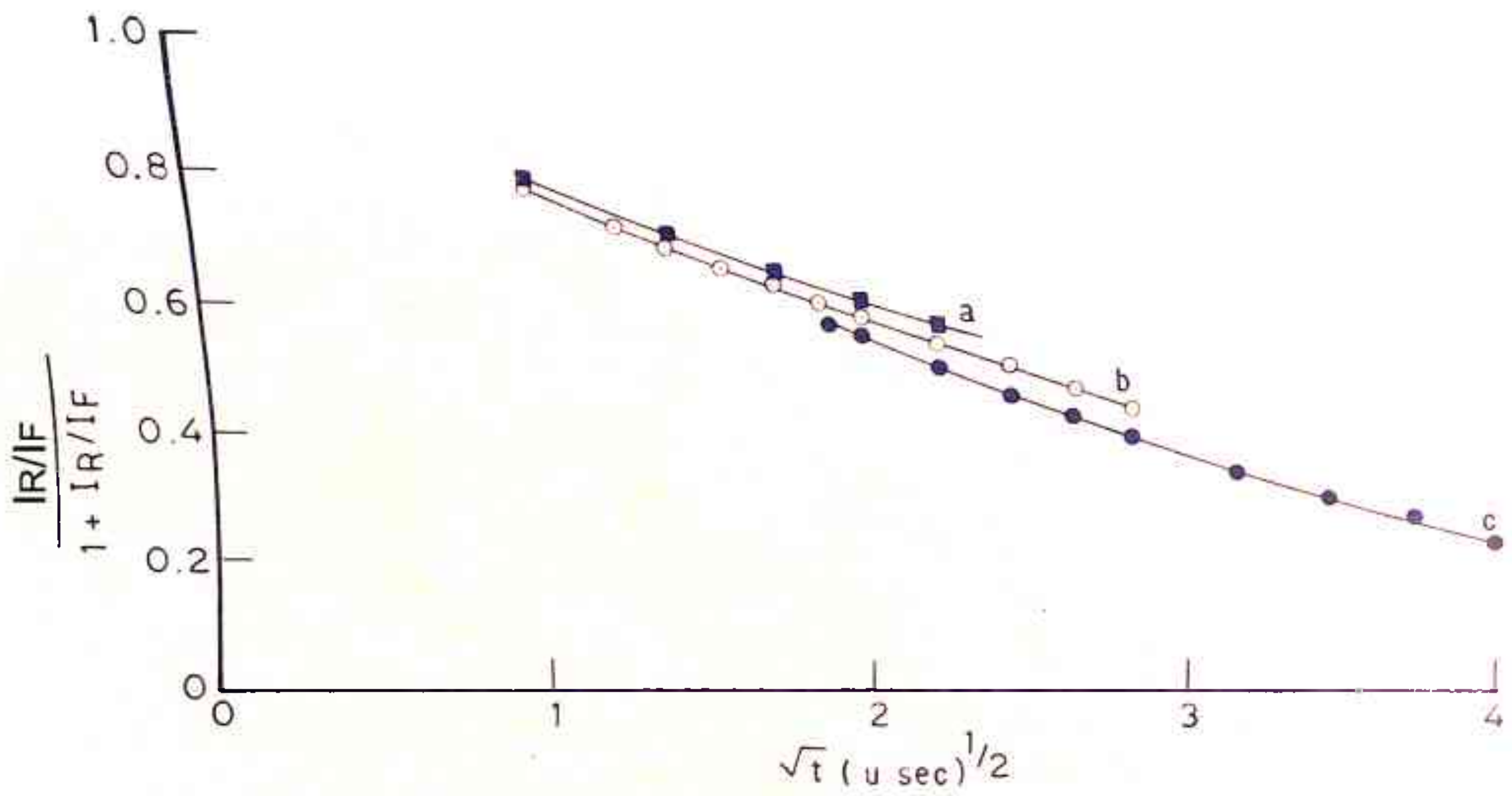

FIG. 4.7

its

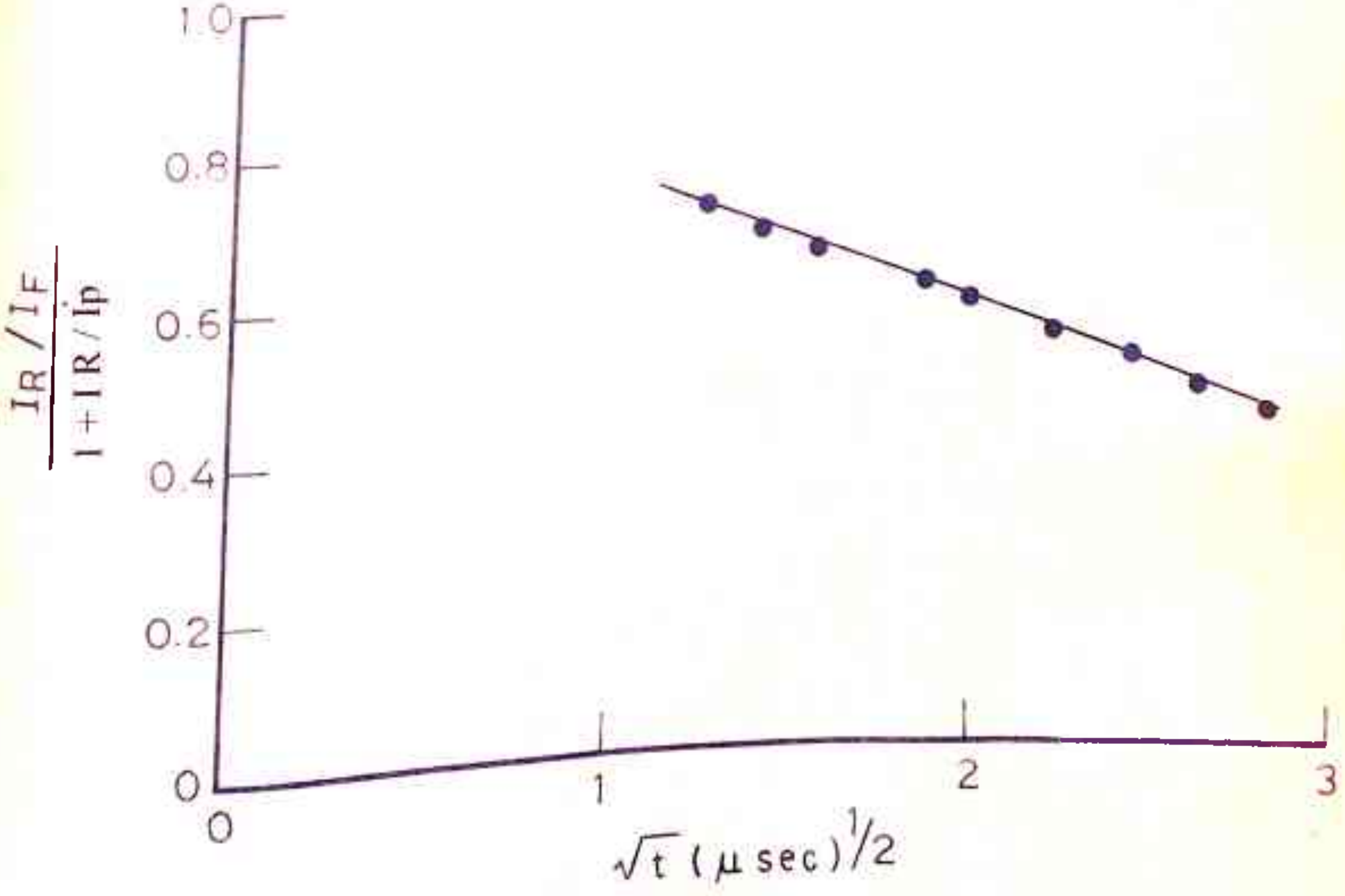

FIG. 4.8

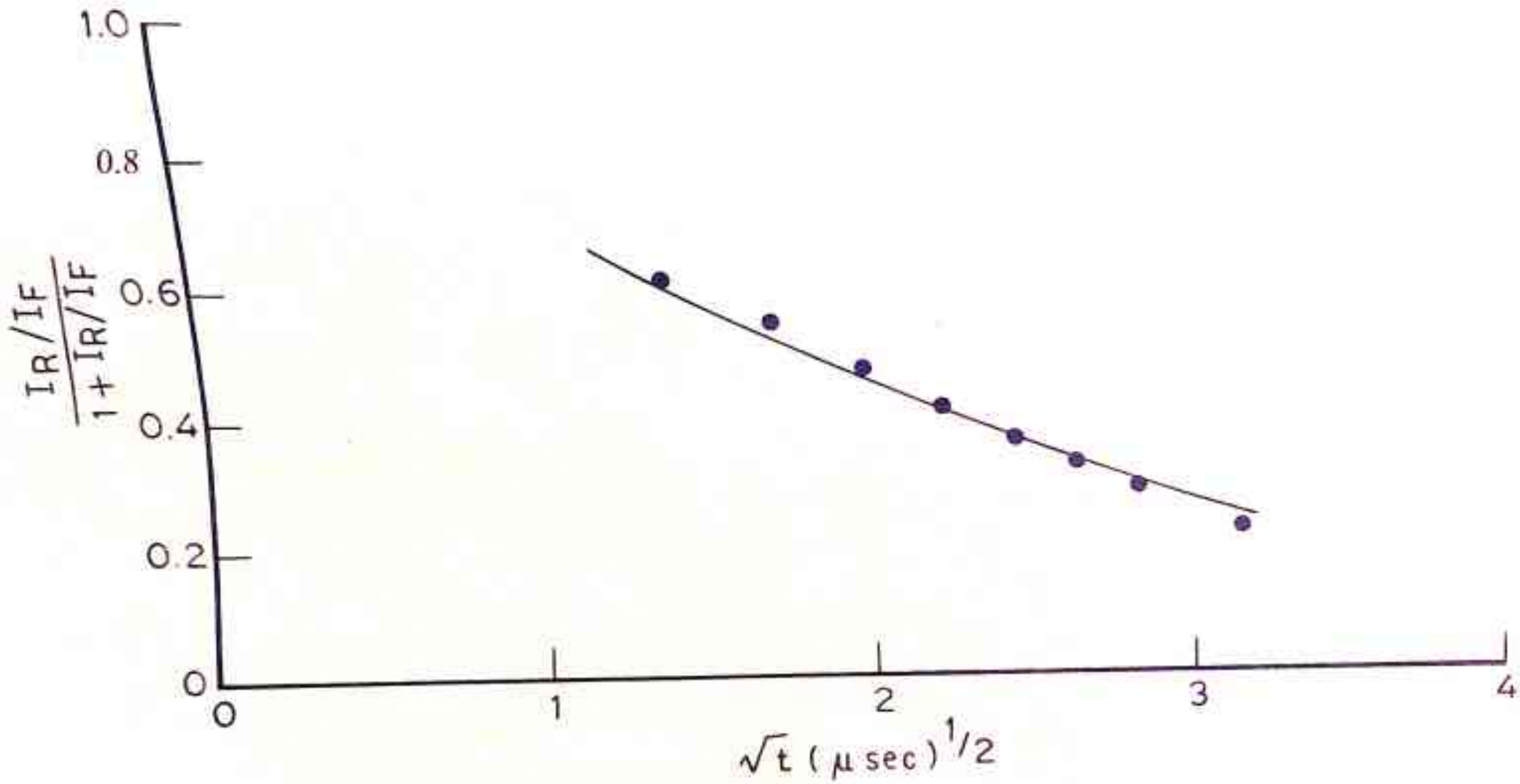

FIG. 4.9

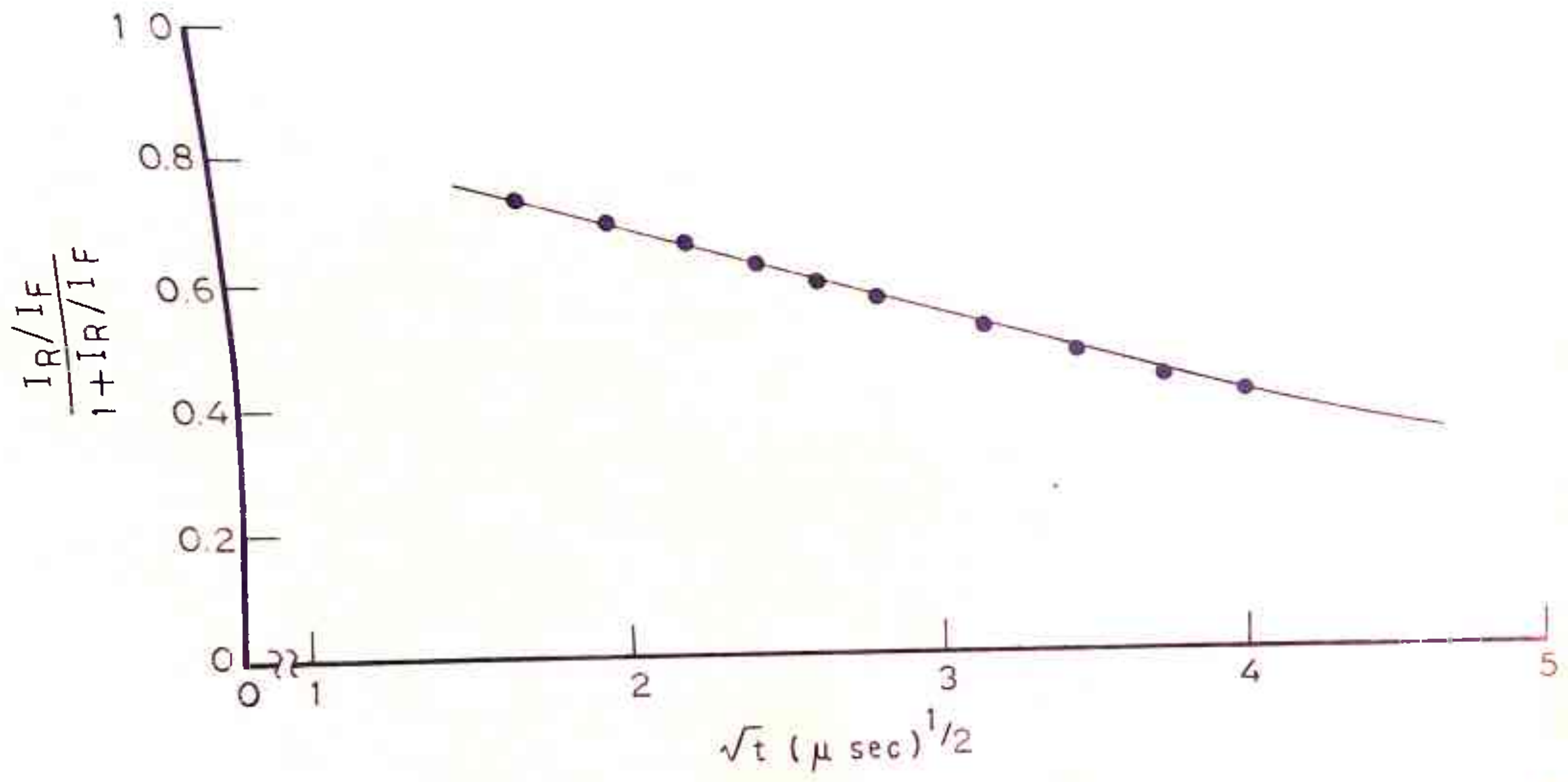

FIG. 4.10

CHAPTER V

PHOTO VOLTAGE DECAY

CHAPTER V

PHOTO VOLTAGE DECAY

Introduction

In last two chapters we have studied two different methods of measuring lifetime of minority carriers in p-n junction diodes. Both methods are based on injection of carriers using electric pulses Both of them can be used to study the transient behaviour of solar cells as well*

A *solar cell, for appU PPiication purposes,* is *almost always exposed to light. The profit* o minority *carriers in the base as* well as emitter emitter region, In case of *exposure to light is different from* w "it one create by *injection of carriers by electrical* *ical* methods d). Hence whether a *solar cell is used in* direct current or *transient (e.g. switching) applications* its response to *optical excitation may be different from that* to an *electrical excitation* (1). For this reason a study of *solar cells under optical* excitation *or minority *carrier lifetime determination,* become. 4 Wortant. *Mahan* et. al *(2) have reported their* *experimental* results of the *study of photo voltage decay of* solar cells by *using a stroboscope. They have used the* theory of OCVD (dark) to Interpret the results of PVD (h voltage decay)

though they find that the voltage decay pattern in the two cases may be different. However, they have not studied the spectral dependence and intensity dependence of photo voltage decay. Jain (1) has given a theory to interpret the results of such an experiment by taking a solar cell equation while neglecting the diffuse layer contribution and has suggested that response will be different for different wavelengths of light.

In this chapter we report our experimental results Of photo voltage decay of a solar cell at different wave-lengths and intensities. Our experimental results of spectral dependence are found to be qualitatively in agreement with the theory proposed in (1). It is also shown that slope of the OCVD and PVD are not much different at large values of time.

2. Theory

We consider a p^n solar cell with abrupt junction at x = *0, front (illuminated surface* at x=-d and back *surface* at *(see Fig. 1.2)*

At t>0 when light is switched off, the continuity equation for minority carriers can be written (4) as

$$D_n \frac{\partial^2 n}{\partial x^2} - \frac{n}{\tau_n} = \frac{dn}{dt} \qquad (5.1)$$

$$D_p \frac{\partial^2 p}{\partial x^2} - \frac{p}{\tau_p} = \frac{\partial p}{\partial t} \qquad (5.2)$$

In eq. (5.1) and *(5.2)* all the r- ■ - symbols have their usual *meaning. The* boundary conditions (3), (4) for the eq. (5.1) and(5.2) are the following,

(i) $D_n \left(\frac{\partial n}{\partial x}\right)_{-d} = s\,n(-d)$ (5.3)

where s is the surface recombination velocity.

(ii) $\frac{n(o)}{n_{po}} = \frac{P(o)}{P_{no}} = \exp(qV/kT) - 1$ (5.4)

where *V is the open circuit voltage.*

(iii) $D_n \left(\frac{\partial n}{\partial x}\right)_{o} + D_p \left(\frac{\partial p}{\partial x}\right)_{o} = 0$ (5.5)

i • e • *t total* current throu h the Junction I_s zero>

(iv) $p(\wedge) = 0$ *(5.6)*

(assuming an ohmic contact at the back)

(v) The steady state carrier profile including the *p-n coupling effect is given* (4) by

$$p(x,o) = K \exp(-VLp) * (1- \frac{cZ N_o \tau_p}{\alpha^2 L_p^2)} \exp [. \alpha (x+d)$$

where

$K'' p_{no}$ f exp(qV/kT) -lj - ot 'tj exp (- α d) / (l- ck^2 l?)

All the symbols have the same meaning as described in chapter 1.

It has not been possible to solve eq.(5.1) and (5.2) with all the above boundary conditions. However, if we *neglect* the contribution due to diffuse layer, the solution (1) for the open circuit voltage (photo voltage) is given as

$$\Delta V = -z^2 + \ln \left[\frac{c\, S(z) - s(cz)}{c-1} \right] \qquad (5.7)$$

where

$$z^2 = \frac{t}{T_p} \qquad (5.8)$$

$$S(z) = e^{z^2} \mathrm{erfc}(z) \qquad (5.9)$$

$$c = \alpha\, i_p \qquad (5.10)$$

$$\text{and } \Delta v = (V(t) - V(o)) \frac{q}{kT} \qquad (5*11)$$

The slope of PVD curve at a point z l_s given

(1) by

$$-T(z) \,'1+c\, csCzy \left[\frac{j\, cS(cz) - S(z)}{sCcz)} \right] \qquad (5.12)'$$

which shows that slope at a point z depends on cL, L_p

and T_p. Hence, if a graph is plotted between AV and kT

t for experimental data and a suitable fit is obtained

with eq (5.7) and for eq.(5«12)' would give the values

of c <- oZ.L_p) and 'tp-

We now examine the large t behaviour of eq.(5.12).

We shall use the asymptotic expansion (eq.(3.47)) to

expand S(z) for large values of z(z >2),

when $z \geq 2$ and zc >2. eq.(5.12) can be written as

$$-T(\hat{}) \approx 1\, t \qquad \frac{1}{2z^2\left[1 - \frac{1}{2z^2} + \frac{1}{2z^2c^2}\right]} \qquad (5.13)$$

Using the expansion

$$(1 + x)^{-1} = 1 - X + \qquad (5.14)$$

we can write eq.(5.13) in the form

$$\frac{1}{2z^2} \quad \frac{1}{4z^4} - \frac{1}{-\gg\!<\!\gg\!>} \;'' \; 1+ + +''' \qquad (5,15)$$

Eq. (5.15) shows that when z >> 1 and zc>> 1, slope of a PVD curve will have a very weak dependence on c. At sufficiently large values of z slope will be independent of the wavelength of light falling on it.

3. Experimental Study

All the measurements reported in this chapter were taken on an SC4 *(Plessey) solar* cell. used General Radio (USA) Type 1531-AB electronic stroboscope to get light *flashes.* *Vie* used its medium speed range *which gives* flashes of 1*2 microseconds duration measured *at* 4 peak intensity.

To monitor traveform a Tektronix Type 556 oscilloscope with 1A1 Plu$_9$ in was used.

Fig. 5.1 r -hows the photo voltage decay patterns for composite f as light and five monochromatic lights. To obtain monochromatic ^4.4- lioht. interference filters ,, d by Toshina (Japan) were used. X_{max} of the filters *SUPP 6* , *90,* 590, 560. 500 and 410 nm.

Fig. 5.2 shows t. the PVD curves for different intensities' wh c h were obtained by changing the distance of solar cell tr ,, from strobe lamp.

Fig. 5.3 shows the same results plotted in the form of (V(t) - V(o)) with respect to t. This figure shows that curves of V(o) 0.5, are identical for first about 80 microseconds.

Fig. 5.4 shows PVD curves for composite and various monochromatic lights (shown in Fig. 5.1) in the form of (V(t) - V(o)) with respect to t.

Fig. 5.5 shows the (v(t) - V(o)) dependence on t for composite (V_Q - 0.5V) as well as monochromatic lights of λ_{maxF} = 690, 590, 560, 500 nm.

rom Fig. 5.1, it is clear that all the filter PVDs (except the one for λ_{max} - 410 nm) — '<«»« °'5V-

If there was no Λ dependence, on a (y(t) - V(oj) vs. t plot, they Should have been identical for first few tens of microseconds. Fig. 5.5 shows that for different λ_{max} slope of the curves *is different.* Also as wavelength decreases (i.e. α increases), slope of PVD curve Increases, which qualitatively confirms the theory proposed in (1).

Mahan et, al. (2) have reported that s> in case *of OCVD (dark) is* different « from the one observed *in PVD for the same sample. To stud*y this we have observed *OCVD (dark) and PVD for SC4 in pi*y* 3.6. Cu^ 3 dotted *in Fig. 5.6 represent OCVD (dark)* $_a$*t <* , curv *initial curr-* represent *17 mA and 54 mA respectively,* 3nd *2* and 5 *of*

PVD at V_Q =■ 0.495, 0.5 and 0.6 respectively. Curve 2 and5 are for composite light (only the distance of cell from lamp is changed) whereas for curve 1 we have used an Interference filter of λ_{max} ® 500 nm, it is apparent that, though the behaviour at t ~ 0 is different, but later (after 20 microseconds) slopes become almost same, and they remain so till the space charge effects set in .The value.* of minority carrier lifetime calculated from the linear region by using the approximate formula (1)

$$T_e = -I^s- \frac{\hat{}r}{Q} \quad (sas)$$

(where $\frac{V_1-V_2}{t_2-t_1}$ *is* the slope of the OCVD (dark or PVD curve) for curves 1 to 5 in Fig. 5.6 is tabulated in the Table 5.1.

This shows, that even by using a very approximate formula (5.15) we get results within 20% of each other.

Another point, which Mahan et. al * (2) have put *forward is that the photo* induced voltage persists for *longer durations* than that of OCVD (dark)• We can see *from Fig,* 5.2 that at least for the curves 1, 2 and 3 the *slopes of PVD (after an initial* difference) are almost *same (see also Fig** 5.3) till approximately 0.4v, where-space charge effects set in (1) and a faster decay starts (5).

If the initial voltage is higher than <~»0.4 V, the curve

has almost the same slope upto 0.4 V and then decays faster. We have studied this phenomenon upto 0.64 V. The conclusion we have drawn that higher the initial voltage, more is the time for which they (almost) straight line region persists and it looks like that the voltage persists for more time.

A study of Fig* 5.6 woulc reveal that if two curves of approximately same V(o) (excluding initial h rp drop for OCVD (dark) case) are taken, there is no appreciable difference in the persistence of voltage sho n in curves representing the two methods, till the space charge effect- start dominating. In fact, for this sample we rina ''nd that for approximately the same V(o) (as described above) it % 4* is the OCVD (dark) curve which persists slightly longer (cuxve Corves 3 & 4). This may mean that decay in this sample at the time when space charge effects are slower when the carriers are injected by <SOmina*1"l method than when they are generated by shining el6Ctr A detailed study of this kind may lead to a b tter light. un derstanding o£ the phenomena taking place in the space charge region and redistribution of carriers•

As proposed in (1), we e*pcrimcntaliy find as the *wavelength of light (falu*no n fh. cell) d 4 that the *waveform starts showing* a *kink st* 0. j»k accr®eses, *been shown in Fig. 5.1 though we* uld not take

in that region because of limitations of measurements. The light pulse also has a finite (of the order of micro-second) decay time which puts limitations on the interpretation of PVD at small times. For these reasons, we find it difficult to fit / in the region of t 0 eq.(5.7) where it is more sensitive. However we shall use eq.(5.12) to interpret the results by finding slope of the curves for various wavelengths in Fig. (5.4) around t 20 micro-seconds. Table 5.2 summarises these results.

Table 5.2 also shows the value of calculated for each curve. The reasons for descrepancy in the value of L may be the following}

1. Space charge effects have been neglected.

2. Thickness of the base is assumed to be infinite whereas in modern solar cells, it is comparable to the diffusion length.

3, The contribution due to diffuse layer and also the p-n coupling have been neglected, it has been already shown (see chapter 3) that p-n coupling can substantially affect the decay pattern.

4* Th theoretical curve is most sensitive to various parameters at t o. whereas It/ was not possible for us to

take data in this region because of experimental limitations. With more sophisticated equipments one may be able to examine the theory in more details.

V(O) for the curve for λ_{max} · 410 nm is already too low (0.435 V) hence the space charge effects will be dominating after a few microseconds, so no calculations for the PVD for (A ») 41n max 7 'J-U nm have been presented here.

4. Conclusion>

1. *In* our investigations we find that PVD curve gives almost a straight line, independent of the intensity or light (upto about 0.64 volts on higher side), till the space charge effects start dominating (on the lower side) It is expected that at higher intensities, saturation effects will start dominating, but those studies have not been carried out in this investigation.

2. With decrease in wavelength slope of the PVD curve increases (at small values of time) as suggested in (1).

3. For our sample, we dl^ot find much differenc in the slope of the straight line for OCVD (dark) and PVD curves. Nor did we find much difference in the time for which voltage persists.

References

1. S.C. Jain^ •'Theory of Photo Induced Open Circuit Voltage Decay in a Solar Cell", Technical Report (1980)/ Solid State Physics Laboratory/ Delhi-110007.

2. • J.E. Mahan et. al. "Measurement of Minority Carrier Lifetime in Solar Cells from Photo Induced Open Circuit Voltage Decay"/ *IEEE* Trans. Electron Devices, Vol. ED-26, p.733, 1979.

3. J.P. McKelvey, Solid State and Semiconductor Physics, New York : Harper & Row, 1966.

4. S.K. Sharma, A. Agarv/ala andV.K. Teuary, -Effect of p-n Coupling on Steady state and Transient Characteristics of a p-n junction solar Cell". To be published in J. *Phys,* D. (Applied Phys.) 1981.

5. J. Basset, .Aweervations on a Method of Determining the carrier Lifetime in P' ln n'- S' -n' Diodes**, Solid state Electron./ Vole 12* P* 385, 1969,

TABLE 5.1

Calculated minority carrier lifetime using eq.(5.16) for SC4 solar cell from the OCVD (dark) and PVD curves shown in Fig. 5.6.

S.No.	Curve	Experiment	Region used for calculation	τ_e (Microseconds)
1.	1	PVD (Filter λ_{max}=500 nanometer)	20 to 40 micro-seconds	18.3
2.	2	PVD (Composite light)	40 to 60 micro-seconds	20.2
3.	3	OCVD (dark) (I_F=17 mA)	20 to 80 micro-seconds	20.0
4.	4	OCVD (dark) (I_F=54 mA)	40 to 80 mitfcro-seconds	20.1
5.	5	PVD (Composite light)	50 to 100 micro-seconds	19.2

TABLE 5.2

A summary of PVD results for different wavelengths of light.

S.No.	Filter λ max	$\frac{\alpha}{kT}$ $\frac{V_1 - V_2}{t_2 - t_1}$	(For = τ_p micro seconds) approximate value of L_P
1.	690 nm	0.045	20 micrometer
2.	590 nm	0.050	80 micrometer
3.	560 nm	0.052	100 micrometer
4.	500 nm	0.057	200 micrometer

Figure Cantions

Fig. 5.1 Photo voltage decay of silicon solar cell (SC4) at different wavelengths of light. The distance of lamp from the cell was kept same for all the sets of readings taken here. Curve 1 is for the composite light given by the lamp. For other curves# interference filters were used to get monochromatic light, curves 2, 3, 4, 5 and 6 correspond respectively to the filters of

QK = 690, 590, 500, 560 and 410 nm.
A max

Fig. 5.2- Photo voltage decay of silicon solar cell (SC4) at different illumination levels. Illumination level was changed by changing the distance of lamp from the cell. Curves 1 to 5 represent increasing distance of lamp from the cell.

Fig. 5.3 Photo voltage decay of silicon solar cells (SC4) at different illumination levels. Curves 1 to 5 of Fig. 5*2 plotted as voltage drop as a function of time. The voltage at t ® 0, i.e. V(o) « 0*64, 0.6, 0.5, 0.45 and 0.44 respectively for curves 1, 2, 3, 4 and 5.

■ ig. 5.4 Photo voltage decay of silicon solar cell (SC4) at different wavelengths of light, plotted as voltage drop as a function of time, curve 1 corresponds to composite light andcurves 2 to 6 correspond respectively to filters of λ max " 690* 590* 560* 500 and 410 nm.

Fig. 5.5 Photo voltage decay of silicon solar cell (SC4) at different wavelengths of light. Curves 2, 3, 4 and 5 correspond respectively to λ_{max} ~ - 690, 590, 560 and 500 nm. Curve 1 corresponds to composite light, but the distance of the lamp was so adjusted that V(o) (i.e. open circuit voltage at t » o) is equal to 0.5 Volts. This has been done to compare it with the PVD corresponding to various^ wavelengths, because V(o) for Λ_{max} « 690,/560 and 500 nm is about 0.5 Volts. The curve corresponding to 410 nm gives V(o) 0.435V and it can be seen from Fig. 5.1 that space charge effects start dominating within a few microseconds, hence PVD for $/_{max}$ • 410 nm has not been put here for comparison. Although it is shown in Fig.5.4 along with curves for other wavelengths.

Fig. 5.6 Λ comparison of open circuit voltage decay and photo voltage decay of silicon solar cell (SC4). Curves 3 and 4 correspond to open circuit voltage decay with forward currents of 17 mΛ and 54 mΛ respectively. Curves 2 and 5 correspond to photo voltage decay for composite light at $V(_o)$ = 0.5V and 0.6 respectively. Curve 1 corresponds to photo voltage decay for filtered light of $7\backslash_{max}$ - 500 nm and V(o) 0.495V.

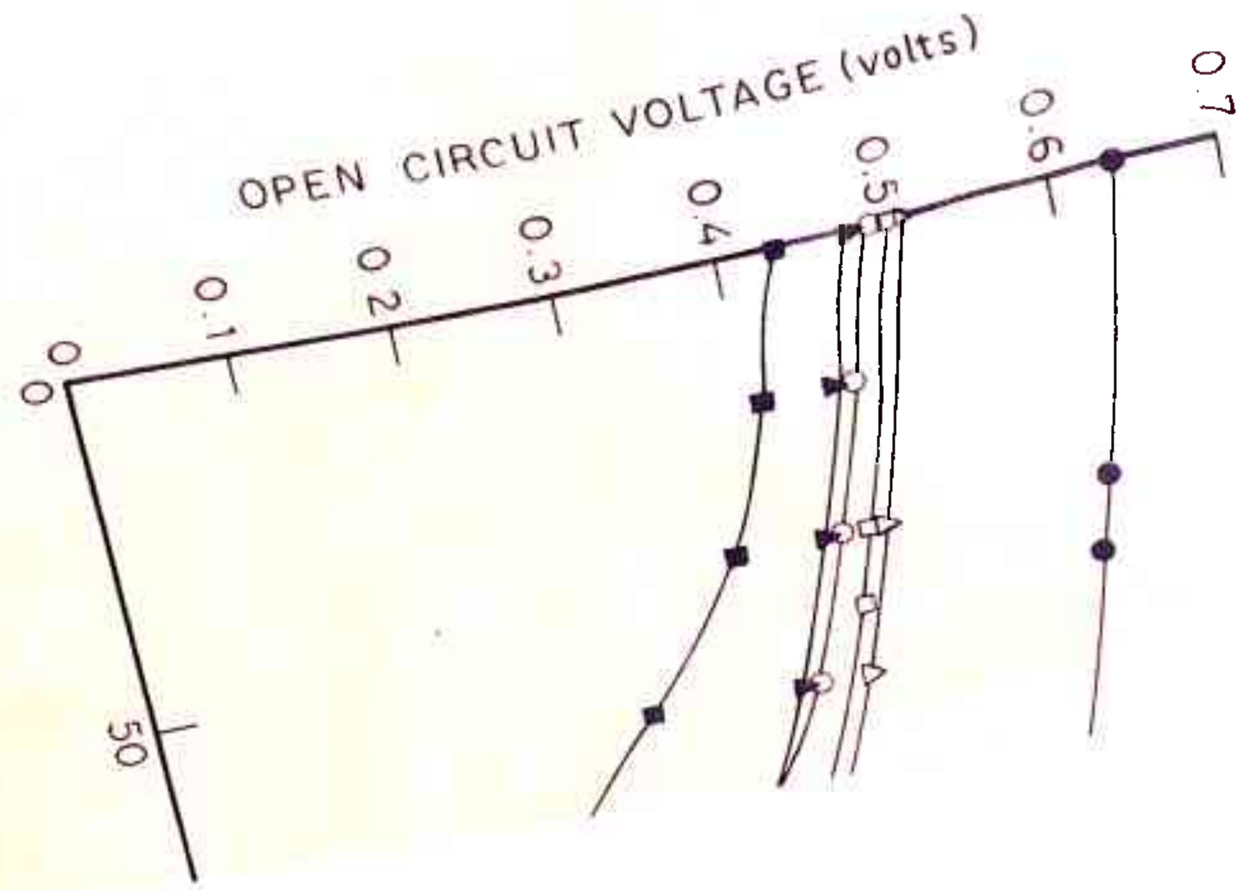
OPEN CIRCUIT VOLTAGE (volts)
0.7
0.6
0.5
0.4
0.3
0 2
0.1
0
0
50

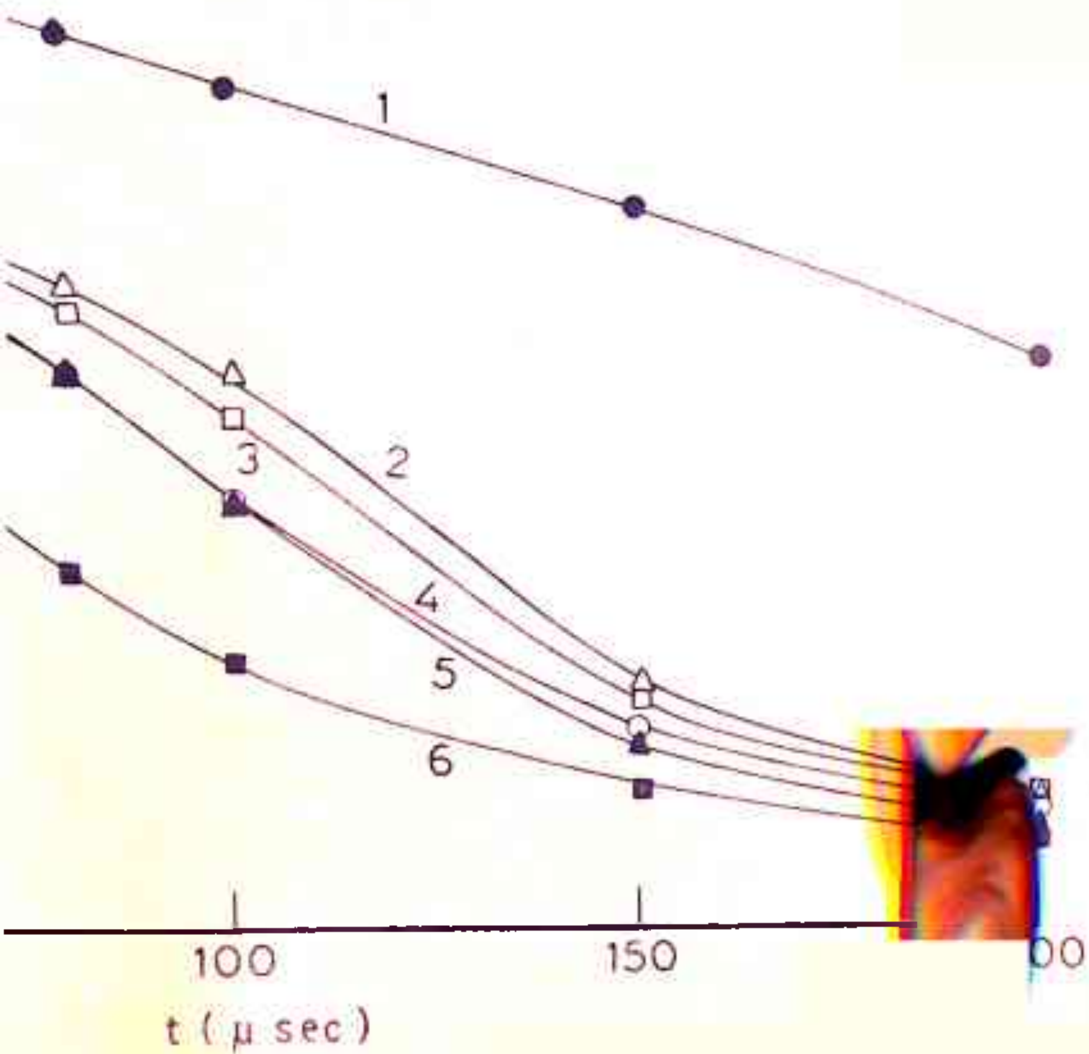

FIG. 5.1

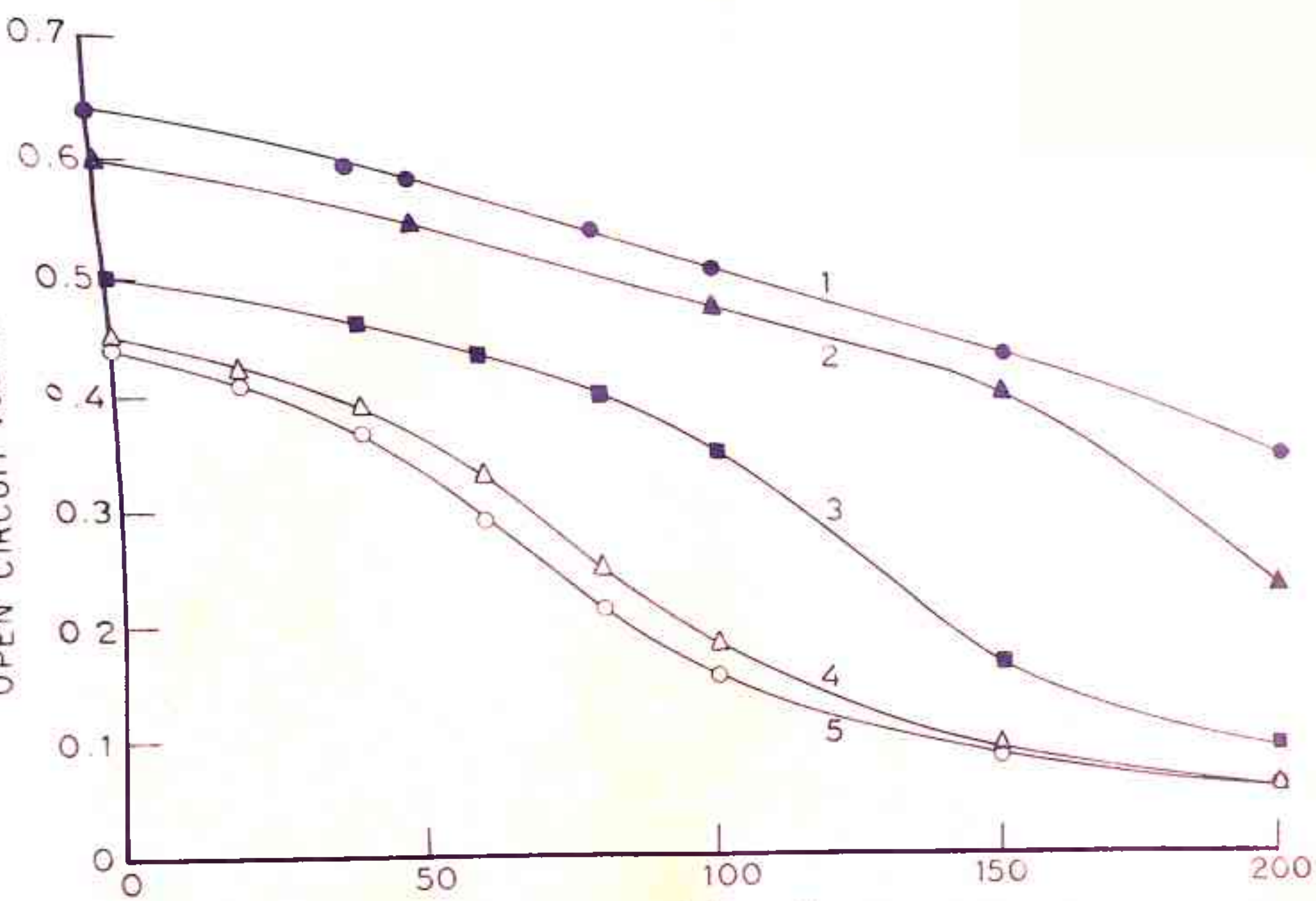

FIG.5.2

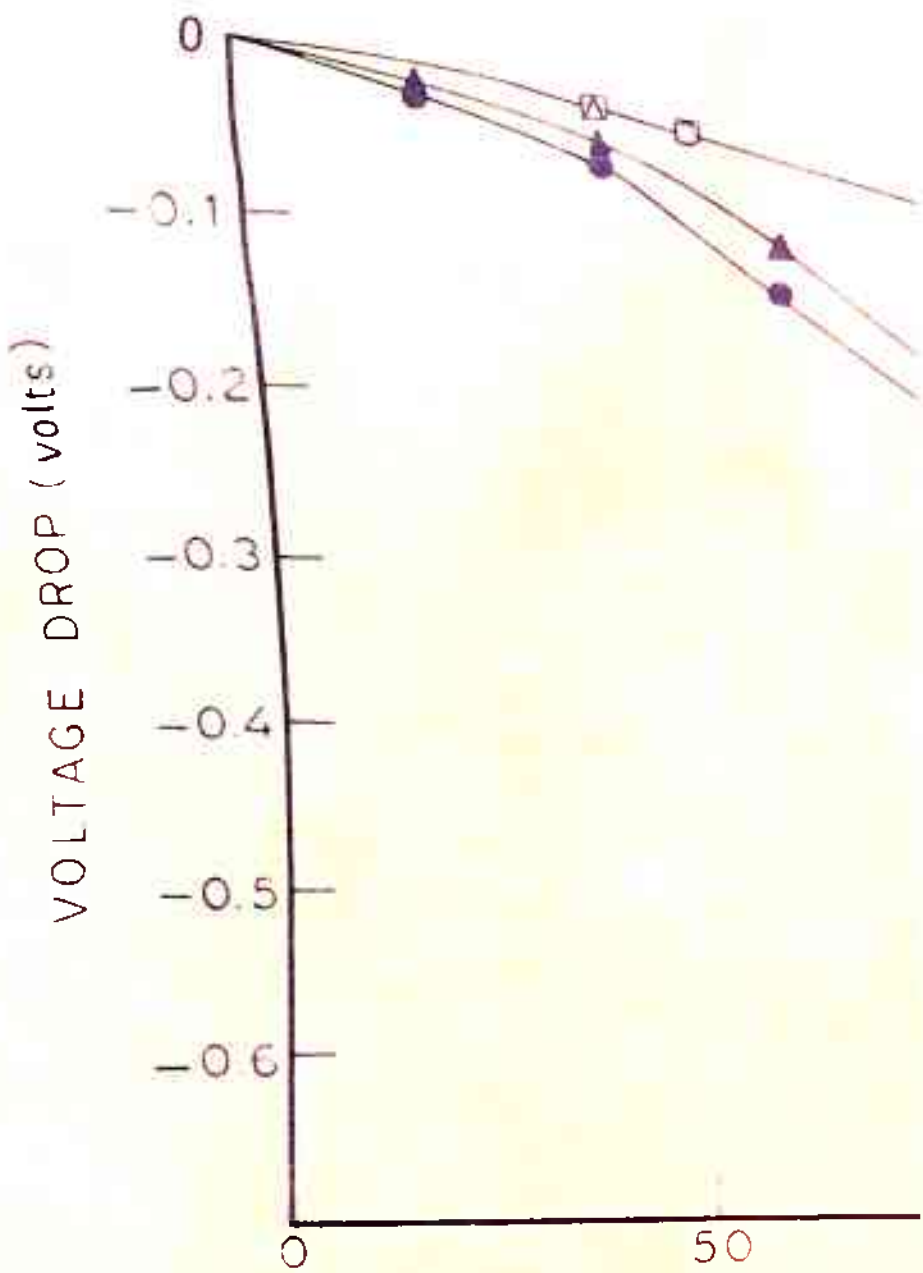

VOLTAGE DROP (volts)
0
-0.1
-0.2
-0.3
-0.4
-0.5
-0.6
0
50

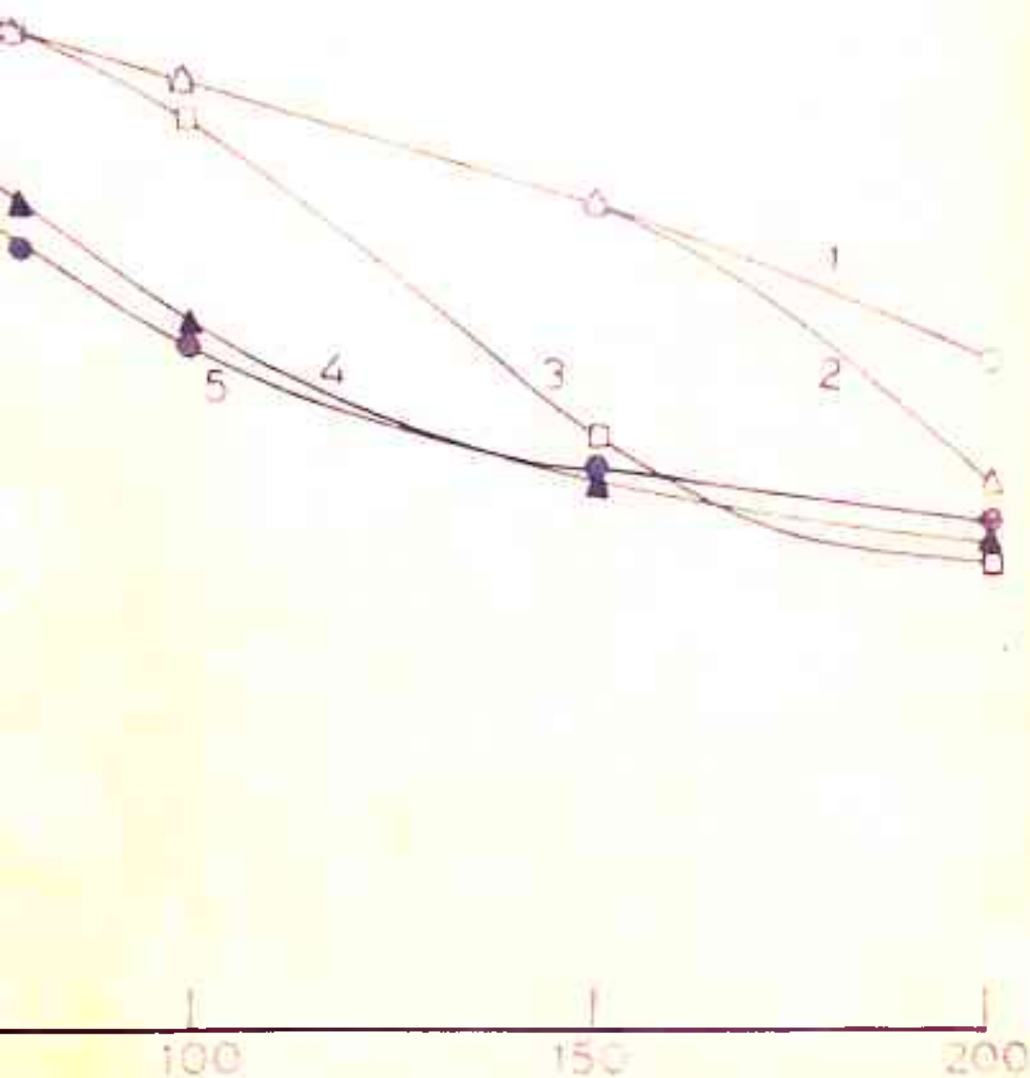

FIG.5.3

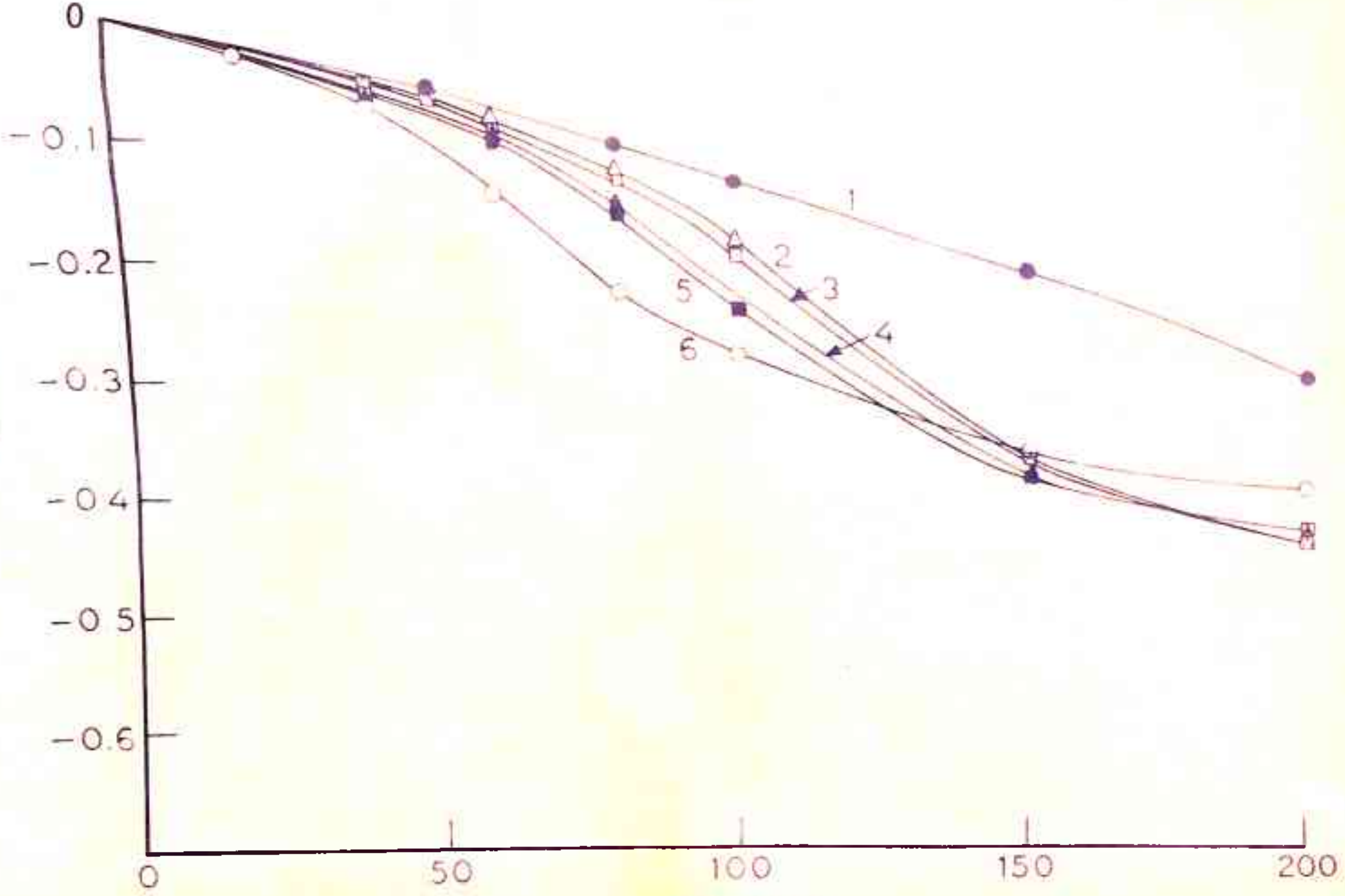

FIG. 5.4

St'S

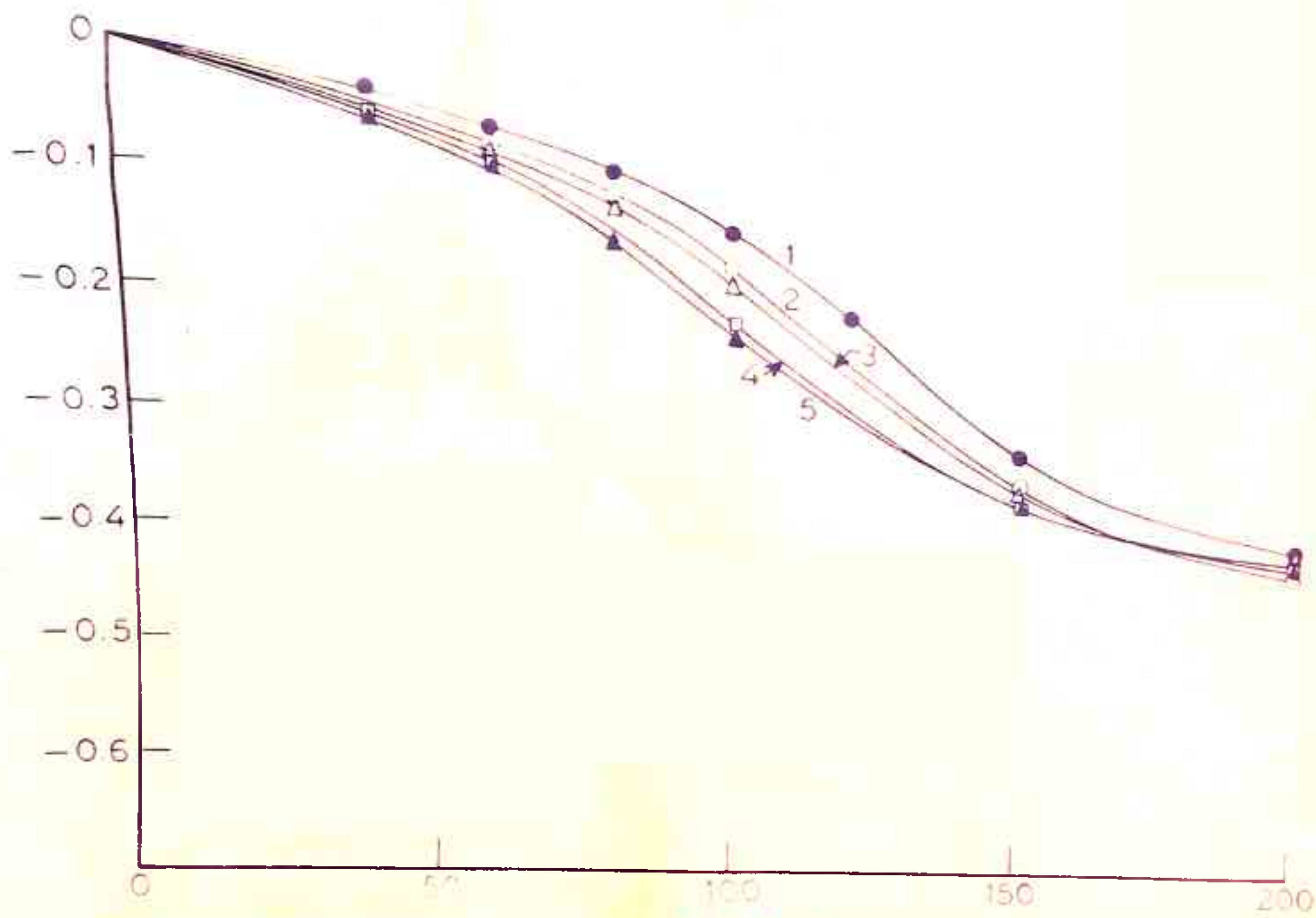

FIG 5.5

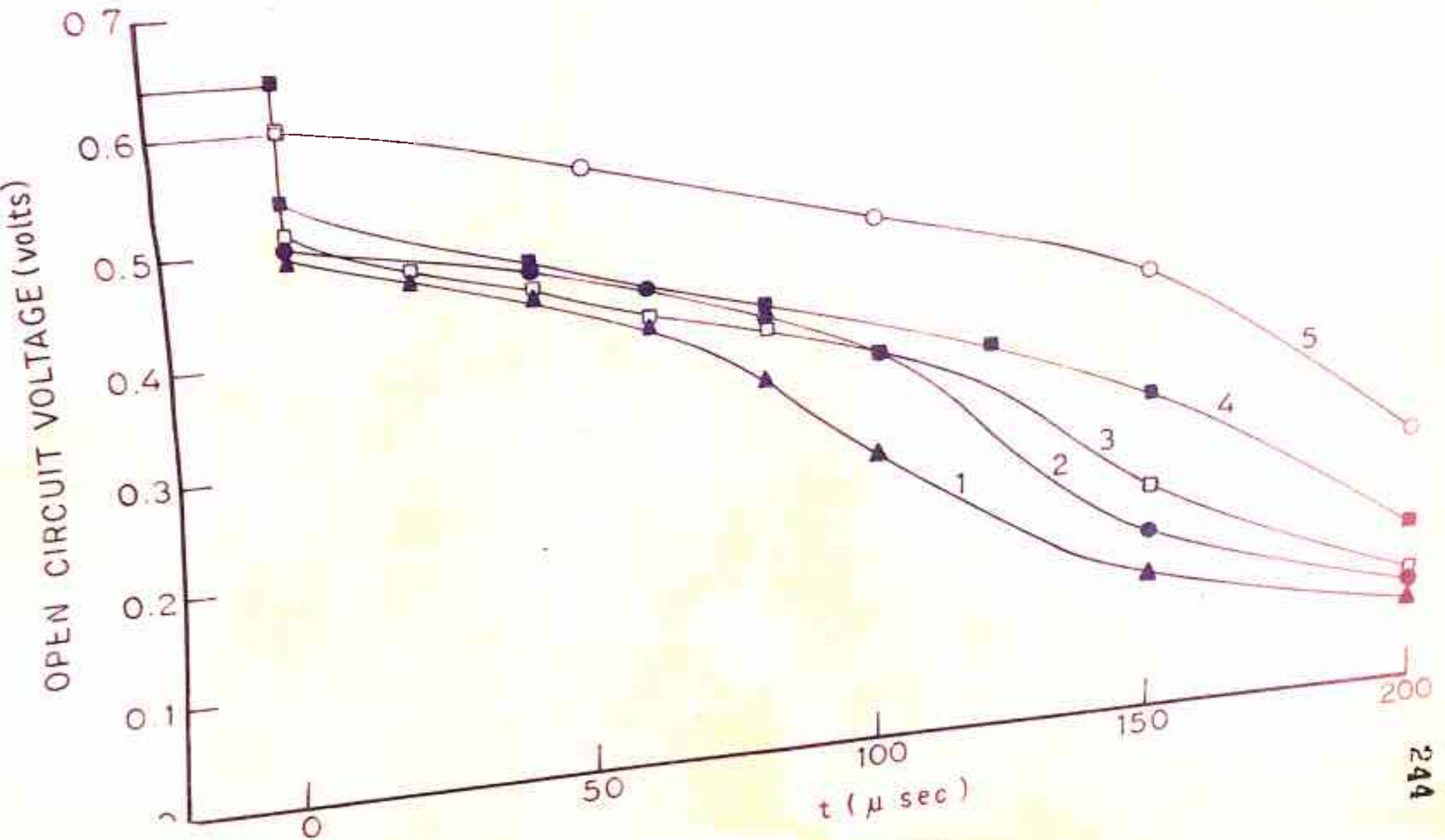

FIG 5.6